EXPLORING MATERNAL-FETAL PHARMACOLOGY THROUGH PBPK MODELING APPROACHES

EDITED BY: André Dallmann and Johannes Nicolaas Van Den Anker
PUBLISHED IN: Frontiers in Pediatrics and Frontiers in Pharmacology

frontiers Research Topics

frontiers

ISSN 1664-8714
ISBN 978-2-88976-335-1
DOI 10.3389/978-2-88976-335-1

About Frontiers

Frontiers is more than just an open-access publisher of scholarly articles: it is a pioneering approach to the world of academia, radically improving the way scholarly research is managed. The grand vision of Frontiers is a world where all people have an equal opportunity to seek, share and generate knowledge. Frontiers provides immediate and permanent online open access to all its publications, but this alone is not enough to realize our grand goals.

Frontiers Journal Series

The Frontiers Journal Series is a multi-tier and interdisciplinary set of open-access, online journals, promising a paradigm shift from the current review, selection and dissemination processes in academic publishing. All Frontiers journals are driven by researchers for researchers; therefore, they constitute a service to the scholarly community. At the same time, the Frontiers Journal Series operates on a revolutionary invention, the tiered publishing system, initially addressing specific communities of scholars, and gradually climbing up to broader public understanding, thus serving the interests of the lay society, too.

Dedication to Quality

Each Frontiers article is a landmark of the highest quality, thanks to genuinely collaborative interactions between authors and review editors, who include some of the world's best academicians. Research must be certified by peers before entering a stream of knowledge that may eventually reach the public - and shape society; therefore, Frontiers only applies the most rigorous and unbiased reviews.
Frontiers revolutionizes research publishing by freely delivering the most outstanding research, evaluated with no bias from both the academic and social point of view. By applying the most advanced information technologies, Frontiers is catapulting scholarly publishing into a new generation.

What are Frontiers Research Topics?

Frontiers Research Topics are very popular trademarks of the Frontiers Journals Series: they are collections of at least ten articles, all centered on a particular subject. With their unique mix of varied contributions from Original Research to Review Articles, Frontiers Research Topics unify the most influential researchers, the latest key findings and historical advances in a hot research area! Find out more on how to host your own Frontiers Research Topic or contribute to one as an author by contacting the Frontiers Editorial Office: frontiersin.org/about/contact

EXPLORING MATERNAL-FETAL PHARMACOLOGY THROUGH PBPK MODELING APPROACHES

Topic Editors:
André Dallmann, Bayer, Germany
Johannes Nicolaas Van Den Anker, Children's National Hospital, United States

Citation: Dallmann, A., Van Den Anker, J. N., eds. (2022). Exploring Maternal-Fetal Pharmacology Through PBPK Modeling Approaches. Lausanne: Frontiers Media SA. doi: 10.3389/978-2-88976-335-1

Table of Contents

05 ***Editorial: Exploring Maternal-Fetal Pharmacology Through PBPK Modeling Approaches***
André Dallmann and John N. van den Anker

08 ***Physiologically Based Pharmacokinetics Model in Pregnancy: A Regulatory Perspective on Model Evaluation***
Paola Coppola, Essam Kerwash and Susan Cole

13 ***Physiologically Based Pharmacokinetic Modelling for Nicotine and Cotinine Clearance in Pregnant Women***
Basile Amice, Harvey Ho, En Zhang and Chris Bullen

20 ***Regulatory Considerations for the Mother, Fetus and Neonate in Fetal Pharmacology Modeling***
Dionna J. Green, Kyunghun Park, Varsha Bhatt-Mehta, Donna Snyder and Gilbert J. Burckart

29 ***Mechanistic Modeling of Maternal Lymphoid and Fetal Plasma Antiretroviral Exposure During the Third Trimester***
Babajide Shenkoya, Shakir Atoyebi, Ibrahim Eniayewu, Abdulafeez Akinloye and Adeniyi Olagunju

40 ***Evaluation of Placental Transfer and Tissue Distribution of* cis- *and* Trans-*Permethrin in Pregnant Rats and Fetuses Using a Physiological-Based Pharmacokinetic Model***
Stéphane Personne, Céline Brochot, Paulo Marcelo, Aurélie Corona, Sophie Desmots, Franck Robidel, Anthony Lecomte, Véronique Bach and Florence Zeman

56 ***Mechanistic Coupling of a Novel* in silico *Cotyledon Perfusion Model and a Physiologically Based Pharmacokinetic Model to Predict Fetal Acetaminophen Pharmacokinetics at Delivery***
Paola Mian, Bridget Nolan, John N. van den Anker, Kristel van Calsteren, Karel Allegaert, Nisha Lakhi and André Dallmann

71 ***Characterization of Plasma Protein Alterations in Pregnant and Postpartum Individuals Living With HIV to Support Physiologically-Based Pharmacokinetic Model Development***
Sherry Zhao, Mary Gockenbach, Manuela Grimstein, Hari Cheryl Sachs, Mark Mirochnick, Kimberly Struble, Yodit Belew, Jian Wang, Edmund V. Capparelli, Brookie M. Best, Tamara Johnson, Jeremiah D. Momper and Anil R. Maharaj

82 ***Mechanistic Modeling of Placental Drug Transfer in Humans: How Do Differences in Maternal/Fetal Fraction of Unbound Drug and Placental Influx/Efflux Transfer Rates Affect Fetal Pharmacokinetics?***
Xiaomei I. Liu, Dionna J. Green, John N. van den Anker, Natella Y. Rakhmanina, Homa K. Ahmadzia, Jeremiah D. Momper, Kyunghun Park, Gilbert J. Burckart and André Dallmann

101 ***Maternal-Fetal Pharmacology of Drugs: A Review of Current Status of the Application of Physiologically Based Pharmacokinetic Models***
Nupur Chaphekar, Prerna Dodeja, Imam H. Shaik, Steve Caritis and Raman Venkataramanan

115 ***Physiologically Based Pharmacokinetic Modeling in Pregnant Women Suggests Minor Decrease in Maternal Exposure to Olanzapine***
Liang Zheng, Hongyi Yang, André Dallmann, Xuehua Jiang, Ling Wang and Wei Hu

frontiers | Frontiers in Pediatrics

EDITORIAL
published: 18 May 2022
doi: 10.3389/fped.2022.880402

Editorial: Exploring Maternal-Fetal Pharmacology Through PBPK Modeling Approaches

André Dallmann[1]* *and John N. van den Anker*[2,3]

[1] Pharmacometrics/Modeling and Simulation, Research and Development, Pharmaceuticals, Bayer AG, Leverkusen, Germany, [2] Division of Clinical Pharmacology, Children's National Hospital, Washington, DC, United States, [3] Department of Pediatric Pharmacology and Pharmacometrics, University Children's Hospital Basel, University of Basel, Basel, Switzerland

Keywords: PBPK, pregnancy, maternal-fetal, pharmacokinetics, modeling and simulation, physiologically – based pharmacokinetic model

Editorial on the Research Topic

Exploring Maternal-Fetal Pharmacology Through PBPK Modeling Approaches

While drug intake during pregnancy is frequent (almost 90%) and still increasing (1, 2), only a small fraction of these drugs (<10%) have been properly studied and labeled for use in pregnant individuals (3). The lack of sufficient information to warrant safe and effective pharmacotherapy during pregnancy constitutes a significant public health challenge. This issue is anything but new. In 1993, the Working Group on Women in Clinical Trials including, amongst others, the commissioner of the Food and Drug Administration (FDA) at that time, Dr. David A. Kessler, stated that "maximizing protection of fetuses from potentially toxic therapies is prudent, and fear of liability is understandable, but the result is that many drugs are ultimately used during pregnancy without reliable data on their maternal and fetal effects" (4). More recently, the response to the COVID-19 pandemic can be seen as another worrisome example illustrating the blatant lack of information to support safe and effective healthcare for pregnant individuals (5–7). While there is some hope that the current paradigm of systematic exclusion will shift toward a fair and responsible inclusion of pregnant individuals in clinical trials (8), other approaches may complement our understanding of maternal-fetal pharmacology and hence improve pharmacotherapy.

Among these approaches, physiologically based pharmacokinetic (PBPK) modeling holds exciting promise (9, 10). PBPK models are compartmental models consisting of a plethora of differential equations describing the pharmacokinetics on a (semi)mechanistic basis, meaning that the relationship between the pharmacokinetics and model parameters is specified in terms of the physical, chemical, and biologic processes that are thought to have given rise to the clinically observed pharmacokinetics. This mechanistic basis brings about a predictive performance superior to that of empirical compartmental models (11–13). PBPK models are increasingly being applied to simulate pharmacokinetics throughout pregnancy (14, 15). This is encouraging in view of the many difficulties in conducting pharmacological studies in pregnant individuals and demonstrates how the potential of PBPK models can be leveraged to refine the knowledge about pre- and perinatal pharmacology, especially when clinical data are sparse, missing, or conflicting.

This article Research Topic aims to promote maternal-fetal PBPK modeling as a high-level tool for gaining a better understanding of drug pharmacokinetics during pregnancy. In the first review, Chaphekar et al. discuss when and how PBPK modeling constitutes an alternative approach to clinical studies and provide a comprehensive summary of the status of human PBPK models for predicting maternal and fetal drug exposure.

OPEN ACCESS

Edited by:
Jeffrey Scott Barrett, Critical Path Institute, United States

Reviewed by:
Deni Hardiansyah, University of Indonesia, Indonesia

***Correspondence:**
André Dallmann
andre.dallmann@bayer.com

Specialty section:
This article was submitted to Obstetric and Pediatric Pharmacology, a section of the journal Frontiers in Pediatrics

Received: *22 February 2022*
Accepted: *06 May 2022*
Published: *18 May 2022*

Citation:
Dallmann A and van den Anker JN (2022) Editorial: Exploring Maternal-Fetal Pharmacology Through PBPK Modeling Approaches. Front. Pediatr. 10:880402. doi: 10.3389/fped.2022.880402

Subsequently, several articles of this Research Topic report novel PBPK applications focusing on maternal and/or fetal pharmacokinetics in rats or humans. Personne et al. open this field with a perspective on fetal permethrin exposure throughout gestation in rats. To this end, the authors developed a rat PBPK model for permethrin to estimate placental transfer and prenatal exposure in various tissues including the fetal brain, providing a sound basis for extrapolation to humans.

Another approach to inform placental drug transfer in humans is reported by Mian et al. who present a novel *in silico* cotyledon perfusion model that was used to learn the placental transfer kinetics of acetaminophen from reported data measured in the *ex vivo* cotyledon perfusion system and, upon integration of the learnt transfer kinetics in a whole-body PBPK model, evaluated with clinical data at term delivery.

Along the same line, Liu et al. refined the ordinary differential equation system of an existing pregnancy PBPK model to account for differences in protein binding of drugs between maternal and fetal blood plasma showing that, especially for highly-protein bound drugs, a lower fraction unbound in the fetus vs. mother can markedly affect predicted fetal exposure.

In another work, Amice et al. combined two previously published pregnancy PBPK models for nicotine and cotinine and predict fetal exposure to these substances in plasma and brain after intravenous injection; potential extensions of this model, such as further refinement once more clinical data become available, are also discussed.

While current pregnancy PBPK models typically rely on physiological information from healthy pregnant individuals, they may not fully reflect the underlying physiology of pregnant patients. To tackle this issue, Zhao et al. analyzed serum albumin concentrations collected from large cohorts of pregnant and postpartum women living with HIV and generated functions describing the trajectory of the concentration of each plasma protein in the two cohorts that can be readily utilized for PBPK model development.

This article Research Topic also includes modeling studies with potential implications for clinical practice. Zheng et al. developed a PBPK model for olanzapine; the simulation results in pregnant individuals suggest that dose adjustment can hardly be recommended at the studied stages of pregnancy if treatment before pregnancy was effective and fetal toxicity can be ruled out.

Shenkoya et al. structurally extended a maternal-fetal PBPK model by adding compartments for the lymphatic system and predict the penetration of three antiretroviral drugs in lymphoid tissues-the largest HIV reservoir in the body-indicating that no dose adjustments seem to be necessary in the late third trimester of pregnancy.

Obviously, clinical research involving pregnant individuals can only be carried out within a well-defined regulatory framework. Therefore, two articles from the UK Medicines and Healthcare Products Regulatory Agency (MHRA) and the US Food and Drug Administration (FDA) conclude this Research Topic. Coppola et al. discuss various facets of model evaluation and qualification that are considered necessary if these models are to be used in the context of regulatory application.

Green et al. provide a detailed account of the regulatory framework pertaining to research in mothers, fetuses, and neonates, and discusses multiple aspects of the use of modeling in regulatory submissions concluding that modeling will help fetal pharmacology to quickly move into the mainstream of drug development for the benefit of pregnant individuals and their fetuses.

We hope that this Research Topic will stimulate further research in the field of maternal-fetal PBPK modeling that will ultimately contribute to a more evidence-based approach to pharmacotherapy in pregnancy.

AUTHOR CONTRIBUTIONS

AD wrote the first draft of the manuscript. Both authors contributed to the article and approved the submitted version.

ACKNOWLEDGMENTS

We would like to thank all colleagues who have contributed to this article Research Topic, either as authors of an article, as peer reviewers or as editors.

REFERENCES

1. Smolina K, Hanley GE, Mintzes B, Oberlander TF, Morgan S. Trends and determinants of prescription drug use during pregnancy and postpartum in British Columbia, 2002–2011: a population-based cohort study. *PLoS ONE.* (2015) 10:e0128312. doi: 10.1371/journal.pone.0128312
2. Engeland A, Bjørge T, Klungsøyr K, Hjellvik V, Skurtveit S, Furu K. Trends in prescription drug use during pregnancy and postpartum in Norway, 2005 to 2015. *Pharmacoepidemiol Drug Saf.* (2018) 27:995–1004. doi: 10.1002/pds.4577
3. Van Calsteren K, Gersak K, Sundseth H, Klingmann I, Dewulf L, Van Assche A, et al. Position statement from the European Board and College of Obstetrics & Gynaecology (EBCOG): the use of medicines during pregnancy–call for action. *Eur J Obstetr Gynecol Reprod Biol.* (2016) 201:189–91. doi: 10.1016/j.ejogrb.2016.04.004
4. Merkatz RB, Temple R, Sobel S, Feiden K, Kessleir DA. Women in clinical trials of new drugs–A change in food and drug administration policy. *N Engl J Med.* (1993) 329:292–6. doi: 10.1056/NEJM199307223290429
5. Davis-Floyd R, Gutschow K, Schwartz DA. Pregnancy, birth and the COVID-19 pandemic in the United States. *Med Anthropol.* (2020) 39:413–27. doi: 10.1080/01459740.2020.1761804
6. Male V. Are COVID-19 vaccines safe in pregnancy? *Nat Rev Immunol.* (2021) 21:200–1. doi: 10.1038/s41577-021-00525-y
7. Jaffe EF, Lyerly AD, Goldfarb IT. Advancing research in pregnancy during COVID-19: missed opportunities and momentum in the US. *Medicine.* (2021) 2:460–4. doi: 10.1016/j.medj.2021.04.019
8. Lyerly AD, Faden RR. Mothers matter: ethics and research during pregnancy. *AMA J Ethics.* (2013) 15:775–8. doi: 10.1001/virtualmentor.2013.15.9.pfor1-1309
9. Dallmann A, Mian P, den Anker JV, Allegaert K. Clinical pharmacokinetic studies in pregnant women and the relevance of pharmacometric tools. *Curr Pharmaceut Des.* (2019) 25:483–95. doi: 10.2174/1381612825666190320151137
10. Ke AB, Greupink R, Abduljalil K. Drug dosing in pregnant women: challenges and opportunities in using physiologically based pharmacokinetic modeling and simulations. *CPT Pharmacometr Syst Pharmacol.* (2018) 7:103–10. doi: 10.1002/psp4.12274

11. Thakur AK. *Model: Mechanistic vs Empirical. New Trends in Pharmacokinetics*: Springer (1991). p. 41–51. doi: 10.1007/978-1-4684-8053-5_3
12. Jones HM, Parrott N, Jorga K, Lavé T, A. novel strategy for physiologically based predictions of human pharmacokinetics. *Clin Pharmacokinet.* (2006) 45:511–42. doi: 10.2165/00003088-200645050-00006
13. Jones HM, Gardner IB, Collard WT, Stanley P, Oxley P, Hosea NA, et al. Simulation of human intravenous and oral pharmacokinetics of 21 diverse compounds using physiologically based pharmacokinetic modelling. *Clin Pharmacokinet.* (2011) 50:331–47. doi: 10.2165/11539680-000000000-00000
14. Dallmann A, Pfister M, van den Anker J, Eissing T. Physiologically based pharmacokinetic modeling in pregnancy: a systematic review of published models. *Clin Pharmacol Therap.* (2018) 104:1110–24. doi: 10.1002/cpt.1084
15. van Hoogdalem MW, Wexelblatt SL, Akinbi HT, Vinks AA, Mizuno T. A review of pregnancy-induced changes in opioid pharmacokinetics, placental transfer, and fetal exposure: towards fetomaternal physiologically-based pharmacokinetic modeling to improve the treatment of neonatal opioid withdrawal syndrome. *Pharmacol Therap*. (2021) 2021:108045. doi: 10.1016/j.pharmthera.2021.108045

Conflict of Interest: AD is an employee of Bayer AG and uses Open Systems Pharmacology software, tools, and models in his professional role.

The remaining author declares that the research was conducted in the absence of any commercial or financial relationships that could be construed as a potential conflict of interest.

Publisher's Note: All claims expressed in this article are solely those of the authors and do not necessarily represent those of their affiliated organizations, or those of the publisher, the editors and the reviewers. Any product that may be evaluated in this article, or claim that may be made by its manufacturer, is not guaranteed or endorsed by the publisher.

frontiers in Pediatrics

PERSPECTIVE
published: 23 June 2021
doi: 10.3389/fped.2021.687978

Physiologically Based Pharmacokinetics Model in Pregnancy: A Regulatory Perspective on Model Evaluation

Paola Coppola, Essam Kerwash and Susan Cole*

Medicines and Healthcare Products Regulatory Agency, London, United Kingdom

Physiologically based pharmacokinetics (PBPK) modelling is widely used in medicine development and regulatory submissions. The lack of clinical pharmacokinetic data in pregnancy is widely acknowledged; therefore, one area of current interest is in the use of PBPK modelling to describe the potential impact of anatomical and physiological changes during pregnancy on the medicine's pharmacokinetics. PBPK modelling could possibly represent a predictive tool to support the medicine benefit–risk decision and inform dose adjustment in this population and also to investigate medicine levels in the foetus to support the risk assessment to the foetus. In the context of regulatory application, there are, however, a number of considerations around model evaluation, and this should be tailored to the model purpose, in order to inform the confidence in the model for the intended application. A number of gestational age-related physiological changes are expected to alter the pharmacokinetics of medicines during pregnancy, and there are uncertainties on some parameters; therefore, well-qualified models are needed to improve assurance in the model prediction before this approach can be used to inform with confidence high-impact decisions as part of regulatory submissions.

Keywords: physiologically-based pharmacokinetics modelling, pharmacokinetics, pregnancy PBPK, foetal PBPK, breastfeeding PBPK, PBPK qualification, regulatory submissions

OPEN ACCESS

Edited by:
André Dallmann, Bayer, Germany

Reviewed by:
Gilbert Burckart, United States Food and Drug Administration, United States
Shirley Seo, United States Food and Drug Administration, United States

****Correspondence:***
Paola Coppola
paola.coppola@mhra.gov.uk

Specialty section:
This article was submitted to Obstetric and Pediatric Pharmacology, a section of the journal Frontiers in Pediatrics

Received: *30 March 2021*
Accepted: *10 May 2021*
Published: *23 June 2021*

Citation:
Coppola P, Kerwash E and Cole S (2021) Physiologically Based Pharmacokinetics Model in Pregnancy: A Regulatory Perspective on Model Evaluation. Front. Pediatr. 9:687978. doi: 10.3389/fped.2021.687978

INTRODUCTION

Although drug labels generally recommend to avoid use of medicines in pregnancy and breastfeeding, pharmacological treatment may be necessary for some medical conditions. The lack of clinical pharmacokinetics (PK) data in pregnancy is widely acknowledged; therefore, one area of current interest is in the use of PBPK modelling to describe the potential impact of anatomical and physiological changes during pregnancy on the medicine's PK. PBPK modelling could represent a predictive tool to support the medicine benefit–risk decision and inform dose adjustment in this population. PBPK may also be useful to investigate medicine levels in the foetus to support the risk assessment to the foetus and in breast milk to inform exposure to infants.

Using a mathematical approach, PBPK models predict the expected medicine levels in the target population, as well as how physiological changes may alter those levels. There are, however, a number of considerations around the modelling before it can be used to inform clinical practice or regulatory submissions with confidence. This article provides an overview of considerations around the potential use of modelling to inform clinical practice with confidence,

and considerations are provided regarding the qualification process usually required to support high-impact regulatory uses.

PREGNANCY PHYSIOLOGICALLY BASED PHARMACOKINETICS MODELS

The physiological changes occurring in women during pregnancy may alter the absorption, distribution, metabolism and excretion (ADME) of medicines. Oral drug absorption may be delayed during pregnancy, and decreased levels of plasma proteins albumin and α1-acid glycoprotein may lead to decreased drug plasma protein binding and increased levels of unbound drugs. Moreover, protein binding of drugs, hepatic blood flow and hepatic enzyme activity are altered during pregnancy; and this may affect the elimination pathway of hepatically cleared drugs (1). As a consequence of altered metabolic enzymes activity, the blood concentrations of drugs metabolised through CYP2D6, CYP3A4, CYP2A6, UGT1A4, and UGT2B7 are expected to decrease during pregnancy as compared with those in non-pregnant subjects, while concentrations of drugs that are substrates of other enzymes, e.g., CYP1A2 and CYP2C19, are expected to increase in pregnant women (2).

PBPK modelling can be used as a predictive tool to provide an understanding of drugs disposition in pregnant women. Most gestational age-dependent physiological changes, including the development of the foetal placental compartment, may be incorporated in the model to allow an understanding of the impact of those changes on the PK of medicines in pregnant women compared with non-pregnant subject. Simcyp™ Simulator (Simcyp Ltd, Sheffield, UK, http://www.simcyp.com), GastroPlus™ (Simulations Plus Inc., Lancaster, CA, USA) and PK-Sim® (http://www.open-systems-pharmacology.org/) are PBPK platforms; and all have pregnancy models to predict exposure in pregnancy populations at different stages of pregnancy based on the physiological changes that occur.

The European Medicines Agency (EMA) and US Food and Drug Administration (FDA) recommend that, where possible, PK and pharmacodynamic (PD) studies should be conducted in pregnant women to understand how pregnancy affects the blood levels of medicines commonly used and to inform dosing regimen of medicines to be used in pregnancy (3, 4). The importance of PK studies including pregnant patients has been highlighted in the FDA's draft guidance (4), where the use of PBPK is suggested to support clinical study design in this vulnerable population.

PBPK models have been seen in regulatory submissions by regulators in Europe and the USA; and in some cases, models have been accepted to replace clinical studies and to inform the SmPC (5–7). However, pregnancy PBPK models have, to date, been seen in a very limited number of submissions in Europe.

PBPK may support the understanding of drug systemic exposures in pregnant population and be used to optimise the design of PK clinical trials for investigational medicines in this population. Given the sparsity of data and the need to, on occasions, dose pregnant women, the potential of PBPK modelling to inform this dosing was considered important to explore. The modelling could be used to identify which medicines are more likely to be affected by pregnancy and, therefore, would be a priority to obtain clinical data in pregnant women. Eventually, there may be situations where the confidence in the PBPK model is such that it can be used to support extrapolation of efficacy and safety data from healthy volunteers to pregnant women without any clinical data. Ultimately, the hope is that models could be used by healthcare professionals in the clinic to better inform dosing of these patients.

Dosing based solely on exposure, whether measured or predicted, is considered an extrapolation in EU regulatory terms, and a framework has recently been published for children. This framework could be usefully applied to pregnancy (8). A comprehensive PBPK pregnancy model framework could bridge the gaps in data to support a prospective investigation of the exposure, which should then be considered in terms of the exposure–response relationship. This is important for predicting the necessary dose changes to maintain maternal health (9). The first step in the extrapolation is to understand the exposure in pregnancy, and this could be informed by the PBPK models. Such a use would be considered a high-impact application and would require a robust model evaluation.

FOETAL PHYSIOLOGICALLY BASED PHARMACOKINETICS MODELS

The evaluation of the risk of foetal exposure to drugs, and its toxicity, during pregnancy is crucial in the benefit–risk assessment of medicines for treating either pre-existing or gestational-related maternal medical conditions. Moreover, in some cases, medical treatment may be needed to prevent vertical disease transmission from the mother to the foetus (e.g., HIV infection). PBPK modelling could provide an understanding of the drug transplacental passage and may be helpful to predict expected foetal medicine levels during pregnancy. The umbilical cord/maternal plasma drug concentration ratio may allow some understanding of the transplacental transfer, although it may not always provide a good prediction of the foetal drug exposure, and the majority of data are in late-stage pregnancy/delivery (10).

LACTATION PHYSIOLOGICALLY BASED PHARMACOKINETICS MODELS

Modelling approaches may be useful to estimate mother and infant drug exposure during lactation. PBPK is a potential valuable tool that has been used to predict milk to plasma ratio of potentially harmful medicines and environmental toxins (11). Milk composition varies considerably during and in between breastfeeding sessions, which affects the milk to plasma ratio, leading to variable concentrations of the medicines excreted in milk (12). PBPK may be utilised to estimate the medicine's plasma to milk partition coefficient and calculate the total concentration in milk during breastfeeding, which could be used to calculate the total daily intake by infant. Moreover, PBPK may potentially predict infant exposure during breastfeeding after accounting for the maturation in the drug absorption, distribution and

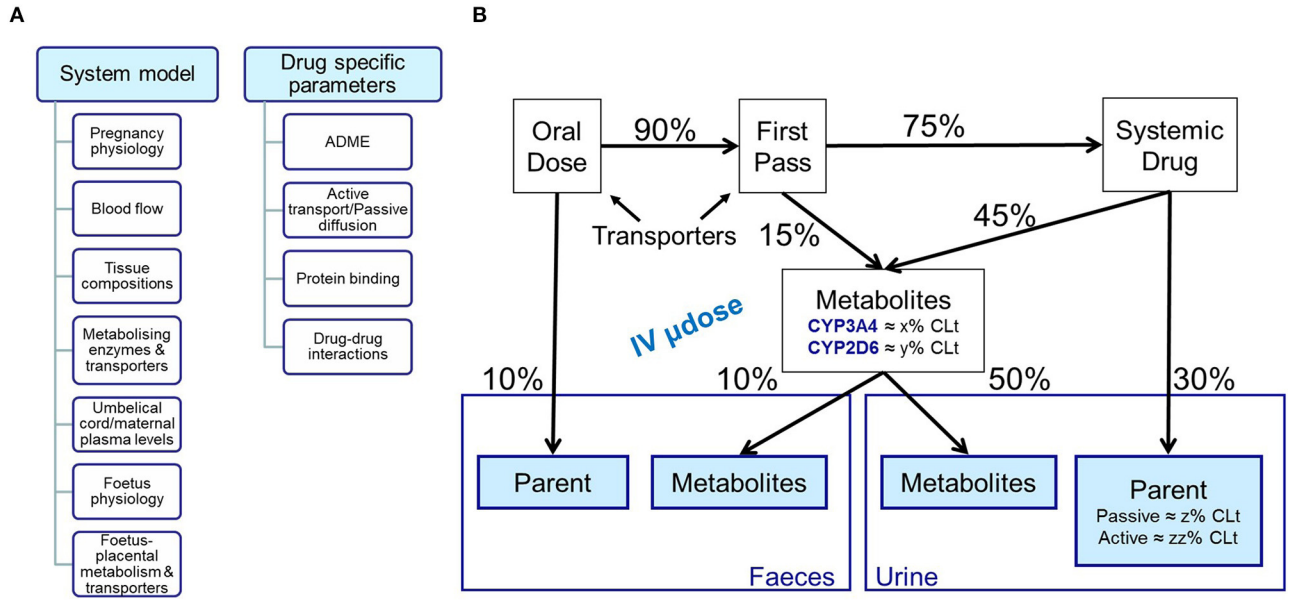

FIGURE 1 | Schematic representation of **(A)** inputs needed for building both system and drug models; **(B)** Mass balance diagram following oral and intravenous dosing.

elimination systems (13). The deposition of drug in various infant tissues such as the kidney, liver, and bone marrow may be also simulated.

EVALUATION OF THE PREGNANCY PHYSIOLOGICALLY BASED PHARMACOKINETICS MODEL

In a previous publication, we introduced a project to investigate PBPK models to inform drug use in pregnancy (9); this publication includes more detail on what should be considered in terms of model evaluation.

The recommendations in terms of considering whether these models are fit for purpose are outlined in the EMA guideline (6), and key aspects are discussed below. Other frameworks exist for the evaluation of models, e.g., the risk-based credibility assessment framework proposed by Kuemmel et al. (14).

Literature data are available on a number of model drugs that we consider to have rich data sets in pregnancy. For these compounds, drug models are needed; these may be sourced from model repositories; or when models are not available, these models can be built from scratch. In both cases, it is important to determine that the input parameters, i.e., drug physicochemical, PK and PD characteristics, are robust and adequately determined. In the drug development environment in pharmaceutical companies, all input parameters will usually be measured *de novo*; however, when building models retrospectively, it is necessary to source data from the literature; and in some cases, parameters are optimised during model development.

The important parameters for constructing an appropriate PBPK model depend on the model purpose. In the context of use in pregnancy, an extensive understanding of the absorption and elimination processes is essential, and parameters describing this should be reliable. A drug disposition diagram (15, 16) is recommended for the drugs of interest (**Figure 1**). The quantitative contribution of all enzymes and transporters involved in the absorption and elimination should be adequately captured in the model, and any uncertainties should be explored with a sensitivity analysis. The quantitation of all pathways to the elimination can be difficult to determine. This may be more challenging for compounds that are substrates of multiple CYPs enzymes, e.g., metronidazole (17), where the specific contribution of each CYP needs to be known, or for substrates of CYP2D6, e.g., metoprolol, as polymorphism may affect the systemic exposure (18). Moreover, the PK of medicines undergoing renal elimination, e.g., amoxicillin, may be altered during pregnancy due to changes in transporters activity/expression; and information about transporters involved in clearance pathways and/or transplacental passage is still limited at the moment (19). The more complex the absorption and elimination processes are for the drug of interest, the more uncertainty this can introduce.

The predictive capability of the drug model should also be determined. The reliability is assessed on the basis of how well important characteristics of the drug model have been tested against *in vivo* PK data. The moiety of interest for predictions should be considered; e.g., parent drug and/or metabolite and the predictive performance of the drug model needs to be demonstrated in healthy volunteers following a range of doses and following single and multiple dosing. Any mis-specification

in healthy volunteers will need to be considered when it comes to considering the results in pregnancy.

QUALIFICATION OF THE PREGNANCY PHYSIOLOGICALLY BASED PHARMACOKINETICS MODEL

Extensive understanding of physiological changes occurring both during and after pregnancy that may affect drug absorption and disposition (system model) are critical to build a robust PBPK model.

Model qualification is used to determine if these physiology changes have been adequately captured by the system model. In the context of regulatory application, the confidence in the model predictions should be supported by the model qualification, which should be related to the intended purpose and the regulatory impact of the modelling (6, 20). For example, extensive qualification is requested for high-impact models, e.g., when the PBPK is aimed to replace clinical studies or to investigate complex drug–drug interactions (6). A number of compounds with similar ADME characteristics to that of the investigational drug should be used to qualify the model. The confidence in the model depends on both the results of drug model evaluation and the qualification level for the use of the PBPK for the intended purpose (5). For pregnancy PBPK models, clinical PK data in pregnant women collected in all gestational trimesters should be used for the model qualification and validation. However, this might be hampered in some cases due to limited available data in this population, in all trimesters.

For maternal pregnancy models, changes in distribution and elimination are important to capture in the models and to determine the compounds in a qualification data set for a given drug. For example, information about renal changes occurring during all gestational trimesters is crucial for developing a PBPK model aimed to investigate the maternal systemic exposure of medicines undergoing renal elimination. The qualification set should then include drugs renally cleared by the same mechanism. For drugs where a specific enzyme or transporter plays a major role in the absorption, distribution and elimination, the qualification set should consist of a set of drugs for which the same enzyme or transporter plays a significant role. In some cases where multiple enzymes or transporters are involved, then a larger qualification data set may be required including drugs with known maternal exposure, which are substrates for at least one of the enzymes or transporters.

In order to understand foetal exposure of drugs, qualification will be required to show the model's ability to predict foetal concentrations or concentrations entering the foetus. In this situation, qualification will need to focus on the model's ability to predict foetal or cord concentrations.

The approach taken could be a comprehensive model with qualification of maternal and foetal concentrations; alternatively, if the maternal model has already been qualified or concentrations are based on measured values, it is suggested that an abbreviated approach could be taken where the qualification is based on prediction of foetal concentrations when the maternal concentrations are known and foetal concentrations are considered in the terms of a ratio to maternal concentrations. In this case, the qualification set of drugs should include drugs with similar properties to the drug of interest.

In order to understand exposure in milk, qualification using drug concentration PK profile in human milk is normally required to show the model's ability to predict milk concentrations. Comparison between foremilk and hindmilk drug concentrations is recommended to account for any time-dependent changes.

The approach taken could be a comprehensive model with qualification of maternal and foetal concentrations; alternatively, if the maternal model has already been qualified or concentrations are based on measured values, again, an abbreviated approach could be taken where the qualification is based on prediction of milk concentrations when the maternal concentrations are known, in the terms of a ratio. In this case, the qualification set of drugs should include drugs with similar properties to the drug of interest.

CONCLUSION

PBPK modelling could be a valuable tool to support the investigation of the expected medicine levels in pregnant women and exposure to the foetus and the infant on breastfeeding and to support the benefit–risk evaluation for drugs to be used in pregnancy.

As a number of gestational age-related physiological changes are expected to alter the PK of medicines during pregnancy, and there are uncertainties on some parameters, well-qualified models are needed to improve assurance in the model prediction before this approach can be used to inform with confidence high-impact decisions as part of regulatory submissions.

DATA AVAILABILITY STATEMENT

The original contributions generated for the study are included in the article/supplementary material, further inquiries can be directed to the corresponding author/s.

AUTHOR CONTRIBUTIONS

All authors listed have made a substantial, direct and intellectual contribution to the work, and approved it for publication.

FUNDING

The MHRA received a grant from the Bill & Melinda Gates Foundation, Seattle, Washington, USA, for a project to investigate the utilisation of PK and PBPK to improve drug use in pregnancy.

REFERENCES

1. Feghali M, Venkataramanan R, Caritis S. Pharmacokinetics of drugs in pregnancy. *Semin Perinatol*. (2015) 39:512–9. doi: 10.1053/j.semperi.2015.08.003
2. Hyunyoung J. Altered drug metabolism during pregnancy: hormonal regulation of drug-metabolizing enzymes. *Expert Opin Drug Metab Toxicol*. (2010) 6:689–99. doi: 10.1517/17425251003677755
3. European Medicines Agency. *EMA Guideline on the Exposure to Medicinal Products During Pregnancy: Need for Post-Authorisation Data*. EMEA/CHMP/313666/2005. London: European Medicines Agency (2005).
4. US FDA. *Pregnant Women: Scientific and Ethical Considerations for Inclusion in Clinical Trials. Guidance for Industry* (Silver Spring, MD) (2018).
5. Luzon E, Blake K, Cole S, Nordmark A, Versantvoort C, Berglund EG. Physiologically based pharmacokinetic modeling in regulatory decision-making at the European Medicines Agency. *Clin Pharmacol Ther*. (2017) 102:98–105. doi: 10.1002/cpt.539
6. European Medicines Agency. *EMA Guideline on the Reporting of Physiologically Based Pharmacokinetic (PBPK) Modelling and Simulation*. EMA/CHMP/458101/2016. London: European Medicines Agency (2018).
7. US FDA. *Physiologically Based Pharmacokinetic Analyses — Format and Content Guidance for Industry* (Silver Spring, MD) (2018).
8. European Medicines Agency. *Reflection Paper on the Use of Extrapolation in the Development of Medicines for Paediatrics*. EMA/189724/2018. London: European Medicines Agency (2018).
9. Cole S, Coppola P, Kerwash E, Nooney J, Lam SP. Pharmacokinetic characterization to enable medicine use in pregnancy, the potential role of physiologically-based pharmacokinetic modeling: a regulatory perspective. *CPT Pharmacometrics Syst Pharmacol*. (2020) 9:547–9. doi: 10.1002/psp4.12551
10. Zhang Z, Imperial MZ, Patilea-Vrana GI, Wedagedera J, Gaohua L, Unadkat JD. Development of a novel maternal-fetal physiologically based pharmacokinetic model I: insights into factors that determine fetal drug exposure through simulations and sensitivity analyses. *Drug Metab Dispos*. (2017) 45:920–38. doi: 10.1124/dmd.117.075192
11. Verstegen RHJ, Anderson PO, Ito S. Infant drug exposure *via* breast milk. *Br J Clin Pharmacol*. (2020) 2020:1–17. doi: 10.1111/bcp.14538
12. Corley RA, Mast TJ, Carney EW, Rogers JM, Daston GP. Evaluation of physiologically based models of pregnancy and lactation for their application in children's health risk assessments. *Crit Rev Toxicol*. (2003) 33:137–211. doi: 10.1080/713611035
13. Delaney SR, Malik PRV, Stefan C, Edginton AN, Colantonio DA, Ito S. Predicting escitalopram exposure to breastfeeding infants: integrating analytical and *in silico* techniques. *Clin Pharmacokinet*. (2018) 57:1603–11. doi: 10.1007/s40262-018-0657-2
14. Kuemmel C, Yang Y, Zhang X, Florian J, Zhu H, Tegenge M, et al. Consideration of a credibility assessment framework in model-informed drug development: potential application to physiologically-based pharmacokinetic modeling and simulation. *CPT Pharmacometrics Syst Pharmacol*. (2020) 9:21–8. doi: 10.1002/psp4.12479
15. Shepard T, Scott G, Cole S, Nordmark A, Bouzom F. Physiologically based models in regulatory submissions: output from the ABPI/MHRA Forum on physiologically based modeling and simulation. *CPT Pharmacometrics Syst Pharmacol*. (2015) 4:221–5. doi: 10.1002/psp4.30
16. Coppola P, Andersson A, Cole S. The importance of the human mass balance study in regulatory submissions. *CPT Pharmacometrics Syst Pharmacol*. (2019) 8:792–804. doi: 10.1002/psp4.12466
17. Amon I, Amon K, Franke G, Mohr C. Pharmacokinetics of metronidazole in pregnant women. *Chemotherapy*. (1981) 27:73–9. doi: 10.1159/000237958
18. Ryu RJ, Eyal S, Easterling TR, Caritis SN, Venkataraman R, Hankins G, et al. Pharmacokinetics of metoprolol during pregnancy and lactation. *J Clin Pharmacol*. (2016) 56:581–9. doi: 10.1002/jcph.631
19. Andrew MA, Easterling TR, Carr DB, Shen D, Buchanan ML, Rutherford T, et al. Amoxicillin pharmacokinetics in pregnant women: modeling and simulations of dosage strategies. *Clin Pharmacol Ther*. (2007) 81:547–56. doi: 10.1038/sj.clpt.6100126
20. US FDA. *The Use of Physiologically Based Pharmacokinetic Analyses —Biopharmaceutics applications for Oral Drug Product Development, Manufacturing Changes, and Controls Guidance for Industry* (Silver Spring, MD) (2020).

Disclaimer: The views expressed in this article are the personal views of the authors and may not be understood or quoted as being made on behalf of or reflecting the position of the regulatory agencies or other organizations with which the authors are affiliated.

Conflict of Interest: The authors are employees of the Medicines and Healthcare products Regulatory Agency, UK.

frontiers in Pharmacology

BRIEF RESEARCH REPORT
published: 20 July 2021
doi: 10.3389/fphar.2021.688597

Physiologically Based Pharmacokinetic Modelling for Nicotine and Cotinine Clearance in Pregnant Women

Basile Amice[1], *Harvey Ho*[2]*, *En Zhang*[3]* *and Chris Bullen*[4]

[1]ENSEEIHT, National Polytechnic Institute of Toulouse, Toulouse, France, [2]Auckland Bioengineering Institute, The University of Auckland, Auckland, New Zealand, [3]Chongqing Institute for Food and Drug Control, Chongqing, China, [4]National Institute for Health Innovation, The University of Auckland, Auckland, New Zealand

Introduction: Physiologically based pharmacokinetic (PBPK) models for the absorption, disposition, metabolism and excretion (ADME) of nicotine and its major metabolite cotinine in pregnant women (p-PBPK) are rare. The aim of this short research report is to present a p-PBPK model and its simulations for nicotine and cotinine clearance.

Methods: The maternal-placental-fetal compartments of the p-PBPK model contain a total of 16 compartments representing major maternal and fetal organs and tissue groups. Qualitative and quantitative data of nicotine and cotinine disposition and clearance have been incorporated into pharmacokinetic parameters.

Results: The p-PBPK model reproduced the higher clearance rates of nicotine and cotinine in pregnant women than non-pregnant women. Temporal profiles for their disposition in organs such as the brain were also simulated. Nicotine concentration reaches its maximum value within 2 min after an intravenous injection.

Conclusion: The proposed p-PBPK model produces results consistent with available data sources. Further pharmacokinetic experiments are required to calibrate clearance parameters for individual organs, and for the fetus.

Keywords: nicotine, cotinine, pregnant women, fetus, PBPK

OPEN ACCESS

Edited by:
André Dallmann, Bayer, Germany

Reviewed by:
Ashwin Karanam, Pfizer, United States
Benjamin Dupont, PhinC Development, France

***Correspondence:**
Harvey Ho
harvey.ho@auckland.ac.nz
En Zhang
Zhangen@cqifdc.org.cn

Specialty section:
This article was submitted to Obstetric and Pediatric Pharmacology, a section of the journal Frontiers in Pharmacology

Received: *31 March 2021*
Accepted: *08 July 2021*
Published: *20 July 2021*

Citation:
Amice B, Ho H, Zhang E and Bullen C (2021) Physiologically Based Pharmacokinetic Modelling for Nicotine and Cotinine Clearance in Pregnant Women. Front. Pharmacol. 12:688597. doi: 10.3389/fphar.2021.688597

INTRODUCTION

Cigarette smoking during pregnancy is associated with many adverse effects, including increased spontaneous abortion, a higher premature delivery rate and lower birth weight (Lambers and Clark, 1996). Clinical and experimental studies on the absorption, disposition, metabolism and excretion (ADME) of nicotine and its major metabolism product, cotinine, in pregnant women have provided important insights (Benowitz and Dempsey, 2004),' such as the significantly higher nicotine and cotinine clearance during pregnancy than post-partum and at different gestation stages (Benowitz and Dempsey, 2004; Dempsey et al., 2002; Taghavi et al., 2018; Benowitz et al., 2006). Possible explanations for this phenomenon include pregnancy-induced metabolism activities for C-oxidation *via* the CYP2A6 and for G-glucuronidation *via* UGT2B10 (Taghavi et al., 2018). Physiological changes during pregnancy may also pay a role, such as the substantially increased renal flow (30–50% higher) and resultant higher renal clearance (Morgan, 1997). To date, however, these findings have

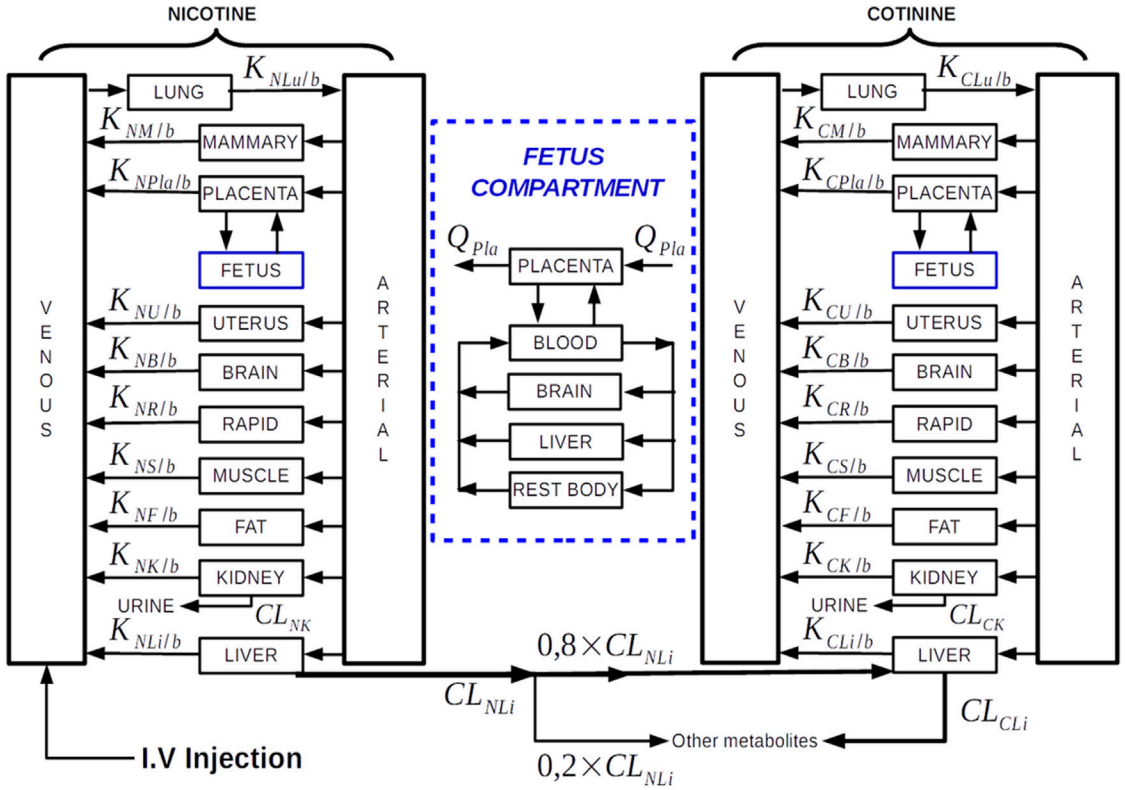

FIGURE 1 | Diagram of the P-PBPK model structure with intravenous nicotine injection as the intake route. The underlying differential equations and parameters are provided in **Supplementary Material**. Details of the fetus PBPK model are shown inside the blue compartment. Note, the "Rapid" compartment in the diagram corresponding to "Vessel-rich Group" compartment in the PBPK model of Robinson et al. (1992).

not been incorporated into physiologically based pharmacokinetic (PBPK) models for pregnancy (p-PBPK), and specifically for nicotine and cotinine clearance during pregnancy.

PBPK is a mathematical modelling technique for predicting the ADME of drugs in humans. An early PBPK model developed for adult men, not pregnant women, used data from intravenous nicotine infusion experiments to find pharmacokinetic parameters (Robinson et al., 1992). Recent PBPK models for nicotine were also reported, e.g., by Kovar et al. (2020) to simulate nicotine brain tissue concentrations after the use of combustible cigarettes, e-cigarettes, nicotine gums, and nicotine patches, and by Saylor and Zhang (2016) where antibody affinity to nicotine was considered in a PBPK model for nicotine disposition in the brains of rats and humans. Specific to p-PBPK model, Gaohua et al. (2012) used it to investigate the PK profiles of three compounds (caffeine, metoprolol and midazolam) in response to the gestational related activities of three cytochrome P450 enzymes. George et al. (2020) used another p-PBPK model to investigate the dosing adjustment of an antidepressant (sertraline) during pregnancy.

In this study, we take advantage of a generic p-PBPK template (Gentry et al., 2003), where nicotine was used as a representative compound for water soluble, semi-volatile chemicals. However, the model did not provide clearance profiles after nicotine administration but rather changes at different gestation stages. The aim of the current work was to combine the two models, i.e. by Robinson et al. (1992) and Gentry et al. (2003), and to incorporate some recently published data.

METHODS

Integrated PBPK Model for Nicotine/Cotinine

We adopted and customised an adult PBPK model consisting of nine compartments for cotinine (COT) and ten for nicotine (NIC), representing key organs and tissues in humans, i.e., the arterial and venous blood, the brain, liver, lung, kidney, rapid (vessel-rich tissues), muscle and fat groups (Robinson et al., 1992) (**Figure 1**). The NIC and COT models are connected from the liver compartment, representing the biotransformation from nicotine to cotinine *via* CYP2A6 (approximately 80% of nicotine is metabolized into cotinine) (Benowitz et al., 2009). In this way the time course of nicotine and cotinine concentrations can be simulated simultaneously. Furthermore, we added an extra brain compartment to simulate the quick uptake of nicotine in the brain (10–20 s after cigarette smoking) (Benowitz et al., 2009).

A significant difference between our PBPK model and the model of (Robinson et al., 1992) is the updated renal and hepatic

TABLE 1 | Nicotine and cotinine hepatic and renal clearance parameters used in the model.

	Parameter for men Curvall et al. (1990), [a]	Parameters for women Dempsey et al. (2002), [b]	Parameters for pregnant women, estimated from Dempsey et al. (2002), Taghavi et al. (2018), [b]
Nicotine hepatic clearance	277.14	16.2	26.6
Nicotine renal clearance	0.6198	0.7	0.3
Cotinine hepatic clearance	6.3635	0.5	1.2
Cotinine renal clearance	0.0248	0.2	0.3

[a]*Unit: ml/h/kg.*
[b]*Unit: ml/min/kg.*

clearance rates since women have a higher nicotine/cotinine clearance (Dempsey et al., 2002) (Curvall et al., 1990). The parameters for NIC/COT hepatic and renal clearance, including those estimated for pregnant women, are shown in **Table 1**.

In addition to the hepatic and renal clearance changes, the clearance rate in the muscle compartment is also updated so that the nicotine concentration in muscle is similar to that in the plasma (Benowitz et al., 2009).

P-PBPK Model Construction

The p-PBPK model has been constructed with extra compartments: the mammary, uterus, placenta and fetus compartments (**Figure 1**). We adopted the p-PBPK template which has a similar NIC-COT compartmental structure to (Gentry et al., 2003). We also used some physiological parameters in this template, as documented in the **Supplementary Material**. In the fetus compartment, in addition to the blood, liver and rest of the body compartments, a brain compartment is added to investigate the nicotine distribution to the fetal brain. Concerning the methods of nicotine administration, three pathways have been implemented including intravenous injection, cigarette smoking and oral dosing.

New clearance rates have been estimated to simulate the accelerated clearance rates for nicotine and cotinine in pregnant women, which are about 60 and 140% higher respectively than non-pregnant women (Dempsey et al., 2002; Taghavi et al., 2018). Corresponding changes to the hepatic and cotinine renal clearances are shown in **Table 1**.

In the p-PBPK model of Gentry et al. (2003), the transfer of drugs across the placenta barrier is modelled in a diffusion-limited equation. However, since the fetal nicotine level is 15% higher than the maternal side, yet the fetal cotinine level is lower than the maternal level (Lambers and Clark, 1996), an influx-efflux model is used to simulate the nicotine/cotinine transfer in the placenta. Different stages of gestation are also incorporated through adjustments of organ/tissue volumes, blood flow supply based on the generic equations (Abduljalil et al., 2012; Brown et al., 1997).

Parameters of the p-PBPK Model

Overall, our model consists of two sets of parameters. The first set of parameters describe the physiological properties in each compartment including the volume, blood flow rate; while the second set of parameters define drug-specific parameters including tissue-to-blood partition coefficients, metabolic and clearance rates. The second set, i.e. nicotine/cotinine related parameters including their respective data sources are provided in **Table 1**. The first set i.e., physiological parameters are provide in the **Supplementary Material**.

There are total 32 differential equations for the p-PBPK model shown in **Figure 1**. The equations are not listed here but provided in the **Supplementary Material** for interested reader's reference. The program was implemented in Matlab, with ODE45 as the differential equation solver. To run the programme, the gestation stage (in months) and body weight (in kg) need to be provided. In this work we used gestation week 30 and body weight 73 kg as the parameters, which can be altered by the user. Furthermore, the body weight is related to the gestation week, which has also been implemented in our model (Sharma et al., 2018).

Validation of the Model

Published plasma NIC/COT concentration data that was used to validate the PBPK model in (Robinson et al., 1992), were employed to validate the non-pregnant woman model. Specifically, the plasma levels of cotinine for four non-smoking subjects after cotinine infusion (0.67 mg/min for 30 min), as reported by De Schepper et al. (1987), and the plasma NIC/COT concentration after nicotine infusion (10 μg/min for 60 min) in six non-smoking subject, as reported by (Curvall et al., 1990), were used to compare with our model simulations.

The studies on plasma NIC/COT levels in pregnant women are very rare. However, there are reports that describe qualitatively some pharmacokinetic features of NIC/COT in pregnant women. For instance (Lambers and Clark, 1986), pointed out that the nicotine level in plasma at the fetal side was about 15% higher than that at the maternal side. These data have been used indirectly in our model for parameter optimisation.

RESULTS

Baseline PBPK Model

At first, we calibrated the adult PBPK model with published nicotine/cotinine PBPK model for man (Robinson et al., 1992),

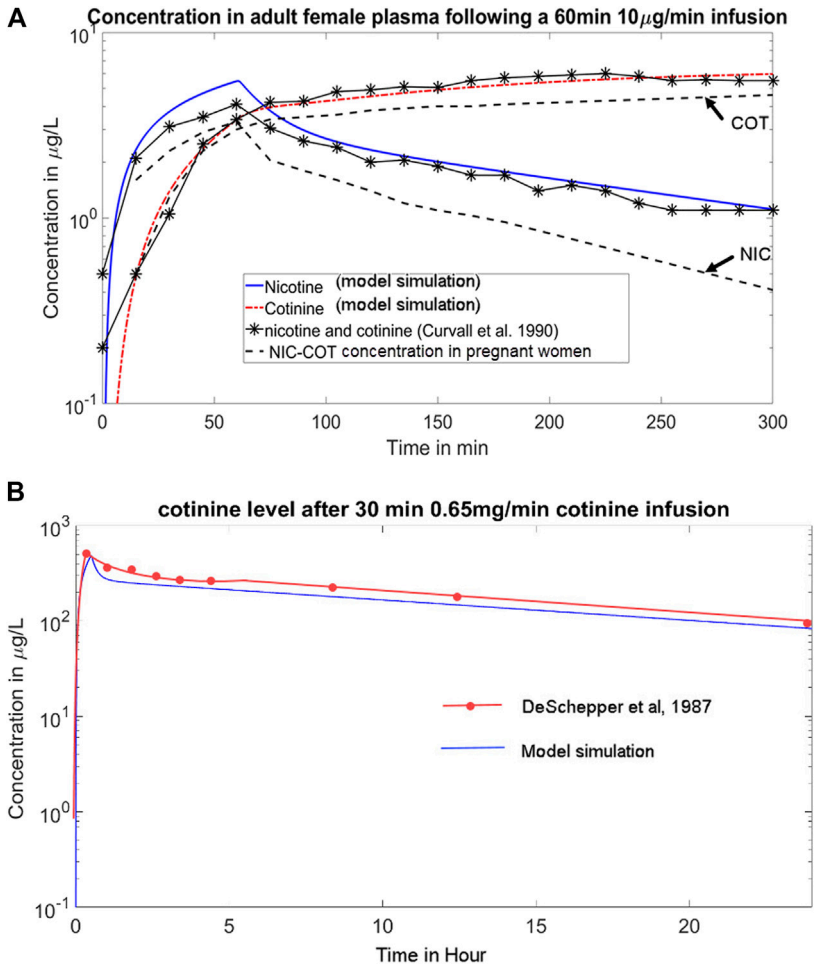

FIGURE 2 | (A) Simulations of the time course of the plasma concentrations of NIC/COT following a 60 min 10 μg/min intravenous infusion of nicotine, per data from Curvall et al. (1990). The blue solid line and red dotted line represent the NIC-COT concentration in adult men, matching experimental data (solid lines with asterisks), which the dashed lines represent plasma concentration of NIC-COT in pregnant women showing higher clearance rates; **(B)** Simulation of the cotinine level after 30 min of 0.65 mg/min continine infusion, per data from De Schepper et al. (1987). The blue line represents model simulation.

which may be used as a proxy for non-pregnant women. The simulations in (Robinson et al., 1992) contain several dose and infusion scenarios, which we chose two regimens to investigate: 1) intravenous nicotine infusion of 10 μg/min for 60 min (Curvall et al., 1990); and 2) intravenous infusion of cotinine of 0.67 mg/min for 30 min (De Schepper et al., 1987). The body weight of the adult women was set as 70 kg, following the adult body weight configuration in (Robinson et al., 1992). **Figure 2** shows the time course of nicotine and cotinine over 5 h. The plasma nicotine concentration reaches the peak value after about 1 h, and then gradually decreases. Its half-life (~3 h) is much shorter than that of cotinine (~16 h), in accordance with the half-life data reported in literature (2 h for nicotine vs. 16.6 h for cotinine) (Dempsey et al., 2002).

The time course of the concentration of nicotine and cotinine in plasma (blue and red lines respectively) resulting from our model match closely (within 5% of deviation) with the pharmacokinetic data reported by Curvall et al. (1990). In addition, the literature reported 22 ± 7.2 μg of unchanged nicotine and 16.1 ± 3.8 μg of cotinine in urine 5 h after the infusion (Curvall et al., 1990), while our model predicted 28.8 μg of nicotine and 15.3 μg of cotinine in urine, consistent with the literature.

p-PBPK Model

The evolvement of nicotine and cotinine centration profiles in pregnant women was simulated. The gestation stage was set as week 30, and the body weight of pregnant woman as 73 kg. At this stage of fetal development the fetal liver has limited nicotine and cotinine metabolism and clearance capacity (Benowitz et al., 2009). Since data related to fetal clearance was not available, assumptions were made that the fetal clearance efficiency was only 20% of maternal hepatic clearance for both nicotine and cotinine. With these assumptions, the plasma nicotine and cotinine profiles are shown as dashed lines in **Figure 1**. As can be seen, the nicotine and cotinine concentrations in the pregnant women model are lower than the adult non-pregnant woman model, reflecting higher clearance rates. This is more

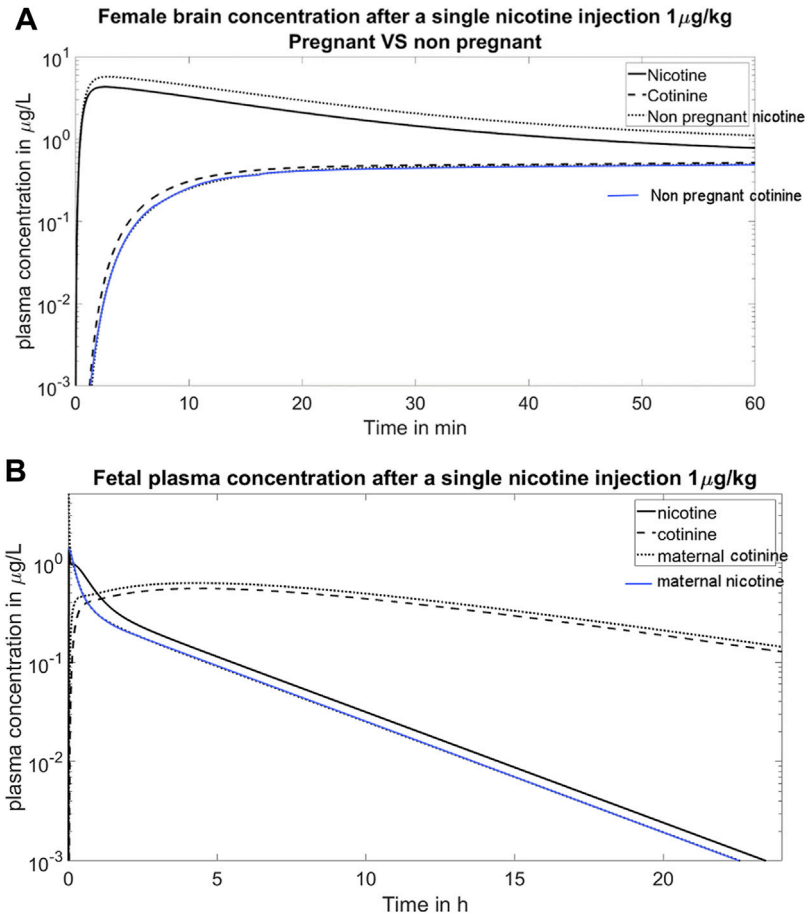

FIGURE 3 | (A) Simulation of the time course of the concentration of nicotine and cotinine in the maternal brain. The nicotine enters brain quickly and reaches its peak value within 2 min. This figure also shows the higher clearance of nicotine in pregnant women than in non-pregnant women; **(B)** Simulation of fetal plasma concentration after a single nicotine injection 1 μg/kg. The simulation reproduces the clinical observation that the fetal nicotine level is higher than the maternal nicotine level, yet the fetal cotinine level is lower than the maternal level (Lambers and Clark, 1996).

pronounced in nicotine (~70% lower) than in cotinine (~30% lower) at 150 min.

After a puff of cigarette smoking, the nicotine concentration in the brain increases rapidly (Benowitz and Dempsey, 2004). This fast entrance phenomenon also occurs with intravenous injection, as shown in the simulation of **Figure 3**, where the nicotine concentration in the brain reaches its maximum value within 2 min. Also shown in **Figure 3** is the higher nicotine clearance in the brain during pregnancy, as the concentration profile of nicotine is lower in pregnant women than non-pregnant women.

DISCUSSION

Approximately 14% of United States women continue to smoke after becoming pregnant (Taghavi et al., 2018), and an estimated 32% of women who are Māori (the indigenous people of New Zealand) smoke during pregnancy (Humphrey et al., 2016). Nicotine replacement therapy (NRT) has been used for smoking cessation assistance during pregnancy in the forms of nicotine gums, transdermal administration and patches (Benowitz and Dempsey, 2004). Still, the pharmacokinetic profiles of nicotine in individual organs of pregnant women, in particular in fetus, remain poorly understood. Most experiments provide measurement data from plasma or urine samples as it is difficult to obtain tissue measurements *in vivo*. This is even more the case when drug clearance in fetus needs to be investigated, as blood samples are taken from the umbilical vein/artery only at the time of delivery. The motivation of the work was to develop an *in silico* p-PBPK model for the prediction of nicotine and cotinine clearance, and to provide an initial computational platform for incorporating new data and/or for evaluating new hypotheses. Another motivation of the model was to incorporate the simulation results into graphic animations for educational purposes. A science-based, visual tool could aid public health workers to explain the pharmacokinetics of nicotine/cotinine in a more understandable manner.

The current model combines two previous PBPK models with an updated set of nicotine and cotinine specific parameters to reflect our

updated knowledge of their clearance in pregnant women (Dempsey et al., 2002; Taghavi et al., 2018). Only a subset of results are presented in this short report due to scarcity of *in vivo* or *in vitro* data to compare with. However, we found that the partition coefficients in the fetal model and its clearance did not have great impacts on the maternal model. Rather, the physiological changes over different gestation stages could exert significant influence on the nicotine clearance. Another important finding was that placental absorption/clearance plays an important role in mediating the overall nicotine/cotinine kinetics in fetus. This effect was previously simplified as a first order diffusion effects (Gentry et al., 2003), which was not sufficient to explain the transportation of nicotine and cotinine across the placenta barrier. For example, to transport cotinine from the fetus to the mother, where the cotinine level is higher, a more sophisticated model than the passive diffusion model is required.

It should be stressed that even though the current p-PBPK model, with a non-trivial set of 32 differential equations, is still highly simplified due to the complexity of drug disposition and clearance in the maternal-placental-fetal compartments. For example, the hepatic and renal clearance parameters for nicotine are gestational age dependent, which in the current model are fixed (corresponding to gestational week 30). Likewise are the partition coefficients, or unbound fractions, which may alter during different stages of gestation. Further investigation into individual nicotine metabolism pathways *via* CYPs and UGTs would require a novel model involving nonlinear metabolism kinetic terms. Such a model should be tested for the liver compartment at first for optimal parameters, before applying it to a larger PBPK model. We refer the interested reader to such an individual enzyme-oriented metabolism model of acetaminophen for reference (Means and Ho, 2019).

It worth noting that the placental barrier plays an important role in the drug transfer between maternal and fetal circulations. While our p-PBPK model has additional influx-efflux terms for the placenta compartment, it is not sufficient to describe the complex transport mechanism of nicotine/cotinine in placenta. Specifically, various transporters play a critical role in the apical and basolateral membrane of trophoblasts, where their mediation kinetics warrants a separate study. We refer the interested reader for an excellent review on this topic by Dallmann et al. (2019).

In this report we only presented simulation results where nicotine intake was *via* intravenous infusion, because the hour-based PK data for verifying simulation results were available (Curvall et al., 1990) (De Schepper et al., 1987). However, it should be noted that the most common route for nicotine intake is *via* smoking, and the oral intake e.g., by chewing nicotine gums is the most common for NRT (Oncken et al., 1996). However, since serum cotinine data were taken after days' of gum use (Oncken et al., 1996), they cannot be used to verify hour-based PK profile simulations.

Due to the difficulty of obtaining data in humans, an extension of the current model is to adapt it to animals, and to compare the results with published data from animal models (Craig et al., 2014). Still, due to the significant differences of nicotine metabolism between different species (Hukkanen et al., 2005), cautions must be taken to extrapolate the model between species.

Concerning application of the p-PBPK framework to other drugs, physiological aspect of the model, i.e., blood flow/volume to individual organs/tissues may still be applicable, or with only minor adjustments required. However, drug-specific parameters, such as the hepatic/renal clearance, the drug's volume of distribution and partition coefficient, must be re-instilled. Moreover, efforts should be made to obtain first-hand pharmacokinetic data where the elimination kinetics are independently informed.

Another extension of the work would be to apply the model to population pharmacokinetics analysis. Several approaches could be employed towards that direction. For example, a Latin Hypercube Sampling analysis could be performed where model parameters are perturbed around their nominal values simultaneously (Zhang et al., 2020). By observing the statistical distribution of pharmacokinetic profiles of NIC/COT in a population, we could determine the influence of a parameter on system dynamics i.e., the sensitivity of a model versus its parameters.

In summary, there are many future extension possibilities, such as longitudinal studies, enzyme activities, hepatic/renal clearance changes, could be incorporated into the current prototype model. While adding these many features would be interesting, adding these features in the model demands multidisciplinary collaborations on data collection, physiological interpretation, and model refining.

CONCLUSION

A p-PBPK model has been developed for nicotine and cotinine disposition and clearance. The model has reproduced some key features of ADME in pregnant women. More data are required to calibrate the parameters in the model.

DATA AVAILABILITY STATEMENT

The datasets presented in this study can be found in online repositories. The names of the repository/repositories and accession number(s) can be found in the article/**Supplementary Material**.

AUTHOR CONTRIBUTIONS

HH and CB: Designed the project. BA: Performed the programming. EZ: Provided pharmacological context of the drugs and insights HH and BA: Wrote the paper.

FUNDING

HH acknowledges the financial support from the Li Ka Shing Foundation. EZ acknowledges the financial support from the Ministry of Science and Technology of China (2017ZX09101001).

SUPPLEMENTARY MATERIAL

The Supplementary Material for this article can be found online at: https://www.frontiersin.org/articles/10.3389/fphar.2021.688597/full#supplementary-material

REFERENCES

Abduljalil, K., Furness, P., Johnson, T. N., Rostami-Hodjegan, A., and Soltani, H. (2012). Anatomical, Physiological and Metabolic Changes with Gestational Age during Normal Pregnancy. *Clin. Pharmacokinet.* 51, 365–396. doi:10.2165/11597440-000000000-00000

Benowitz, N., and Dempsey, D. (2004). Pharmacotherapy for Smoking Cessation during Pregnancy. *Nicotine Tob. Res.* 6, 189–202. doi:10.1080/14622200410001669169

Benowitz, N., Lessovschlaggar, C., Swan, G., and Jacobiii, P. (2006). Female Sex and Oral Contraceptive Use Accelerate Nicotine Metabolism. *Clin. Pharmacol. Ther.* 79, 480–488. doi:10.1016/j.clpt.2006.01.008

Benowitz, N. L., Hukkanen, J., and Jacob, P. (2009). "Nicotine Chemistry, Metabolism, Kinetics and Biomarkers," in *In Nicotine Psychopharmacology Handbook of Experimental Pharmacology* (Berlin, Heidelberg: Springer), 29–60. doi:10.1007/978-3-540-69248-5_2

Brown, R. P., Delp, M. D., Lindstedt, S. L., Rhomberg, L. R., and Beliles, R. P. (1997). Physiological Parameter Values for Physiologically Based Pharmacokinetic Models. *Toxicol. Ind. Health* 13, 407–484. doi:10.1177/074823379701300401

Craig, E. L., Zhao, B., Cui, J. Z., Novalen, M., Miksys, S., and Tyndale, R. F. (2014). Nicotine Pharmacokinetics in Rats Is Altered as a Function of Age, Impacting the Interpretation of Animal Model Data. *Drug Metab. Dispos* 42, 1447–1455. doi:10.1124/dmd.114.058719

Curvall, M., Elwin, C.-E., Kazemi-Vala, E., Warholm, C., and Enzell, C. R. (1990). The Pharmacokinetics of Cotinine in Plasma and Saliva from Non-smoking Healthy Volunteers. *Eur. J. Clin. Pharmacol.* 38, 281–287. doi:10.1007/BF00315031

Dallmann, A., Liu, X. I., Burckart, G. J., and den Anker, J. (2019). Drug Transporters Expressed in the Human Placenta and Models for Studying Maternal-Fetal Drug Transfer. *J. Clin. Pharmacol.* 59, S70–S81. doi:10.1002/jcph.1491

De Schepper, P. J., Van Hecken, A., Daenens, P., and Van Rossum, J. M. (1987). Kinetics of Cotinine after Oral and Intravenous Administration to Man. *Eur. J. Clin. Pharmacol.* 31 (5), 583–588. doi:10.1007/bf00606635

Dempsey, D., Jacob, P., and Benowitz, N. L. (2002). Accelerated Metabolism of Nicotine and Cotinine in Pregnant Smokers. *J. Pharmacol. Exp. Ther.* 301, 594–598. doi:10.1124/jpet.301.2.594

Gaohua, L., Abduljalil, K., Jamei, M., Johnson, T. N., and Rostami-Hodjegan, A. (2012). A Pregnancy Physiologically Based Pharmacokinetic (P-PBPK) Model for Disposition of Drugs Metabolized by CYP1A2, CYP2D6 and CYP3A4. *Br. J. Clin. Pharmacol.* 74 (5), 873–885. doi:10.1111/j.1365-2125.2012.04363.x

Gentry, P. R., Covington, T. R., and Clewell, H. J. (2003). Evaluation of the Potential Impact of Pharmacokinetic Differences on Tissue Dosimetry in Offspring during Pregnancy and Lactation. *Regul. Toxicol. Pharmacol.* 38, 1–16. doi:10.1016/S0273-2300(03)00047-3

George, B., Lumen, A., Nguyen, C., Wesley, B., Wang, J., Beitz, J., et al. (2020). Application of Physiologically Based Pharmacokinetic Modeling for Sertraline Dosing Recommendations in Pregnancy. *NPJ Syst. Biol. Appl.* 6 (1), 1–9. doi:10.1038/s41540-020-00157-3

Hukkanen, J., Jacob, P., and Benowitz, N. L. (2005). Metabolism and Disposition Kinetics of Nicotine. *Pharmacol. Rev.* 57, 79–115. doi:10.1124/pr.57.1.3

Humphrey, G., Rossen, F., Walker, N., and Bullen, C. (2016). Parental Smoking during Pregnancy: Findings from the Growing up in New Zealand Cohort. *N. Z. Med. J.* 129, 60–74.

Kovar, L., Selzer, D., Britz, H., Benowitz, N., St. Helen, G., Kohl, Y., et al. (2020). Comprehensive Parent-Metabolite PBPK/PD Modeling Insights into Nicotine Replacement Therapy Strategies. *Clin. Pharmacokinet.* 59 (9), 1119–1134. doi:10.1007/s40262-020-00880-4

Lambers, D. S., and Clark, K. E. (1996). The Maternal and Fetal Physiologic Effects of Nicotine. *Semin. Perinatology* 20, 115–126. doi:10.1016/S0146-0005(96)80079-6

Means, S. A., and Ho, H. (2019). A Spatial-Temporal Model for Zonal Hepatotoxicity of Acetaminophen. *Drug Metab. Pharmacokinet.* 34 (1), 71–77. doi:10.1016/j.dmpk.2018.09.266

Morgan, D. J. (1997). Drug Disposition in Mother and Foetus. *Clin. Exp. Pharmacol. Physiol.* 24, 869–873. doi:10.1111/j.1440-1681.1997.tb02707.x

Oncken, C. A., Hatsukami, D. K., Lupo, V. R., Lando, H. A., Gibeau, L. M., and Hansen, R. J. (1996). Effects of Short-Term Use of Nicotine Gum in Pregnant Smokers*. *Clin. Pharmacol. Ther.* 59 (6), 654–661. doi:10.1016/s0009-9236(96)90005-3

Robinson, D. E., Balter, N. J., and Schwartz, S. L. (1992). A Physiologically Based Pharmacokinetic Model for Nicotine and Cotinine in Man. *J. Pharmacokinet. Biopharmaceutics* 20, 591–609. doi:10.1007/BF01064421

Saylor, K., and Zhang, C. (2016). A Simple Physiologically Based Pharmacokinetic Model Evaluating the Effect of Anti-nicotine Antibodies on Nicotine Disposition in the Brains of Rats and Humans. *Toxicol. Appl. Pharmacol.* 307, 150–164. doi:10.1016/j.taap.2016.07.017

Sharma, R. P., Schuhmacher, M., and Kumar, V. (2018). The Development of a Pregnancy PBPK Model for Bisphenol A and its Evaluation with the Available Biomonitoring Data. *Sci. total Environ.* 624, 55–68. doi:10.1016/j.scitotenv.2017.12.023

Taghavi, T., Arger, C. A., Heil, S. H., Higgins, S. T., and Tyndale, R. F. (2018). Longitudinal Influence of Pregnancy on Nicotine Metabolic Pathways. *J. Pharmacol. Exp. Ther.* 364, 238–245. doi:10.1124/jpet.117.245126

Zhang, S., Zhang, E., and Ho, H. (2020). Extrapolation for a Pharmacokinetic Model for Acetaminophen from Adults to Neonates: A Latin Hypercube Sampling Analysis. *Drug Metab. Pharmacokinet.* 35 (3), 329–333. doi:10.1016/j.dmpk.2020.03.004

Conflict of Interest: The authors declare that the research was conducted in the absence of any commercial or financial relationships that could be construed as a potential conflict of interest.

frontiers in Pediatrics

POLICY AND PRACTICE REVIEWS
published: 26 July 2021
doi: 10.3389/fped.2021.698611

Regulatory Considerations for the Mother, Fetus and Neonate in Fetal Pharmacology Modeling

Dionna J. Green[1], *Kyunghun Park*[2], *Varsha Bhatt-Mehta*[2], *Donna Snyder*[1] *and Gilbert J. Burckart*[2]*

[1] Office of Pediatric Therapeutics, Office of the Commissioner, US Food and Drug Administration, Silver Spring, MD, United States, [2] Office of Clinical Pharmacology, Center for Drug Evaluation and Research, US Food and Drug Administration, Silver Spring, MD, United States

The regulatory framework for considering the fetal effects of new drugs is limited. This is partially due to the fact that pediatric regulations (21 CFR subpart D) do not apply to the fetus, and only US Health and Human Service (HHS) regulations apply to the fetus. The HHS regulation 45 CFR Part 46 Subpart B limits research approvable by an institutional review board to research where the risk to the fetus is minimal unless the research holds out the prospect of a direct benefit to the fetus or the pregnant woman (45 CFR 46.204). Research that does not meet these requirements, but presents an opportunity to understand, prevent, or alleviate a serious problem affecting the health of pregnant women, fetuses, or neonates, may be permitted by the Secretary of the HHS after expert panel consultation and opportunity for public review and comment (45 CFR 46.407). If the product is regulated by the US Food and Drug Administration (FDA), FDA may get involved in the review process. The FDA does however have a Reviewer Guidance on Evaluating the Risks of Drug Exposure in Human Pregnancies from 2005 and this guidance does discuss the intensity of drug exposure. Estimation of that exposure using physiologically based pharmacokinetic (PBPK) modeling has been suggested by some investigators. Given that drug exposure during pregnancy will impact the fetus, a number of new guidances in the last 2 years also address inclusion of pregnant women in clinical drug trials. Therefore, the drug-specific information on fetal pharmacology will increase dramatically in the next decade due to interest in drugs administered in pregnancy and with the assistance of model-informed drug development.

Keywords: drug development, fetal, regulatory, pediatrics, Food and Drug Administration, model-informed drug development

OPEN ACCESS

Edited by:
Wei Zhao,
Shandong University, China

Reviewed by:
Andrea N. Edginton,
University of Waterloo, Canada
Tamorah Rae Lewis,
Children's Mercy Hospital,
United States

***Correspondence:**
Gilbert J. Burckart
gilbert.burckart@fda.hhs.gov

Specialty section:
This article was submitted to Obstetric and Pediatric Pharmacology, a section of the journal Frontiers in Pediatrics

Received: *21 April 2021*
Accepted: *28 June 2021*
Published: *26 July 2021*

Citation:
Green DJ, Park K, Bhatt-Mehta V, Snyder D and Burckart GJ (2021) Regulatory Considerations for the Mother, Fetus and Neonate in Fetal Pharmacology Modeling. Front. Pediatr. 9:698611. doi: 10.3389/fped.2021.698611

INTRODUCTION

In his 1966 treatise on perinatal pharmacology, Sumner Yaffe stated that "The administration of a drug to a pregnant woman presents a unique problem to the physician; not only must he consider maternal pharmacologic mechanisms, but he must also be aware of the fetus as a potential recipient of the drug" (1). This dilemma is still a problem today; how can we assess the effects of a drug administered to the mother on the fetus? For 50 years after Yaffe's publication, researchers and regulators had few options to address this question.

A more recent review of obstetric and fetal pharmacology is available (2), and has led to the development of Obstetric-Fetal Pharmacology Research Centers sponsored by the National

Institutes of Health (3). Today we are presented with a unique method of performing a pharmacologic assessment on the fetus without the risk of direct blood sampling. This unique method uses sophisticated modeling, which is being increasingly used in drug development. The critical reasons for this assessment are multiple.

While the teratogenic effects of drugs administered to the mother on the fetus have had a central role in safety assessment since the time of thalidomide, questions are increasingly being ask about the long-term effects of perinatal drug exposure. The potential for this serious consequence of perinatal drug exposure was not lost on Sumner Yaffe 50 years ago. Yaffe and colleagues studied the long-term effects of phenobarbital exposure in the perinatal period on sex hormones in rats, and found that phenobarbital perinatal exposure affected adult rat testosterone levels (4). This research continues today as pharmacoepidemiology studies examine these associations, such as for the maternal use of antidepressants with autism spectrum disorders in children (5). This type of research and its findings are complicated by the exclusion of pregnant women from drug development studies, and the off-label use of drugs in pregnancy (6). Additionally, such post-marketing pharmacoepidemiologic studies require a long time to gain such knowledge. Associations between in-utero drug exposure and long-term outcomes may be able to be addressed by modeling approaches.

Modeling will also assist the development of fetal therapeutics. Knowledge gained from classical approaches of administering medications to the mother intended to benefit the fetus, such as in the treatment of fetal arrhythmias, in conjunction with modeling approaches can be used to advance the science of fetal therapeutics. The antenatal administration of drugs such as corticosteroids to the mother at risk of preterm birth to accelerate fetal lung maturation and prevent neonatal disorders results in highly variable outcomes, and modeling and systems pharmacology may be able to provide consistency to this process. Finally gene and stem cell therapy for the fetus will depend on a high degree of understanding of fetal pharmacology and dosing (7).

These modeling efforts for the fetus can be facilitated by regulatory science and regulatory approaches to requiring and assessing the information generated during drug development. Therefore, the objective of this presentation is to review the ethical and guidance-related regulations and recommendations that affect drug therapy in pregnant women and their fetuses. These current regulations will undoubtedly influence the use of modeling to advance the care of these women and babies.

HHS REGULATIONS ON RESEARCH IN MOTHER, FETUS, AND NEONATE

Regulations to protect individuals in research supported or conducted by the Department of Health and Human Services (HHS) evolved from a series of reports released by the National Commission for the Protection of Human Subjects of Biomedical and Behavioral Research (8) in the 1970s. The Belmont Report (9) or the "Ethical Principles and Guidelines for the Protection of Human Subjects of Research," the most prominent document issued by National Commission, informed regulations found under 45 CFR 46, subpart A (10), otherwise known as the Basic Policy for Protection of Human Research Subjects as subpart A has been adopted by some federal agencies and is known as the Common Rule. HHS regulations also include three other subparts that are intended to protect specific populations that might be involved in research, including the vulnerable populations of prisoners (subpart C) and children (subpart D) (11). Subpart B, the "Additional Protections for Pregnant Women, Human Fetuses and Neonates (12), is pertinent to the topic of this manuscript.

With the adoption of the New Common Rule in 2018, pregnant women are no longer considered as a vulnerable population under 45 CFR 46.111 (a) (3); nonetheless, the considerations under 45 CFR 46.204 of subpart B (12) still apply. Pregnant women may be included in research approvable by an Institutional Review Board (IRB) only if:

(a) "Where scientifically appropriate, preclinical studies on pregnant animals, and clinical studies, including studies on non pregnant women, have been conducted and provide data for assessing potential risks to pregnant women and fetuses;
(b) The risk to the fetus is caused solely by interventions or procedures that hold out the prospect of direct benefit for the woman or the fetus; or, if there is no such prospect of benefit, the risk to the fetus is not greater than minimal and the purpose of the research is the development of important biomedical knowledge which cannot be obtained by any other means;
(c) Any risk is the least possible for achieving the objectives of the research;
(d) If the research holds out the prospect of direct benefit to the pregnant woman, the prospect of a direct benefit both to the pregnant woman and the fetus, or no prospect of benefit for the woman nor the fetus when risk to the fetus is not greater than minimal and the purpose of the research is the development of important biomedical knowledge that cannot be obtained by any other means, her consent is obtained in accord with the informed consent provisions of subpart A of this part;
(e) If the research holds out the prospect of direct benefit solely to the fetus then the consent of the pregnant woman and the father is obtained in accord with the informed consent provisions of subpart A of this part, except that the father's consent need not be obtained if he is unable to consent because of unavailability, incompetence, or temporary incapacity or the pregnancy resulted from rape or incest;
(f) Each individual providing consent under paragraph (d) or (e) of this section is fully informed regarding the reasonably foreseeable impact of the research on the fetus or neonate;
(g) For children as defined in § 46.402 (a) who are pregnant, assent and permission are obtained in accord with the provisions of subpart D of this part;
(h) No inducements, monetary or otherwise, will be offered to terminate a pregnancy;

TABLE 1 | Summary of FDA guidances for the mother, fetus and neonate.

Guidance title	Month, Year	Key contents	Reference [this text]
Guidance for Industry: Pregnant Women: Scientific and Ethical Considerations for Inclusion in Clinical Trials	April, 2018	• General scientific and ethical considerations to encourage the inclusion of pregnant women in clinical trials when appropriate. • Evaluation of drugs in clinical trials for conditions to treat medical conditions or acute illnesses that are common in women of reproductive potential.	(14)
Reviewer Guidance: Evaluating the Risks of Drug Exposure in Human Pregnancies	April, 2005	• Guidance to reviewers for evaluation of human fetal outcome data generated after medical product exposure during pregnancy. • Critical factors to consider when evaluating the effects of drug exposure in human pregnancies, sources of human data on drug exposures, methods for overall assessment of post-marketing human data and labeling.	(15)
Guidance for Industry: General Clinical Pharmacology Considerations for Neonatal Studies for Drugs and Biological Products	July, 2019	• Clinical pharmacology considerations specific to the newborn and emphasizes the need for input from a multidisciplinary team when planning for studies enrolling neonates.	(16)
Guidance for Industry: Post-approval Pregnancy Safety Studies	May, 2019	• Recommendations on how to design investigations to assess the outcomes of pregnancies in women exposed to drugs and biological products.	(17)
Guidance for Industry: Nonclinical Safety Evaluation of the Immunotoxic Potential of Drugs and Biologics	February, 2020	• Immunomodulating potential of drugs and biologicals, and use of ICH guidances	(18)
Guidance for Industry: Safety Testing of Drug Metabolites	March 2020	• Recommended studies for assessing the safety of metabolites such as: general toxicity studies, genotoxicity studies, carcinogenicity studies, and embryo-fetal development toxicity studies.	(19)
Guidance for Industry: Pregnancy, Lactation, and Reproductive Potential: Labeling for Human Prescription Drug and Biological Products — Content and Format	July, 2020	• Recommendations on complying with the Pregnancy and Lactation Labeling Rule (PLLR) to assist with the content and format requirements for 8.1, 8.2, and 8.3 of the USE IN SPECIFIC POPULATIONS subsections.	(20)

(i) Individuals engaged in the research will have no part in any decisions as to the timing, method, or procedures used to terminate a pregnancy; and
(j) Individuals engaged in the research will have no part in determining the viability of a neonate."

If an IRB cannot approve the research under these provisions, but the IRB determines that the "research presents a reasonable opportunity to further the understanding, prevention, or alleviation of a serious problem affecting the health or welfare of pregnant women, fetuses or neonates," the IRB may refer the research to the Secretary of the HHS, who after consultation with a panel of experts and a period for public comment, may allow the research to proceed (13).

The FDA is not a Common Rule agency but has parallel regulations for the basic protection of human subjects to those in 45 CFR 46, subpart A. These regulations are found under 21 CFR parts 50 and 56. FDA also has parallel regulations for children found under 21 CFR 50, subpart D. FDA does not have parallel regulations to those under 45 CFR 46, subpart B, for protection of pregnant women, human fetuses and neonates in research. However, any FDA regulated research that is federally funded would be subject to the requirements under 45 CFR 46 as well as the requirements under 21 CFR parts 50 and 56. FDA considers the requirements under 45 CFR 46, subpart B, when reviewing research that includes pregnant women, fetuses and neonates but FDA does not have a formal regulatory process for review of such research.

FDA GUIDANCES FOR THE MOTHER, FETUS AND NEONATE

Guidance for Industry: Pregnant Women: Scientific and Ethical Considerations for Inclusion in Clinical Trials (April, 2018)

The draft guidance [(14), see **Table 1**] includes general scientific and ethical considerations to encourage the inclusion of pregnant women in clinical trials when appropriate, noting that the decision to do so necessitates a complex risk benefit analysis that involves both the pregnant woman and the fetus. In addition to studies that might be required to treat pregnancy-specific conditions, the guidance discusses the evaluation of drugs in clinical trials for conditions to treat medical conditions or acute illnesses that are common in women of reproductive potential. These drugs are often used during pregnancy without a clear scientific understanding of the risks and benefits to the mother or to the developing fetus (21). Women should be included in clinical trials because (1) safe and effective treatments are needed during pregnancy, (2) lack of data on dosing, safety and effectiveness of drugs may compromise

pregnant women and fetuses, (3) there may be a direct benefit to participation that is not available outside of the research, and (4) limited accessible treatment options for pregnant women is a public health issue. The physiologic changes that occur during pregnancy are unique. Drug pharmacokinetics (PK) and pharmacodynamics (PD) may be altered during pregnancy impacting drug absorption, distribution, metabolism, and excretion (ADME) and consequently, impacting safety and effectiveness (22).

As noted earlier, although FDA does not have specific regulations that govern the participation of pregnant women in clinical trials, the general considerations for the participation of individuals as human subjects (23) or as unemancipated minors (24) do apply. Research risks differ based on whether the drug is given as part of clinical care or as a research intervention. In the latter situation, the risk of study participation exceeds minimal risk because of the exposure to the drug whereas an observational study collecting data on a drug administered as part of clinical care might be considered minimal risk (25). A decision to expose the fetus to more than minimal risk includes a determination that the exposure to the drug offers a potential clinical benefit to the mother or to the fetus (12).

FDA considers it ethically justifiable to include pregnant women with a disease or medical condition in a post-marketing clinical trial if there are adequate nonclinical studies to support a clinical trial in pregnant women, there are supportive safety data from nonpregnant women in clinical trials, or from literature or other sources, and if efficacy cannot be extrapolated and/or safety cannot be assessed by other means. In the premarket setting, pregnant women may be included in clinical trials if there are adequate nonclinical data to support study in pregnant women and the study intervention holds out a prospect of direct benefit to the mother or fetus, and the pregnant woman has not responded to other treatment options or the study interventions are not available outside of the research setting. Pregnant women with severe disease with limited treatment options may be the most appropriate for clinical studies. PK data should be collected in these studies; data from phase two studies can be used to guide dosing in phase 3. Drug exposure in the fetus/newborn can be assessed by collection of cord blood or from the neonate at the time of delivery, depending on drug exposure and the half-life of the drug. Safety monitoring in any trial where pregnant women will take part should include adequate obstetrical and perinatal expertise in order to recognize safety concerns unique to the pregnant woman and the fetus.

If a woman becomes pregnant during a clinical trial, unblinding should occur and the risk and benefits of continued treatment with the investigational product should be reviewed. A woman may continue in a clinical trial and receive investigational treatment if the benefits of treatment outweigh the risks of continued fetal exposure vs. transition to other treatment options. Informed consent should be obtained for continued study participation. These situations offer an opportunity to collect steady state PK data in the pregnant woman to inform drug modeling and simulation (14, 26) and dosing during pregnancy. The outcome of the pregnancy should be recorded regardless of whether the woman continues to participate in the study.

Reviewer Guidance: Evaluating the Risks of Drug Exposure in Human Pregnancies (April, 2005)

Despite the lack of information on the safety of drug use during pregnancy, most pregnant women likely will be exposed to drugs. Knowledge of teratogenic potential is a critical part of a drug's benefit/risk profile. However, pregnant women are rarely included in clinical trials. Currently, majority of the data on teratogenicity are derived from inadvertent pregnancy exposures during clinical trials of new products, fetal exposure occurring before a woman knows she is pregnant or from some women who enter pregnancy with medical conditions that require continuing drug therapy. Such data are usually insufficient to permit an adequately powered statistical analysis.

The guidance on Evaluating the Risks of Drug Exposure in Human Pregnancies developed in 2005 [(15), see **Table 1**] is aimed at guiding reviewers to evaluate human fetal outcome data generated after medical product (including drug and biological products including vaccines) exposure during pregnancy. The guidance describes critical factors to consider when evaluating the effects of drug exposure in human pregnancies, sources of human data on drug exposures, methods for overall assessment of post-marketing human data and labeling of such products. This guidance should be used in conjunction with more recent guidances, such as the Reproductive and Developmental Toxicities—Integrating Study Results to Assess Concerns Guidance for Industry (27).

Critical factors to consider during evaluation of a product for teratogenic potential include consideration of background prevalence of adverse pregnancy outcomes, combined vs. individual rates of birth defects, major vs. minor birth defects, timing and intensity of exposure, variability of response and class effects. Typically, a drug must cross the placenta and reach the fetus in sufficient concentration to cause an effect. Most teratogens have a threshold below which adverse effects do not occur. Conversely, almost all exposures can be toxic to the fetus if the dose is high enough, even if only indirectly through maternal toxicity. Dosing, including frequency and duration of exposure, is therefore an important consideration in fetal drug exposure. This guidance does not discuss the detailed methodologies for estimating in-utero intensity of drug exposure possibly due to its publication at a time when physiologically based pharmacokinetic (PBPK) modeling was still in its infancy. Recent developments in PBPK models of pregnancy for understanding maternal-fetal drug transfer look promising (28). However, these models need significant refinement before they can be used routinely in drug development to predict intensity of fetal exposure during maternal fetal drug transfer.

Information on human gestational drug exposures will emerge during the post-marketing phase for virtually all drug products. Evidence from all sources, including human data from case reports, epidemiology studies, and animal data, should be considered collectively to determine the strength

of the relationship between drug exposure and teratogenicity. Data from embryo-fetal developmental toxicity studies of drug metabolites in animals must also be considered (19).

The only data on fetal effects initially available in the product labeling usually comes from animal reproductive toxicology studies. As part of the Periodic Safety Update Report (PSUR) sponsors are asked to specifically report on "positive or negative experiences during pregnancy or lactation," by evaluating new human data as they become available, in the context of what is already known about the reproductive effects of the drug, and, if clinically relevant, communicate conclusions regarding risk or lack of risk associated with gestational exposure in the product labeling.

Guidance for Industry: General Clinical Pharmacology Considerations for Neonatal Studies for Drugs and Biological Products (July, 2019)

The neonatal population is a highly heterogenous patient group that has historically been understudied in clinical research. FDA-approved product labeling is often devoid of neonatal-specific information on drug dosing, safety and efficacy, and most drugs administered in neonatal intensive care units (NICUs) are used off-label. As such, when treating this vulnerable population, health care professionals frequently must rely on professional judgment to inform their clinical decision-making. In order to gain the needed information on the safety and efficacy of medications used in neonates, it is imperative to encourage their inclusion in clinical research, as well as encourage the development of new therapies for conditions unique to the newborn. In response to a provision included in the FDA Reauthorization Act (FDARA) of 2017, FDA published a draft guidance on general clinical pharmacology considerations for neonatal studies [(16), see **Table 1**]. The draft guidance discusses clinical pharmacology considerations specific to the newborn and emphasizes the need for input from a multidisciplinary team when planning for studies enrolling neonates.

Similar to the International Council for Harmonization (ICH) E11 addendum (29), this draft guidance defines the neonatal period for the term and post-term newborn as the day of birth plus 27 days, and for the preterm newborn as the day of birth, through the expected date of delivery plus 27 days. It also describes subgroup classifications for the neonatal population [e.g., based on gestational age, postnatal age (PNA), post-menstrual age (PMA), birth weight] and notes the importance of considering stratification as a means for defining more homogenous groups of neonates in a trial. Compared to adults and older children, neonates exhibit unique ADME characteristics. Drug ADME in the neonate can be affected by body size, growth/maturation trajectories, underlying illness and concomitant medications which can result in inter- and intra-individual variability in PK measures. Evaluating products in neonatal studies that include a wide spectrum of PMA and PNA subgroups can help to account for this variability.

Characterization of the PK and PD of a drug can inform rational dosing recommendations for the neonatal population if the ontogeny of factors affecting ADME is considered (30, 31). It is important to leverage all existing PK and PD data from other populations (e.g., adults and other pediatric subgroups) to help determine an initial dose for neonatal studies. Quantitative approaches, such as modeling and simulation, can have utility in helping to predict neonatal doses and optimize clinical trial designs. When designing neonatal studies, sparse sampling is a practical approach for obtaining PK data; opportunistic and scavenged sampling can also be considered. For analysis, a previously developed population PK model in an older population can be redeveloped using the newly acquired neonatal data to create a PopPK model that is applicable for neonates to adults. In the absence of prior neonatal data for which a model is built, sparse data can be used to confirm a neonatal PBPK model that has been appropriately scaled to neonates or a population PK model that has incorporated expected changes in growth and maturation on PK parameters. Age-appropriate formulations are required for neonatal studies and safety data should be obtained.

Guidance for Industry: Post-approval Pregnancy Safety Studies (May, 2019)

The purpose of this draft guidance [(17), see **Table 1**] is to provide recommendations on how to design investigations to assess the outcomes of pregnancies in women exposed to drugs and biological products. Section 505(o) (3) of the Federal Food, Drug, and Cosmetic Act (FD&C Act) authorizes FDA to require certain post-marketing studies or clinical trials for prescription drugs. The goal of post-approval pregnancy safety studies is to provide clinically relevant information about the use and safety of the products during pregnancy, through inclusion of the information in a product's labeling. This guidance describes three general approaches that can be used in the post-marketing setting to evaluate the product safety during pregnancy:

- Pharmacovigilance—Case reports have been most useful and influential in situations where the adverse pregnancy outcome rarely occurs. Examples include: isotretinoin (32), and oligohydramnios with trastuzumab (33). However, it remains challenging to determine whether a causal relationship exists between a product exposure and an adverse pregnancy outcome. Therefore, observational studies such as pregnancy registries usually are needed to provide additional information.
- Pregnancy Registries—A pregnancy registry actively collects information on product exposures during pregnancy and associated pregnancy outcomes by enabling voluntary participation of women who have been exposed to a specific drug of interest. While it is useful to collect data on the effects of rare exposures during pregnancy, it alone may not be sufficient to assess the safety of products, due to challenges of achieving sufficient enrollment. Use of complementary studies with different study designs may help address these limitations and provide greater confidence in the conclusions.
- Complementary Studies—Additional studies that complement data obtained from pregnancy registries and other sources can be implemented to better understand the specific effects of a product during pregnancy, and to more precisely quantify the

magnitude of an association between a pregnancy exposure and a specific outcome.

Guidance for Industry: Nonclinical Safety Evaluation of the Immunotoxic Potential of Drugs and Biologics (February, 2020)

This draft guidance [(18), see **Table 1**] deals with the immunomodulating potential of drugs and biologicals, and makes extensive use of ICH guidances such as:

- S8 Immunotoxicity Studies for Human Pharmaceuticals (April 2006)
- M3(R2) Nonclinical Safety Studies for the Conduct of Human Clinical Trials and Marketing Authorization for Pharmaceuticals (January 2010)
- S6(R1) Preclinical Safety Evaluation of Biotechnology-Derived Pharmaceuticals (May 2012)
- S5(R3) Detection of Toxicity to Reproduction for Human Pharmaceuticals (November 2017)

Since the immune system is a very complex and highly regulated network, the assessment of the potential toxicity of a new drug or biologic agent is difficult to characterize. This guidance stresses the "weight-of-evidence" approach for general immunotoxicity assessments, as discussed in ICH S8.

Immune suppression or stimulation could potentially produce deleterious effects on the mother and fetus. Immunostimulation is a particular concern, in view of the previous experience with cytokine release due to the monoclonal antibody TGN 1412 (34). There are now *in vitro* assays that can assess this risk, and the expectation is that these cytokine release and immune activations assays will be conducted to establish the effective concentration (EC) values such as EC_{20}, EC_{50} and EC_{80}. Additional studies of antibody-mediated immune stimulation, autoimmune reactions, or effects on innate immunity may be necessary.

In some cases, more extensive testing with developmental animal studies may be warranted. These studies may be necessary in situations where the drug product has been shown to elicit immunotoxicity in nonclinical studies with adult animals; the drug or drug class is known to directly affect the immune; or there is reasonable evidence that the mechanism of action or the pharmacology of the drug product could affect the developing immune system. If an evaluation of existing nonclinical toxicity studies indicates the potential for enhanced toxicity in pediatric patients, juvenile animal studies should be considered for products being developed in some therapeutic indications.

Guidance for Industry: Safety Testing of Drug Metabolites (March 2020)

Drug metabolites may need to be determined in nonclinical studies when there are disproportionate drug metabolites, that is, metabolites identified only in humans or present at higher plasma concentrations in humans than in any of the animal species used during standard nonclinical toxicology testing. It is not standard practice for drug metabolites to be evaluated separately in a cross-species safety assessment. As a result, their specific contribution to the overall toxicity of the parent drug has often remained unknown. Technological advances, however, have greatly improved the analytical abilities to detect, identify, and characterize metabolites and may allow a better understanding of the role metabolites play in drug safety assessment. This guidance [(19), see **Table 1**] describes recommended studies for assessing the safety of metabolites such as: general toxicity studies, genotoxicity studies, carcinogenicity studies, and embryo-fetal development toxicity studies. It notes that embryo-fetal development toxicity studies with the drug metabolite are required when a drug is intended for use in a population that includes women of childbearing potential, and that the FDA may ask for other reproductive toxicity studies on a case-by-case basis, depending on these study results.

Guidance for Industry: Pregnancy, Lactation, and Reproductive Potential: Labeling for Human Prescription Drug and Biological Products — Content and Format (July, 2020)

On December 4, 2014, the FDA published the final rule "Content and Format of Labeling for Human Prescription Drug and Biological Products; Requirements for Pregnancy and Lactation Labeling," referred to as the pregnancy and lactation labeling rule (PLLR). This draft guidance [(20), see **Table 1**] provides recommendations on complying with the PLLR to assist with the content and format requirements for the 8.1 Pregnancy, 8.2 Lactation, and 8.3 Females and Males of Reproductive Potential of the USE IN SPECIFIC POPULATIONS subsections.

- 8.1 Pregnancy—This subsection contains information on what is known about the drug's effect on pregnancy, including labor and/or delivery, and the availability of a pregnancy exposure registry. The information about Clinical Considerations for this subsection can include: Disease-Associated Maternal and/or Embryo/Fetal Risk; Dose Adjustments During Pregnancy and the Postpartum Period; Maternal Adverse Reactions; Fetal/Neonatal Adverse Reactions; and Labor/Delivery.
- 8.2 Lactation—This subsection contains information about clinical considerations such as minimizing exposure and monitoring for adverse reactions. Some other areas of information that can belong in this subsection include the presence of the drug in human milk and effects of the drug on the breastfed child.
- 8.3 Females and Males of Reproductive Potential—This subsection provides information on pregnancy testing, contraception, and infertility. In information on infertility, a cross-reference to the carcinogenesis, mutagenesis, impairment of fertility subsection of the Nonclinical Toxicology section, can be made. Even when the data from the animal studies do not raise concern with respect to human fertility and/or loss effects, such information should be described in the Carcinogenesis, Mutagenesis, Impairment of Fertility subsection.

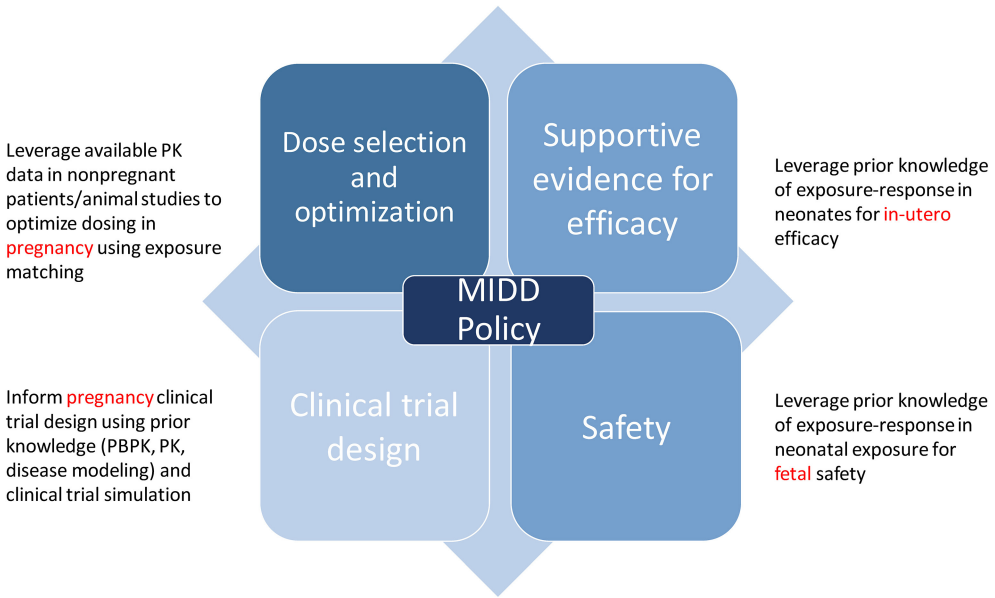

FIGURE 1 | Regulatory application of model informed drug development.

USE OF MODELING IN REGULATORY SUBMISSIONS

The use of quantitative models that leverage our understanding of physiology, disease processes, and pharmacology are routinely applied to inform drug development. Model-informed drug development (MIDD) was formally recognized as an important application for drug development and included in the Prescription Drug User Fee Act (PDUFA) reauthorization performance goals and procedures for 2018 through 2022 (PDUFA VI) (35). The regulatory application of MIDD is broadly classified into four categories: dose optimization, supportive evidence for efficacy, clinical trial design, and safety, all of which inform policy (**Figure 1**) (36).

Given that there is a finite number of dosing regimens that can be formally evaluated in clinical efficacy trials, dosing regimen optimization can often be informed by modeling and simulation strategies [e.g., through nonlinear mixed effect population PK and exposure-response (ER) analyses]. MIDD is also useful in dose optimization of subgroups where therapeutic dose individualization is needed e.g., pediatrics, pregnancy, or extremes of body weight. In such conditions, model based analyses such as PBPK models and population PK models can be used to derive dosing regimens for these specific subgroups with the goal of matching the safe and effective exposure achieved in the reference patient group under the proposed dosing regimen that was studied in the efficacy and safety trials. This strategy relies on the assumption that the ER relationships for both efficacy and safety are similar between the reference group and the specific subgroups. MIDD is also useful to address complex questions regarding efficacy of drugs based on established exposure (dose)-response relationships. It allows for improving clinical trial efficiency during early phases of drug development through modeling and simualtion to determine dose selection, patient selection, trial duration and trial design. In its April 17, 2018 Federal Register Notice, FDA announced a MIDD meeting pilot program to facilitate the development and application of exposure-based, biological, and statistical models derived from preclinical and clinical data sources. The MIDD pilot program is designed to provide a process for drug developers and FDA to discuss the application of MIDD approaches, including PBPK modeling and simulation, to a specific drug development program (37). The goals of including MIDD in PDUFA VI are reducing uncertainty and attrition in drug development, providing a regulatory pathway forward for practically challenging drug development contexts, and informing appropriate use of a drug once approved.

A PBPK approach enables integration of physiologic, chemical, and drug-dependent preclinical and clinical data to model an investigational drug's ADME to generate initial PK parameters and leverage their use in subsequent simulation of untested clinical scenarios (38, 39). Currently, most applications of PBPK in regulatory decision making are limited to drug–drug interactions and initial clinical trial design. Active research is being conducted to further explore the utility of PBPK modeling in other areas to potentially expand the scope of PBPK applications (40). Pediatric PBPK models have generated attention in the last decade, because physiological parameters for model building are increasingly available and regulatory guidelines require pediatric studies during drug development.

The use of modeling and simulation to optimize design of "first-in-pediatric" PK, safety and efficacy clinical studies has increased. PBPK models have the potential to replace or inform

clinical studies in children (40). Currently, the main intended application of a pediatric PBPK model is to propose an initial dosing recommendation for clinical trials at the investigational new drug (IND) application stage. PBPK/PD modeling may also provide a quantitative assessment of assumptions supporting pediatric extrapolation and pediatric trial design (41). Some researchers have suggested that for children younger than 2 years of age, the PBPK approach for predicting PK may be preferred over an allometric scaling approach in cases where ontogeny is an important determinant of drug's ADME (42, 43).

Recent studies have demonstrated the potential utility of PBPK for assessing fetal concentrations from maternal concentrations (44, 45). These PBPK assessments can be extended to assessing neonatal blood concentrations from drugs administered to mothers, which also serves as verification of the fetal model (46).

In summary, quantitative models may help provide insight on safety and efficacy to inform innovation, policy, and ultimately benefit the patient. Despite advances made in MIDD, leveraging data that are generated from all stages of drug development into appropriate modeling and simulation techniques that inform decisions remains challenging, especially in special populations. Additional discussions regarding the application of quantitative modeling approaches to drug development decisions, such as through the MIDD pilot program, may be crucial for both the sponsor(s) and regulatory review teams. As the use of MIDD by regulators and industry expands, standards and best practices must be developed to establish when and where MIDD can be applied, and what methods are appropriate in disparate settings.

CONCLUSIONS

The need for maternal and fetal studies has now been established, and regulatory approaches are catching up quickly. Ethical considerations and FDA guidances have now established the need to include pregnant women in drug development studies when appropriate, and these studies will allow an assessment of the drug therapy in fetuses using modeling. PBPK modeling for the prediction of fetal drug concentrations is being explored in preliminary studies, and this approach is expected to mature quickly.

Science always should drive regulatory approaches. The additional needs to advance the science of fetal pharmacology are obvious and were clearly stated by Sumner Yaffe 55 years go: "Hopefully, the descriptive phase of research will be supplanted by a more sophisticated molecular approach. Only in this way will drug administration during the perinatal period truly represent optimal therapeusis instead of dogmatic posology, and contributions to a better understanding of developmental physiology be made" (1). Modeling will help fetal pharmacology to quickly move into the mainstream of drug development for the benefit of pregnant women and their fetuses.

AUTHOR CONTRIBUTIONS

DG, KP, VB-M, DS, and GB wrote the manuscript. All authors contributed to the article and approved the submitted version.

REFERENCES

1. S.J. Yaffe. Some aspects of perinatal pharmacology. *Annu Rev Med.* (1966) 17:213–34. doi: 10.1146/annurev.me.17.020166.001241
2. Giacoia GP, Mattison DR. Obstetric and fetal pharmacology. *Glob Libr Women's Med*. (2009). doi: 10.3843/GLOWM.10196
3. National Institutes of Health: Obstetric-Fetal Pharmacology Research Centers (OPRC) Network. Available online at: https://www.nichd.nih.gov/research/supported/opru_network (accessed June 16, 2021).
4. Gupta C, Yaffe SJ, Shapiro BH. Prenatal exposure to phenobarbital permanently decreases testosterone and causes reproductive dysfunction. *Science.* (1982) 216:640–2. doi: 10.1126/science.7200262
5. Mezzacappa A, Lasica PA, Gianfagna F, Cazas O, Hardy P, Falissard B. et al. Risk for Autism Spectrum Disorders According to Period of Prenatal Antidepressant Exposure: A Systematic Review and Meta-analysis. *JAMA Pediatrics.* (2017) 171:555–63. doi: 10.1001/jamapediatrics.2017.0124
6. Cleary KL, Roney K, Costantine M. Challenges of studying drugs in pregnancy for off-label indications: pravastatin for preeclampsia prevention. *Semin Perinatol.* (2014) 38:523–7. doi: 10.1053/j.semperi.2014.08.019
7. O'Connell AE, Guseh S, Lapteva L, Cummings CL, Wilkins-Haug L, Chan J, et al. Gene and Stem Cell Therapies for Fetal Care: A Review. *JAMA Pediatr.* (2020) 174:985–91. doi: 10.1001/jamapediatrics.2020.1519
8. HHS Office for Human Research Protection: Related Historical Documents from the National Commission for the Protection of Human Subjects of Biomedical and Behavioral Research. Available online at: https://www.hhs.gov/ohrp/regulations-and-policy/belmont-report/access-other-reports-by-the-national-commission/index.html (accessed March 20, 2021).
9. HHS Office for Human Research Protections: The Belmont Report. Available online at: https://www.hhs.gov/ohrp/regulations-and-policy/belmont-report/read-the-belmont-report/index.html (accessed March 20, 2021).
10. Code of Federal Regulations, Title 45, Subtitle A, Subchapter A, Part 46, Subpart A: Basic Policy for Protection of Human Research Subjects. Available online at: https://www.ecfr.gov/cgi-bin/retrieveECFR?gp=&SID=83cd09e1c0f5c6937cd9d7513160fc3f&pitd=20180719&n=pt45.1.46&r=PART&ty=HTML (accessed March 20, 2021).
11. Code of Federal Regulations, 45 CFR 46.111(a)(3). Available online at: https://www.ecfr.gov/cgi-bin/retrieveECFR?gp=&SID=83cd09e1c0f5c6937cd9d7513160fc3f&pitd=20180719&n=pt45.1.46&r=PART&ty=HTML (accessed March 20, 2021).
12. Code of Federal Regulations, 45 CFR 46, subpart B. Available online at: https://www.ecfr.gov/cgi-bin/retrieveECFR?gp=&SID=83cd09e1c0f5c6937cd9d7513160fc3f&pitd=20180719&n=pt45.1.46&r=PART&ty=HTML (accessed March 20, 2021).
13. Code of Federal Regulations, 45 CFR 46.207. Available online at: https://www.ecfr.gov/cgi-bin/retrieveECFR?gp=&SID=83cd09e1c0f5c6937cd9d7513160fc3f&pitd=20180719&n=pt45.1.46&r=PART&ty=HTML (accessed March 20, 2021).
14. US Food and Drug Administration: Guidance for Industry: Pregnant Women: Scientific and Ethical Considerations for Inclusion in Clinical Trials (2018). Available online at: https://www.fda.gov/media/112195/download (accessed March 21, 2021).
15. US Food and Drug Administration: Reviewer Guidance: Evaluating the Risks of Drug Exposure in Human Pregnancies (2005). Available online at: https://www.fda.gov/media/71368/download (accessed March 24, 2021).
16. US Food and Drug Administration: Guidance for Industry: General Clinical Pharmacology Considerations for Neonatal Studies for Drugs and Biological Products (2019). Available online at: https://www.fda.gov/media/129532/download (accessed March 21, 2021).
17. US Food and Drug Administration: Guidance for Industry: Postapproval Pregnancy Safety Studies (2019). Available online at: https://www.fda.gov/media/124746/download (accessed March 21, 2021).

18. US Food and Drug Administration: Guidance for Industry: Nonclinical Safety Evaluation of the Immunotoxic Potential of Drugs and Biologics (2020). Available online at: https://www.fda.gov/media/135312/download (accessed March 21, 2021).
19. US Food and Drug Administration: Guidance for Industry: Safety Testing of Drug Metabolites (2020). Available online at: https://www.fda.gov/media/72279/download (accessed March 21, 2021).
20. US Food and Drug Administration: Guidance for Industry: Pregnancy, Lactation, and Reproductive Potential: Labeling for Human Prescription Drug and Biological Products — Content and Format (2020). Available online at: https://www.fda.gov/media/90160/download (accessed March 21, 2021).
21. Lyerly AD, Little MO, Faden R. The second wave: toward responsible inclusion of pregnant women in research. *Int J Fem Approaches Bioeth.* (2008) 1:5–22. doi: 10.3138/ijfab.1.2.5
22. Sheffield JS, Siegel D, Mirochnick M, Heine RP, Nguyen C, Bergman KL, et al. Designing drug trials: considerations for pregnant women. *Clin Infect Dis.* (2014) 59:S437–44. doi: 10.1093/cid/ciu709
23. Code of Federal Regulations, 21 CFR. Part 50, subparts A and B. Available online at: https://www.ecfr.gov/cgi-bin/text-idx?tpl=/ecfrbrowse/Title21/21cfr50_main_02.tpl (accessed March 20, 2021).
24. Code of Federal Regulations, 21 CFR 50, subpart D. Available online at: https://www.ecfr.gov/cgi-bin/text-idx?tpl=/ecfrbrowse/Title21/21cfr50_main_02.tpl (accessed March 20, 2021).
25. Code of Federal Regulations, 21 CFR 50.3(k). Available online at: https://www.ecfr.gov/cgi-bin/text-idx?tpl=/ecfrbrowse/Title21/21cfr50_main_02.tpl (accessed March 20, 2021).
26. Xia B, Heimbach T, Gollen R, Nanavati C, He H. A simplified PBPK modeling approach for prediction of pharmacokinetics of four primarily renally excreted and CYP3A metabolized compounds during pregnancy. *AAPS J.* (2013) 15:1012–24. doi: 10.1208/s12248-013-9505-3
27. US Food and Drug Administration: Guidance for Industry: Reproductive and Developmental Toxicities — Integrating Study Results to Assess Concerns, September 2011. Available online at: https://www.fda.gov/media/72231/download (accessed June 16, 2021).
28. Dallmann A, Liu XI, Burckart GJ, van den Anker J. Drug Transporters Expressed in the Human Placenta and Models for Studying Maternal-Fetal Drug Transfer. *J Clin Pharmacol.* (2019) 59:S70–81. doi: 10.1002/jcph.1491
29. US Food and Drug Administration: Guidance for Industry: E11(R1) Addendum: Clinical Investigation of Medicinal Products in the Pediatric Population (2018). Available online at: https://www.fda.gov/media/101398/download (accessed March 21, 2021).
30. Burckart GJ, van den Anker JN. Pediatric Ontogeny: Moving From Translational Science to Drug Development. *J Clin Pharmacol.* (2019) 59:S7–8. doi: 10.1002/jcph.1481
31. Burckart GJ, Seo S, Pawlyk AC, McCune SK, Yao LP, Giacoia GP, et al. Scientific and Regulatory Considerations for an Ontogeny Knowledge Base for Pediatric Clinical Pharmacology. *Clin Pharmacol Ther.* (2020) 107:707–9. doi: 10.1002/cpt.1763
32. Rosa FW. Teratogenicity of isotretinoin. *Lancet.* (1983) 2:513. doi: 10.1016/S0140-6736(83)90538-X
33. Zagouri F, Sergentanis TN, Bartsch R, Berghoff AS, Chrysikos D, de Azambuja E, et al. Intrathecal administration of trastuzumab for the treatment of meningeal carcinomatosis in HER2-positive metastatic breast cancer: a systematic review and pooled analysis. *Breast Cancer Res Treat.* (2013) 139:13–22. doi: 10.1007/s10549-013-2525-y
34. Schneider CK. First-in-human trials with therapeutic proteins: regulatory rethink? *Expert Rev Clin Pharmacol.* (2008) 1:327–31. doi: 10.1586/17512433.1.3.327
35. US Food and Drug Administration: PDUFA reauthorization performance goals and procedures fiscal years 2018 through 2022. Available online at: https://www.fda.gov/downloads/ForIndustry/UserFees/PrescriptionDrugUserFee/UCM511438.pdf (accessed March 18, 2021).
36. Wang Y, Zhu H, Madabushi R, Liu Q, Huang SM, Zineh I. Model-informed drug development: current us regulatory practice and future considerations. *Clin Pharmacol Ther.* (2019) 105:899–911. doi: 10.1002/cpt.1363
37. U.S. Food and Drug Administration: Pilot meetings program for model-informed drug development approaches. 83 FR 16868. Notice. 16868-16870. Available online at: https://www.federalregister.gov/documents/2018/04/17/2018-08010/pilot-meetings-program-for-model-informed-drug-development-approaches (accessed March 18, 2021).
38. Zhao P, Rowland M, Huang SM. Best practice in the use of physiologically based pharmacokinetic modeling and simulation to address clinical pharmacology regulatory questions. *Clin Pharmacol Ther.* (2012) 92:17–20. doi: 10.1038/clpt.2012.68
39. Zhao P, Zhang L, Grillo JA, Liu Q, Bullock JM, Moon YJ, et al. Applications of physiologically based pharmacokinetic (PBPK) modeling and simulation during regulatory review. *Clin Pharmacol Ther.* (2011) 89:259–67. doi: 10.1038/clpt.2010.298
40. Grimstein M, Yang Y, Zhang X, Grillo J, Huang SM, Zineh I, et al. Physiologically Based Pharmacokinetic Modeling in Regulatory Science: An Update From the US Food and Drug Administration's Office of Clinical Pharmacology. *J Pharm Sci.* (2019) 108:21–5. doi: 10.1016/j.xphs.2018.10.033
41. Green DJ, Zineh I, Burckart GJ. Pediatric Drug Development: Outlook for Science-Based Innovation. *Clin Pharmacol Ther.* (2018) 103:376–8. doi: 10.1002/cpt.1001
42. Zhou W, Johnson TN, Bui KH, Cheung SYA, Li J, Xu H, et al. Predictive performance of physiologically based pharmacokinetic (PBPK) modeling of drugs extensively metabolized by major cytochrome P450s in children. *Clin Pharmacol Ther.* (2018) 104:188–200. doi: 10.1002/cpt.905
43. Calvier EA, Krekels EH, Valitalo PA, Rostami-Hodjegan A, Tibboel D, Danhof M, et al. Allometric scaling of clearance in paediatric patients: when does the magic of 0.75 fade? *Clin Pharmacokinet.* (2017) 56:273–285. doi: 10.1007/s40262-016-0436-x
44. Liu XI, Momper JD, Rakhmanina N, van den Anker JN, Green DJ, Burckart GJ, et al. Physiologically Based Pharmacokinetic Models to Predict Maternal Pharmacokinetics and Fetal Exposure to Emtricitabine and Acyclovir. *J Clin Pharmacol.* (2020) 60:240–55. doi: 10.1002/jcph.1515
45. Liu XI, Momper JD, Rakhmanina NY, Green DJ, Burckart GJ, Cressey TR, et al. Prediction of maternal and fetal pharmacokinetics of dolutegravir and raltegravir using physiologically based pharmacokinetic modeling. *Clin Pharmacokinet.* (2020) 59:1433–50. doi: 10.1007/s40262-020-00897-9
46. Liu XI, Momper JD, Rakhmanina NY, Green DJ, Burckart GJ, Cressey TR, et al. Physiologically based pharmacokinetic modeling framework to predict neonatal pharmacokinetics of transplacentally acquired Emtricitabine, Dolutegravir, and Raltegravir. *Clin Pharmacokinet* (2021) 60:795–809. doi: 10.1007/s40262-020-00977-w

Author Disclaimer: The opinions expressed in this article are those of the authors and should not be interpreted as the position of the U.S. Food and Drug Administration.

Conflict of Interest: The authors declare that the research was conducted in the absence of any commercial or financial relationships that could be construed as a potential conflict of interest.

Publisher's Note: All claims expressed in this article are solely those of the authors and do not necessarily represent those of their affiliated organizations, or those of the publisher, the editors and the reviewers. Any product that may be evaluated in this article, or claim that may be made by its manufacturer, is not guaranteed or endorsed by the publisher.

frontiers in Pediatrics

ORIGINAL RESEARCH
published: 20 September 2021
doi: 10.3389/fped.2021.734122

Mechanistic Modeling of Maternal Lymphoid and Fetal Plasma Antiretroviral Exposure During the Third Trimester

Babajide Shenkoya[1], *Shakir Atoyebi*[1,2], *Ibrahim Eniayewu*[1,3], *Abdulafeez Akinloye*[1] *and Adeniyi Olagunju*[1,2*]

[1] Department of Pharmaceutical Chemistry, Obafemi Awolowo University, Ile-Ife, Nigeria, [2] Department of Pharmacology and Therapeutics, Institute of Systems, Molecular and Integrative Biology, University of Liverpool, Liverpool, United Kingdom, [3] Department of Pharmaceutical and Medicinal Chemistry, University of Ilorin, Ilorin, Nigeria

Pregnancy-induced changes in plasma pharmacokinetics of many antiretrovirals (ARV) are well-established. Current knowledge about the extent of ARV exposure in lymphoid tissues of pregnant women and within the fetal compartment is limited due to their inaccessibility. Subtherapeutic ARV concentrations in HIV reservoirs like lymphoid tissues during pregnancy may constitute a barrier to adequate virological suppression and increase the risk of mother-to-child transmission (MTCT). The present study describes the pharmacokinetics of three ARVs (efavirenz, dolutegravir, and rilpivirine) in lymphoid tissues and fetal plasma during pregnancy using materno-fetal physiologically-based pharmacokinetic models (m-f-PBPK). Lymphatic and fetal compartments were integrated into our previously validated adult PBPK model. Physiological and drug disposition processes were described using ordinary differential equations. For each drug, virtual pregnant women ($n = 50$ per simulation) received the standard dose during the third trimester. Essential pharmacokinetic parameters, including Cmax, Cmin, and AUC (0–24), were computed from the concentration-time data at steady state for lymph and fetal plasma. Models were qualified by comparison of predictions with published clinical data, the acceptance threshold being an absolute average fold-error (AAFE) within 2.0. AAFE for all model predictions was within 1.08–1.99 for all three drugs. Maternal lymph concentration 24 h after dose exceeded the reported minimum effective concentration (MEC) for efavirenz (11,514 vs. 800 ng/ml) and rilpivirine (118.8 vs. 50 ng/ml), but was substantially lower for dolutegravir (16.96 vs. 300 ng/ml). In addition, predicted maternal lymph-to-plasma AUC ratios vary considerably (6.431—efavirenz, 0.016—dolutegravir, 1.717—rilpivirine). Furthermore, fetal plasma-to-maternal plasma AUC ratios were 0.59 for efavirenz, 0.78 for dolutegravir, and 0.57 for rilpivirine. Compared with rilpivirine (0 h), longer dose forgiveness was observed for dolutegravir in fetal plasma (42 h), and for efavirenz in maternal lymph (12 h). The predicted low lymphoid tissue penetration of dolutegravir appears to be significantly offset by its extended dose forgiveness and adequate fetal compartment exposure. Hence, it is unlikely to be a predictor of maternal virological failure or MTCT risks. Predictions from our m-f-PBPK models align with recommendations of no dose adjustment despite moderate

OPEN ACCESS

Edited by:
André Dallmann, Bayer, Germany

Reviewed by:
Karthik Lingineni, Novartis, United States
Stein Schalkwijk, GlaxoSmithKline, United Kingdom

***Correspondence:**
Adeniyi Olagunju
olagunju@liverpool.ac.uk

Specialty section:
This article was submitted to Obstetric and Pediatric Pharmacology, a section of the journal Frontiers in Pediatrics

Received: *30 June 2021*
Accepted: *23 August 2021*
Published: *20 September 2021*

Citation:
Shenkoya B, Atoyebi S, Eniayewu I, Akinloye A and Olagunju A (2021) Mechanistic Modeling of Maternal Lymphoid and Fetal Plasma Antiretroviral Exposure During the Third Trimester. Front. Pediatr. 9:734122. doi: 10.3389/fped.2021.734122

changes in exposure during pregnancy for these drugs. This is an important new application of PBPK modeling to evaluate the adequacy of drug exposure in otherwise inaccessible compartments.

Keywords: pregnancy, antiretroviral, lymph, pharmacokinetics, PBPK, fetus, adherence

INTRODUCTION

Pregnancy-induced physiological changes reduce plasma concentrations of antiretrovirals (ARV), especially in the third trimester (1–4). Mother-to-child transmission (MTCT) of HIV is reduced significantly at the standard dose of current ARVs in use (1, 4–7). Cases of perinatal transmission, although not common, and vaginal shedding of HIV RNA among pregnant women with undetectable or low plasma HIV RNA suggest that declining MTCT may not be attributed to low plasma HIV RNA viral load alone (8–10).

The use of ARVs suppresses plasma HIV RNA levels below the limit of detection (11). However, rapid viral rebound in non-adhering patients suggests that replication-competent viruses persist in HIV reservoirs during treatment (12, 13). Suboptimal adherence may therefore cause a viral rebound in pregnant women, which can increase the risk of mother-to-child transmission (MTCT) (14–16). The lymphoid tissues constitute the largest HIV reservoir sites because they are the primary sites for viral replication, and therefore contain a high proportion of viral genetic components and free virions (15, 17, 18). Furthermore, persistent isolates of HIV particles in lymph nodes of patients on active ART also suggest that the virus may be capable of evading lethal ARV concentrations in maternal plasma. This has constituted a major barrier in HIV eradication (12, 19–22). Penetration of ARVs into the lymphatic tissues is crucial for prevention of viral replication, rebound, drug resistance and MTCT (23).

Quantification of drug distribution into the lymphatic system of living persons has not been studied due to the challenges with sample collection. Macaque mass spectrometry imaging, human lymph node mononuclear cells, and human primary lymphoid endothelial cells are methods that have been reported so far in the literature for drug quantification in lymphoid tissues (24–26). Ethical considerations around sample collection and safety concerns limit fetal pharmacokinetics studies before delivery (27). These gaps may be filled through physiologically-based pharmacokinetic (PBPK) modeling and simulation.

Materno-fetal PBPK (m-f-PBPK) modeling strategy has advanced from simple models to using highly representative models that include gestational-age dependent changes in maternal and fetal anatomy and physiology (27–30). M-f-PBPK models have been used to reliably estimate fetal concentrations of emtricitabine, tenofovir, nevirapine, darunavir, efavirenz, and thalidomide (28–30). These predictions sometimes rely on a number of assumptions based on data derived from *in vitro* or animal models in the absence of relevant clinical pregnancy data. However, a robust mechanistic workflow on PBPK models starting from simple non-pregnant models validated with available clinical data to more complex materno-fetal models, often builds confidence in the data output from such models. Applications of such models to HIV tissue reservoirs could support the development of molecules with optimal characteristics for enhanced distribution in HIV eradication studies. There is currently no published description of ARV distribution into lymphoid tissues during pregnancy.

In the current work, we describe the extension of our previous m-f PBPK model (28) to describe the penetration of efavirenz, dolutegravir and rilpivirine into the lymph and fetal plasma during pregnancy.

METHOD

Model Structure and Parameterisation

The present model is an extension of a previously described materno-fetal PBPK model composed of integrated whole-body maternal model and multi-compartmental fetal model (**Supplementary Figure 1**) (28). The model was implemented in Simbiology® (v. 9.5, MATLAB® 2018b, Mathworks Inc., Natick, Massachusetts, USA) and extended to include the lymphatic circulation (**Figure 1**). Organ weights in the maternal model were predicted anthropometrically using the population physiology model described by Bosgra et al. (31). The compartments

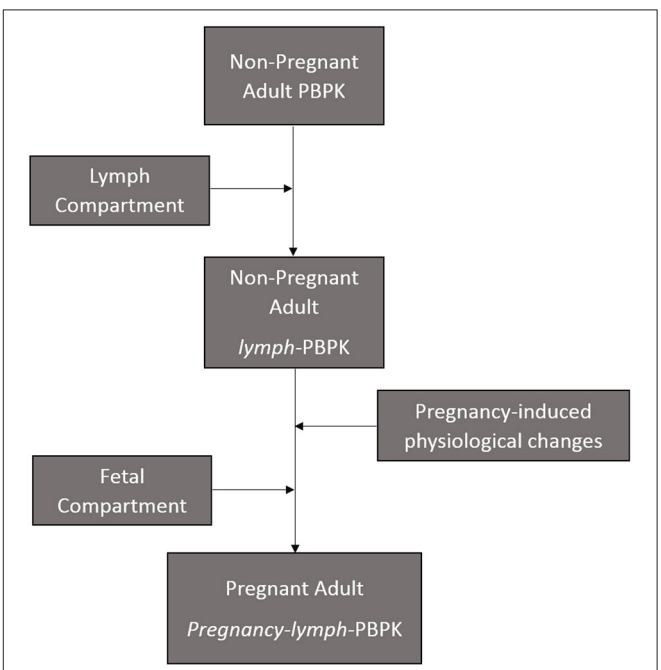

FIGURE 1 | PBPK Model development workflow adopted.

TABLE 1 | Drug-specific parameters for efavirenz, dolutegravir, and rilpivirine used in building the lymph-PBPK model.

Parameters	Description	Efavirenz (34)	Dolutegravir (34)	Rilpivirine (34)
MW (g)	Molecular weight	316	419	366
Log P_{ow}	Octanol-water partition coefficient	4.60	2.20	4.32
pKa	Dissociation constant	10.2	8.3	3.26
R	Blood-to-Plasma ratio	0.74	0.535	0.67
PSA ($Å^2$)	Polar Surface Area	38.33	–	–
HBD	Hydrogen Bond Donor	1	–	–
f_u	Fraction unbound	0.015	0.007	0.003
V_d (L/kg)	Volume of distribution	3.6	–	–
P_{eff} (10^{-6} cm/s)	Effective permeability (Caco-2)	2.5	–	12.0
ClintCYP2A6 (μL/min/pmol)	CYP2A6 Intrinsic Hepatic clearance	0.08	–	–
ClintCYP2B6 (μL/min/pmol)	CYP2B6 Intrinsic Hepatic clearance	0.55	–	–
ClintCYP1A2 (μL/min/pmol)	CYP1A2 Intrinsic Hepatic clearance	0.07	–	–
ClintCYP3A4 (μL/min/pmol)	CYP3A4 Intrinsic Hepatic clearance	0.007	3.0	2.04
ClintCYP3A5 (μL/min/pmol)	CYP3A5 Intrinsic Hepatic clearance	0.03	–	–
ClintUGT1A1 (μL/min/pmol)	UGT1A1 Intrinsic Hepatic clearance	–	3.2	–
d	Particle size (Mean ± SD)	2.35 ± 0.48 μm (35)	5.7 μm (36)	200 nm (37)
Plasma MEC (μg/mL)	Minimum Effective Concentration	8E-1 (38)	3.0E-1 (39)	5.0E-2 (40)
In-vitro adjusted PBIC (μg/mL)	Protein Binding Inhibitory Concentration	1.26E-1	6.40E-2	2.03E-2
Water Solubility (mg/mL)	Water solubility at 25°C	0.093	0.095	0.094

TABLE 2 | Lymph flow draining various tissues in the human body (44).

Tissues	Lymph flow (% CO)	Fraction of extracellular water
Adipose	12.8	0.141
Bone	0.00	0.098
Brain	1.05	0.092
Gut	12.0	0.267
Heart	1.00	0.313
Kidney	8.50	0.283
Liver	33.0	0.165
Lung	3.00	0.348
Muscle	16.0	0.091
Pancreas	0.30	0.120
Skin	7.30	0.623
Spleen	0.00	0.208
Subcutaneous	0.04	0.623

CO, Cardiac output.

represented in the fetal model included the placenta, the amniotic fluid, fetal kidney, fetal liver, and fetal brain. Other organs were lumped together and represented by a single compartment as previously described (32). The structure of the fetal circulatory system was based on a published description (33) and organ blood flows were modeled using equations described by Zhang et al. (32).

Efavirenz, dolutegravir, and rilpivirine were selected for this study because they are approved for use in pregnancy and there is sufficient clinical data available on the pharmacokinetics of these drugs in pregnancy. Values of parameters representing the physicochemical properties of the study drugs (efavirenz, dolutegravir, and rilpivirine) such as octanol-water partition coefficient, acid dissociation constant and blood-to-plasma ratio, as well as their intrinsic hepatic clearances were obtained from literature (**Table 1**). Maternal and fetal anatomical and physiological adaptations to pregnancy were accounted for by the use of gestational-age dependent parameters where relevant (41). In some cases where necessary parameter values were not reported, published graph-plots of changes in the parameters: the placental thickness (18), rates of blood flow through the foramen ovale and ductus arteriosus (42), over the course of pregnancy were digitized (Plotdigitizer® version 2.6.6, Free Software Foundation, Boston, MA, USA). The data points obtained were used to generate equations of best-fit which were subsequently inputted into the model as previously described (28). Sensitivity analyses was conducted to observe the extent in which uncertainty in placental diffusion constant propagated into the fetal plasma predictions in the model (**Supplementary Figure 2**).

Modeling the Lymphatic Circulation

The lymph node draining each organ was collected into a central lymph node compartment. The lymph returns back to the venous circulation at 1.7% rate of cardiac output to maintain body fluid balance (33, 43). The lymph flow and volume of extracellular water for each organ represented in the model is presented in **Table 2** (44). Small drug molecules disintegrating from formulation matrix were assumed to be equilibrated between plasma and interstitial fluid (45). The model assumed transfer of drug from interstitial fluid into the lymphatic circulation by diffusion due to low transporter expression in

the lymph nodes (16). The diffusion process was described by adapting Fick's diffusion equation (46) as shown below:

$$Q_{lymph,\,drug} = \frac{k_{drug} \times TSA_{lymph} \times f_u \times \left(C_{int} - C_{lym}\right)}{LT} \quad (1)$$

where k_{drug} is the diffusion coefficient of the drug, TSA_{lymph} is the total surface area of initial lymphatics, f_u is the fraction of unbound drug, $\left(C_{int} - C_{lym}\right)$ is the drug concentration gradient across interstitial-lymph barrier, and LT is the wall thickness of initial lymphatics.

The diffusion coefficient of each drug, k_{drug}, was calculated based on the Stokes-Einstein equation (47), as shown below:

$$k_{drug} = \frac{RT}{6\pi \times N_a \times r_{drug} \times \eta} \quad (2)$$

where RT is the product of gas constant and body temperature at 37°C = 2.5×10^5 Ncm/mol, N_a is the Avogadro's constant = 6.022×10^{23} /mol, r_{drug} is radius of drug, and η is the viscosity of water = 1.17×10^{-9} Nmin/cm^2.

Lymph is collected by diffusion through the initial lymphatics in various organs. The shape of initial lymphatics was modeled to be a cone with a closed smaller end because it has a blinded (closed) end with a small diameter, which increases along the lymphatic vessels up to the pre-collecting lymphatic vessels (47, 48). The formula for the surface area of a cone was used to represent the surface area of a lymphatic vessels, SA_{lymph}, as shown in the equation below:

$$SA_{lymph} = \pi r_{il}\left(r_{il} + \sqrt{{l_{il}}^2 + {r_{il}}^2}\right) \quad (3)$$

where r_{il} and l_{il} are the radius and length of the initial lymphatic vessel, respectively. The mean (±standard deviation) diameter and length of the closed end of an initial lymphatics had earlier been determined to be 30.8 ± 9.5 μm and 834 ± 796 μm, respectively (48). The suggested number of lymph nodes in the body is 500–600 (43), it was therefore assumed that the total surface area of initial lymphatic vessels, TSA_{lymph}, is 500 times the surface area of an initial lymphatic vessel. The wall thickness of initial lymphatics has been reported to be in the range of 50–100 nm (47).

Absorption, distribution, metabolism and elimination were modeled as previously described for the base model (28). Previously undescribed model equations are presented in **Supplementary Table 1** for reference.

Model Verification and Model Simulation

Model predictions for key system parameters, including organ weights and blood flow, were compared with published reference values (41, 49–51). Published clinical pharmacokinetic studies on efavirenz, dolutegravir, and rilpivirine during pregnancy were searched through PubMed using combinations of drug name, pharmacokinetics, fetal exposure, infant washout, and pregnancy as keywords. In each case, the predicted steady-state pharmacokinetic parameters computed from simulated concentration-time data were compared with published data. Importantly, to ensure that the introduction of the lymphatic model into our previously published materno-fetal model does not affect key predictions, the model was revalidated for key system parameters relevant to drug disposition, and pharmacokinetic parameters in virtual populations of non-pregnant adults and pregnant women. To facilitate validation against clinical pharmacokinetic data from non-pregnant adult populations, non-pregnant equivalent of relevant model parameters and equations describing key processes were created. This allowed for easy activation/deactivation of model equations for the pregnant population while running simulation for the non-pregnant population. An absolute average fold error of <2.0 in predictions when compared with clinical data was set as acceptance threshold for model verification.

Verified models were used to predict the lymph and fetal concentration-time profiles of efavirenz, dolutegravir and rilpivirine following 100% adherence to therapy. Each simulation consisted of a virtual population of 50 females, non-pregnant or pregnant. Study drugs were administered orally at standard doses, 600 mg for efavirenz, 50 mg for dolutegravir, and 25 mg for rilpivirine. Concentration-time data were collected at steady state over a 24 h dosing period at 30 min and then hourly. Infant washout delivery was modeled by dose cessation in the maternal PBPK submodel. The extent of exposure to study drug was calculated as the ratio of AUC in compartments of interest within the same time interval. Non-adherence was modeled by dose cessation at steady state. Dose forgiveness was estimated in lymph and fetal compartment as the time it takes for drug concentration to decrease below the published minimum effective concentration (MEC) after the last dosing interval for each drug: 800 for efavirenz, 300 for rilpivirine and 50 ng/ml for dolutegravir (52–54).

Essential pharmacokinetic parameters, including Cmax, Cmin, and AUC (0–24) at steady state, for both maternal lymph and fetal compartments were computed from the corresponding concentration-time data. Dose input was stopped at delivery, and infant plasma exposure was predicted by measuring drug concentration 2–10 h post dose.

RESULT

Model Validation

The predicted plasma pharmacokinetic parameters in the non-pregnant adult model were within 1.19–1.80 average fold difference of clinically observed data (**Table 3**). Predicted plasma concentration-time curves were superimposed on clinically observed plasma concentration-time profiles (**Figure 2**) of each drug to visually assess predictive performance of the model. There is lack of clinical data to validate the lymph pharmacokinetics predictions. Maternal plasma pharmacokinetic predictions of the m-f-PBPK model developed were validated with clinically observed pharmacokinetics data in third trimester, and were within 1.13–1.76 average fold difference of clinically observed data (**Table 4**). The predicted concentration-time

TABLE 3 | Median Plasma and Lymph pharmacokinetic parameters for efavirenz, dolutegravir, and rilpivirine in non-pregnant adult.

	Plasma			Lymph		Lymph-to-plasma ratio	
	Predicted	**Observed**	**AAFE**	**Predicted**	**Observed**	**Predicted**	**Reported***
Efavirenz 600 mg							
$AUC_{css,0-24/\infty}$ (nghr/mL)	57,763	56,630 (55), 67,200 (56)	1.46, 1.48	408,184	–	7.07	0.86–7.14 (16, 24)
$C_{max,css}$ (ng/mL)	3,950	3,659 (55), 3,660 (56)	1.36, 1.36	22,497	–		
$C_{24,css}$ (ng/mL)	1,315	1,557 (55), 1,820 (56)	1.70, 1.80	11,285	–		
Dolutegravir 50 mg							
$AUC_{css,0-24/\infty}$ (nghr/mL)	46,114	47,137 (57), 50,300 (58)	1.24, 1.26	765.7	–	0.017	0.082 (24)
$C_{max,css}$ (ng/mL)	2,924	3,250 (57), 2,650 (58)	1.18, 1.19	46.3	–		
$C_{24,css}$ (ng/mL)	992.0	950.0 (57), 750.0 (58)	1.46, 1.55	17.4	–		
Rilpivirine 25 mg							
$AUC_{css,0-24/\infty}$ (nghr/mL)	2,981	2,526 (59), 2,582 (60)	1.46, 1.45	4,653	–	1.57	>1 (24, 37)
$C_{max,css}$ (ng/mL)	152	173 (59) 175 (60)	1.36, 1.37	225	–		
$C_{24,css}$ (ng/mL)	97.2	91.0 (59), 92.0 (60)	1.57, 1.57	161	–		

AAFE, Absolute Average Fold Error.

**Lymph-to-plasma ratios in vitro, ex vivo, and animal studies.*

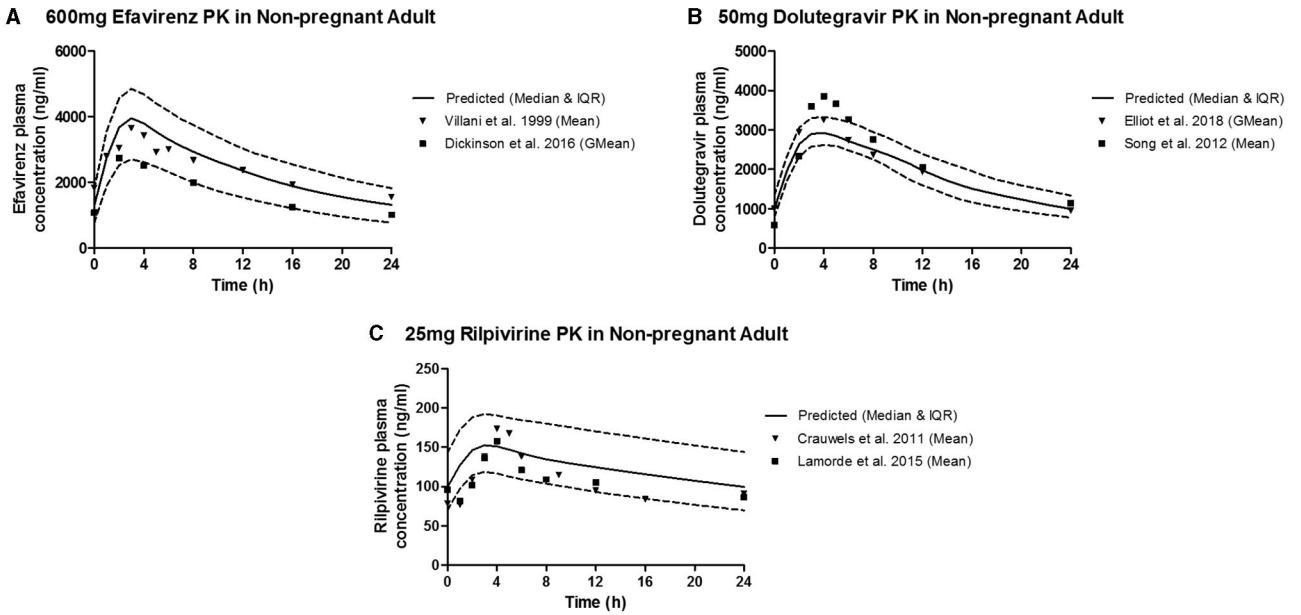

FIGURE 2 | Median (IQR) Predicted vs. Observed plasma concentration-time profile following standard dose of **(A)** 600 mg efavirenz, **(B)** 50 mg dolutegravir, and **(C)** 25 mg rilpivirine in non-pregnant adults.

profiles were comparable with clinically observed maternal plasma concentration-time profiles in third trimester (**Figure 3**).

Obtaining fetal plasma pharmacokinetic parameters for many drugs during clinical studies remains a challenge, but some clinical data on concentration of efavirenz and dolutegravir in non-breastfed infants shortly after delivery (2–10 h) are available (2, 63). However, the time of delivery was not reported in any of these studies. Thus, a delivery time of 12:00 after the last maternal dose was assumed in the model. The model-predicted infant plasma concentration 2–10 h post-delivery was similar to the reported infant concentration for efavirenz and dolutegravir within the same period. The model-predicted infant median concentration for rilpivirine 2–10 h post-delivery was 44.59 ng/mL.

The result of the sensitivity analysis showed that placental diffusion constant is a significant parameter that affect movement of drugs studied into the fetal compartment (**Supplementary Figure 2**). Also, possible influence of the lymph component on accuracy of prediction in the full m-f-PBPK model was evaluated. The median maternal and fetal plasma AUC (0–24) for efavirenz (58,120 vs. 51,984 ng.h/ml; and 34,404 vs. 30,864 ng.h/ml) in the full m-f-PBPK model was

TABLE 4 | Pharmacokinetic parameters of efavirenz, dolutegravir, and rilpivirine in third trimester of pregnancy and infant washout after delivery.

	Maternal plasma (3rd trimester)				Infant washout after delivery		
	Predicted	**Observed**	**AAFE**		**Predicted**	**Observed**	**AAFE**
Efavirenz 600 mg							
$AUC_{css,0-24/\infty}$ (ng.h/mL)	58,120	42,943 (61), 55,400 (62), 60,020 (63)	1.57, 1.47, 1.46	C_{2-10h}	1,016	1,100 (63)	1.08
$C_{max,css}$ (ng/mL)	3,270	3,331 (61), 5,440 (62), 5,130 (63)	1.33, 1.76, 1.68				
$C_{24,css}$ (ng/mL)	1,724	1,002 (61), 1,600 (62), 1,480 (63)	1.99, 1.66, 1.68				
Dolutegravir 50 mg							
$AUC_{css,0-24/\infty}$ (ng.h/mL)	41,166	40,800 (64)[§], 49,119 (2), 35,322 (65)	1.18, 1.24, 1.24	C_{2-10h}	907.4	1,730 (2)	1.91
$C_{max,css}$ (ng/mL)	2,899	3,150 (64), 3,137 (2), 2,534 (65)	1.13, 1.13, 1.18				
$C_{24,css}$ (ng/mL)	1,035	1,000 (64), 921.5 (2), 642 (65)	1.28, 1.30, 1.68				
Rilpivirine 25 mg							
$AUC_{css,0-24/\infty}$ (nghr/mL)	2,205	1,684 (65), 1,762 (3)[§], 1,710 (66)[§]	1.46, 1.43, 1.45	C_{2-10h}	44.59	–	–
$C_{max,css}$ (ng/mL)	121.8	108 (65), 123 (3), 110 (66)	1.29, 1.26, 1.28				
$C_{24,css}$ (ng/mL)	66.9	56 (65), 53 (3), 50 (66)	1.55, 1.58, 1.61				

AAFE, Absolute Average Fold Error. All values are reported in median; [§]Mean values.

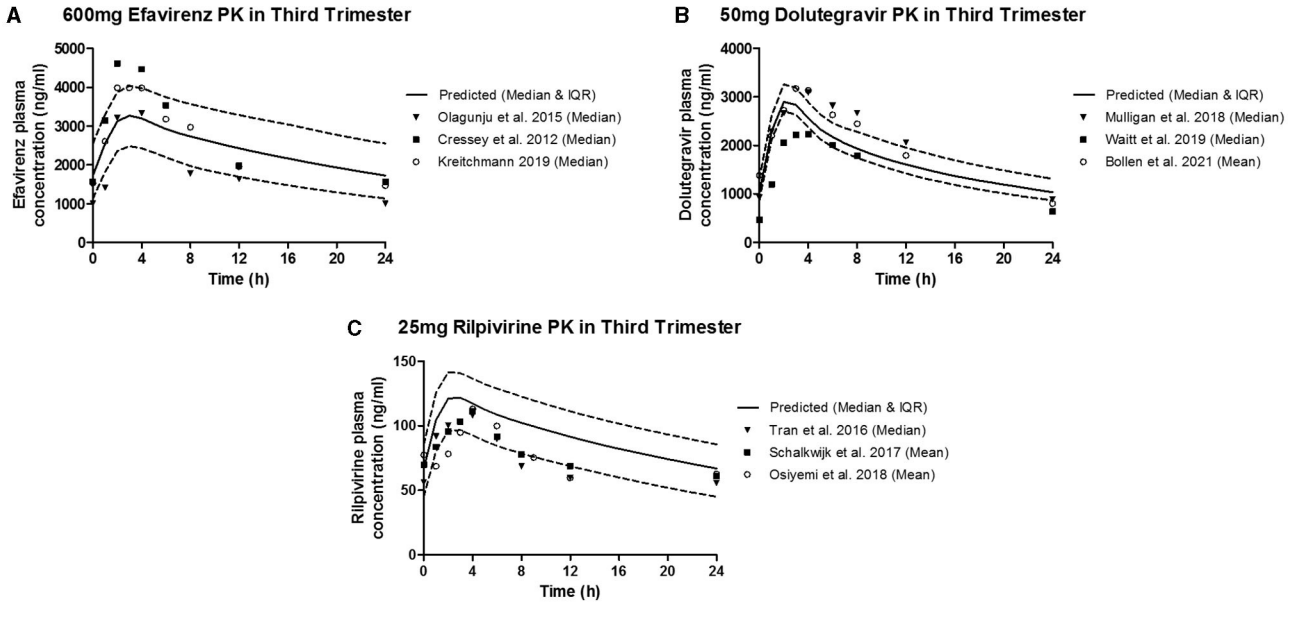

FIGURE 3 | Median (IQR) Predicted vs. Observed plasma concentration-time profile following standard dose of **(A)** 600 mg efavirenz, **(B)** 50 mg dolutegravir, and **(C)** 25 mg rilpivirine in third trimester.

similar to predictions in the m-f-PBPK model without lymphatic component (*data not shown*).

Model Predictions

Simulation was run for 50 virtual patients with mean ± SD age and gestational age of 29 ± 12 years and 39 ± 2.25 weeks, respectively. Each virtual patient was administered a single dose of 600 mg of efavirenz, 50 mg of dolutegravir, or 25 mg of rilpivirine. Concentration-time data was collected after reaching steady state. The validated model was employed to predict the maternal lymph and fetal plasma pharmacokinetics of 600 mg, 50 mg and 25 mg daily dose of efavirenz, dolutegravir, and rilpivirine, respectively (**Figure 4**). The maternal lymph-to-plasma and fetal-to-maternal plasma AUC ratios of 0.592, 0.781, and 0.573 were obtained for efavirenz, dolutegravir and rilpivirine, respectively (**Table 5**). Efavirenz was predicted to accumulate in maternal lymph by over 6-folds and rilpivirine accumulated by <2-folds. Poor lymph penetration was predicted for dolutegravir with only 1.6% of plasma dolutegravir entering the lymph. Predictions of fetal plasma concentrations of efavirenz, dolutegravir, and rilpivirine were 59.2, 78.1, and 57.3% of maternal plasma concentrations, respectively.

Dose forgiveness of 600 mg efavirenz, 50 mg dolutegravir, and 25 mg rilpivirine were determined in order to estimate the time

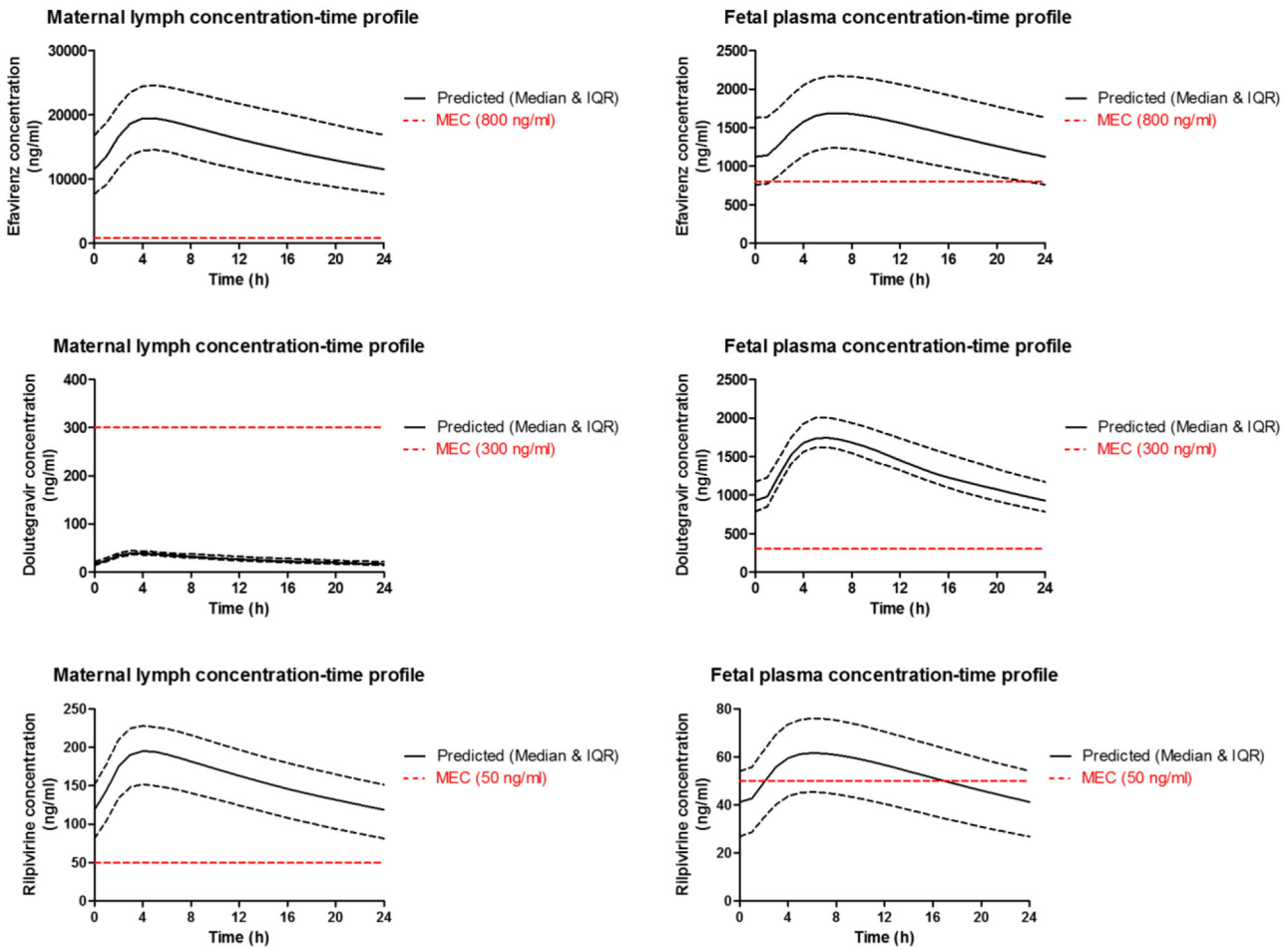

FIGURE 4 | Median (IQR) Predicted maternal plasma and lymph; and fetal plasma concentration-time profile following standard dose of 600 mg efavirenz, 50 mg dolutegravir, and 25 mg rilpivirine in third trimester. Dotted line represent the reported minimum effective concentration (MEC) for each drug at the standard dose.

it takes for the drug concentration to persist above the MEC in the maternal lymph and fetal plasma after dose cessation in third trimester. Model-predicted efavirenz and rilpivirine maternal lymph concentration remained above MEC for 150 and 56 h, respectively, but dolutegravir concentration was persistently below the MEC. In fetal plasma however, dolutegravir and efavirenz were above MEC for 36 and 66 h, respectively, but rilpivirine concentration persisted below the MEC (**Table 6**).

DISCUSSION

Our extended m-f-PBPK model which incorporated lymphatic circulation into an existing whole-body pregnancy model was successfully used to predict maternal lymph and fetal plasma pharmacokinetics of the ARVs efavirenz, dolutegravir, and rilpivirine. Model predictions for maternal plasma pharmacokinetics during the third trimester and infant delivery drug exposures were within 1.08–1.99 average fold difference of clinical data. Predicted maternal lymph-to-plasma AUC ratio was highest for efavirenz at 6.4, followed by rilpivirine at 1.7 and lowest for dolutegravir at 0.016. Model-predicted fetal plasma-to-maternal plasma AUC ratios were 0.59 for efavirenz, 0.78 for dolutegravir, and 0.57 for rilpivirine. The median predicted lymph concentration at 24 h after dose was above the published MEC for efavirenz and rilpivirine only. The predicted low lymphoid tissue penetration of dolutegravir appears to be significantly counterbalanced by its extended dose forgiveness (42 h compared with 12 h for efavirenz and 0 h for rilpivirine) and adequate fetal compartment exposure. Hence, it is unlikely to be a predictor of maternal virological failure or mother-to-child transmission risks.

Although ART suppresses plasma viraemia below the limit of detection, persistence of latent but replication-competent HIV in sanctuary tissues during active treatment constitutes a challenge in HIV cure research (38). Despite lymphoid tissues having the highest proportion of latent HIV (14, 15), no comprehensive assessment of lymph pharmacokinetics of ARVs in humans (pregnant and non-pregnant) is available due to the invasiveness of the conventional lymph node aspiration technique. Although, a number of studies have used *in-vitro*, *ex-vivo*, and *in vivo* animals models to determine lymphatic exposure of efavirenz, dolutegravir, and rilpivirine (16, 24, 67), such models are known

TABLE 5 | Predicted median (IQR) maternal plasma and lymph in third trimester; and fetal plasma pharmacokinetic parameters of efavirenz, dolutegravir and rilpivirine.

	Pharmacokinetic parameters		
	AUC (ng.h/mL)	**Cmax (ng/mL)**	**C24 (ng/mL)**
Efavirenz 600 mg ($n = 50$)			
Maternal Plasma	58,120 (41,149–78,030)	3,270 (2,478–4,035)	1,724 (1,132–2,547)
Maternal Lymph	373,790 (264,477–502,688)	19,470 (14,560–24,579)	11,514 (7,666–16,852)
Lymph-to-plasma AUCratio	6.431		
Fetal Plasma	34,404 (24,236–46,364)	1,689 (1,235–2,170)	1,123 (758.4–1,630)
Fetal-to-plasma ratio	0.5919		
Dolutegravir 50 mg ($n = 50$)			
Maternal Plasma	41,166 (36,660–48,827)	2,899 (2,707–3,259)	1,035 (865.3–1,313)
Maternal Lymph	643.7 (571.7–759.9)	39.26 (35.74–44.01)	16.96 (14.29–21.49)
Lymph-to-plasma ratio	0.0156		
Fetal Plasma	32,152 (28,905–38,541)	1,742 (1,620–2,007)	927.4 (784.7–1,170)
Fetal-to-plasma ratio	0.781		
Rilpivirine 25 mg ($n = 50$)			
Maternal Plasma	22,05 (1,649–2,674)	121.8 (96.71–141.4)	66.91 (45.01–85.67)
Maternal Lymph	3,788 (2,841–4,592)	195.1 (151.8–227.8)	118.8 (81.43–151.4)
Lymph-to-plasma ratio	1.717		
Fetal Plasma	1,263 (888.5–1,591)	61.66 (45.46–76.0)	41.26 (26.83–54.11)
Fetal-to-plasma ratio	0.573		

TABLE 6 | Predicted maternal lymph and fetal plasma dose forgiveness of 600 mg efavirenz, 50 mg dolutegravir and 25 mg rilpivirine during third trimester.

$n = 50$	**Efavirenz**	**Dolutegravir**	**Rilpivirine**
Maternal Lymph			
Duration of action (h)	150	0	56
Dosing interval (h)	24	24	24
Forgiveness (h)	126	0	32
Forgiveness index	5.25	0	1.33
Fetal Plasma			
Duration of action (h)	36	66	0
Dosing interval (h)	24	24	24
Forgiveness (h)	12	42	0
Forgiveness index	0.5	1.75	0

to be inadequate representations of what is expected in humans. It is known that suboptimal adherence to ART may lead to subtherapeutic drug levels in the systemic circulation, stimulating latent HIV in lymphoid tissues to resume active replication, thereby causing viral rebound (19). Detectable viral load is a known risk factor for MTCT and optimal adherence during pregnancy remains critical.

Administration of ARVs during pregnancy has several benefits, notably PMTCT which may be partly due to fetal prophylactic pre-exposure to ARVs. Past studies have relied on umbilical cord blood concentration at delivery to measure the extent of fetal exposure of ARVs. This method has limitations such as single time-point measurement and sample-time variation relative to maternal dosing. In this study, the infant plasma concentration prediction was validated with efavirenz and dolutegravir clinical data for infant washout in non-breastfed babies 2–10 h post-delivery. Post-delivery scenarios were simulated by stopping maternal dosing at term, and then estimating median fetal concentration after 2–10 h. The results were within the acceptable 2-fold difference for efavirenz and dolutegravir. The validated model was applied to rilpivirine and its fetal plasma concentration-time profile was also predicted successfully. The predicted fetal-to-maternal plasma ratio of efavirenz, dolutegravir, and rilpivirine were 0.591, 0.781 and 0.573, respectively. The predicted median fetal concentration at 24 h was higher than MEC for efavirenz (1,123 vs. 800 ng/mL) and dolutegravir (927.4 vs. 300 ng/mL), but lower for rilpivirine (41.26 vs. 50 ng/mL). Differential concentrations of efavirenz, dolutegravir and rilpivirine in maternal lymph and fetal plasma is, to a certain extent, as a result of differences in their physicochemical properties such as plasma protein binding, log P, molecular weight, and pKa (68–70). For instance, high pKa, log P and hydrophobicity of efavirenz were identified to be responsible for high penetration of efavirenz into human lymphoid endothelial cells compared to dolutegravir (24).

Our present study predicted C_{trough} of 992 ng/mL and AUC of 46,114 ng/mL for dolutegravir in non-pregnant women, these are similar to predictions by Freriksen et al. (71), and Liu et al. (72)

respectively, and are within 1.5-fold error to clinically observed data of the drug. This further indicated a strong reliability in the non-pregnant model and the confidence to extend it to incorporate the pregnancy model. Furthermore, the maternal dolutegravir PK parameters during pregnancy predicted by the model employed in this present study were similar to those predicted by Liu et al. (72). Additionally, the predicted fetal exposure to dolutegravir in the present study was comparable to that reported by Freriksen et al. (71). Although, fetal-to-maternal AUC plasma exposure ratio was predicted in our study, it was assumed to be similar to and within the range of the cord blood-to-maternal blood concentration ratios predicted in their study and observed clinical data. Likewise, the C_{max} and the C_{min} of the maternal plasma concentration predicted by our model was lower and higher, respectively, in comparison to their reported values (71). Further studies are still suggested to establish this assumption of similarity.

Dose forgiveness was used to estimate how long it would take for drug concentration in maternal lymph and fetal plasma to reduce below MEC in non-adhering pregnant mothers. Efavirenz and rilpivirine lymph concentrations remained above MEC for 126 and 32 h, respectively; efavirenz may therefore offer a longer protection in lymph against latent HIV in non-adhering pregnant women. While this may be an advantage, the ability of wild-type HIV to develop resistance to efavirenz monotherapy is of concern (67). Therefore, further investigation is required to know the extent of lymph exposure of tenofovir and emtricitabine which are commonly used in combination with efavirenz. In fetal plasma, efavirenz and dolutegravir concentration remained above MEC for 12 and 42 h, respectively. These results showed that efavirenz and rilpivirine may offer adequate protection against viral rebound from the maternal lymph nodes, but in rare situations where the virus enters the systemic circulation, efavirenz and dolutegravir may offer adequate fetal pre-exposure prophylaxis. Longer dose forgiveness of dolutegravir in fetal plasma offers sustained pre-exposure prophylaxis to fetus in pregnant women with suboptimal adherence. These results do not reflect the enzyme induction or inhibition effect of other drugs used as combination therapy. Therefore, interpretation of these results may be limited clinically.

Although, the current model reliably predicted lymphatic and fetal exposure to efavirenz, dolutegravir, and rilpivirine during the third trimester, a number of limitations are identifiable. Firstly, our model did not account for the possible role of transporter activities in placental drug transfer due to lack of sufficient data for model parameterization. The use of data from cell lines expressing relevant transporters such the BeWo monolayer are possible options to mechanistically describe these processes. Unfortunately, these data are not currently available in the literature and thus the option of relying only on passive processes for our predictions. Additionally, such models do not adequately recapitulate these processes in humans. The inclusion of drug transporters and associated variability in their expression can potentially improve the accuracy of model predictions, particularly for drugs that are substrates for these transporters. Secondly, due to lack of data we relied on key assumptions supported by sensitivity analyses for placental diffusion constants of study drugs. Model predictions were fitted to clinically observed infant plasma concentration at delivery. While this resulted in adequate predictions of infant exposure of the study drugs at delivery, further enhancement is desirable in future studies. Thirdly, there was no previous study to validate rilpivirine infant washout data. The validated model with available clinical data on infant washout for efavirenz and dolutegravir was extended to predict for rilpivirine. Furthermore, there are no clinical data available in humans to validate the predictions of the lymphatic model. Although lymph exposure data are available from *ex-vivo*, *in-vitro*, and animal studies, we could not rely on them to assess the predictive performance of the lymphatic model due to well-established inter-species variation.

In conclusion, predictions from our extended m-f-PBPK model showed differences in the distribution of efavirenz, rilpivirine, and dolutegravir into the lymph during pregnancy and the fetal compartment. Importantly, the inclusion of dose forgiveness predictions indicate alignment with recommendations of no dose adjustment despite moderate changes in exposure during pregnancy observed in clinical studies. This is an important new application of PBPK modeling strategy to evaluate the adequacy of drug exposure in an otherwise inaccessible compartment.

DATA AVAILABILITY STATEMENT

The original contributions presented in the study are included in the article/**Supplementary Material**, further inquiries can be directed to the corresponding author/s.

AUTHOR CONTRIBUTIONS

All co-authors contributed equally to the conception of the ideas presented here, the conduct of the research, and the preparation of this manuscript.

SUPPLEMENTARY MATERIAL

The Supplementary Material for this article can be found online at: https://www.frontiersin.org/articles/10.3389/fped.2021.734122/full#supplementary-material

REFERENCES

1. Dooley KE, Denti P, Martinson N, Cohn S, Mashabela F, Hoffmann J, et al. Pharmacokinetics of efavirenz and treatment of HIV-1 among pregnant women with and without tuberculosis coinfection. *J Infect Dis.* (2015) 211:197–205. doi: 10.1093/infdis/jiu429
2. Mulligan N, Best BM, Wang J, Capparelli EV, Stek A, Barr E, et al. Dolutegravir pharmacokinetics in pregnant and postpartum women living with HIV. *AIDS.* (2018) 32:729–37. doi: 10.1097/QAD.0000000000001755
3. Osiyemi O, Yasin S, Zorrilla C, Bicer C, Hillewaert V, Brown K, et al. Pharmacokinetics, antiviral activity, and safety of rilpivirine in pregnant

women with hiv-1 infection: results of a phase 3b, multicenter, open-label study. *Infect Dis Ther.* (2018) 7:147–59. doi: 10.1007/s40121-017-0184-8
4. Colbers A, Greupink R, Burger D. Pharmacological considerations on the use of antiretrovirals in pregnancy. *Curr Opin Infect Dis.* (2013) 26:575–88. doi: 10.1097/QCO.0000000000000017
5. Nduati R, John G, Mbori-Ngacha D, Richardson B, Overbaugh J, Mwatha A, et al. Effect of breastfeeding and formula feeding on transmission of HIV-1: a randomized clinical trial. *JAMA.* (2000) 283:1167–74. doi: 10.1001/jama.283.9.1167
6. Zorrilla CD, Wright R, Osiyemi OO, Yasin S, Baugh B, Brown K, et al. Total and unbound darunavir pharmacokinetics in pregnant women infected with HIV-1: results of a study of darunavir/ritonavir 600/100 mg administered twice daily. *HIV Med.* (2014) 15:50–6. doi: 10.1111/hiv.12047
7. Kreitchmann R, Best BM, Wang J, Stek A, Caparelli E, Watts DH, et al. Pharmacokinetics of an increased atazanavir dose with and without tenofovir during the third trimester of pregnancy. *JAIDS J Acquired Immune Defic Syndr.* (2013) 63:59–66. doi: 10.1097/QAI.0b013e318289b4d2
8. Tubiana R, Le Chenadec J, Rouzioux C, Mandelbrot L, Hamrene K, Dollfus C, et al. Factors associated with mother-to-child transmission of HIV-1 despite a maternal viral load <500 copies/ml at delivery: a case-control study nested in the French Perinatal cohort (EPF-ANRS CO1). *Clin Infect Dis.* (2010) 50:585–96. doi: 10.1086/650005
9. Launay O, Tod M, Tschöpe I, Si-Mohamed A, Bélarbi L, Charpentier C, et al. Residual HIV-1 RNA and HIV-1 DNA production in the genital tract reservoir of women treated with HAART: the prospective ANRS EP24 GYNODYN study. *Antiviral Ther.* (2011) 16:843–52. doi: 10.3851/IMP1856
10. European Collaborative Study. Mother-to-child transmission of HIV infection in the era of highly active antiretroviral therapy. *Clin Infect Dis.* (2005) 40:458–65. doi: 10.1086/427287
11. Quinn TC, Wawer MJ, Sewankambo N, Serwadda D, Li C, Wabwire-Mangen F, et al. Viral load and heterosexual transmission of human immunodeficiency virus type 1. Rakai Project Study Group. *N Engl J Med.* (2000) 342:921–9. doi: 10.1056/NEJM200003303421303
12. Eisele E, Siliciano RF. Redefining the viral reservoirs that prevent HIV-1 eradication. *Immunity.* (2012) 37:377–88. doi: 10.1016/j.immuni.2012.08.010
13. Jilek BL, Zarr M, Sampah ME, Rabi SA, Bullen CK, Lai J, et al. A quantitative basis for antiretroviral therapy for HIV-1 infection. *Nat Med.* (2012) 18:446–51. doi: 10.1038/nm.2649
14. Estes JD, Kityo C, Ssali F, Swainson L, Makamdop KN, Del Prete GQ, et al. Defining total-body AIDS-virus burden with implications for curative strategies. *Nat Med.* (2017) 23:1271–6. doi: 10.1038/nm.4411
15. Henrich TJ, Deeks SG, Pillai SK. Measuring the size of the latent human immunodeficiency virus reservoir: the present and future of evaluating eradication strategies. *J Infect Dis.* (2017) 215:S134–41. doi: 10.1093/infdis/jiw648
16. Burgunder E, Fallon JK, White N, Schauer AP, Sykes C, Remling-Mulder L, et al. Antiretroviral drug concentrations in lymph nodes: a cross-species comparison of the effect of drug transporter expression, viral infection, and sex in humanized mice, nonhuman primates, and humans. *J Pharmacol Exp Ther.* (2019) 370:360–8. doi: 10.1124/jpet.119.259150
17. Embretson J, Zupancic M, Ribas JL, Burke A, Racz P, Tenner-Racz K, et al. Massive covert infection of helper T lymphocytes and macrophages by HIV during the incubation period of AIDS. *Nature.* (1993) 362:359–62. doi: 10.1038/362359a0
18. Pantaleo G, Graziosi C, Demarest JF, Butini L, Montroni M, Fox CH, et al. HIV infection is active and progressive in lymphoid tissue during the clinically latent stage of disease. *Nature.* (1993) 362:355–8. doi: 10.1038/362355a0
19. Barton K, Winckelmann A, Palmer S. HIV-1 reservoirs during suppressive therapy. *Trends Microbiol.* (2016) 24:345–55. doi: 10.1016/j.tim.2016.01.006
20. Rothenberger MK, Keele BF, Wietgrefe SW, Fletcher CV, Beilman GJ, Chipman JG, et al. Large number of rebounding/founder HIV variants emerge from multifocal infection in lymphatic tissues after treatment interruption. *Proc Natl Acad Sci USA.* (2015) 112:E1126–34. doi: 10.1073/pnas.1414926112
21. Kuo HH, Lichterfeld M. Recent progress in understanding HIV reservoirs. *Curr Opin HIV AIDS.* (2018) 13:137–42. doi: 10.1097/COH.0000000000000441
22. Kulpa DA, Chomont N. HIV persistence in the setting of antiretroviral therapy: when, where and how does HIV hide? *J Virus Erad.* (2015) 1:59–68. doi: 10.1016/S2055-6640(20)30490-8
23. Fletcher CV, Podany AT. Antiretroviral drug penetration into lymphoid tissue. In: Hope TJ, Stevenson M, Richman D, editors. *Encyclopedia of AIDS.* New York, NY: Springer (2014). pp. 1–9.
24. Dyavar SR, Gautam N, Podany AT, Winchester LC, Weinhold JA, Mykris TM, et al. Assessing the lymphoid tissue bioavailability of antiretrovirals in human primary lymphoid endothelial cells and in mice. *J Antimicrob Chemother.* (2019) 74:2974–8. doi: 10.1093/jac/dkz273
25. Thompson CG, Cohen MS, Kashuba ADM. Antiretroviral pharmacology in mucosal tissues. *J Acquired Immune Defic Syndr.* (2013) 63:S240–S7. doi: 10.1097/QAI.0b013e3182986ff8
26. Fletcher CV, Staskus K, Wietgrefe SW, Rothenberger M, Reilly C, Chipman JG, et al. Persistent HIV-1 replication is associated with lower antiretroviral drug concentrations in lymphatic tissues. *Proc Natl Acad Sci USA.* (2014) 111:2307–12. doi: 10.1073/pnas.1318249111
27. Zhang Z, Unadkat JD. Development of a novel maternal-fetal physiologically based pharmacokinetic model II: verification of the model for passive placental permeability drugs. *Drug Metab Dispos.* (2017) 45:939–46. doi: 10.1124/dmd.116.073957
28. Atoyebi SA, Rajoli RKR, Adejuyigbe E, Owen A, Bolaji O, Siccardi M, et al. Using mechanistic physiologically-based pharmacokinetic models to assess prenatal drug exposure: thalidomide versus efavirenz as case studies. *Eur J Pharmaceut Sci.* (2019) 140:105068. doi: 10.1016/j.ejps.2019.105068
29. De Sousa Mendes M, Lui G, Zheng Y, Pressiat C, Hirt D, Valade E, et al. A physiologically-based pharmacokinetic model to predict human fetal exposure for a drug metabolized by several CYP450 pathways. *Clin Pharmacokinet.* (2017) 56:537–50. doi: 10.1007/s40262-016-0457-5
30. Schalkwijk S, Buaben AO, Freriksen JJM, Colbers AP, Burger DM, Greupink R, et al. Prediction of fetal darunavir exposure by integrating human *ex-vivo* placental transfer and physiologically based pharmacokinetic modeling. *Clin Pharmacokinet.* (2018) 57:705–16. doi: 10.1007/s40262-017-0583-8
31. Bosgra S, van Eijkeren J, Bos P, Zeilmaker M, Slob W. An improved model to predict physiologically based model parameters and their inter-individual variability from anthropometry. *Crit Rev Toxicol.* (2012) 42:751–67. doi: 10.3109/10408444.2012.709225
32. Zhang Z, Imperial MZ, Patilea-Vrana GI, Wedagedera J, Gaohua L, Unadkat JD. Development of a novel maternal-fetal physiologically based pharmacokinetic model I: insights into factors that determine fetal drug exposure through simulations and sensitivity analyses. *Drug Metab Dispos Biol Fate Chem.* (2017) 45:920–38. doi: 10.1124/dmd.117.075192
33. ICRP. Basic anatomical and physiological data for use in radiological protection: reference values: ICRP Publication 89. *Ann ICRP.* (2002) 32:5–265. doi: 10.1016/S0146-6453(03)00002-2
34. Rajoli RKR, Back DJ, Rannard S, Freel Meyers CL, Flexner C, Owen A, et al. Physiologically based pharmacokinetic modelling to inform development of intramuscular long-acting nanoformulations for HIV. *Clin Pharmacokinet.* (2015) 54:639–50. doi: 10.1007/s40262-014-0227-1
35. Fandaruff C, Segatto Silva MA, Galindo Bedor DC, de Santana DP, Rocha HVA, Rebuffi L, et al. Correlation between microstructure and bioequivalence in Anti-HIV Drug Efavirenz. *Eur J Pharmaceut Biopharmaceut.* (2015) 91:52–8. doi: 10.1016/j.ejpb.2015.01.020
36. Australian Government Department of Health. *Australian Public Assessment Report for Dolutegravir* (as *Sodium)* (2014).
37. van 't Klooster G, Hoeben E, Borghys H, Looszova A, Bouche MP, van Velsen F, et al. Pharmacokinetics and disposition of rilpivirine (TMC278) nanosuspension as a long-acting injectable antiretroviral formulation. *Antimicrob Agents Chemother.* (2010) 54:2042–50. doi: 10.1128/AAC.01529-09
38. Davey RT, Bhat N, Yoder C, Chun TW, Metcalf JA, Dewar R, et al. HIV-1 and T cell dynamics after interruption of highly active antiretroviral therapy (HAART) in patients with a history of sustained viral suppression. *Proc Natl Acad Sci USA.* (1999) 96:15109–14. doi: 10.1073/pnas.96.26.15109
39. Song I, Borland J, Chen S, Peppercorn A, Wajima T, Piscitelli SC. Effect of fosamprenavir-ritonavir on the pharmacokinetics of dolutegravir in healthy subjects. *Antimicrob Agents Chemother.* (2014) 58:6696–700. doi: 10.1128/AAC.03282-14
40. Néant N, Gattacceca F, Lê MP, Yazdanpanah Y, Dhiver C, Bregigeon S, et al. Population pharmacokinetics of Rilpivirine in HIV-1-infected patients treated with the single-tablet regimen rilpivirine/tenofovir/emtricitabine. *Eur J Clin Pharmacol.* (2018) 74:473–81. doi: 10.1007/s00228-017-2405-1

41. Abduljalil K, Furness P, Johnson TN, Rostami-Hodjegan A, Soltani H. Anatomical, physiological and metabolic changes with gestational age during normal pregnancy: a database for parameters required in physiologically based pharmacokinetic modelling. *Clin Pharmacokinet.* (2012) 51:365–96. doi: 10.2165/11597440-000000000-00000
42. Sutton MS, Groves A, MacNeill A, Sharland G, Allan L. Assessment of changes in blood flow through the lungs and foramen ovale in the normal human fetus with gestational age: a prospective Doppler echocardiographic study. *Br Heart J.* (1994) 71:232–7. doi: 10.1136/hrt.71.3.232
43. Moore JE, Bertram CD. Lymphatic system flows. *Ann Rev Fluid Mech.* (2018) 50:459–82. doi: 10.1146/annurev-fluid-122316-045259
44. Gill KL, Gardner I, Li L, Jamei M. A Bottom-up whole-body physiologically based pharmacokinetic model to mechanistically predict tissue distribution and the rate of subcutaneous absorption of therapeutic proteins. *AAPS J.* (2016) 18:156–70. doi: 10.1208/s12248-015-9819-4
45. Niederalt C, Kuepfer L, Solodenko J, Eissing T, Siegmund HU, Block M, et al. A generic whole body physiologically based pharmacokinetic model for therapeutic proteins in PK-Sim. *J Pharmacokinet Pharmacodyn.* (2018) 45:235–57. doi: 10.1007/s10928-017-9559-4
46. Griffiths SK, Campbell JP. Placental structure, function and drug transfer. *Continuing Educ Anaesth Crit Care Pain.* (2015) 15:84–9. doi: 10.1093/bjaceaccp/mku013
47. Margaris KN, Black RA. Modelling the lymphatic system: challenges and opportunities. *J R Soc Interface.* (2012) 9:601–12. doi: 10.1098/rsif.2011.0751
48. Sloas DC, Stewart SA, Sweat RS, Doggett TM, Alves NG, Breslin JW, et al. Estimation of the pressure drop required for lymph flow through initial lymphatic networks. *Lymph Res Biol.* (2016) 14:62–9. doi: 10.1089/lrb.2015.0039
49. Molina DK, DiMaio VJM. Normal organ weights in women: part II-the brain, lungs, liver, spleen, and kidneys. *Am J Forensic Med Pathol.* (2015) 36:182–7. doi: 10.1097/PAF.0000000000000175
50. Molina DK, DiMaio VJM. Normal organ weights in men: part I-the heart. *Am J Forensic Med Pathol.*. (2012) 33:362–7. doi: 10.1097/PAF.0b013e31823d298b
51. Archie JG, Collins JS, Lebel RR. Quantitative standards for fetal and neonatal autopsy. *Am J Clin Pathol.* (2006) 126:256–65. doi: 10.1309/FK9D5WBA1UEPT5BB
52. Cerrone M, Wang X, Neary M, Weaver C, Fedele S, Day-Weber I, et al. Pharmacokinetics of Efavirenz 400 mg once daily coadministered with isoniazid and rifampicin in human immunodeficiency virus–infected individuals. *Clin Infect Dis.* (2019) 68:446–52. doi: 10.1093/cid/ciy491
53. Aouri M, Barcelo C, Guidi M, Rotger M, Cavassini M, Hizrel C, et al. Population pharmacokinetics and pharmacogenetics analysis of rilpivirine in HIV-1-infected individuals. *Antimicrob Agents Chemother.* (2016) 61:e00899-16. doi: 10.1128/AAC.00899-16
54. Dailly E, Allavena C, Grégoire M, Reliquet V, Bouquié R, Billaud E, et al. Influence of nevirapine administration on the pharmacokinetics of dolutegravir in patients infected with HIV-1. *J Antimicrob Chemother.* (2015) 70:3307–10. doi: 10.1093/jac/dkv245
55. Villani P, Regazzi MB, Castelli F, Viale P, Torti C, Seminari E, et al. Pharmacokinetics of efavirenz (EFV) alone and in combination therapy with nelfinavir (NFV) in HIV-1 infected patients. *Br J Clin Pharmacol.* (1999) 48:712–5. doi: 10.1046/j.1365-2125.1999.00071.x
56. Dickinson L, Amin J, Else L, Boffito M, Egan D, Owen A, et al. Pharmacokinetic and pharmacodynamic comparison of once-daily efavirenz (400 mg vs. 600 mg) in treatment-naïve HIV-infected patients: results of the ENCORE1 study. *Clin Pharmacol Therapeut.* (2015) 98:406–16. doi: 10.1002/cpt.156
57. Elliot ER, Cerrone M, Challenger E, Else L, Amara A, Bisdomini E, et al. Pharmacokinetics of dolutegravir with and without darunavir/cobicistat in healthy volunteers. *J Antimicrob Chemother.* (2019) 74:149–56. doi: 10.1093/jac/dky384
58. Song I, Borland J, Chen S, Patel P, Wajima T, Peppercorn A, et al. Effect of food on the pharmacokinetics of the integrase inhibitor dolutegravir. *Antimicrob Agents Chemother.* (2012) 56:1627–9. doi: 10.1128/AAC.05739-11
59. Crauwels H, Vingerhoets J, Ryan R, Witek J, Anderson D. Pharmacokinetic parameters of once-daily rilpivirine following administration of efavirenz in healthy subjects. *Antiviral Ther.* (2011) 17:439–46. doi: 10.3851/IMP1959
60. Lamorde M, Walimbwa S, Byakika-Kibwika P, Katwere M, Mukisa L, Sempa JB, et al. Steady-state pharmacokinetics of rilpivirine under different meal conditions in HIV-1-infected Ugandan adults. *J Antimicrob Chemother.* (2015) 70:1482–6. doi: 10.1093/jac/dku575
61. Olagunju A, Bolaji O, Amara A, Waitt C, Else L, Adejuyigbe E, et al. Breast milk pharmacokinetics of efavirenz and breastfed infants' exposure in genetically defined subgroups of mother-infant pairs: an observational study. *Clin Infect Dis.* (2015) 61:453–63. doi: 10.1093/cid/civ317
62. Cressey TR, Stek A, Capparelli E, Bowonwatanuwong C, Prommas S, Sirivatanapa P, et al. Efavirenz pharmacokinetics during the third trimester of pregnancy and postpartum. *JAIDS J Acquired Immune Defic Syndr.* (2012) 59:245–52. doi: 10.1097/QAI.0b013e31823ff052
63. Kreitchmann R, Schalkwijk S, Best B, Wang J, Colbers A, Stek A, et al. Efavirenz pharmacokinetics during pregnancy and infant washout. *Antiviral Ther.* (2019) 24:95–103. doi: 10.3851/IMP3283
64. Bollen P, Freriksen J, Konopnicki D, Weizsäcker K, Hidalgo Tenorio C, Moltó J, et al. The effect of pregnancy on the pharmacokinetics of total and unbound dolutegravir and its main metabolite in women living with human immunodeficiency virus. *Clin Infect Dis.* (2021) 72:121–7. doi: 10.1093/cid/ciaa006
65. Tran AH, Best BM, Stek A, Wang J, Capparelli EV, Burchett SK, et al. Pharmacokinetics of rilpivirine in HIV-infected pregnant women. *JAIDS J Acquired Immune Defic Syndr.* (2016) 72:289–96. doi: 10.1097/QAI.0000000000000968
66. Schalkwijk S, Colbers A, Konopnicki D, Gingelmaier A, Lambert J, van der Ende M, et al. Lowered rilpivirine exposure during the third trimester of pregnancy in human immunodeficiency virus type 1–infected women. *Clin Infect Dis.* (2017) 65:1335–41. doi: 10.1093/cid/cix534
67. Clotet B. Efavirenz: resistance and cross-resistance. *Int J Clin Pract Suppl.* (1999) 103:21–5.
68. Pacifici GM, Nottoli R. Placental transfer of drugs administered to the mother. *Clin Pharmacokinet.* (1995) 28:235–69. doi: 10.2165/00003088-199528030-00005
69. Ali Khan A, Mudassir J, Mohtar N, Darwis Y. Advanced drug delivery to the lymphatic system: lipid-based nanoformulations. *Int J Nanomed.* (2013) 8:2733–44. doi: 10.2147/IJN.S41521
70. Kashuba ADM, Dyer JR, Kramer LM, Raasch RH, Eron JJ, Cohen MS. Antiretroviral-drug concentrations in semen: implications for sexual transmission of human immunodeficiency virus type 1. *Antimicrob Agents Chemother.* (1999) 43:1817–26. doi: 10.1128/AAC.43.8.1817
71. Freriksen JJM, Schalkwijk S, Colbers AP, Abduljalil K, Russel FGM, Burger DM, et al. Assessment of maternal and fetal dolutegravir exposure by integrating *ex vivo* placental perfusion data and physiologically-based pharmacokinetic modeling. *Clin Pharmacol Therapeut.* (2020) 107:1352–61. doi: 10.1002/cpt.1748
72. Liu XI, Momper JD, Rakhmanina NY, Green DJ, Burckart GJ, Cressey TR, et al. Prediction of maternal and fetal pharmacokinetics of dolutegravir and raltegravir using physiologically based pharmacokinetic modeling. *Clin Pharmacokinet.* (2020) 59:1433–50. doi: 10.1007/s40262-020-00897-9

Conflict of Interest: The authors declare that the research was conducted in the absence of any commercial or financial relationships that could be construed as a potential conflict of interest.

Publisher's Note: All claims expressed in this article are solely those of the authors and do not necessarily represent those of their affiliated organizations, or those of the publisher, the editors and the reviewers. Any product that may be evaluated in this article, or claim that may be made by its manufacturer, is not guaranteed or endorsed by the publisher.

frontiers in Pediatrics

ORIGINAL RESEARCH
published: 23 September 2021
doi: 10.3389/fped.2021.730383

Evaluation of Placental Transfer and Tissue Distribution of *cis*- and *Trans*-Permethrin in Pregnant Rats and Fetuses Using a Physiological-Based Pharmacokinetic Model

Stéphane Personne[1,2], *Céline Brochot*[2], *Paulo Marcelo*[3], *Aurélie Corona*[1], *Sophie Desmots*[2], *Franck Robidel*[2], *Anthony Lecomte*[2], *Véronique Bach*[1] *and Florence Zeman*[2]*

[1] *Péritox, UMR_I 01, Université de Picardie Jules Verne, Amiens, France,* [2] *Institut National de l'Environnement Industriel et des Risques (INERIS), Unité Toxicologie Expérimentale et Modélisation (TEAM), Parc ALATA BP2, Verneuil en Halatte, France,* [3] *Plateforme ICAP, ICP FR CNRS 3085, Université de Picardie Jules Verne, Amiens, France*

OPEN ACCESS

Edited by:
André Dallmann, Bayer, Germany

Reviewed by:
Raju Prasad Sharma, Leiden University, Netherlands
Steven Jan Van Cruchten, University of Antwerp, Belgium

***Correspondence:**
Florence Zeman
florence.zeman@ineris.fr

Specialty section:
This article was submitted to Obstetric and Pediatric Pharmacology, a section of the journal Frontiers in Pediatrics

Received: *24 June 2021*
Accepted: *24 August 2021*
Published: *23 September 2021*

Citation:
Personne S, Brochot C, Marcelo P, Corona A, Desmots S, Robidel F, Lecomte A, Bach V and Zeman F (2021) Evaluation of Placental Transfer and Tissue Distribution of cis- and Trans-Permethrin in Pregnant Rats and Fetuses Using a Physiological-Based Pharmacokinetic Model. Front. Pediatr. 9:730383. doi: 10.3389/fped.2021.730383

Biomonitoring studies have highlighted the exposure of pregnant women to pyrethroids based on the measurement of their metabolites in urine. Pyrethroids can cross the placental barrier and be distributed in the fetus as some pyrethroids were also measured in the meconium of newborns. Prenatal exposure to pyrethroids is suspected to alter the neurodevelopment of children, and animal studies have shown that early life exposure to permethrin, one of the most commonly used pyrethroid in household applications, can alter the brain development. This study aimed to characterize the fetal permethrin exposure throughout gestation in rats. We developed a pregnancy physiologically based pharmacokinetic (pPBPK) model that describes the maternal and fetal kinetics of the *cis*- and *trans*- isomers of permethrin during the whole gestation period. Pregnant Sprague–Dawley rats were exposed daily to permethrin (50 mg/kg) by oral route from the start of gestation to day 20. Permethrin isomers were quantified in the feces, kidney, mammary gland, fat, and placenta in dams and in both maternal and fetal blood, brain, and liver. *Cis*- and *trans*-permethrin were quantified in fetal blood and tissues, with higher concentrations for the *cis*-isomer. The pPBPK model was fitted to the toxicokinetic maternal and fetal data in a Bayesian framework. Several parameters were adjusted, such as hepatic clearances, partition coefficients, and intestinal absorption. Our work allowed to estimate the prenatal exposure to permethrin in rats, especially in the fetal brain, and to quantitatively estimate the placental transfer. These transfers could be extrapolated to humans and be incorporated in a human pPBPK model to estimate the fetal exposure to permethrin from biomonitoring data.

Keywords: pesticides, PBPK model, permethrin, pyrethroids, rat, pregnancy, fetus, brain

INTRODUCTION

Pyrethroids are the most commonly used group of insecticides with a wide range of applications in agricultural, commercial, industrial, and residential settings. They are also used in veterinary and human medicine and for public health vector control (1). Given their broad spectrum of applications and the restriction of other classes of insecticides, their use has increased over the years, exposing a large population worldwide (2, 3). In humans, pyrethroids are rapidly metabolized in the gastro-intestinal tract and the liver and excreted as metabolites in urine (4). Permethrin metabolism involved hydrolysis by carboxylesterases and oxidation by cytochrome P450 enzymes. The exposure of human populations to pyrethroids is often based on the measurement of five urinary biomarkers: *cis*- and *trans*-3-(2,2-dichlorovinyl)-2,2-dimethyl-(1-cyclopropane) carboxylic acid, 4-fluoro-3-phenoxybenzoic acid, 3-(2,2-dibromovinyl)-2,2-dimethyl cyclopropane carboxylic acid, and 3-phenoxybenzoic acid (3-PBA). Biomonitoring studies in pregnant women have shown a widespread exposure to pyrethroids in many countries (5–11), which increased with the use of domestic insecticides (12). Pyrethroids can cross the placenta and have been measured in cord blood at delivery (7, 13, 14) and in the meconium (15–17).

According to the Developmental Origin of Health and Disease hypothesis, exposure to environmental toxicants during fetal development and childhood can contribute to the development of chronic diseases, including neurodevelopmental disorders in later stages of life (18). The nervous system is particularly vulnerable during the critical window of prenatal development due to high cellular plasticity and the differentiation of neurons or glial cells at this stage (19). Fetal exposure to pyrethroids during this critical period of brain development is of concern and could impact child neurodevelopment (20). Associations between prenatal exposure to pyrethroids and child neurobehavioral disorders have been investigated in limited studies (21–28). A positive association between pyrethroid pesticides and autism spectrum disorder, attention deficit hyperactivity disorder, or neurocognitive development has only been observed in a few studies (21, 26, 27). However, human exposure was based on the assessment of urinary metabolites, which can be common to several pyrethroids (29) and may not reflect the internal effective dose of the fetus in target tissues during critical time windows.

Among pyrethroids, permethrin [3-phenoxybenzyl (*1RS*, *3RS*;*1RS*, *3SR*)-*cis*, *trans*-3-(2,2-dichlorovinyl)-2,2-dimethylcyclopropanecarboxylate] is one of the most frequently used pyrethroids (30, 31). Permethrin is composed of a mixture of *cis*- and *trans*-isomers. Experimental studies in rodents have shown that prenatal exposure to permethrin can alter neurodevelopment and cognitive abilities (32–36). To better understand the exposure dose–response relationship, it is critical to determine the concentration of the active compound in the brain, the target tissue. Physiologically based pharmacokinetic (PBPK) models can be used to simulate internal dosimetry from an external dose and can support the extrapolations between species based on the physiological and biochemical differences (37). PBPK models for permethrin have been developed in rats (38–40) and humans at different life stages (30, 38, 40–43) but did not cover prenatal life.

In this paper, we present the development of a pregnancy pPBPK model in rats to predict the kinetic of permethrin isomers in fetal tissues and their capacity to reach the developing brain. The proposed model is an extension of our previous PBPK model for permethrin in adult rats (38). An experimental toxicokinetic study was performed in pregnant rats after single and repeated dose administrations until the end of gestation. The measured concentrations in blood and several organs and tissues were used to calibrate the gestation PBPK model in a Bayesian framework.

MATERIALS AND METHODS

Toxicokinetic Studies in Rats

Chemicals

Cis-permethrin and *trans*-permethrin were obtained from Dr. Ehrenstorfer (Augsburg, Germany). The internal standards, $^{13}C_6$-*cis*-permethrin and $^{13}C_6$–*trans*-permethrin, were purchased from Cambridge Isotope Laboratories (Andover, MA, USA).

For the toxicokinetic studies, permethrin in powder form (99% purity, 40 and 60% of *cis* and *trans*-isomers, respectively) was also purchased from Dr. Ehrenstorfer. Corn oil was acquired from Sigma-Aldrich (St. Quentin Fallavier, France).

Animals and Experimental Design

Our experimental protocol was approved by a regional ethics committee on experiments using animals (CREMEAP no. 96) and the French Ministry of Research with the permit number 01812.01. Sprague–Dawley female rats were housed with adult males overnight (Janvier Labs, Le Genest Saint Isle, France) after a minimum of 5 days of acclimatization. Mating was confirmed by a microscopic analysis of vaginal smears on the following morning. The day when a positive vaginal smear was observed was considered as day 0 of gestation. The female rats weighed 277 ± 27 g [mean body weight (BW) ± standard deviation (SD)] at day 0. Each pregnant rat was housed in a cage with a 12-h light/12-h dark cycle. Temperature and relative humidity were maintained at 22 ± 2°C and 55 ± 15%, respectively. The animals were provided with food (Altromin rodent diet for growing animals, Genestril, Royaucourt, France) and tap water *ad libitum*. The pregnant rats were dosed orally daily by gavage with 50 mg/kg permethrin dissolved in corn oil (2 ml/kg) from the first day of gestation until the day of sacrifice at gestational day (GD) 1, GD15, or GD20. GD15 and GD20 were selected to characterize the kinetic profile in rats during the last week of pregnancy as the placental and conceptus weights increase exponentially during this period. Groups of four animals were sacrificed at 1, 2, 3, 4, 6, 10, and 24 h post-dose by an overdose intra-peritoneal injection of pentobarbital at each gestational day. The dose of 50 mg/kg (40:60 cis/trans), corresponding to 20 and 30 mg/kg of the *cis*- and *trans*-isomer, respectively, was similar to the 25 mg/kg dose used by Willemin et al. (38) in the same strain of rat. The mean body weights at GD15 and GD20 were 356 ± 24 and 422 ± 28 g, respectively, and the mean number of fetuses per litter was 13.5 ± 2.

Sample Collection and Chemical Analyses

At each time point, blood, whole brain, kidneys, liver, mammary glands, and abdominal fat were collected. For blood, formic acid (1%) was added v/v to blood to inhibit the metabolism of permethrin by carboxylesterases. At GD1 and GD15, the pregnant rats were kept in individual metabolic cages for 24 h to collect the feces. The placentas were collected at GD15 and GD20. Fetal blood, liver, and brain were collected at GD20. The placenta and fetal samples were pooled by litter to provide an adequate sample size for analysis. All samples were stored at −80°C until analysis.

Extraction and analyses were performed by liquid chromatography–tandem mass spectrometry (LC-MS/MS) according to the analytical method developed by our team (44). Briefly, samples of 500 mg were used except for mammary gland, fat, and feces, where a sample of 50 mg was used. For blood, an aliquot of 1.5 ml was used. The samples were transferred in vials and spiked with $^{13}C_6$-*trans*-permethrin as surrogate standard. Extraction was performed by liquid–liquid extraction using acetone/hexane (2:8, vol/vol) with three consecutive extractions. The combined organic phases were evaporated to dryness under nitrogen before reconstitution for LC-MS/MS analysis. For fat, mammary gland, and feces, an additional purification step was performed using a blend of Sepra ZT-WAX and Na_2SO_4. All dried extracts were then reconstituted in 500 µL of acetonitrile and transferred to autosampler vials with the addition of $^{13}C_6$-*cis*-permethrin as the internal standard. The analysis was conducted with an Acquity UPLC® H-Class (Waters) coupled to a triple quadrupole mass spectrometer Xevo TQ-S (Waters) with a HSS T3 column (1.8 µm; 100 | 2.1 mm, Waters). The limits of quantification (LOQs) for *cis*-permethrin were 4 ng/g in placenta and feces, 20 ng/g in the liver, brain, fat, and mammary gland, 40 ng/g in the kidneys, and 26 ng/ml in blood. The LOQs for *trans*-permethrin were 20 ng/g in the brain and placenta, 40 ng/g in feces, 80 ng/g in the liver, kidney, fat, and mammary gland, and 52 ng/ml in blood.

Model Development

Model Structure

The adult male rat PBPK model for permethrin, as published by Willemin et al. (38), was extended to include gestation. The gestational PBPK model includes a maternal sub-model and a fetal sub-model that are linked via the placenta (**Figure 1**). The maternal sub-model includes the same 10 compartments as the adult male model by Willemin et al. (38) (blood, brain, liver, muscle, kidney, fat, stomach, intestinal lumen, and slowly perfused and rapidly perfused tissues) except that the testes compartment was removed and the mammary gland was added as a compartment. All the model equations can be found in the former paper. The fetal sub-model includes four compartments: blood, liver, brain, and a lumped compartment for the rest of the body. All fetuses from a single litter were modeled as one large fetal model.

In pregnant rats, oral absorption was modeled using a two-compartment model with the stomach and gastro-intestinal tract and a single constant of absorption (K_{aI}) located in the GI tract. Distribution in compartments was assumed to be limited by diffusion in the brain, muscle, fat, kidney, slowly perfused tissues, and mammary tissues because of the lipophilicity of permethrin and of the experimental observations in animals. For the intestines, liver, rapidly perfused tissue, and placenta, the distribution was blood flow-limited. Similar to the adult model, permethrin is metabolized in blood and liver and excreted in feces. Fetal exposure was through the placenta with transfers described as bi-directional between the placenta and the fetal blood. Placental transfer was modeled as a diffusion process with a first-order rate constant (*Ktrans1* and *Ktrans2*), and the amount of *cis*- or *trans*-permethrin in the placenta (A_{Pla}) was given by:

$$\frac{d(A_{Pla})}{dt} = Q_{Pla} \times \left(C_{Art} - \frac{C_{Pla}}{PC_{Pla}} \right) - Ktrans1 \times \frac{C_{Pla}}{PC_{Pla}} + Ktrans2 \times C_{Art,F}$$

where Q_{Pla} is the blood flow to the placenta, C_{Art} and C_{Pla} are the maternal arterial and placental concentrations, PC_{Pla} is the placenta/blood partition coefficient, and $C_{Art,F}$ is the arterial concentration in the fetus. The distribution in fetal compartments was assumed to be flow-limited, with the exception of the brain. Fetal metabolism was assumed to be

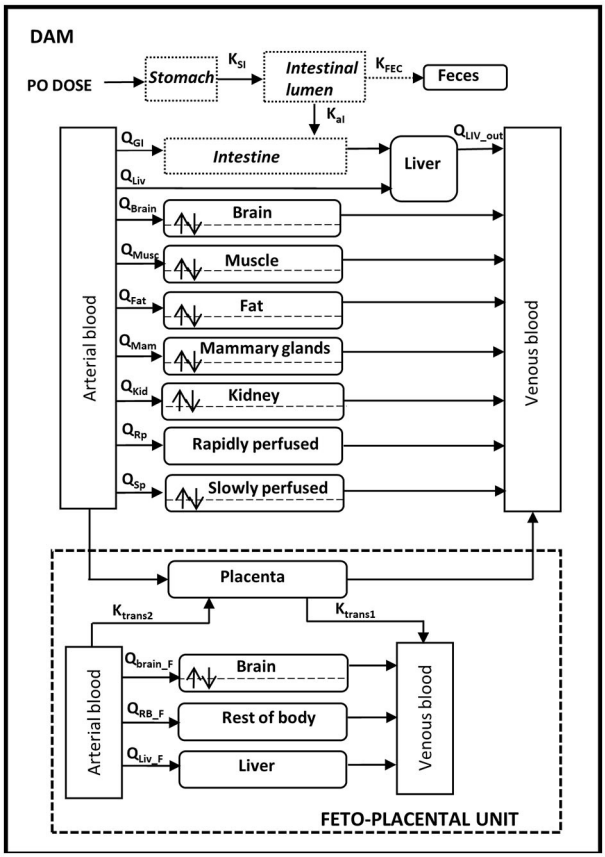

FIGURE 1 | Physiologically based pharmacokinetic model of *cis*- and *trans*-permethrin in pregnant rats and fetuses.

TABLE 1 | Physiological parameters of the maternal and fetal physiologically based pharmacokinetic models for *cis*- and *trans*-permethrin.

Parameters	Value	Source
Pregnant rats		
Body weight (BW, kg)	0.277–0.422[a]	This study
Cardiac output index (QCI, L/h/kg)	24.56–21.6[a]	Dowell and Kauer (45)
Tissue volumes (fraction of initial BW, unitless)		
Blood (V_{Blood})	0.06	Brown et al. (46)
GI tract (V_{GI})	0.027	Brown et al. (46)
Liver (V_{Liv})	0.0351	This study
Muscle (V_{Musc})	0.404	Brown et al. (46)
Brain (V_{Brain})	0.0073	Brown et al. (46)
Kidney (V_{Kid})	0.0076	Brown et al. (46)
Non-perfused (V_{NP})	0.05	Brown et al. (46)
Rapidly perfused (V_{RP})	0.046	Brown et al. (46)
Slowly perfused (V_{SP})	1—all organs, non-perfused	
Tissue volume (changing during gestation, L)		
Mammary gland (V_{Mam})	0.0024–0.013[a]	Hanwell and Linzell (47); Rosso et al. (48)
Fat (V_{Fat})	0.017–0.024[a]	Brown et al. (46); Naismith et al. (49)
Placenta (V_{Pla})	0–0.167[a]	Clewell (50); O'Flaherty et al. (51); Yoon et al. (52)
Blood flows (fraction of initial cardiac output, unitless)		
Liver (total) (Q_{Livout})	0.174	Brown et al. (46)
Portal (GI tract) (Q_{GI})	0.151	Brown et al. (46)
Arterial (GI tract) (Q_{Liv})	0.024	Brown et al. (46)
Muscle (Q_{Musc})	0.278	Brown et al. (46)
Brain (Q_{Brain})	0.02	Brown et al. (46)
Kidney (Q_{Kid})	0.141	Brown et al. (46)
Slowly perfused (Q_{Rp})	0.063	Brown et al. (46)
Blood flow (changing during gestation, L/h)		
Mammary gland (Q_{Mam})	0.012–0.064[a]	Hanwell and Linzell (47)
Fat (Q_{Fat})	0.21–0.29[a]	Clewell (50); O'Flaherty et al. (51); Yoon et al. (52)
Placenta (Q_{Pla})	0–1.42[a]	Clewell (50); O'Flaherty et al. (51); Yoon et al. (52)
Rapidly perfused (Q_{Rp})	Difference between cardiac output and the sum of the other tissue blood flows	
Blood volume (fraction of tissue, unitless)		
Brain (BV_{Brain})	0.03	Brown et al. (46)
Muscle (BV_{Musc})	0.04	Tornero-Velez et al. (40)
Kidney (BV_{Kid})	0.16	Brown et al. (46)
Fat (BV_{Fat})	0.02	Tornero-Velez et al. (40)
Mammary glands (BV_{Mam})	0.02	Assimilated to fat
Fetuses		
Body weight for individual fetus (V_{1Fet}, kg)	0–0.0068[a]	Sikov and Thomas (53)
Cardiac output index (QCI_{1F}, L/h/kg)	22.8	Girard et al. (54); Yoon et al. (52)
Tissue volumes (fraction of BW)		
Blood (V_{Blood_1F})	0.0676	Brown et al. (46)
Tissue volume (changing during fetal growth, L)		
Brain (V_{Brain_1F})	0–0.0034	Sikov and Thomas (53)
Liver (V_{Liv_1F})	0–0.0044	Sikov and Thomas (53)
Rest of the body (V_{RB_1F})	BW—sum of other tissue volumes	
Tissue blood flow (fraction of cardiac output)		
Brain (Q_{Brain_1F})	0.1055	Carter and Gu (55); Yoon et al. (52)

(Continued)

TABLE 1 | Continued

Parameters	Value	Source
Liver (Q_{Liv_1F})	0.061	Itskovitz et al. (56); Yoon et al. (52)
Rest of the body (Q_{RB_1F})	Cardiac output—sum of other tissue blood flows	
Blood volume (fraction of tissue)		
Brain (BV_{Brain_1F})	0.03	Set to adult value from Willemin et al. (38)
Rest of the body (BV_{RB_1F})	0.05	Set to adult value from Willemin et al. (38)

[a] *Range during the gestation period.*

negligible. The model structure is identical for both isomers. The model code is provided in the **Supplementary Material**.

Model Parameterization

Physiological Parameters

The physiological parameters (cardiac output, blood flow, and tissue volume) for the pregnant dam and the fetus are summarized in **Table 1** and were obtained from the literature or measured in this study. The model accounted for the gestation-induced changes in maternal tissue volumes and fetal growth during the whole gestation period. The equations used for the growth of maternal and fetal tissues and also the changes in blood flows occurring during gestation can be found in **Supplementary Table S1**.

Chemical Specific Parameters

Chemical specific parameters for pregnant dams and fetuses were estimated using the measured concentrations in our toxicokinetic study, with the exception of the rate constants for absorption and for blood and intestinal metabolism. The parameters were estimated simultaneously in a Bayesian calibration framework using our experimental data. Separate calibrations were performed with data generated at GD1 or at GD15/GD20 after repeated daily administration. In a Bayesian approach, all parameters are considered as random variables. A prior distribution was defined for each parameter based on the knowledge on the values of the parameter. In conjunction with a likelihood function of the data, a posterior distribution was determined by random sampling methods (57).

For absorption, two metabolic rate constants are considered in the model: the intestinal absorption rate constant (K_{aI}) and the stomach–intestine transfer rate constant (K_{sI}). As it was not possible to estimate both parameters based on our experimental data, the K_{aI} values of the adult model of Willemin et al. (38) were used. Only the K_{sI} values were estimated as K_{sI} is considered as a sensitive parameter according to previous PBPK models published for pyrethroids (58). For metabolic clearances, as the liver is the main site of metabolism (59), only metabolic rate constants for permethrin isomers in the liver were estimated. Blood and intestinal rate constant values were set to the optimized values of the adult model of Willemin et al. (38).

A truncated normal distribution was assigned to the parameters for which values were reported in previous PBPK models for permethrin in adult rats (38, 40). The mean values of the prior distribution were taken from the PBPK model of Willemin et al. (38), with the exception of the liver clearance for which the values of the PBPK model of Tornero et al. (40) were used. For all other parameters, a uniform distribution was applied. The coefficients of variation were set to 50% for all parameters. The prior distributions of all parameters are reported in **Table 2**. The likelihood of the data was assumed to follow a lognormal distribution with 15% of error. The posterior distributions were estimated by Markov Chain Monte Carlo simulations using MCSim (ver.5.6.6) software. Three independent Markov chains of 10,000 iterations were run, and one in two of the last 4,000 iterations were recorded to check the convergence using the potential scale reduction factor $\hat{R}$. An acceptable convergence was considered as reached when the $\hat{R}$ value was 1.2 or less (60).

Sensitivity Analyses

A global sensitivity analysis (GSA) using the Sobol method was conducted on the PBPK model to identify the compound-specific parameters that have the most impact on the internal maternal and fetal exposures of permethrin (*cis*-isomer) following the same exposure scenario of the *in vivo* experiments. Three model outputs were selected: the arterial concentrations of the mother and the fetus and the concentration in the fetal brain. Truncated normal distributions were assigned to the specific compound parameters, with a mean estimated mean value (**Table 2**) and a coefficient of variation of 30%. The SA was run at three time points at GD15 and GD20 (4, 6, and 12 h after the oral administration). The SA results are presented as two indices: the first order index, which is the variance contribution of one parameter to the total model variance, and the total order index, which is the result of the main effect of the parameter and of its interactions with the other parameters.

RESULTS

Toxicokinetic Profiles in Pregnant Rats and Fetuses

In pregnant rats, *cis*-permethrin was quantified in blood, feces, and all tissues after a single administration at GD1 and

TABLE 2 | Distribution of the chemical specific parameters of the model for permethrin isomers in pregnant rats and fetuses.

Parameters	Prior distribution		Posterior distribution		
	***cis*-Permethrin**	***trans*-Permethrin**		***cis*-Permethrin**	***trans*-Permethrin**
Pregnant dam					
Partition coefficients					
Liver: blood (PC_{Liv})	0.89 ± 0.445 (10^{-3}-20)	(10^{-3}-20)	GD1	**2.33** (2.14–2.61)	–
			GD15/20	**1.48** (1.37–1.61)	**1.36** (1.19–1.61)
GI: blood (PC_{GI})	Equal to PC_{Kid}	Equal to PC_{Kid}	–	–	–
Fat: blood (PC_{Fat})	225 ± 112.5 (5–900)	76 ± 38 (5–900)	GD1	**345** (195–592)	**60.5** (28.9–154)
			GD15/20	**545** (414–744)	**165** (119–234)
Mammary gland: blood (PC_{Mam})	225 ± 112.5 (5–900)	76 ± 38 (5–900)	GD1	**212** (65.8–487)	**5.09** (5–5.52)
			GD15/20	**436** (312–654)	**46.7** (42.9–52.1)
Muscle: blood (PC_{Musc})	Fixed to 1.2	Fixed to 0.82	–	–	–
Brain: blood (PC_{Brain})	1.60 ± 0.80 (10^{-3}-20)	0.57 ± 0.285 (10^{-3}-20)	GD1	**2.67** (2.37–3.12)	**0.72** (0.39–1.34)
			GD15/20	**1.15** (1.08–1.26)	**0.64** (0.58–0.73)
Kidney: blood (PC_{Kid})	1.10 ± 0.55 (10^{-3}-20)	Fixed to 0.21	GD1	**5.61** (5.09–6.30)	–
			GD15/20	**3.00** (2.78–3.32)	–
Placenta: blood (PC_{Pla})	(10^{-3}-20)	(10^{-3}-20)	GD15/20	**3.52** (3.14–4.03)	**3.00** (2.67–3.47)
Slowly perfused: blood (PC_{Sp})	19 ± 9.50 (10^{-3}-20)	8.4 ± 4.20 (10^{-3}-20)	GD1	**14.7** (5.5–20.0)	**9.5** (3.2–18.8)
			GD15/20	**4.55** (3.42–6.21)	**1.55** (0.35–12.8)
Rapidly perfused: blood (PC_{Rp})	Fixed to 1.1	Fixed to 0.21	–	–	–
Permeability coefficients (L/h)					
Brain (PS_{Brain})	1.0. ± 0.5.10^{-3} (10^{-5}-1)	1.2. ± 0.6.10^{-3} (10^{-5}-1)	GD1	**5.6.10^{-3}**(5.2–6.3.10^{-3})	**1.6.10^{-3}**(1.1–2.6.10^{-3})
			GD15/20	**3.5.10^{-3}**(3.1–4.1.10^{-3})	**2.2.10^{-3}**(1.8–2.8.10^{-3})
Kidney (PS_{Kid})	(10^{-5}-1)	(10^{-5}-1)	GD1	**1.3.10^{-2}**(1–2.10^{-2})	**1.3.10^{-2}**(1–2.10^{-2})
			GD15/20	**0.24** (0.14–0.3)	**0.24** (0.14–0.3)
Fat (PS_{Fat})	4.8 ± 2.4.10^{-2} (10^{-5}-1)	0.11 ± 0.055 (10^{-5}-1)	GD1	**0.10** (0.09–0.11)	**0.07** (0.06–0.09)
			GD15/20	**4.5.10^{-2}**(4–5.4.10^{-2})	**9.2.10^{-3}**(8.3–10.6.10^{-3})
Mammary gland (PS_{Mam})	(10^{-5}-1)	(10^{-5}-1)	GD1	**0.252** (0.23–0.283)	**0.522** (0.443–0.631)
			GD15/20	**0.125** (0.112-0.147)	**0.253** (0.172–0.368)
Muscle (PSMusc)	Fixed to 0.32	Fixed to 0.48	–	–	–
Slowly perfused (PS_{Sp})	0.31 ± 0.055 (10^{-5}-1)	0.065 ± 0.032 (10^{-5}-1)	GD1	**0.20** (0.02–0.55)	**0.07** (0.02–0.15)
			GD15/20	**0.79** (0.58–0.99)	**0.11** (0.03–0.19)
Rate constant (h^{-1})					
Stomach–intestine transfer (K_{si})	0.35 ± 0.175 (0–2)	0.20 ± 0.10 (0–2)	GD1	**0.15** (0.14–0.16)	**0.058** (0.043-0.071)
			GD15/20	**0.18** (0.17–0.19)	**0.084** (0.075–0.096)
Intestinal absorption (K_{ai})	Fixed to 0.52	Fixed to 1.30	–	–	–
Fecal excretion (K_{Fec})	0.39 ± 0.195 (0–2)	0.85 ± 0.42 (0–2)	GD1	**0.07** (0.06–0.10)	**0.09** (0.07–0.12)
			GD15/20	**0.020** (0.018–0.024)	**0.033** (0.028–0.040)
Metabolic clearance (L/h/kg)					
Intestinal metabolism (CL_{GI})	Fixed to 0.04	Fixed to 0.3	–	–	–
Blood metabolism (CL_{Blood})	Fixed to 0.07	Fixed to 0.29	–	–	–
Liver metabolism (CL_{Liv})	6.20 ± 3.10 (1–15)	24.30 ± 12.15 (1–50)	GD1	**8.44** (7.92–9.10)	**19.4** (15.7–23.6)
			GD15/20	**2.40** (2.3–2.6)	**20.5** (19.3–22.2)
Placental transfer (L/h/kg $^{0.75}$)					
Dam to fetus (scK_{trans1})	(0–6)	(0–6)		**1.91** (1.39–2.65)	**1.91** (1.39–2.65)
Fetus to dam (scK_{trans2})	(0–6)	(0–6)		**2.52** (1.85–3.22)	**2.52** (1.85–3.22)
Fetuses					
Partition coefficients					
Liver: blood (PC_{Liv_F})	(10^{-3}-20)	(10^{-3}-20)		**5.41** (4.97–6.11)	**5.41** (4.97–6.11)
Brain: blood (PC_{Brain_F})	(10^{-3}-20)	(10^{-3}-20)		**2.01** (1.84–2.24)	**2.01** (1.84–2.24)
Rest of the body: blood (PC_{RB_F})	(10^{-3}-900)	(10^{-3}-900)		**57.20** (45–75.5)	**57.20** (45–75.5)
Permeability coefficients (L/h)					
Brain (PS_{Brain_F})	(10^{-5}-1)	(10^{-5}-1)		**7.9.10^{-3}**(5.9–14.2.10^{-3})	**7.9.10^{-3}** (5.9–14.2.10^{-3})

Posterior distributions are represented by mean (value in bold) with the 2.5th and 97.5th percentiles.

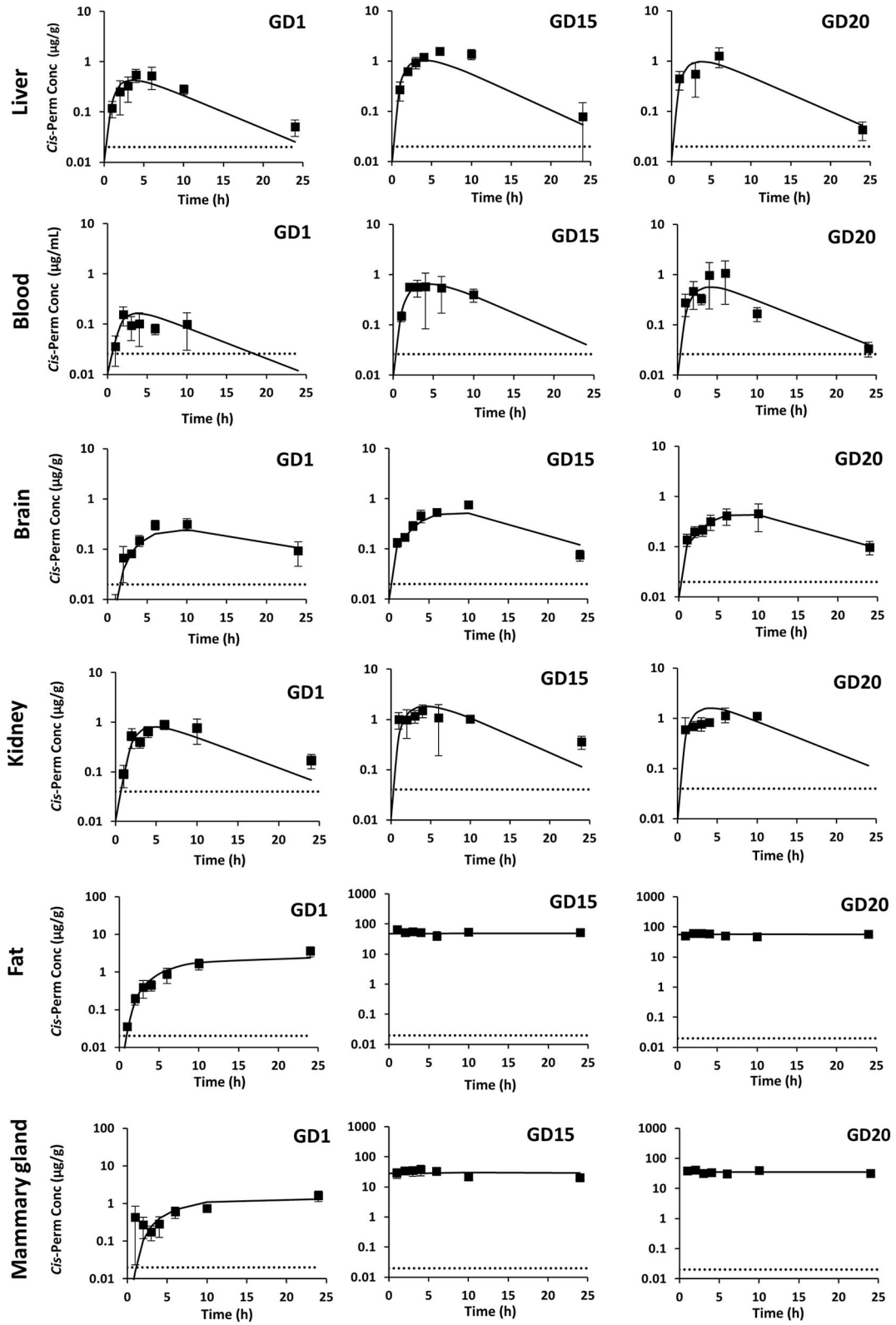

FIGURE 2 | Measured concentrations (squares) and toxicokinetic profiles estimated with the physiologically based pharmacokinetic model (solid line) of *cis*-permethrin in pregnant rats at GD1, GD15, and GD20. The gray dotted line stands for the limit of quantification.

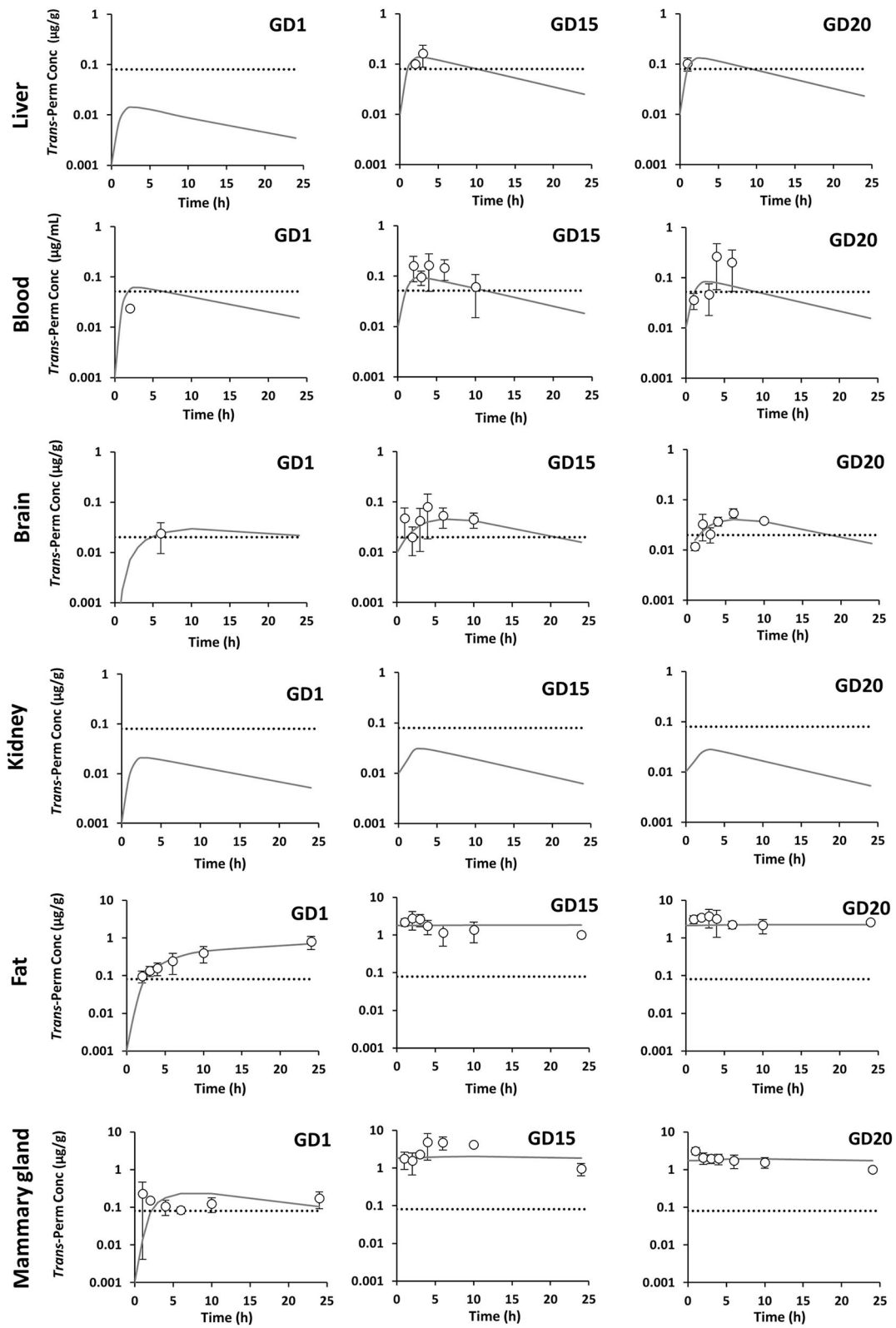

FIGURE 3 | Measured concentrations (dots) and toxicokinetic profiles estimated with the physiologically based pharmacokinetic model (solid line) of *trans*-permethrin in pregnant rats at GD1, GD15, and GD20. The gray dotted line stands for the limit of quantification.

repeated administrations until GD15 and GD20. Because *trans*-permethrin is eliminated more rapidly from the body than *cis*-permethrin, *trans*-permethrin was not quantified in several samples. Quantification was performed at the three time points studied (GD1, GD15, and GD20) in fat, mammary gland, and feces and only performed at GD15 and GD20 in blood, brain, and liver. *Trans*-permethrin was not quantified in the kidneys. For the samples where compounds were detected but below the LOQ, the concentration was set to LOQ/2. The kinetic profiles of *cis*- and *trans*-permethrin in blood and tissues at GD1, GD15, and GD20 in pregnant rats are presented in **Figures 2**, **3**, respectively. *Cis*-permethrin was quantified in placenta, fetal blood, fetal liver, and fetal brain, whereas *trans*-permethrin could only be quantified in placenta and fetal

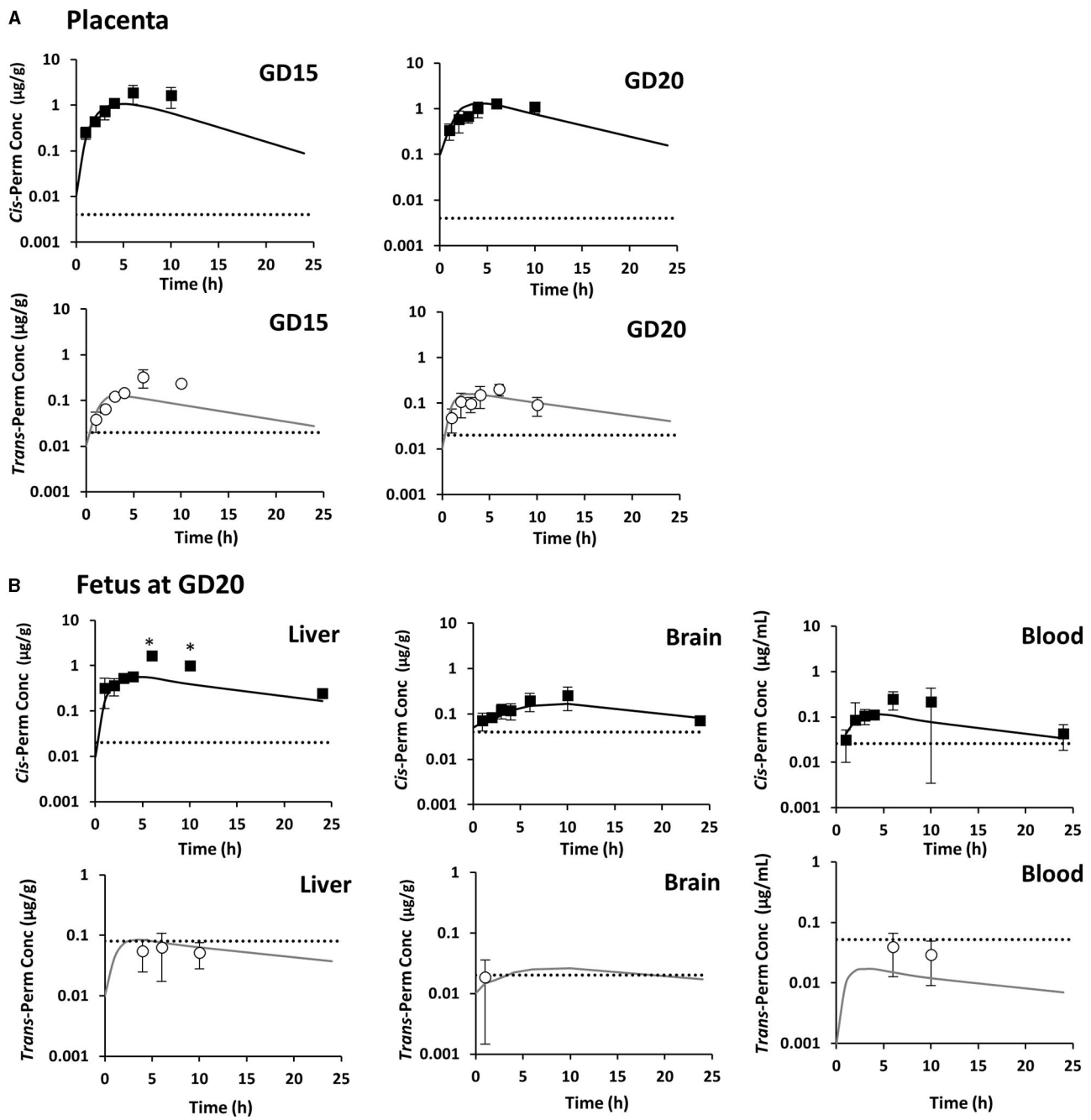

FIGURE 4 | Measured concentrations of *cis*-permethrin (squares) and *trans*-permethrin (dots) and toxicokinetic profiles estimated with the physiologically based pharmacokinetic model (solid lines) in the placenta **(A)** and fetal tissues **(B)**. Mean values ± SD for $n = 4$ at each time point except for the point marked with an asterisk ($n = 1$). The gray dotted line stands for the limit of quantification.

TABLE 3 | Maximum time concentration (T_{max}, h)/half-lives ($T_{1/2}$, h) of *cis*- and *trans*-permethrin in the blood and tissues of pregnant rats at GD1, GD15, and GD20.

	***cis*-Permethrin**						***trans*-Permethrin**					
	GD1		**GD15**		**GD20**		**GD1**		**GD15**		**GD20**	
	T_{max}	$T_{1/2}$	T_{max}	$T_{1/2}$	T_{max}	$T_{1/2}$	T_{max}	$T_{1/2}$	T_{max}	$T_{1/2}$	T_{max}	$T_{1/2}$
Blood	6	3.7	4	2.6	6	3.6	–	–	4	3.2	4	–[a]
Liver	4	5.7	6	3.4	6	3.7	–	–	3	–[a]	–	–
Brain	10	7.9	10	4.2	10	6.3	–	–	4	5.4	2	–[a]
Kidney	6	6.5	4	6.7	6	–[a]	–	–	–	–	–	–
Fat	24	–[a]	1	–[a]	2	–[a]	10	–[a]	3	–[a]	3	–[a]
Mammary gland	24	–[a]	4	–[a]	10	–[a]	1	–[a]	4	–[a]	1	–[a]
Placenta	na	na	6	3.2	6	4.5	na	na	6	–[a]	6	–[a]

–[a], no half-life was computed due to insufficient data in the elimination phase.
na, not applicable.
–, no compound was quantified.

TABLE 4 | Area under the curve (μg h/ml or μg h/g) of the observed concentrations (AUC_{obs}) and the estimated concentrations (AUC_{est}) for *cis*-permethrin in the blood and tissues of pregnant rats.

	GD1		**GD15**		**GD20**	
	AUC_{obs}	AUC_{est}	AUC_{obs}	AUC_{est}	AUC_{obs}	AUC_{est}
Blood	1.26	1.60	6.71	7.72	7.52	6.53
Liver	6.20	4.72	21.22	11.79	15.79	10.75
Brain	4.80	3.88	10.28	8.07	7.05	6.86
Kidney	12.89	9.45	20.34	21.59	–	18.26
Fat	43.97	37.18	1,247.08	1,171.88	1,260.18	1,357.83
Mammary gland	21.23	22.06	606.71	690.07	856.41	840.45
Placenta	na	na	23.92	12.80	17.67	16.13

–, no data available.
na, not applicable.

TABLE 5 | Area under the curve (μg h/ml or μg h/g) of the observed concentrations (AUC_{obs}) and the estimated concentrations (AUC_{est}) for *trans*-permethrin in the blood and tissues of pregnant rats.

	GD1		**GD15**		**GD20**	
	AUC_{obs}	AUC_{est}	AUC_{obs}	AUC_{est}	AUC_{obs}	AUC_{est}
Blood	–	0.42	1.18[a]	0.75	1.04[a]	0.61
Liver	–	–	–	1.54	–	0.95
Brain	–	0.52	0.77[a]	0.71	0.53[a]	0.59
Kidney	–	–	–	–	–	–
Fat	10.60[a]	10.06	34.41	44.10	61.77	53.29
Mammary gland	–	3.94	73.20	46.66	37.53	44.18
Placenta	na	na	–	1.72	–	2.26

[a]Value of extrapolated AUC.
na, not applicable.
–, no data available.

brain, even if it could be detected in fetal liver and blood (**Figure 4**).

For *cis*-permethrin, after a single administration at GD1, the maximal concentration (C_{max}) was reached between 4 and 6 h in blood, liver, and kidney and declined rapidly, with an observed half-life of 3.7, 5.7, and 6.5 h (**Table 3**). In the brain, fat, and mammary gland, a slower diffusion was observed, with the peak concentrations occurring later; at 10 h in the brain and at 24 h in fat and mammary gland. In the brain, the estimated half-life was 7.9 h. After repeated administration, there were no significant

changes in T_{max} values at GD15 and GD20. However, the values of half-life were reduced compared to GD1, with the lowest values reported at GD15.

In order to compare maternal and fetal exposure, the 24-h area under the curve (AUC_{obs}) for *cis*-permethrin in blood and tissues was computed using the measured concentrations in pregnant rats and fetuses and are presented in **Tables 4**, **6**, respectively. In pregnant dams, the fat and the mammary gland had the highest AUC_{obs}, which were respectively 44- and 21-fold higher to that in blood at GD1 (**Table 4**). No significant accumulation was observed after repeated administration in the kidney, liver, and brain, with AUC_{obs} ratios between GD1 and GD15 or GD20 values ranging from 1.5 to 3.4. On the contrary, in blood, fat, and mammary gland, the AUC_{obs} values at GD15 and GD20 were increased by 5.3- and 6-fold in blood, 28.4- and 28.7-fold in fat, and 28.6- and 40.3-fold in mammary gland compared to GD1. The AUC_{obs} in placenta for the *cis*-isomer was similar at GD15 and GD20 and was 3.6- and 2.3-fold the AUC_{obs} in blood, respectively (**Table 6**). In fetuses, the liver had the highest exposure, and the lowest exposure was observed in blood. The exposure in fetal blood and fetal brain was lower than the exposure of the dam to *cis*-permethrin. In the brain, the AUC ratio (fetus/dam) was 0.54. On the contrary, the exposure in the fetal liver was 1.6 times greater than the exposure of the dam in the liver.

Regarding *trans*-permethrin, the concentrations of the *trans*-isomer were always lower than those measured for the *cis*-isomer even if the administration of the *trans* isomer was slightly higher than the *cis*-isomer. For the *trans*-isomer, due to the low number of time points for which the concentration measured was above the LOQ, AUC_{obs} could only be estimated in pregnant rats at GD15 and GD20 in blood, brain, and fat and at GD1, GD15, and GD20 in the mammary gland (**Table 5**). The highest exposures were observed in fat and mammary gland as identified for the *cis*-isomer and were 29- and 62-fold and 59- and 36-fold the AUC_{obs} in blood at GD15 and GD20, respectively.

TABLE 6 | Area under the curve (μg h/ml or μg h/g) of the observed concentrations (AUC_{obs}) and the estimated concentrations (AUC_{est}) for *cis*-permethrin in fetal blood, liver, and brain.

	***cis*-Permethrin**	
	AUC_{obs}	**AUC_{est}**
Blood	3.35	1.66
Liver	17.86	8.18
Brain	3.83	2.94

Model Calibration

Convergence Analysis and Posterior Distributions

The convergence criterion $\hat{R}$ was computed for the three chains for all parameters calibrated with datasets of GD1 or GD15 and GD20. All the $\hat{R}$ values were below 1.2, indicating that the convergence was reached in both cases. The posterior distributions of the estimated parameters at GD1 or GD15/GD20 are reported in **Table 2** as the mean with 95% confidence interval. The means of the posterior distributions of the estimated parameters at GD1 or GD15/GD20 were compared to prior distribution and between them.

At GD1, the estimated means were close to prior estimates for tissue/blood partition coefficient (PC) in slowly perfused tissue for both isomers and for the hepatic clearance of the *trans*-isomer only. For the *cis*-isomer, the hepatic clearance was modestly increased by 36%. For all other parameters, the posterior means differed from their prior values. A decrease was observed for the parameters of absorption (K_{sI}) and fecal excretion (K_{Fec}), with a decrease of 57 and 72% for K_{sI} and 82 and 90% for K_{Fec} for *cis*- and *trans*-permethrin, respectively. On the contrary, the PC values were markedly increased for *cis*-permethrin. The mean PC values for the posterior distribution were 1.5-, 2.6-, and 5.1-fold higher than the prior mean values for fat, liver, and kidney.

When compared together, the estimated means at GD15 and GD20 were substantially different from those calibrated with concentration data at GD1, with the exception of K_{sI} values for both isomers and also hepatic clearance and PC in brain for *trans*-permethrin. The mean values of all parameters were decreased compared to GD1 values, with the exception of the PC in fat and mammary gland and permeability coefficients in slowly perfused tissue. For *cis*-permethrin, the hepatic clearance and fecal excretion were decreased by 3.5- and 3.6-fold, respectively. The PCs were decreased by a factor of 1.6, 1.9, 2.3, and 3.2 in the liver, kidney, brain, and slowly perfused tissues, respectively.

In fetuses, the PCs in the brain and liver were highest than their respective values in dams. Asymmetric placental rate constants were observed between maternal placenta and fetal blood, with the majority of the transfer being in the fetal-to-maternal direction. A 0.76 ratio was estimated between transfer rates from the dam to the fetus (scKTrans1) and from the fetus to the dam (scKTrans2).

Comparison of Predictions With Experimental Data

The experimental data at GD1, GD15, and GD20 were compared with the model predictions with estimated parameters at GD1 or at GD15 and GD20 (**Figures 2**–**4**). The estimated concentrations were generally in good agreement with the observed data in blood and tissues in dams. The estimated and observed AUC in pregnant rats and fetuses are reported in **Tables 4**–**6**. The estimated to observed AUC ratios for *cis*- and *trans*-permethrin were within a range between 0.5 and 1.5, indicating acceptable prediction results with the exception of fetal liver. For fetal liver, the AUC ratio was 0.46. However, at time points +6h and +10h, *cis*-permethrin was only quantifiable in one sample.

Using the model, it was possible to estimate AUC for *trans*-permethrin in pregnant rats notably after a single administration at GD1 even if the lack of measured concentrations prevents the computation of an observed AUC_{obs} (**Table 5**). At GD1, the tissue/blood ratios for AUC_{est} were 1.2 in the brain and 9.4 and 24 in mammary gland and fat, respectively. In fat and mammary gland, these

ratios were ∼2-fold lower than those observed with *cis*-permethrin, similar to the observed ratio in fat in toxicokinetic studies performed in male rats with permethrin (*cis*/*trans*, 40:60) (40).

Based on AUC_{est}, the AUC values for the *cis*-isomer were 3.7- to 5.6-fold greater than that of the *trans*-isomer in blood and tissues at GD1. At GD15 and GD20, the *cis*/*trans* AUC_{est} ratios were increased compared to those calculated at GD1.

Sensitivity Analyses

The GSA identified the parameters to which the maternal and fetal blood concentrations and fetal brain concentrations are sensitive at GD15 and GD20. Three parameters mostly influenced the maternal blood concentration at the three time points (4, 6, and 12 h after the oral administration), i.e., the hepatic clearance and absorption parameters, partition coefficient (**Supplementary Figure S1**). The influence of the other model parameters is quite negligible. Regarding the fetal dosimetry in blood and brain, the hepatic clearance is still the most influential parameter (**Supplementary Figures S2**, **S3**). The absorption parameters also have an impact on the blood concentration, with a decreasing influence over time. As it could have been expected, the fetal blood and brain concentrations are sensitive to the two parameters driving the placental transfer (K_{trans1} and K_{trans2}). Due to its high volume, the compartment "rest of the body" also influences the kinetics in fetal blood. In the brain, the partitioning in the tissues (PC_{BrainF}) and the permeability (PS_{BrainF}) become influential parameters. For all model outputs, the rankings of the parameters by the first order and total order indices were similar, and significant interactions were observed between the most influential parameters.

DISCUSSION

Gestation induces numerous physiological, biochemical, and metabolic changes that can affect the disposition of xenobiotics (61). Assessing the fetal exposure during the whole gestation will then require careful considerations of the maternal exposure. In this paper, we extended the structure of a PBPK model for permethrin in adult male rats (38, 40) to integrate the dynamic changes occurring during gestation. Published toxicokinetic data for permethrin isomers were obtained in male rats after a single-dose administration (38, 40, 62). The existence of gender differences in kinetics of pyrethroids has not been experimentally studied for the parent compounds but only for some metabolites, 3-phenoxybenzyl alcohol and 3-phenoxybenzaldehyde, in rats for which gender differences were observed (63). To characterize these potential differences for permethrin, we collected toxicokinetic data after a single oral dose at the first day of gestation (GD1), as the modifications due to gestation are supposed to be negligible at GD1.

Compared to the known toxicokinetic profile of permethrin in male rats, female rats demonstrated a similar hepatic clearance but with a slower absorption rate. Indeed the estimated stomach intestine rate transfers (K_{si}) in females were 2.3- and 3.6-fold lower compared to those in males for *cis*- and *trans*-permethrin, respectively. These results are in accordance with the sex differences in the gastrointestinal tract that have been reported in rats (64) and the higher gastric mucosal blood flow observed in male than in female rats (65).

Cis- and *trans*-permethrin were mainly distributed in tissues, with a high accumulation in fat and mammary glands. The estimated AUCs for *cis*- and *trans*-permethrin in blood (normalized by the dose) were similar to those reported by Tornero et al. (40) at 10 mg/kg but 2.7 and 5.7 lower than those reported in Willemin et al. (38) at 25 mg/kg for each isomer, respectively. However, in the study of Willemin et al., the blood concentrations exceeded the binding capacity of rat plasma, impacting the estimation of partition coefficients (66). In our study, the observed C_{max} in blood for *cis*-permethrin was 260 nM, in the linear range of the binding in plasma. Highest tissue/blood partitions coefficients were estimated in our study compared to those reported for males in the study of Tornero et al. (40). In rats, *cis*- and *trans*-permethrin are primarily bound by plasma proteins (50–60%) and, to a lesser amount, by lipoproteins (30–35%) (67). Sex differences in plasma apolipoprotein profiles have been reported in rats, with higher concentrations observed in males than in females (68), which could explain these differences observed between the studies.

Using estimated parameters at GD1, corresponding to a non-pregnant rat, the model was not able to capture the toxicokinetic at GD15 and GD20, demonstrating an impact of gestation on the toxicokinetic profile of permethrin. The main observed differences were related to hepatic clearance and tissue/blood PC. The predicted hepatic clearance of *cis*-permethrin at GD15 and GD20 was reduced by 3.5 compared to the prediction at GD1.

The calibration was performed in a Bayesian interference framework, allowing the integration of informative prior knowledge on the parameters and experimental data to optimize the model parameter values and inform on their variability. The sensitivity analysis identified hepatic clearance, absorption parameters, and partition coefficients as having the most impact on blood and brain concentrations. These results were in agreement with previously published sensitivity analyses on the kinetics of permethrin and deltamethrin in rodents or humans (41, 42, 58). Because the model was not able to capture the kinetics observed at GD1, GD15, and GD20 with the same set of parameter values, the model was calibrated independently with the data generated at GD1 after a single-dose administration and the data generated at GD15 or GD20 after repeated daily yielding to two different sets of parameters for GD1 and GD15/GD20. The main differences between these two sets of estimated values were related to the hepatic clearance and the tissue/blood partition coefficients. The predicted hepatic clearance of *cis*-permethrin at GD15 and GD20 was reduced by a 3.5 factor compared to the value estimated at GD1.

Gestation is associated with a small decrease in total rodent liver P450 content and/or activity (69, 70), which can explain these differences in the metabolic rate of the *cis*-isomer. For *trans*-permethrin, it was not possible to observe such a reduction due to the limited number of time points at which the isomer was quantified. The respective values of the PCs for fat and mammary gland were markedly increased by 1.6 and 2.1 for *cis*-permethrin and 2.7 and 9.2 for *trans*-permethrin. This evolution might be

explained by the fact that blood lipid levels can increase up to 4-fold during gestation (71) and affect the disposition of lipophilic compounds such as permethrin [log $P = 6.1$; (40)]. Moreover, maternal fat content progressively increases during gestation and mammary fat accumulation increases intensely from day 12 of gestation, contributing to maternal fat storage (48, 72). These differences in blood and tissue composition during the gestation may explain the changes in PC values and the changes in pharmacokinetic profile after chronic administration during the whole gestation, with a marked accumulation in fat tissues and mammary glands.

The other main objective of our PBPK model in rat was to predict the internal dose in the fetal brain to help in risk assessment. PBPK models allow inter-species extrapolations (73) and can be used to estimate human fetal exposure in inaccessible compartments such as the brain (74). The estimated concentrations in the fetal brain could aid in the selection of appropriate doses to investigate the neurodevelopmental toxicity using human *in vitro* systems. To assess exposure in the fetal brain and to facilitate its use in a risk assessment context, a compartmental structure was established for the fetal PBPK model, with mass communication via the blood–placenta barrier. Using estimated parameters in pregnant rats and fetuses, the model was able to reproduce correctly the kinetics of both *cis*- and *trans*-isomers in fetal blood and tissues even if *trans*-permethrin was only quantifiable in fetal brain due to analytical limitations. The fetal brain was exposed to permethrin, demonstrating that exposure during pregnancy is of concern for the developing brain even if fetal exposure was less than maternal exposure with a feto/maternal (FM) ratio of 0.54. In blood, the FM ratio was 0.25 for *cis*-permethrin, which is close to the FM ratio of 0.5 reported for cypermethrin, another pyrethroid in placental perfusion studies in humans (75). In our model, transfers from the placenta to the fetuses were considered as a simple diffusion with an estimated placental rate constant value from the dam to the fetuses of 1.91 $L/h/kg^{0.75}$. This value was close to that reported for other pesticides, such as atrazine in rats (76). However, the placental transfer of permethrin could also involve active transports, and further data are needed to characterize placental transfer.

In conclusion, we developed a gestation PBPK model in rats, allowing the identification of key parameters affecting maternal exposure to *cis*- and *trans*-permethrin during gestation and an accurate prediction of fetal brain tissue distribution in rats. In rodents, permethrin and other pyrethroids have shown neurodevelopmental effects. The interpretation of animal studies is challenging due to the lack of assessment of the internal exposure and variable exposure periods and doses used. This model could be used to predict brain levels in reported studies in animals during gestational exposure to aid in risk assessment. Moreover, the mechanisms by which chronic early-life permethrin and pyrethroids could exert developmental neurotoxicity was not well-understood (77). The model allows the estimation of relevant concentrations in the fetal brain in rats. The model could be extrapolated to humans by including specific human values for parameters required for the PBPK model and relevant *in vitro* data for clearance-specific parameters (78). The human pregnancy PBPK model could then be used to estimate relevant concentrations in the fetal brain to test in *in vitro* systems. Once more data will be available, these data could be integrated in specific adverse outcome pathways to assess developmental neurotoxicity in humans.

DATA AVAILABILITY STATEMENT

The raw data supporting the conclusions of this article will be made available by the authors, without undue reservation.

ETHICS STATEMENT

The animal study was reviewed and approved by a regional Ethic Committee on experiments using animals (CREMEAP no.96) and the French Ministry of Research with the permit number 01812.01.

AUTHOR CONTRIBUTIONS

SP and FZ formulated the research questions and designed the studies. SD, FR, and AL performed the experimental study in rats. SP, PM, and AC performed the chemical analysis. SP, FZ, and CB performed the PBPK modeling. CB ran the sensitivity analyses. SP wrote the manuscript. FZ and CB provided critical review and comments. FZ and VB were the supervisors of this research. All authors contributed to the article and approved the submitted version.

FUNDING

This work was supported by the French Ministry of Ecology and Sustainable Development (Program 190) and by the HBM4EU project.

SUPPLEMENTARY MATERIAL

The Supplementary Material for this article can be found online at: https://www.frontiersin.org/articles/10.3389/fped.2021.730383/full#supplementary-material

REFERENCES

1. Saillenfait A-M, Ndiaye D, Sabaté J-P. Pyrethroids: exposure and health effects – an update. *Int J Hyg Environ Health*. (2015) 218:281–92. doi: 10.1016/j.ijheh.2015.01.002
2. Feo ML, Eljarrat E, Barceló D, Barceló D. Determination of pyrethroid insecticides in environmental samples. *TrAC Trends Anal Chem*. (2010) 29:692–705. doi: 10.1016/j.trac.2010.03.011
3. Weston DP, Holmes RW, You J, Lydy MJ. Aquatic toxicity due to residential use of pyrethroid insecticides. *Environ Sci Technol*. (2005) 39:9778–84. doi: 10.1021/es0506354

4. Heudorf U, Angerer J. Metabolites of pyrethroid insecticides in urine specimens: current exposure in an urban population in Germany. *Environ Health Perspect*. (2001) 109:213. doi: 10.1289/ehp.01109213
5. Dereumeaux C, Saoudi A, Pecheux M, Berat B, de Crouy-Chanel P, Zaros C, et al. Biomarkers of exposure to environmental contaminants in French pregnant women from the Elfe cohort in 2011. *Environ Int*. (2016) 97:56–67. doi: 10.1016/j.envint.2016.10.013
6. Castorina R, Bradman A, Fenster L, Barr DB, Bravo R, Vedar MG, et al. Comparison of current-use pesticide and other toxicant urinary metabolite levels among pregnant women in the CHAMACOS cohort and NHANES. *Environ Health Perspect*. (2010) 118:856–63. doi: 10.1289/ehp.0901568
7. Dewailly E, Forde M, Robertson L, Kaddar N, Laouan Sidi EA, Côté S, et al. Evaluation of pyrethroid exposures in pregnant women from 10 Caribbean countries. *Environ Int*. (2014) 63:201–6. doi: 10.1016/j.envint.2013.11.014
8. Lewis RC, Cantonwine DE, Anzalota Del Toro LV, Calafat AM, Valentin-Blasini L, et al. Urinary biomarkers of exposure to insecticides, herbicides, and one insect repellent among pregnant women in Puerto Rico. *Environ Health*. (2014) 13:97. doi: 10.1186/1476-069X-13-97
9. Watkins DJ, Fortenberry GZ, Sánchez BN, Barr DB, Panuwet P, Schnaas L, et al. Urinary 3-phenoxybenzoic acid (3-PBA) levels among pregnant women in Mexico City: Distribution and relationships with child neurodevelopment. *Environ Res*. (2016) 147:307–13. doi: 10.1016/j.envres.2016.02.025
10. Woodruff TJ, Zota AR, Schwartz JM. Environmental chemicals in pregnant women in the United States: NHANES 2003–2004. *Environ Health Perspect*. (2011) 119:878–85. doi: 10.1289/ehp.1002727
11. Zhang J, Hisada A, Yoshinaga J, Shiraishi H, Shimodaira K, Okai T, et al. Exposure to pyrethroids insecticides and serum levels of thyroid-related measures in pregnant women. *Environ Res*. (2013) 127:16–21. doi: 10.1016/j.envres.2013.10.001
12. Dereumeaux C, Saoudi A, Goria S, Wagner V, De Crouy-Chanel P, Pecheux M, et al. Urinary levels of pyrethroid pesticides and determinants in pregnant French women from the Elfe cohort. *Environ Int*. (2018) 119:89–99. doi: 10.1016/j.envint.2018.04.042
13. Neta G, Goldman LR, Barr D, Apelberg BJ, Witter FR, Halden RU. Fetal exposure to chlordane and permethrin mixtures in relation to inflammatory cytokines and birth outcomes. *Environ Sci Technol*. (2011) 45:1680–7. doi: 10.1021/es103417j
14. Pérez JJ, Williams MK, Weerasekera G, Smith K, Whyatt RM, Needham LL, et al. Measurement of pyrethroid, organophosphorus, and carbamate insecticides in human plasma using isotope dilution gas chromatography–high resolution mass spectrometry. *J Chromatogr B*. (2010) 878:2554–62. doi: 10.1016/j.jchromb.2010.03.015
15. Berton T, Mayhoub F, Chardon K, Duca R-C, Lestremau F, Bach V, et al. Development of an analytical strategy based on LC–MS/MS for the measurement of different classes of pesticides and theirs metabolites in meconium: application and characterisation of foetal exposure in France. *Environ Res*. (2014) 132:311–20. doi: 10.1016/j.envres.2014.03.034
16. Meyer-Monath M, Chatellier C, Cabooter D, Rouget F, Morel I, Lestremau F. Development of liquid chromatography methods coupled to mass spectrometry for the analysis of substances with a wide variety of polarity in meconium. *Talanta*. (2015) 138:231–9. doi: 10.1016/j.talanta.2015.02.058
17. Cassoulet R, Haroune L, Abdelouahab N, Gillet V, Baccarelli AA, Cabana H, et al. Monitoring of prenatal exposure to organic and inorganic contaminants using meconium from an Eastern Canada cohort. *Environ Res*. (2019) 171:44–51. doi: 10.1016/j.envres.2018.12.044
18. Tran NQV, Miyake K. Neurodevelopmental disorders and environmental toxicants: epigenetics as an underlying mechanism. *Int J Genomics*. (2017) 2017:1–23. doi: 10.1155/2017/7526592
19. Rodier PM. Developing brain as a target of toxicity. *Environ Health Perspect*. (1995) 103(Suppl. 6):73–6.
20. Shafer TJ, Meyer DA, Crofton KM. developmental neurotoxicity of pyrethroid insecticides: critical review and future research needs. *Environ Health Perspect*. (2004) 113:123–36. doi: 10.1289/ehp.7254
21. Viel J-F, Warembourg C, Le Maner-Idrissi G, Lacroix A, Limon G, Rouget F, et al. Pyrethroid insecticide exposure and cognitive developmental disabilities in children: the PELAGIE mother–child cohort. *Environ Int*. (2015) 82:69–75. doi: 10.1016/j.envint.2015.05.009
22. Viel J-F, Rouget F, Warembourg C, Monfort C, Limon G, Cordier S, et al. Behavioural disorders in 6-year-old children and pyrethroid insecticide exposure: the PELAGIE mother–child cohort. *Occup Env Med*. (2017) 74:275–81. doi: 10.1136/oemed-2016-104035
23. Shelton JF, Geraghty EM, Tancredi DJ, Delwiche LD, Schmidt RJ, Ritz B, et al. Neurodevelopmental disorders and prenatal residential proximity to agricultural pesticides: The CHARGE study. *Environ Health Perspect*. (2014) 122:1103–9. doi: 10.1289/ehp.1307044
24. Horton MK, Rundle A, Camann DE, Boyd Barr D, Rauh VA, Whyatt RM. Impact of prenatal exposure to piperonyl butoxide and permethrin on 36-month neurodevelopment. *Pediatrics*. (2011) 127:e699–706. doi: 10.1542/peds.2010-0133
25. Ostrea EM, Bielawski DM, Posecion NC, Corrion M, Villanueva-Uy E, Bernardo RC, et al. Combined analysis of prenatal (maternal hair and blood) and neonatal (infant hair, cord blood and meconium) matrices to detect fetal exposure to environmental pesticides. *Environ Res*. (2009) 109:116–22. doi: 10.1016/j.envres.2008.09.004
26. von Ehrenstein OS, Ling C, Cui X, Cockburn M, Park AS, Yu F, et al. Prenatal and infant exposure to ambient pesticides and autism spectrum disorder in children: population based case-control study. *BMJ*. (2019) 364:l962. doi: 10.1136/bmj.l962
27. Dalsager L, Fage-Larsen B, Bilenberg N, Jensen TK, Nielsen F, Kyhl HB, et al. Maternal urinary concentrations of pyrethroid and chlorpyrifos metabolites and attention deficit hyperactivity disorder (ADHD) symptoms in 2-4-year-old children from the Odense Child Cohort. *Environ Res*. (2019) 176:108533. doi: 10.1016/j.envres.2019.108533
28. Barkoski JM, Philippat C, Tancredi D, Schmidt RJ, Ozonoff S, Barr DB, et al. *In utero* pyrethroid pesticide exposure in relation to autism spectrum disorder (ASD) and other neurodevelopmental outcomes at 3 years in the MARBLES longitudinal cohort. *Environ Res*. (2021) 194:110495. doi: 10.1016/j.envres.2020.110495
29. Ueyama J, Saito I, Kamijima M. Analysis and evaluation of pyrethroid exposure in human population based on biological monitoring of urinary pyrethroid metabolites. *J Pestic Sci*. (2010) 35:87–98. doi: 10.1584/jpestics.R10-01
30. Darney K, Bodin L, Bouchard M, Côté J, Volatier J-L, Desvignes V. Aggregate exposure of the adult French population to pyrethroids. *Toxicol Appl Pharmacol*. (2018) 351:21–31. doi: 10.1016/j.taap.2018.05.007
31. US EPA. *Pesticides : Industry Sales and Usage : 2006 and 2007 Market Estimate* (2007).
32. Carloni M, Nasuti C, Fedeli D, Montani M, Amici A, Vadhana MSD, et al. The impact of early life permethrin exposure on development of neurodegeneration in adulthood. *Exp Gerontol*. (2012) Washington, 47:60–6. doi: 10.1016/j.exger.2011.10.006
33. Carloni M, Nasuti C, Fedeli D, Montani M, Vadhana MSD, Amici A, et al. Early life permethrin exposure induces long-term brain changes in Nurr1, NF-kB and Nrf-2. *Brain Res*. (2013) 1515:19–28. doi: 10.1016/j.brainres.2013.03.048
34. Imanishi S, Okura M, Zaha H, Yamamoto T, Akanuma H, Nagano R, et al. Prenatal exposure to permethrin influences vascular development of fetal brain and adult behavior in mice offspring: prenatal Exposure to Permethrin Influences Brain in Offspring. *Environ Toxicol*. (2013) 28:617–29. doi: 10.1002/tox.20758
35. Nasuti C, Carloni M, Fedeli D, Gabbianelli R, Di Stefano A, Laura Serafina C, et al. Effects of early life permethrin exposure on spatial working memory and on monoamine levels in different brain areas of pre-senescent rats. *Toxicology*. (2013) 303:162–8. doi: 10.1016/j.tox.2012.09.016
36. Saito H, Hara K, Tominaga T, Nakashima K, Tanemura K. Early-life exposure to low levels of permethrin exerts impairments in learning and memory with the effects on neuronal and glial population in adult male mice. *J Appl Toxicol*. (2019) 39:1651–62. doi: 10.1002/jat.3882
37. US EPA. *Approaches for the Application of Physiologically Based Pharmacokinetic (PBPK) Models and Supporting Data in Risk Assessment* (2006) Washington.

38. Willemin M-E, Desmots S, Le Grand R, Lestremau F, Zeman FA, Leclerc E, et al. PBPK modeling of the cis- and trans-permethrin isomers and their major urinary metabolites in rats. *Toxicol Appl Pharmacol*. (2016) 294:65–77. doi: 10.1016/j.taap.2016.01.011
39. Song G, Moreau M, Efremenko A, Lake BG, Wu H, Bruckner JV, et al. Evaluation of age-related pyrethroid pharmacokinetic differences in rats: physiologically-based pharmacokinetic model development using *in vitro* data and *in vitro* to *in vivo* extrapolation. *Toxicol Sci*. (2019) 169:365–79. doi: 10.1093/toxsci/kfz042
40. Tornero-Velez R, Davis J, Scollon EJ, Starr JM, Setzer RW, Goldsmith M-R, et al. A pharmacokinetic model of cis- and trans-permethrin disposition in rats and humans with aggregate exposure application. *Toxicol Sci*. (2012) 130:33–47. doi: 10.1093/toxsci/kfs236
41. Wei B, Isukapalli SS, Weisel CP. Studying permethrin exposure in flight attendants using a physiologically based pharmacokinetic model. *J Expo Sci Environ Epidemiol*. (2013) 23:416–27. doi: 10.1038/jes.2013.12
42. Quindroit P, Beaudouin R, Brochot C. Estimating the cumulative human exposures to pyrethroids by combined multi-route PBPK models: application to the French population. *Toxicol Lett*. (2019) 312:125–38. doi: 10.1016/j.toxlet.2019.05.007
43. Mallick P, Moreau M, Song G, Efremenko AY, Pendse SN, Creek MR, et al. Development and application of a life-stage Physiologically Based Pharmacokinetic (PBPK) model to the assessment of internal dose of pyrethroids in humans. *Toxicol Sci*. (2020) 173:86–99. doi: 10.1093/toxsci/kfz211
44. Personne S, Marcelo P, Pilard S, Baltora-Rosset S, Corona A, Robidel F, et al. Determination of maternal and foetal distribution of cis- and trans-permethrin isomers and their metabolites in pregnant rats by liquid chromatography tandem mass spectrometry (LC-MS/MS). *Anal Bioanal Chem*. (2019) 411:8043–52. doi: 10.1007/s00216-019-02157-7
45. Dowell T, Kauer CD. Maternal hemodynamics and uteroplacental blood flow throughout gestation in conscious rats. *Methods Find Exp Clin Pharmacol*. (1997) 19:613–25.
46. Brown RP, Delp MD, Lindstedt SL, Rhomberg LR, Beliles RP. Physiological parameter values for physiologically based pharmacokinetic models. *Toxicol Ind Health*. (1997) 13:407–84. doi: 10.1177/074823379701300401
47. Hanwell A, Linzell JL. The time course of cardiovascular changes in lactation in the rat. *J Physiol*. (1973) 233:93–109. doi: 10.1113/jphysiol.1973.sp010299
48. Rosso P, Keyou G, Bassi JA, Slusser WM. Effect of malnutrition during pregnancy on the development of the mammary glands of rats. *J Nutr*. (1981) 111:1937–41. doi: 10.1093/jn/111.11.1937
49. Naismith DJ, Richardson DP, Pritchard AE. The utilization of protein and energy during lactation in the rat, with particular regard to the use of fat accumulated in pregnancy. *Br J Nutr*. (1982) 48:433. doi: 10.1079/BJN19820125
50. Clewell RA. Predicting fetal perchlorate dose and inhibition of iodide kinetics during gestation: a physiologically-based pharmacokinetic analysis of perchlorate and iodide kinetics in the rat. *Toxicol Sci*. (2003) 73:235–55. doi: 10.1093/toxsci/kfg081
51. O'Flaherty EJ, Scott W, Schreiner C, Beliles RP. A physiologically based kinetic model of rat and mouse gestation: disposition of a weak acid. *Toxicol Appl Pharmacol*. (1992) 112:245–56. doi: 10.1016/0041-008X(92)90194-W
52. Yoon M, Nong A, Clewell HJ, Taylor MD, Dorman DC, Andersen ME. Evaluating placental transfer and tissue concentrations of manganese in the pregnant rat and fetuses after inhalation exposures with a PBPK model. *Toxicol Sci*. (2009) 112:44–58. doi: 10.1093/toxsci/kfp198
53. Sikov MR, Thomas JM. Prenatal growth of the rat. *Growth*. (1970) 34:1–14.
54. Girard H, Klappstein S, Bartag, I, Moll, W. Blood circulation and oxygen transport in the fetal guinea pig. *J Dev Physiol*. (1983) 5:181–93.
55. Carter, AM, Gu W. Cerebral blood fow in the fetal guinea pig. *J Dev Physiol*. (1988) 10:123–9. doi: 10.1016/0143-4004(89)90089-1
56. Itskovitz J, LaGamma EF, Rudolph AM. Effects of cord compression on fetal blood flow distribution and O2 delivery. *Am J Physiol Heart Circ Physiol*. (1987) 252:H100–9. doi: 10.1152/ajpheart.1987.252.1.H100
57. Gelman A, Meng X-L, Stern H. Posterior predictive assessment of model fitness via realized discrepancies. *Stat Sin*. (1996) 6:733–807.
58. Godin SJ, DeVito MJ, Hughes MF, Ross DG, Scollon EJ, Starr JM, et al. Physiologically based pharmacokinetic modeling of deltamethrin: development of a rat and human diffusion-limited model. *Toxicol Sci*. (2010) 115:330–43. doi: 10.1093/toxsci/kfq051
59. Crow J, Borazjani A, Potter P, Ross M. Hydrolysis of pyrethroids by human and rat tissues: examination of intestinal, liver and serum carboxylesterases. *Toxicol Appl Pharmacol*. (2007) 221:1–12. doi: 10.1016/j.taap.2007.03.002
60. Gelman A, Bois F, Jiang J. Physiological pharmacokinetic analysis using population modeling and informative prior distributions. *J Am Stat Assoc*. (1996) 91:1400–12. doi: 10.1080/01621459.1996.10476708
61. Lu G, Abduljalil K, Jamei M, Johnson TN, Soltani H, Rostami-Hodjegan. Physiologically-based Pharmacokinetic (PBPK) models for assessing the kinerics of xenobiotics during pregnancy: achievements and shortcomings. *Curr Drug Metab*. (2012) 13:695–720. doi: 10.2174/138920012800840374
62. Anadon A, Martinez-Larranaga MR, Diaz MJ, Bringas P. Toxicokinetics of permethrin in the rat. *Toxicol Appl Pharmacol*. (1991) 110:1–8. doi: 10.1016/0041-008X(91)90284-L
63. Ueyama J, Hirosawa N, Mochizuki A, Kimata A, Kamijima M, Kondo T, et al. Toxicokinetics of pyrethroid metabolites in male and female rats. *Environ Toxicol Pharmacol*. (2010) 30:88–91. doi: 10.1016/j.etap.2010.03.017
64. Afonso-Pereira F, Dou L, Trenfield SJ, Madla CM, Murdan S, Sousa J, et al. Sex differences in the gastrointestinal tract of rats and the implications for oral drug delivery. *Eur J Pharm Sci*. (2018) 115:339–44. doi: 10.1016/j.ejps.2018.01.043
65. Shore R, Björne H, Omoto Y, Siemiatkowska A, Gustafsson J-Å, Lindblad M, et al. Sex differences and effects of oestrogen in rat gastric mucosal defence. *World J Gastroenterol*. (2017) 23:426. doi: 10.3748/wjg.v23.i3.426
66. Sethi P, Bruckner JV, Mortuza TB, Cummings BS, Muralidhara S, White CA. Plasma protein and lipoprotein binding of *Cis* - and *Trans* -permethrin and deltamethrin in adult humans and rats. *Drug Metab Dispos*. (2019) 47:941–8. doi: 10.1124/dmd.118.085464
67. Sethi PK, Muralidhara S, Bruckner JV, White CA. Measurement of plasma protein and lipoprotein binding of pyrethroids. *J Pharmacol Toxicol Methods*. (2014) 70:106–11. doi: 10.1016/j.vascn.2014.06.002
68. Van Lenten BJ, Jenkins CH, Roheim PS. Plasma apolipoprotein profiles of male and female rats. *Atherosclerosis*. (1980) 37:569–77. doi: 10.1016/0021-9150(80)90064-7
69. He XJ, Ejiri N, Nakayama H, Doi K. Effects of pregnancy on CYPs protein expression in rat liver. *Exp Mol Pathol*. (2005) 78:64–70. doi: 10.1016/j.yexmp.2004.08.011
70. He XJ, Yamauchi H, Suzuki K, Ueno M, Nakayama H, Doi K. Gene expression profiles of drug-metabolizing enzymes (DMEs) in rat liver during pregnancy and lactation. *Exp Mol Pathol*. (2007) 83:428–34. doi: 10.1016/j.yexmp.2006.05.002
71. McMullin TS, Lowe ER, Bartels MJ, Marty MS. Dynamic changes in lipids and proteins of maternal, fetal, and pup blood and milk during perinatal development in CD and wistar rats. *Toxicol Sci*. (2008) 105:260–74. doi: 10.1093/toxsci/kfn124
72. López-Luna P, Maier I, Herrera E. Carcass and tissue fat content in the pregnant rat. *Neonatology*. (1991) 60:29–38. doi: 10.1159/000243385
73. Andersen ME. Development of physiologically based pharmacokinetic and physiologically based pharmacodymamic models for applications in toxicology and risk assessment. *Decis Subtances Methodol Hum Health Risk Assess Toxic Subst*. (1995) 79:35–44. doi: 10.1016/0378-4274(95)03355-O
74. Sager JE, Yu J, Ragueneau-Majlessi I, Isoherranen N. Physiologically Based Pharmacokinetic (PBPK) modeling and simulation approaches: a systematic review of published models, applications, and model verification. *Drug Metab Dispos*. (2015) 43:1823–37. doi: 10.1124/dmd.115.065920
75. Mathiesen L, Mørck TA, Poulsen MS, Nielsen JKS, Mose T, Long M, et al. Placental transfer of pesticides studied in human placental perfusion. *Basic Clin Pharmacol Toxicol*. (2020) 127:505–15. doi: 10.1111/bcpt.13456
76. Lin Z, Fisher JW, Wang R, Ross MK, Filipov NM. Estimation of placental and lactational transfer and tissue distribution of atrazine and its main metabolites in rodent dams, fetuses, and neonates with physiologically based pharmacokinetic modeling. *Toxicol Appl Pharmacol*. (2013) 273:140–58. doi: 10.1016/j.taap.2013.08.010

77. Pitzer EM, Williams MT, Vorhees CV. Effects of pyrethroids on brain development and behavior: deltamethrin. *Neurotoxicol Teratol.* (2021) 87:106983. doi: 10.1016/j.ntt.2021.106983
78. Dallmann A, Solodenko J, Ince I, Eissing T. Applied concepts in PBPK modeling: how to extend an open systems pharmacology model to the special population of pregnant women: pregnancy PBPK models in open systems pharmacology. *CPT Pharmacomet Syst Pharmacol.* (2018) 7:419–31. doi: 10.1002/psp4.12300

Conflict of Interest: The authors declare that the research was conducted in the absence of any commercial or financial relationships that could be construed as a potential conflict of interest.

Publisher's Note: All claims expressed in this article are solely those of the authors and do not necessarily represent those of their affiliated organizations, or those of the publisher, the editors and the reviewers. Any product that may be evaluated in this article, or claim that may be made by its manufacturer, is not guaranteed or endorsed by the publisher.

frontiers in Pediatrics

ORIGINAL RESEARCH
published: 23 September 2021
doi: 10.3389/fped.2021.733520

Mechanistic Coupling of a Novel *in silico* Cotyledon Perfusion Model and a Physiologically Based Pharmacokinetic Model to Predict Fetal Acetaminophen Pharmacokinetics at Delivery

Paola Mian[1]*, Bridget Nolan[2,3], John N. van den Anker[4,5], Kristel van Calsteren[6,7], Karel Allegaert[6,8,9], Nisha Lakhi[2,3] and André Dallmann[10]

[1] Department of Clinical Pharmacy, Medisch Spectrum Twente, Enschede, Netherlands, [2] Department of Obstetrics and Gynecology, Richmond University Medical Center, Staten Island, NY, United States, [3] Department of Obstetrics and Gynecology, New York Medical College, Valhalla, NY, United States, [4] Division of Clinical Pharmacology, Children's National Hospital, Washington, DC, United States, [5] Department of Pediatric Pharmacology and Pharmacometrics, University Children's Hospital Basel, Basel, Switzerland, [6] Department of Development and Regeneration, KU Leuven, Leuven, Belgium, [7] Department of Gynecology and Obstetrics, UZ Gasthuisberg, Leuven, Belgium, [8] Department of Pharmaceutical and Pharmacological Sciences, KU Leuven, Leuven, Belgium, [9] Department of Hospital Pharmacy, Erasmus Medical Center Rotterdam, Rotterdam, Netherlands, [10] Pharmacometrics/Modeling and Simulation, Research and Development, Pharmaceuticals, Bayer AG, Leverkusen, Germany

OPEN ACCESS

Edited by:
Venkata Kashyap Yellepeddi, The University of Utah, United States

Reviewed by:
Alexandre Bonnin, University of Southern California, United States
Vijay K. Siripuram, University of Florida, United States

***Correspondence:**
Paola Mian
Paola.Mian@mst.nl
orcid.org/0000-0002-3551-1201

Specialty section:
This article was submitted to Obstetric and Pediatric Pharmacology, a section of the journal Frontiers in Pediatrics

Received: *30 June 2021*
Accepted: *20 August 2021*
Published: *23 September 2021*

Citation:
Mian P, Nolan B, van den Anker JN, van Calsteren K, Allegaert K, Lakhi N and Dallmann A (2021) Mechanistic Coupling of a Novel in silico Cotyledon Perfusion Model and a Physiologically Based Pharmacokinetic Model to Predict Fetal Acetaminophen Pharmacokinetics at Delivery. Front. Pediatr. 9:733520. doi: 10.3389/fped.2021.733520

Little is known about placental drug transfer and fetal pharmacokinetics despite increasing drug use in pregnant women. While physiologically based pharmacokinetic (PBPK) models can help in some cases to shed light on this knowledge gap, adequate parameterization of placental drug transfer remains challenging. A novel *in silico* model with seven compartments representing the *ex vivo* cotyledon perfusion assay was developed and used to describe placental transfer and fetal pharmacokinetics of acetaminophen. Unknown parameters were optimized using observed data. Thereafter, values of relevant model parameters were copied to a maternal-fetal PBPK model and acetaminophen pharmacokinetics were predicted at delivery after oral administration of 1,000 mg. Predictions in the umbilical vein were evaluated with data from two clinical studies. Simulations from the *in silico* cotyledon perfusion model indicated that acetaminophen accumulates in the trophoblasts; simulated steady state concentrations in the trophoblasts were 4.31-fold higher than those in the perfusate. The whole-body PBPK model predicted umbilical vein concentrations with a mean prediction error of 24.7%. Of the 62 concentration values reported in the clinical studies, 50 values (81%) were predicted within a 2-fold error range. In conclusion, this study presents a novel *in silico* cotyledon perfusion model that is structurally congruent with the placenta

implemented in our maternal-fetal PBPK model. This allows transferring parameters from the former model into our PBPK model for mechanistically exploring whole-body pharmacokinetics and concentration-effect relationships in the placental tissue. Further studies should investigate acetaminophen accumulation and metabolism in the placenta as the former might potentially affect placental prostaglandin synthesis and subsequent fetal exposure.

Keywords: acetaminophen, *ex vivo* cotyledon perfusion, physiologically-based pharmacokinetics, placental transfer, maternal-fetal, pregnancy

INTRODUCTION

Despite frequent and increasing drug use in pregnant women (1, 2), little is known about placental drug transfer and pharmacokinetics in the fetus. To address this knowledge gap, numerous physiologically based pharmacokinetic (PBPK) models for pregnant women were developed over the past years and used to simulate fetal pharmacokinetics (3, 4). Yet, adequate parameterization of placental drug transfer in these models remains challenging. While some models relied on various *in vitro* information, such as the drug's physicochemical properties or permeability across Caco-2 cell membranes, to estimate placental drug transfer (5–8), other models integrated kinetic data obtained from the *ex vivo* cotyledon perfusion assay (9–14) or fitted the placental permeability to clinical data (15).

The kinetic *in silico* models representing the *ex vivo* cotyledon perfusion system typically consist of few compartments and lump various tissue portions of the cotyledon, e.g., intravillous vascular, interstitial, and intracellular space, in a single compartment. Although in general these models appear to scale well with the placental drug transfer kinetics simulated in whole-body models, the relatively simple structure prevents a more mechanistic understanding of the transfer kinetics. For example, drug accumulation in the trophoblasts of the cotyledon—which may lengthen fetal drug exposure *in vivo* (16)—cannot be described by these models. Along the same line, the understanding of placental concentration-time profiles enables modeling concentration-effects profiles in the placental tissue, as the placenta is not only a 'transfer' organ but an 'active' organ with endocrine and metabolic functions. Hence, tissue-specific pharmacology of a given drug within the placenta and potential interactions with its endocrine synthesis and secretion of hormones (e.g., prostaglandins) may also affect fetal development and pregnancy outcome (e.g., preterm induction of labor).

In the obstetric clinical pharmacology field, pharmacokinetic data in pregnant women are sparse and data sharing can be an important step to advance the development and validation of PBPK models. Here, we used data on acetaminophen pharmacokinetics in the umbilical cord from two clinical studies (17, 18) to re-evaluate and refine a recently developed maternal-fetal PBPK model (13, 19). In our previous work, acetaminophen transfer across the placenta in the PBPK model was informed based on published data from the *ex vivo* cotyledon perfusion assay (20). Therefore, an *in silico* cotyledon perfusion model was previously developed to learn the transfer kinetics in the *ex vivo* cotyledon perfusion assay before implementing them in the PBPK model. However, the previously developed *in silico* cotyledon perfusion model consisted of 4 compartments only, namely the maternal and fetal reservoir and the maternal and fetal tissue portions of the cotyledon (13). It was therefore structurally different than the placental sub-structure implemented in the PBPK model (see **Figures 1**, **2**) (19). Consequently, the parameters of the former model are not directly transferable to the latter and hence translatability across these models may not be guaranteed.

To this end, a novel *in silico* cotyledon perfusion model was developed herein that constitutes a congruent, albeit minimized, replicate of the placental structure implemented in the maternal-fetal PBPK model. Additionally, it was intended that the novel *in silico* cotyledon perfusion model better reflected the cotyledon physiology so that potential drug accumulation in the tissue could be considered in the simulations. Several parameters of the *in silico* cotyledon perfusion model relevant to maternal-fetal drug transfer were then optimized using previously published data for acetaminophen. The optimization results were then transferred into the PBPK model and the predicted pharmacokinetics in the umbilical vein at delivery were re-evaluate using the pooled data of Nitsche et al. (17) and Mehraban et al. (18).

MATERIALS AND METHODS

Software

PBPK models were built with PK-Sim® and MoBi® which are available as open source tools through the Open Systems Pharmacology (OSP) software, version 9.1, via GitHub (https://github.com/Open-Systems-Pharmacology) (21). The software R, version 3.6.3 (R Foundation for Statistical Computing, http://www.r-project.org) was used for graphics creation and statistical analysis. The R-package "ospsuite", version 9.0.79 (https://github.com/Open-Systems-Pharmacology/OSPSuite-R), was used to conduct pharmacokinetic simulations in virtual populations of pregnant women. The tool WebPlotDigitizer, version 4.0 (https://automeris.io/WebPlotDigitizer/) was used to extract data from figures and conversion into numerical format.

General Workflow

In our previous study, we successfully translated an adult, non-pregnant PBPK model for acetaminophen including its metabolites generated by uridine 5′-diphospho-glucuronosyltransferase (UGT) 1A1, sulfotransferase (SULT)

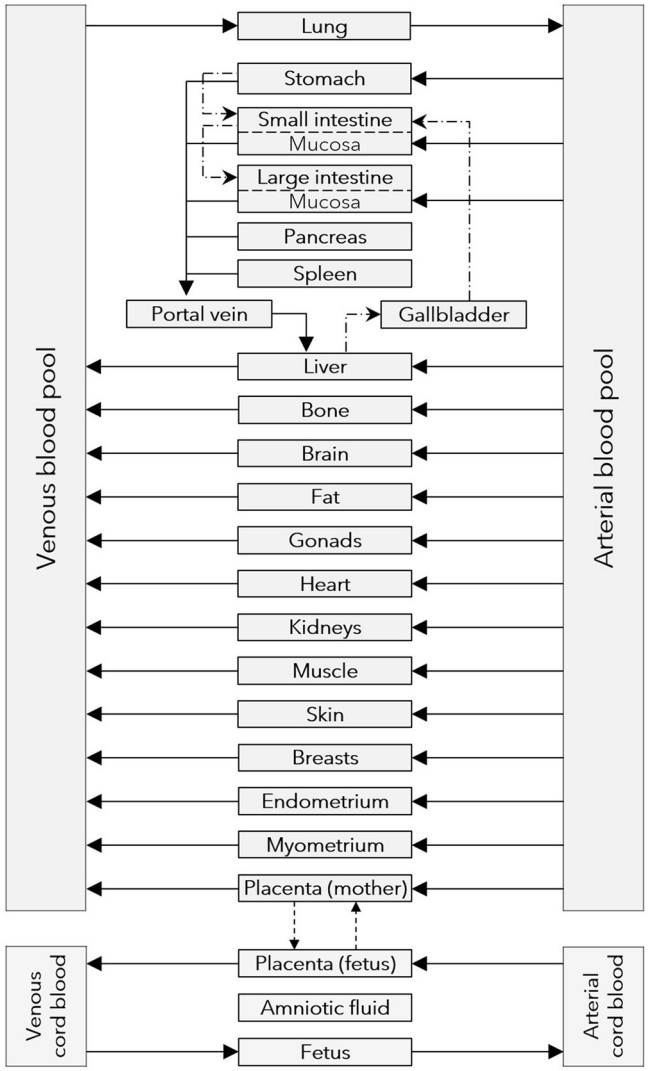

FIGURE 1 | Structure of the maternal-fetal PBPK model. Gray boxes represent compartments of the physiologically based pharmacokinetic (PBPK) model; solid arrows denote drug transport via the organ blood flow; dashed arrows denote drug transport via passive diffusion; dash dotted lines denote drug transport via gastrointestinal motility or the biliary excretion route.

1A1 and cytochrome-P-450 (CYP) 2E1 to pregnancy (13, 19). The predicted acetaminophen pharmacokinetics in the maternal blood were previously verified in the first trimester with clinical data from Beaulac-Baillargeon and Rocheleau (22); predicted acetaminophen pharmacokinetics in the maternal and umbilical vein blood at delivery were previously evaluated with data from Allegaert et al. (23) and Nitsche et al. (17), respectively.

In this study, we developed a novel *in silico* cotyledon perfusion model that is structurally equivalent with the placenta implemented in the PBPK model. We used this *in silico* cotyledon perfusion model to learn placental transfer kinetics of acetaminophen by fitting relevant model parameters to observed data obtained in the *ex vivo* perfusion cotyledon assay (20). Once this model captured the observed *ex vivo* kinetics adequately, the values of relevant model parameters were copied to the maternal-fetal PBPK model. Note that the structure of the PBPK model was not changed in this study and is thus consistent with the structure of the PBPK model reported in our previous publication (13). Thereafter, fetal pharmacokinetics were predicted in the umbilical vein compartment of the PBPK model and predictions were evaluated with clinical data from Nitsche et al. (17) and Mehraban et al. (18).

In silico Cotyledon Perfusion Model

Description of the Model

A novel *in silico* cotyledon perfusion model structure, schematically depicted in **Figure 3**, was developed that closely reflects the physiological structure of the cotyledon *ex vivo*. Note that the maternal intracellular compartment representing mainly the decidua basalis is only present in the PBPK model, but not in the *in silico* cotyledon perfusion model. Since the decidua is shed off during childbirth, it is not part of the cotyledon tissue used in the *ex vivo* experiment and only present in utero. Although there will still be decidual remnants on the delivered placenta, they come off during flushing and rinsing for experimental preparation. Hence, the *in silico* cotyledon perfusion model consists of seven compartments: The maternal perfusate in the maternal reservoir and in the intervillous space of the cotyledon; the intervillous interstitial compartment representing fibrous tissue adhering to the cotyledon on the maternal-facing side; the trophoblasts; the interstitial space representing fibrous tissue in the fetal villous; and the fetal perfusate in the fetal villous and fetal reservoir. **Table 1** gives an overview of the tissue components present *in vivo*/*ex vivo* and their corresponding compartments in the *in silico* cotyledon perfusion model (**Figure 3**) and the placental sub-structure of the PBPK model (**Figure 2**).

The ordinary differential equations (ODE) given in the following were used in the novel *in silico* cotyledon perfusion model. Note that in MoBi®, the ODEs are first defined for intercompartmental exchange processes in the passive transports building block; during set-up of a simulation, the ODEs are then generated for each compartment. In the following, the ODEs are first introduced for each intercompartmental exchange transport and then defined for the compartments.

The following equations were used to describe drug transfer in perfusate between the maternal reservoir and the cotyledon (Equation 1) and between the fetal reservoir and the cotyledon (Equation 2):

$$\frac{dN_{M\_perf}}{dt} = Q_M \times \left(C_{M\_res} - C_{M\_perf}\right) \quad (1)$$

$$\frac{dN_{F\_perf}}{dt} = Q_F \times \left(C_{F\_res} - C_{F\_perf}\right) \quad (2)$$

Here, N_{M_perf} and N_{F_perf} denote the molar drug amount in the maternal and fetal perfusate, respectively, that fills the intervillous space of the cotyledon [μmol]; Q_M and Q_F denote the flow rate of the perfusate in maternal and fetal

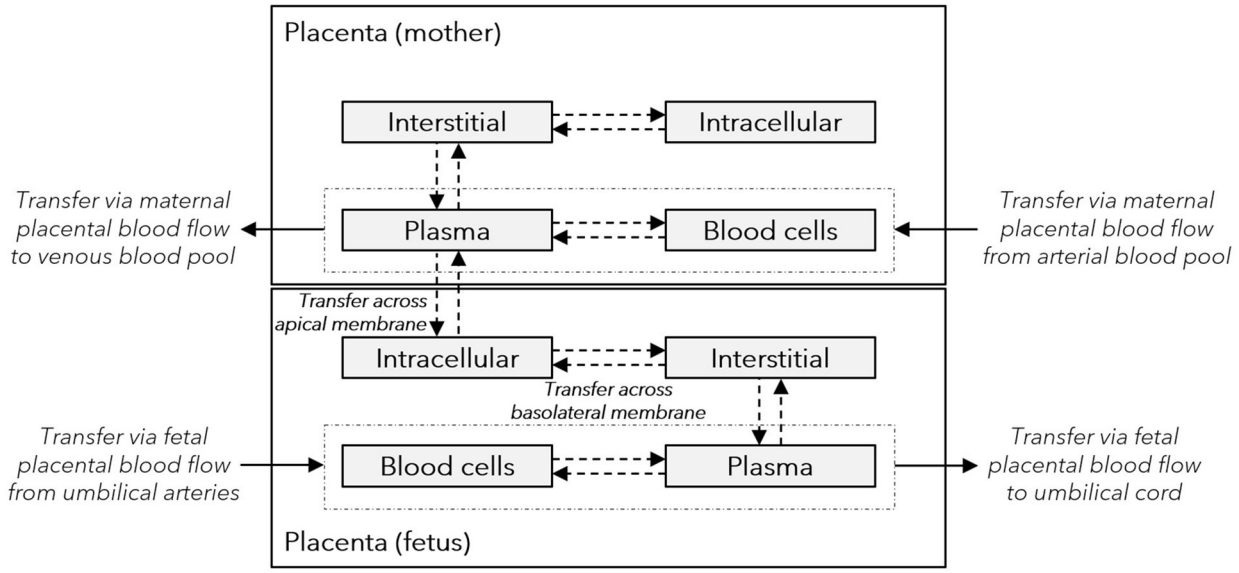

FIGURE 2 | Structure of the placenta sub-model integrated in the maternal-fetal PBPK model. Gray boxes represent sub-compartments of the placenta structure implemented in the maternal-fetal physiologically based pharmacokinetic (PBPK) model; dash-dotted boxes represent the vascular space; solid arrows denote drug transport via the organ blood flow; and dashed arrows denote drug transport via passive diffusion. The maternal plasma and blood cell compartments represent the intervillous space, and the maternal interstitial and intracellular space represent the placental septae and the decidua basalis, respectively. The fetal intracellular compartment represents the (syncytio-)trophoblasts with the apical membrane facing the maternal plasma compartment and the basolateral membrane facing the fetal interstitial compartment. The fetal interstitial space represents intravillous fibrous tissue and the plasma and blood cell compartments represent the intravillous vascular system.

system, respectively [L/min]; C_{M_res} and C_{F_res} the molar drug concentration in maternal and fetal perfusate in the reservoir, respectively [μmol/L]; and C_{M_perf} and C_{F_perf} the molar drug concentration in maternal and fetal perfusate in the cotyledon, respectively [μmol/L]. Q_M and Q_F as well as the volumes of the maternal and fetal reservoirs were set to the values reported by Conings et al. (20); 14 mL/min and 6 mL/min for the flow rate in the maternal and fetal system, respectively; and 280 and 284 mL for the maternal and fetal reservoir volume. Drug amount was converted to drug concentration by dividing the drug amount by the compartment's volume.

Drug transfer between maternal perfusate in the cotyledon and intervillous interstitial space and fetal perfusate in the cotyledon and intravillous interstitial space was described by Equations 3, 4, respectively:

$$\frac{dN_{M\_int}^{M\_int\leftrightarrow M\_perf}}{dt} = f_u \times P_{endo} \times SA_{M\_perf\,:\,int} \times \left(C_{M\_perf} - \frac{C_{M\_int}}{K_{M\_int\,:\,perf}}\right) \quad (3)$$

$$\frac{dN_{F\_int}^{F\_int\leftrightarrow F\_perf}}{dt} = f_{u\_fetus} \times P_{endo} \times SA_{F\_perf\,:\,int} \times \left(C_{F\_perf} - \frac{C_{F\_int}}{K_{F\_int\,:\,perf}}\right) \quad (4)$$

Here, $N_{M\_int}^{M\_int\leftrightarrow M\_perf}$ denotes molar drug amount in the intervillous interstitial compartment when drug exchange is only considered to occur between the intervillous interstitial space and maternal perfusate in the cotyledon [μmol]; $N_{F\_int}^{F\_int\leftrightarrow F\_perf}$ denotes molar drug amount in the intravillous interstitial compartment when drug exchange is only considered to occur between the intravillous interstitial space and fetal perfusate in the cotyledon [μmol]; f_u and f_{u_fetus} denote the drug's fraction unbound in maternal and fetal perfusate, respectively; P_{endo} is the drug's permeability through the endothelial membrane of blood vessels and was assumed to be equal for maternal and fetal endothelial membranes [dm/min]; $SA_{M\_perf\,:\,int}$ and $SA_{F\_perf\,:\,int}$ denote the surface area between maternal perfusate and intervillous interstitial space and fetal perfusate and intravillous interstitial space, respectively [dm^2]; C_{M_int} and C_{F_int} the molar drug concentration in intervillous and intravillous interstitial space of the cotyledon, respectively [μmol/L]; $K_{M\_int\,:\,perf}$ is the intervillous interstitial-to-perfusate partition coefficient of the drug; and $K_{F\_int\,:\,perf}$ is the intravillous interstitial-to-perfusate partition coefficient of the drug.

The unbound fraction of acetaminophen was scaled from an adult value of 0.82 (19) as described previously (24). The bovine serum albumin concentrations present in the maternal and fetal perfusate of the *ex vivo* cotyledon perfusion assay were 40 and 30 mg/mL, respectively (20). This resulted in an unbound fraction of 0.84 and 0.88 in maternal and fetal perfusate,

respectively. Permeability across the endothelial membrane in the intervillous and intravillous space (P_{endo}) was assumed to be not the rate-limiting step for tissue distribution and was hence set to a value of 100 cm/min as has been done for other organ compartments (except the brain) in whole-body PBPK models (24). Note that for drugs that are substrates to efflux transporters expressed in the endothelial membrane, this rate may have to be reduced. $SA_{M\_perf\,:\,int}$ and $SA_{F\_perf\,:\,int}$ were estimated by scaling the local surface area from the cotyledon volume assuming that organ structure is geometrically similar among species (24). The volumes of the intervillous and intravillous cotyledon fraction were assumed to be 23 and 35 mL, respectively (25). $K_{M\_int\,:\,perf}$ was calculated from the biochemical tissue composition of the cotyledon and the drug's physicochemical properties using the equation published by Schmitt (26). Values for the biochemical composition of the placenta have been reported previously (27). Finally, $K_{F\_int\,:\,perf}$ was calculated accordingly, except that the fraction unbound in the original equation by Schmitt (26) was replaced by the fetal fraction unbound (Equation 5):

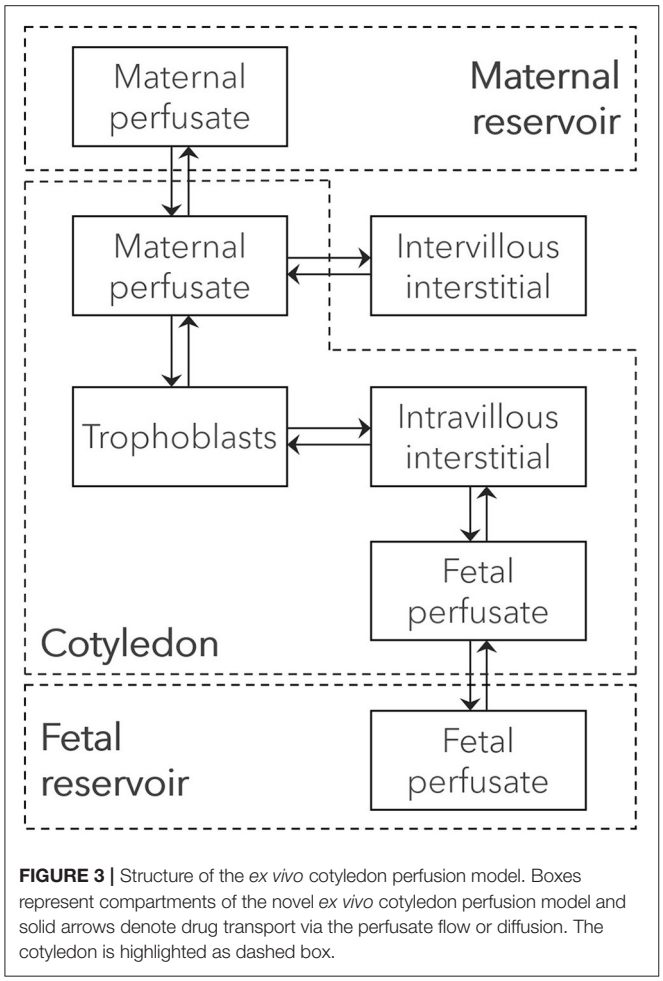

FIGURE 3 | Structure of the *ex vivo* cotyledon perfusion model. Boxes represent compartments of the novel *ex vivo* cotyledon perfusion model and solid arrows denote drug transport via the perfusate flow or diffusion. The cotyledon is highlighted as dashed box.

$$K_{F\_int\,:\,perf} = \left(f_{water}^{int} + \frac{f_{protein}^{int}}{f_{protein}^{perf}} \times \left(\frac{1}{f_{u\_fetus}} - f_{water}^{perf} \right) \right) \times f_{u\_fetus} \quad (5)$$

In this equation, f_{water}^{int} and f_{water}^{perf} denote the fractional water content in intravillous interstitial space and perfusate, respectively; and $f_{protein}^{int}$ and $f_{protein}^{perf}$ the fractional protein content in intravillous interstitial space and perfusate, respectively. f_{water}^{int} was assumed to be the same than for the intervillous interstitial space [0.935 (28)] and f_{water}^{perf} was assumed to be similar to the fractional volume content reported for plasma [0.926 (28)]. The value for the ratio $\frac{f_{protein}^{int}}{f_{protein}^{perf}}$ in the *ex vivo* cotyledon was assumed to be the same as in adult tissue [0.37 (26)].

Intravillous drug transfer between interstitial and intracellular space (i.e., the trophoblasts) was described by Equation 6:

$$\frac{dN_{F\_cell}^{F\_cell \leftrightarrow F\_int}}{dt} = P \times SA_{F\_int\,:\,cell} \times \left(K_{F\_water\,:\,int} \times C_{F\_int} - K_{F\_water\,:\,cell} \times C_{F\_cell} \right) \quad (6)$$

Here, $N_{F\_cell}^{F\_cell \leftrightarrow F\_int}$ denotes molar drug amount in the intracellular space when drug exchange is only considered to occur between the intracellular and intravillous interstitial

TABLE 1 | Overview of different tissue components and their corresponding compartments in the novel *in silico* cotyledon perfusion model and the PBPK model.

Physiological tissue component	Compartment name in the novel *in silico* cotyledon perfusion model	Compartment name in the PBPK model
Maternal blood in the intervillous space of the cotyledon	Maternal perfusate in the cotyledon	Plasma and blood cells in the maternal part of the placenta
Placental septae	Intervillous interstitial	Interstitial space in the maternal part of the placenta
Decidua basalis	*NA*[a]	Intracellular space in the maternal part of the placenta
(Syncytio)trophoblasts	Trophoblasts	Intracellular space in the fetal part of the placenta
Fibrous tissue in the fetal villi	Intravillous interstitial	Interstitial space in the fetal part of the placenta
Fetal blood in the blood capillaries of the fetal villi	Fetal perfusate in the cotyledon	Plasma and blood cells in the fetal part of the placenta

[a] *During childbirth the decidua basalis is shed off and hence not present in the ex vivo cotyledon.*

compartment [μmol]; P is the drug's membrane permeability [dm/min] which was calculated from the drug's effective molecular weight and lipophilicity as described elsewhere (24); $SA_{F\_int:cell}$ is the surface area between the intravillous interstitial space and the intracellular space (i.e. trophoblasts) [dm^2]; $K_{F\_water:int}$ the partition coefficient between water and intravillous interstitial space; $K_{F\_water:cell}$ the partition coefficient between water and intracellular space of the trophoblasts; and C_{F_cell} the molar drug concentration in the trophoblasts [μmol/L]. The local surface area in this equation was calculated as already described above. $K_{F\_water:int}$ and $K_{F\_water:cell}$ were expressed as follows:

$$K_{F\_water:int} = \frac{f_{u\_fetus}}{K_{F\_int:perf}} \tag{7}$$

$$K_{F\_water:cell} = \frac{f_{u\_fetus}}{K_{F\_cell:perf}} \tag{8}$$

where $K_{F\_int:perf}$ is calculated according to the Equation 5 and $K_{F\_cell:perf}$ according to the cell-to-plasma partition coefficient equation. In the developed *in silico* cotyledon perfusion model, several equations were implemented to calculate these partition coefficients from the biochemical tissue composition of the placenta (27) and the drug's physicochemical properties using, namely the PK-Sim Standard equation (29) and the equations proposed by Schmitt et al. (26), Rodgers et al. (30, 31), and Poulin et al. (32, 33). For acetaminophen, the partition coefficient equation by Rodgers et al. (30, 31) was used. Note that in the presented model, $K_{F\_cell:perf}$ was included as global parameter that used per default the maternal fraction unbound; to correct for the fetal fraction unbound, $K_{F\_cell:perf}$ was multiplied by the ratio of fetal-to-maternal fraction unbound. Hence, inserting Equations 5, 7, 8 into Equation 6 as well as correcting for the fetal fraction unbound yields Equation 9 which was implemented in the model:

$$\frac{dN_{F\_cell}^{F\_cell\leftrightarrow F_i nt}}{dt} = P \times SA_{F\_int:cell} \times \left(C_{F\_int} \times \left(f_{water}^{int} + \frac{f_{protein}^{int}}{f_{protein}^{perf}} \times \left(\frac{1}{f_{u\_fetus}} - f_{water}^{perf} \right) \right)^{-1} \right) \left(-C_{F\_cell} \times \frac{f_{u\_fetus}}{K_{F\_cell:perf} \times \frac{f_{u\_fetus}}{f_u}} \right) \tag{9}$$

Or, alternatively and in a shorter form (Equation 10):

$$\frac{dN}{dt} = P \times SA_{F\_int:cell} \times \left(C_{F\_int} \times \frac{f_{u\_fetus}}{K_{F\_int:perf}} - C_{F\_cell} \times \frac{f_u}{K_{F\_cell:perf}} \right) \tag{10}$$

Finally, maternal-fetal drug transfer across the apical side of the trophoblast was modeled between maternal perfusate in the intervillous space and the trophoblasts using Equation 11:

$$\frac{dN_{F\_cell}^{F\_cell\leftrightarrow M\_perf}}{dt} = P \times SA_{villi} \times f_u \times \left(f_{in} \times C_{M\_perf} - f_{out} \times \frac{C_{F\_cell}}{K_{FM\_cell:perf}} \right) \tag{11}$$

In this equation, $N_{F\_cell}^{F\_cell\leftrightarrow M\_perf}$ denotes molar drug amount in the intracellular space when drug exchange is only considered to occur between the intracellular space and maternal perfusate in the cotyledon [μmol]; SA_{villi} is the surface area of the fetal villi at the interface of maternal perfusate in the cotyledon and trophoblasts [dm^2]; f_{in} and f_{out} are factors modifying the influx and efflux permeability of the drug (i.e. in maternal→fetal and fetal→maternal direction), respectively; and $K_{FM\_cell:perf}$ is the drug's partition coefficient between fetal intracellular space (trophoblasts) and maternal perfusate in the cotyledon.

Per default, f_{in} and f_{out} in Equation 11 are set to 1 (i.e. equal permeability in both directions). SA_{villi} was estimated by diving the absolute surface area of all fetal villi in the term placenta, ∼1178 dm^2 (27), by the average number of cotyledons in the placenta which varies around 35 at term (34). The drug's permeability across the trophoblasts' membrane was calculated from the drug's effective molecular weight and lipophilicity as described elsewhere (24) resulting in a value of $4.29 \cdot 10^{-2}$ cm/min for acetaminophen. $K_{FM\_cell:perf}$ was estimated as described above, i.e. according to the method described by Rodgers et al. (30, 31). Of note, the value of $K_{FM\_cell:perf}$ in Equation 11 is similar to that of $K_{F\_cell:perf}$ in Equation 10 because both partition coefficients refer to the same intracellular compartment (trophoblast). $K_{FM\_cell:perf}$ is located at the apical membrane and $K_{F\_cell:perf}$ at the basolateral membrane of the trophoblasts.

Hence, combining the ODEs above for the specific intercompartmental exchange processes gives the full ODE system of the novel *in silico* cotyledon perfusion model:

$$dt \begin{bmatrix} N_{M\_res} \\ N_{M\_perf} \\ N_{M\_int} \\ N_{F\_cell} \\ N_{F\_int} \\ N_{F\_perf} \\ N_{F\_res} \end{bmatrix} = E \begin{bmatrix} C_{M\_res} \\ C_{M\_perf} \\ C_{M\_int} \\ C_{F\_cell} \\ C_{F\_int} \\ C_{F\_perf} \\ C_{F\_res} \end{bmatrix} \tag{12}$$

Here, N and C denote molar drug amount [μmol] and molar drug concentration [μmol/L] in the compartment specified by the subscript and E describes the intercompartmental drug exchange processes that have been specified in Equations 1–11. More specifically, E can be written as the following 7 × 7 matrix:

$$E = \begin{bmatrix} -Q_M & Q_M & 0 & 0 & 0 & 0 & 0 \\ Q_M & -Q_M - f_u \times \left(P_{endo} \times SA_{M\_perf:int} + P \times SA_{villi} \times f_{in}\right) & P_{endo} \times SA_{M\_perf:int} \times f_u & P \times SA_{villi} \times f_{out} \times \frac{f_u}{K_{F\_cell:perf}} & 0 & 0 & 0 \\ 0 & P_{endo} \times SA_{M\_perf:int} \times f_u & P_{endo} \times SA_{M\_perf:int} \times \frac{f_u}{K_{M\_int:perf}} & 0 & 0 & 0 & 0 \\ 0 & P \times SA_{villi} \times f_{in} \times f_u & 0 & -P \times f_u \times \left(f_{out} \times \frac{SA_{villi}}{K_{FM\_cell:perf}} + \frac{SA_{F\_int:cell}}{K_{F\_cell:perf}}\right) & P \times SA_{F\_int:cell} \times \frac{f_u}{K_{F\_cell:perf}} & 0 & 0 \\ 0 & 0 & 0 & P \times SA_{F\_int:cell} \times \frac{f_{u\_fetus}}{K_{F\_int:perf}} & -\frac{f_{u\_fetus}}{K_{F\_int:perf}} \times \left(P \times SA_{F\_int:cell} + P_{endo} \times SA_{F\_perf:int}\right) & P_{endo} \times SA_{F\_perf:int} \times f_{u\_fetus} & 0 \\ 0 & 0 & 0 & 0 & P_{endo} \times SA_{F\_perf:int} \times \frac{f_{u\_fetus}}{K_{F\_int:perf}} & -Q_F - P_{endo} \times SA_{F\_perf:int} \times f_{u\_fetus} & 0 \\ 0 & 0 & 0 & 0 & 0 & Q_F & -Q_F \end{bmatrix} \quad (13)$$

Model Optimization

After the model has been implemented as described above, it was used to simulate acetaminophen concentrations in the maternal and fetal reservoir. Model parameters relevant for placental drug transfer, namely f_{in}, f_{out} and the placental partition coefficients ($K_{FM\_cell:perf}$ on the apical side and $K_{F\_cell:perf}$ on the basolateral side of the trophoblast), were optimized to better capture the observed data reported by Conings et al. (20). More specifically, the following optimization scenarios were tested:

- Optimizing symmetrical drug transfer: f_{in} and f_{out} were both fitted together so that the permeability in maternal→fetal and fetal→maternal direction was modified by the same factor.
- Optimizing asymmetrical drug transfer: f_{in} and f_{out} were fitted separately from each other, resulting in different permeability values in maternal→fetal and fetal→maternal direction.
- Optimizing symmetrical drug transfer and the placental partition coefficients: In addition to fitting f_{in} and f_{out} together, $K_{FM\_cell:perf}$ and $K_{F\_cell:perf}$ were also fitted together (i.e. both partition coefficients had the same fitted value). Hence, the permeability in maternal→fetal and fetal→maternal direction was modified by the same factor as were the partition coefficients. Fitting $K_{FM\_cell:perf}$ and $K_{F\_cell:perf}$ facilitated changes in intracellular drug concentrations (e.g., causing drug accumulation in the trophoblasts).
- Optimizing asymmetrical drug transfer and the placental partition coefficients: f_{in} and f_{out} were fitted separately from each other, while $K_{FM\_cell:perf}$ and $K_{F\_cell:perf}$ were fitted together (i.e. both partition coefficients had the same fitted value). This resulted in different permeability values in maternal→fetal and fetal→maternal direction and in modified additionally intracellular drug concentrations.

Parameter optimizations were conducted using the built-in module in MoBi® and the Monte-Carlo algorithm. All observed data [in total 18 data sets comprising 455 data values (20)] were included in the parameter optimization.

Fetal-Maternal PBPK Model for Acetaminophen

Description of the Model

After training the novel *in silico* cotyledon perfusion model to learn placental transfer kinetics of acetaminophen from the *ex vivo* cotyledon perfusion data, the fitted parameter values were copied to the PBPK model to predict acetaminophen pharmacokinetics in the umbilical vein at delivery. The structure of this whole-body model is schematically shown in **Figure 1** and the sub-structure of the placenta implemented in that model is depicted in **Figure 2**. In this placental sub-structure, the maternal plasma and blood cell compartments represent together the intervillous space, the maternal interstitial represents the placental septae and the maternal intracellular space represents the decidua basalis which is distorted during labor-induced contraction of the myometrium and eventually destroyed by the hemorrhages during delivery. The fetal intracellular compartment represents the (syncytio-)trophoblasts with the apical membrane facing the maternal plasma compartment

TABLE 2 | Patient characteristics.

	Study by Nitsche et al. (17)	Study by Mehraban et al. (18)
No. of patients	34	43
Maternal age [years]	32 [25–39]	30 [20–35]
Maternal weight [kg]	82 [62–100]	76 [46–136]
Maternal height [cm]	*not reported*	178 [149–209]
Gestational age at delivery [weeks]	39 [38–40]	39 [37–41]

Data are expressed as median [range].

and the basolateral membrane facing the fetal interstitial compartment. The fetal interstitial space represents intravillous fibrous tissue and the plasma and blood cell compartments represent the intravillous vascular system.

The PBPK model was corrected for the drug's unbound fraction in fetal compartments. Unbound maternal and fetal fraction of acetaminophen were calculated from the albumin plasma concentrations using a previously reported function (24). For the mother, albumin plasma concentrations were calculated for each patient's gestational age (27), while for the fetus, a concentration of 32 g/L was used as has been reported for the gestational age range from 35 to 38 weeks (35). Placental transfer parameters in the PBPK model were replaced with the fitted values from the *in silico* cotyledon perfusion model (see section Model Optimization). Of note, while the permeability across the placenta in the PBPK model was the same as in the *in silico* cotyledon perfusion model ($4.29 \cdot 10^{-2}$ cm/min), the transfer rate in the PBPK model was scaled with the villi surface area resulting thus in a larger transfer clearance for the total placenta compared to the cotyledon. All other model parameters were kept the same as published previously (13, 19).

Model Simulations

Pharmacokinetics were predicted in the venous plasma of the umbilical cord. For each patient, a virtual population of 100 pregnant women with the patient's body weight and height as well as gestational week was created using the population creation algorithm of the R-package 'ospsuite'. Unfortunately, the study by Nitsche et al. (17) did not report the individual body weight and height of each patient and, thus, a virtual population with standard body weight at term delivery (24) was used for the simulations. The population simulation results for all patients were pooled for calculation of the overall median and percentiles and for further analysis.

Patients and Data

Nitsche et al. (17) studied maternal and fetal pharmacokinetics in 34 women without medical or obstetrical complications following a single oral dose of 1,000 mg acetaminophen upon admission for scheduled cesarean delivery. Patient characteristics are listed in **Table 2**. Pharmacokinetic data were extracted from the concentration-time profile figure published by Nitsche et al. (17). From the 34 women, only 28 data values could be extracted.

Additional concentration data in the umbilical cord were obtained from the study by Mehraban et al. (18). From the 121 patients with intrapartum fever of whom blood samples were collected in this study, we included the 45 patients who received a single oral dose of 1,000 mg acetaminophen. Two additional patients were excluded from our analysis because of unusually high acetaminophen concentrations in the umbilical cord which we attributed to documentation errors (the umbilical vein concentrations of these patients were 14.5 and 3.1 mg/L at 18 and 55 h after dose administration). Characteristics of the patients included in our analysis are listed in **Table 2**.

Few measured concentrations in the study by Mehraban et al. (18) fell below the lower limit of quantification (LLOQ). These data were included as LLOQ/2 in this analysis. It has to be noted that in the study by Mehraban et al. (18), maternal concentrations were not measured.

PBPK Model Evaluation

Predicted concentrations in the umbilical vein were visually compared to clinical data obtained from clinical studies. Additionally, goodness-of-fit plots depicting predicted vs. observed concentrations and residuals vs. time plots were created and the mean prediction error (MPE) and mean absolute prediction error (MAPE) were calculated.

Ethics

Ethics and study registration related aspects are clearly mentioned in the original publications (17, 18) that served as source of this refinement effort, and no additional registration or procedures were needed.

RESULTS

In silico Cotyledon Perfusion Model

Of the four tested optimization scenarios, optimizing asymmetrical drug transfer and the placental partition coefficients yielded the lowest simulation error. The fitted value ± 95% confidence interval for the placental partition coefficients, $K_{FM\_cell:perf}$ and $K_{F\_cell:perf}$, was 4.31 ± 0.57 [vs. 0.76 when being estimating according to the method described by Rodgers et al. (30, 31)] resulting in a substantial amount of acetaminophen accumulating in the trophoblasts of the cotyledon.

The fitted values ± 95% confidence intervals for f_{in} and f_{out} were 0.060 ± 0.0058 and 0.051 ± 0.0061, respectively. This resulted in permeability values in maternal→fetal and fetal→maternal direction of 2.56×10^{-3} and 2.18×10^{-3} cm/min, respectively, vs. 4.29×10^{-2} cm/min when the permeability was estimated from the physicochemical properties of acetaminophen. **Figure 4** presents the observed and simulated concentration-time profiles of acetaminophen in maternal and fetal perfusate in the reservoirs of the *ex vivo* cotyledon perfusion assay.

The results of a local sensitivity analysis are presented in **Figure 5**. In this figure, simulation results are shown when $K_{FM\_cell:perf}$ and $K_{F\_cell:perf}$ were set to 0.76 [i.e., the value estimated according to the method described by Rodgers et al.

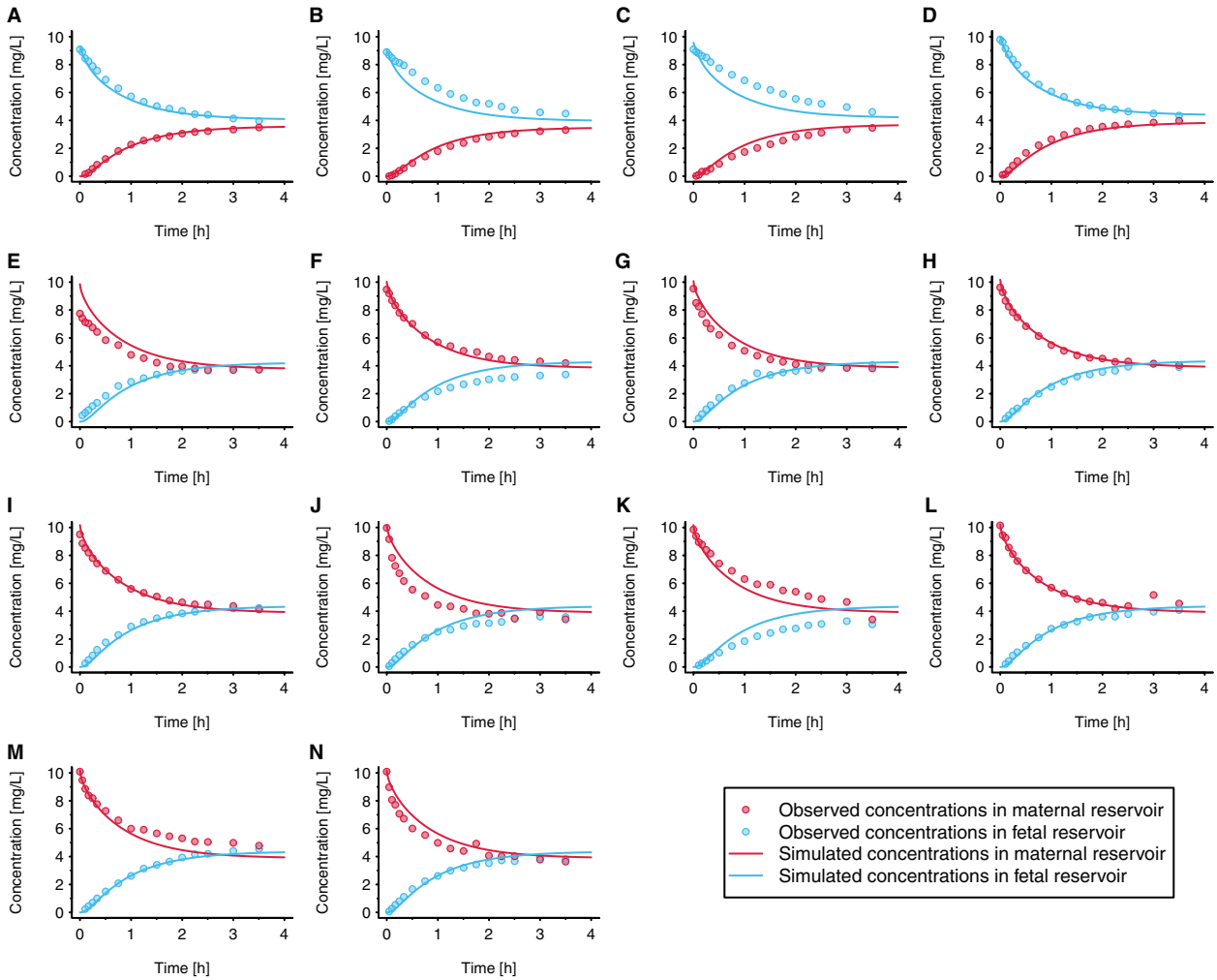

FIGURE 4 | Observed and simulated concentration time profiles in the novel *ex vivo* cotyledon perfusion model. In each experiment, acetaminophen was either administered to the fetal reservoir **(A–D)** or maternal reservoir **(E–N)** at time = 0h. The initial concentration was 10 mg/L in all experiments (to reflect clinically relevant concentrations); each panel refers to an individual experiment. All experiments were conducted under similar conditions. Observed data were taken from Conings et al. (20).

(30, 31)], 2.5, and 4.31 (i.e., the fitted value). All other model parameter values were kept unchanged in this sensitivity analysis. Pooled over all individual experiments, the MPE was 375%, 131, and −62.6% when using placental partition coefficient values of 0.76, 2.5, and 4.31, respectively.

PBPK Model Evaluation

Figure 6 presents the concentration-time profile predicted in the umbilical vein together with the clinical data reported by Nitsche et al. (17) and Mehraban et al. (18). The observed inter-individual variability, especially in the data reported by Mehraban et al. (18), was considerably larger than the predicted variability. For the pooled data sets, MPE and MAPE were 24.7 and 68.7%, respectively. For the data reported by Nitsche et al. (17), MPE and MAPE were −10.4 and 29.9%, respectively; and for the data reported by Mehraban et al. (18), MPE and MAPE were 49.3 and 96.0%, respectively.

Figure 7 presents the goodness-of-fit plot and the residuals plotted against time. For the pooled data sets, 50 (81%) out of 62 concentration values were predicted within a 2-fold error range (excluding values below LLOQ). For the data reported by Nitsche et al. (17), 25 (89%) out of 28 concentrations were predicted within the 2-fold error range, whereas for the data reported by Mehraban et al. (18), 25 (74%) out of 34 concentrations that were above LLOQ were predicted within that range.

DISCUSSION

The *ex vivo* cotyledon perfusion assay is often used to quantify drug transfer across the placenta and the results obtained from this assay can be leveraged in a PBPK modeling framework

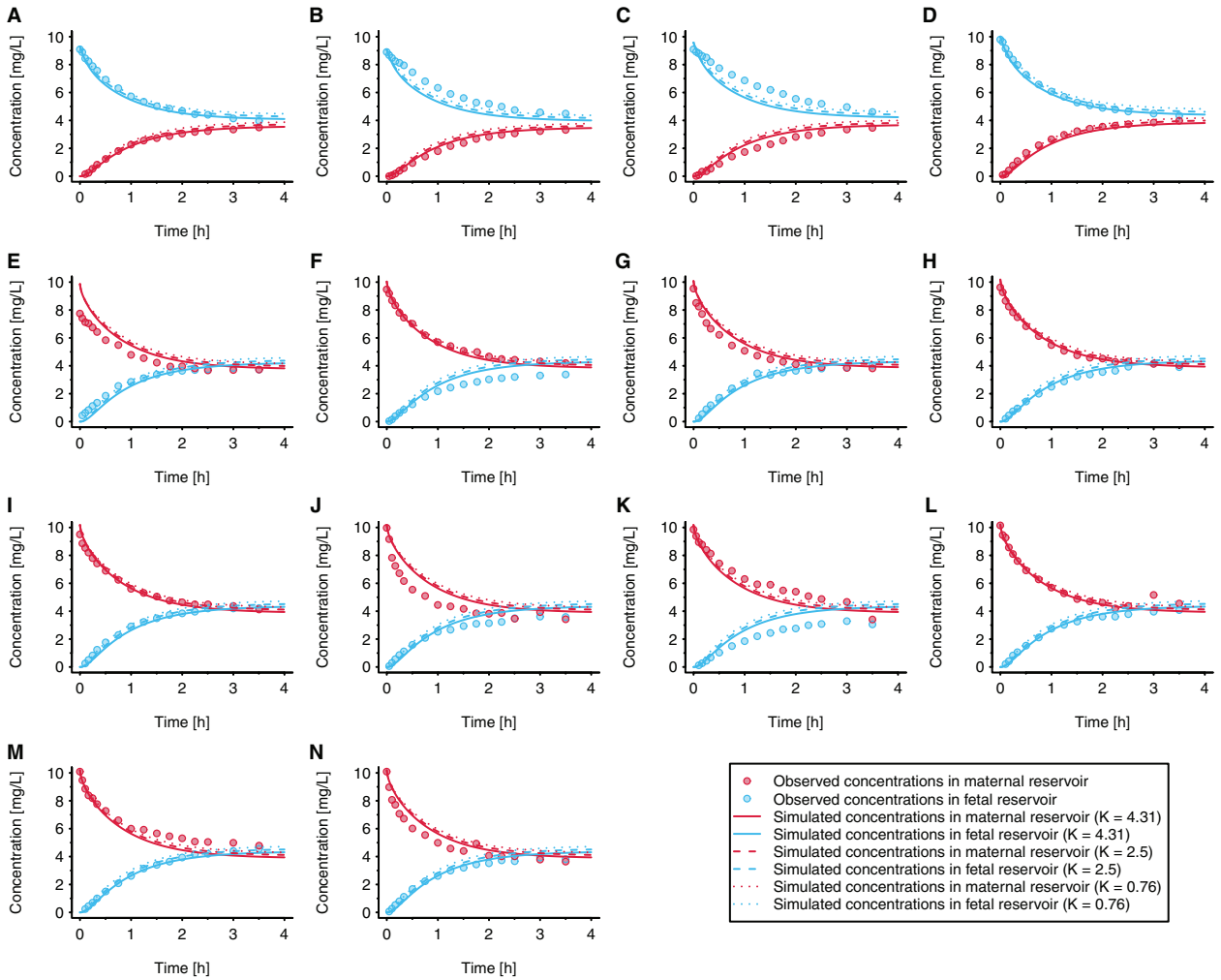

FIGURE 5 | Local sensitivity analysis for the placental partition coefficients ($K_{FM\_cell:perf}$ and $K_{F\_cell:perf}$). In each experiment, acetaminophen was either administered to the fetal reservoir **(A–D)** or maternal reservoir **(E–N)** at time = 0 h. The initial concentration was 10 mg/L in all experiments (to reflect clinically relevant concentrations); each panel refers to an individual experiment. All experiments were conducted under similar conditions. Observed data were taken from Conings et al. (20).

(36). While the previously developed *in silico* cotyledon perfusion model for acetaminophen directly links maternal with fetal perfusate (13), the PBPK model separates maternal from fetal blood plasma by interposing the fetal intracellular compartment (representing the trophoblasts) and the fetal interstitial compartment (representing stroma tissue in the fetal villi) (19). Owing to these structural differences, parameters in the *in silico* cotyledon perfusion model did not translate directly to parameters in the PBPK model. For example, the partition coefficient between maternal and fetal perfusate in the former model did not have an equivalent parameter in the PBPK model. Hence, this study aimed at developing an *in silico* cotyledon perfusion model with a more physiologic representation of the cotyledon and a compartmentalization of different tissue portions. Subsequently, this model was optimized to simulate published data for acetaminophen (20). Several parameters relevant to maternal-fetal drug transfer were optimized in this model and the best optimization results were then transferred into a previously developed whole-body PBPK model for acetaminophen (13, 19) to predict pharmacokinetics in the umbilical vein at delivery. The predictive performance of the PBPK model was then assessed with clinical data reported by Nitsche et al. (17) and Mehraban et al. (18).

The developed *in silico* cotyledon perfusion model consisted of seven compartments (**Figure 3**). It could be argued that the fetal compartment is missing the fetal endothelial cells since they represent an additional barrier to diffusion into the fetal plasma and blood cells which may become relevant, especially when it constitutes the rate-limiting step for drug distribution into the fetal reservoir. In this case, this barrier could be technically simulated by reducing the permeability across the endothelial membrane in the intravillous space (P_{endo}). This

also applies to drugs that are substrates to efflux transporters expressed in the endothelial membrane. While the transfer rate across the endothelial cells could be technically simulated, drug accumulation in the endothelial cells cannot be described by this model. For this case, a structural refinement of the model is necessary.

Data measured in the *ex vivo* cotyledon perfusion assay for acetaminophen (20) were used to optimize the model so that the observed data could be adequately reproduced (**Figure 4**). Obviously, the volume of the cotyledon [23 and 35 mL for the intervillous and intravillous cotyledon fraction, respectively (25)] appeared not always correctly parameterized since some simulations overestimated the observed concentrations at time point zero (see e.g., **Figure 4E**), although experimental sampling or measurement errors could also have given rise to these deviations.

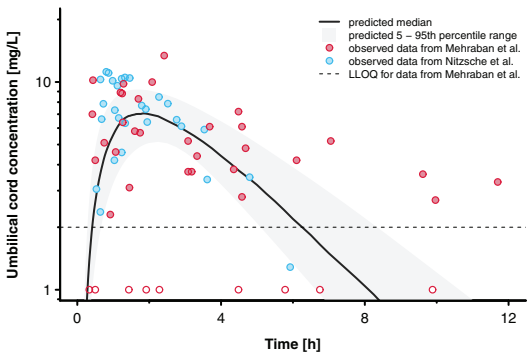

FIGURE 6 | Concentration time profiles for acetaminophen in the umbilical cord. Blue and red circles indicate observed clinical data reported by Nitsche et al. (17) and Mehraban et al. (18). Data from Mehraban et al. (18) below the lower limit of quantification (LLOQ), shown as dashed line, are included as LLOQ/2 and empty circles in the figure. The black line indicates the predicted median and the shaded area the predicted 5–95th percentile range.

It was observed that when increasing the placental partition coefficients, steady state acetaminophen concentrations in the maternal and fetal reservoir were slightly better simulated as indicated by the lower MPE, although the overall effect of higher placental partition coefficients on the concentrations in the reservoirs was rather small (**Figure 5**). The results of the sensitivity analysis (**Figure 5**) indicated that the measured acetaminophen concentrations in the maternal and fetal reservoirs were somewhat sensitive when accumulation in the trophoblasts was increased. Hence, the information content in these data was rather limited and results should be interpreted considering this uncertainty. Even though some uncertainty with respect to acetaminophen accumulation in the trophoblasts remains, the model simulations, especially the simulated steady state concentrations in the reservoirs, improved when acetaminophen was, at least to some extent, 'removed' from the reservoirs by either shifting it into other compartments (e.g., the trophoblasts) or completely removing it from the system. In the *ex vivo* experiment, this could have been caused by either accumulation in the cotyledon, by binding to the experimental equipment (e.g., the inner wall of the tubes) or by the loss of acetaminophen due to e.g., the sampling procedure or metabolism in the cotyledon. Here, rather than modeling acetaminophen metabolism, the partition coefficients $K_{FM\_cell:perf}$ and $K_{F\_cell:perf}$ were fitted allowing an accumulation in the trophoblasts. The fitted value (4.31) indicated that simulated acetaminophen concentrations at steady state are more than 4-fold greater in the trophoblasts vs. the maternal perfusate. Although various clinical studies have shown that several drugs accumulate in placental tissue, including ciprofloxacin (37), sildenafil (38), and tacrolimus (39), it is unclear whether acetaminophen also accumulates in placental tissue. If so, acetaminophen might affect prostaglandin synthesis

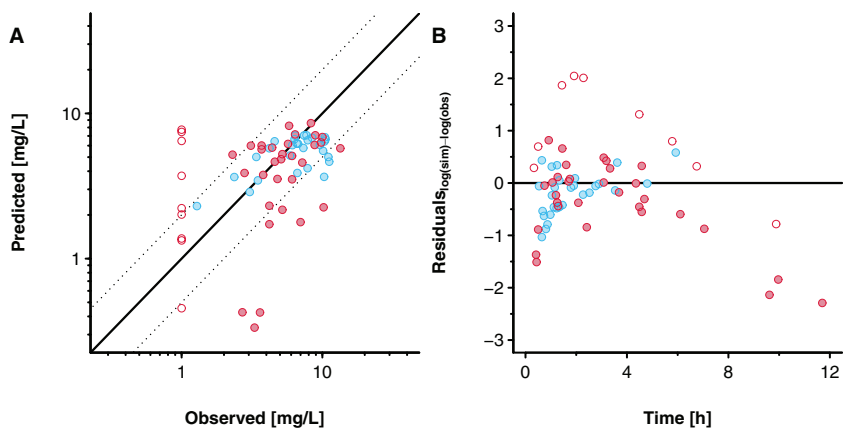

FIGURE 7 | Goodness-of-fit plot **(A)** and residuals versus time plot **(B)** for the predicted acetaminophen concentrations in the umbilical vein**.** Blue and red circles indicate clinical data reported by Nitsche et al. (17) and Mehraban et al. (18). Data from Mehraban et al. (18) below the lower limit of quantification (LLOQ) are included as LLOQ/2 and empty circles in the figure. In **(A)**, the solid line indicates the line of identity and the dashed lines limit the 2-fold error range. In **(B)**, the solid line indicates the level where the residuals are zero.

in the placenta, and subsequent fetal exposure with potentially deleterious effects on fetal development, future studies may further investigate this point.

However, metabolism could, at least partly, also be an explanation why the amount of acetaminophen in the maternal and fetal perfusate at steady state was lower than initially expected. Acetaminophen is predominantly metabolized by members of the UGT1A subgroup (mainly UGT1A1), members of the SULT1A subgroup (mainly SULT1A1), whereas a very minor extent is metabolized by CYP1A2, 2E1 and 3A4 to the toxic metabolite *N*-acetyl-*p*-benzoquinone imine (NAPQI). Although expression studies show somewhat conflicting results, it appears that most of these enzymes, including UGT1A, CYP1A2, and CYP2E1, can only be detected in placentae collected in the first trimester, but not in term placentae, whereas CYP3A4 is expressed, but apparently not functionally active in the term placenta (40, 41). SULT1A was reported to be expressed and active in the term placenta (42). However, Conings et al. (20) observed that during *ex vivo* cotyledon perfusion experiments with acetaminophen, the phase II metabolites acetaminophen glucuronide and sulfate could not be detected, whereas in perfusion experiments with acetaminophen glucuronide and sulfate, back-conversion to acetaminophen (deglucuronidation and desulfation) seemed to occur. Hence, placental metabolism of acetaminophen—and the potential conversion of phase II metabolites to the parent compound—is currently poorly understood. This aspect should be further investigated in future studies to disentangle acetaminophen accumulation and metabolism in the placenta as well as formation from its phase II metabolites. Accounting (even partially) for metabolism could improve the value of the model. This issue could potentially be addressed more specifically when selecting another drug with a better characterization of its placental metabolism profile.

The presented model enables to explore the concentration-time and concentration-effect profiles in placental tissue. To illustrate the relevance of this construct, with acetaminophen as example, we should be aware that the placenta is also a highly active secreting endocrine organ. This includes prostaglandins secreted to the fetal circulation to ensure high prostaglandin exposure throughout fetal life. In the event of transient placental acetaminophen accumulation, it is likely that this will affect prostaglandin synthesis, and subsequent fetal exposure. This may provide additional insight in the side effects associated with maternal acetaminophen (neurodevelopmental, fetal patent ductus constriction, atopy, fertility) intake during pregnancy, in addition or besides the subsequent fetal acetaminophen exposure (43–46). Finally, the concept of accumulation in placental tissue as observed for different compounds, and integrated in the current PBPK model should stimulate researchers to also consider conducting *ex vivo* cotyledon perfusion studies in both naïve as well as in placentas already exposed to a given compound before delivery.

The maternal-fetal PBPK model was used in a second step to predict acetaminophen concentrations in the umbilical cord at delivery. It was assumed that, apart from the pregnancy-induced physiological changes, neither labor nor the patient's condition (e.g., intrapartum maternal fever) would influence acetaminophen pharmacokinetics. The only adjustment related to labor and/or drugs administered in the peripartum period, such as opioids, was the 3-fold increase in gastric emptying time in the model as discussed previously (13). While all patients in the dataset by Mehraban et al. (18) received epidurals, pharmacokinetic data for the mother were not measured. The maternal pharmacokinetic data reported by Nitsche et al. (17) suggest that a 3-fold increase in gastric emptying time in the PBPK model is adequate to capture the data (13). Similar findings were also reported by Mendes et al. (9), although the authors changed the absorption rate and not gastric emptying time in their PBPK model.

The prediction results indicated that acetaminophen pharmacokinetics in the umbilical vein were overall satisfactory (**Figure 6**). However, inter-individual variability was substantially underestimated. This findings is not surprising because the physiological variability implemented in the PBPK model was derived from healthy pregnant women who were not in labor (27). Obviously, relatively little data is available that quantifies inter-individual variability in relevant physiological parameters (gastric emptying, organ blood flows, glomerular filtration rate etc.) during labor and hence the integration of physiological variability in PBPK models can at best be driven by plausible assumptions that are subsequently evaluated with clinical data. The predicted median concentration-time profile captured the observed data reasonably, though, as indicated by the relatively small MPE of 25.9%. Future studies should hence focus on reasonably capturing the large variability. This might also help assessing whether e.g., the two patients excluded from this analysis should really be treated as outliers (or documentation errors) or whether the unusually high concentrations from these patients could be attributed to e.g., variations in placental permeability as a consequence of labor, concomitant drug intake and/or diseases.

Unfortunately, observed maternal concentration data were not available for all patients. Such data could have helped better identifying the reasons why for some patients the fetal concentrations were rather poorly predicted. For example, a relatively large proportion of the fetal concentrations reported by Mehraban et al. (18) fell below the LLOQ. Without corresponding maternal data, is it difficult to determine whether acetaminophen poorly crossed the placenta barrier in these patients or whether maternal pharmacokinetics (e.g., delayed absorption or very fast metabolism) were responsible for the low fetal concentrations. A disease-related effect on placental drug transfer might, at least to some extent, explain the low concentrations in the umbilical cord. From the 43 patients included in this analysis, three were hypertensive and four additional patients were diabetic. Both conditions appear to be associated with impaired uteroplacental blood flow (47, 48). Additionally, it has been found that placentae from pregnancies complicated by gestational diabetes, especially if poorly controlled, show a decrease in the fluidity and a thickening of the syncytiotrophoblasts' membrane (49–51). These alterations could, at least partly, reduce placental drug transfer. In fact, from the seven hypertensive or diabetic patients

included in this analysis, five umbilical cord samples yielded concentrations below the LLOQ, whereas the concentrations from the other hypertensive or diabetic patients did not appear to differ from the remaining data. Interestingly, although one of the two patients excluded from this analysis was also suffering from gestational hypertension, the umbilical cord concentration obtained from this patient was unusually high (3.1 mg/L at 55 h) which seems inconsistent with a reduced placental drug transfer. Still, these considerations illustrate that the influence of diseases on the physiology in pregnant women should ideally be integrated in PBPK models, if applied to a clinical setting.

Several limitations pertain to the presented findings and models. In the *in silico* cotyledon perfusion model, many parameters could not be adequately identified, and hence biologically plausible assumptions had to be made. For example, the biochemical tissue composition of the placenta and cotyledon—a relevant input parameter for estimating the partition coefficients—was assumed to be similar. Currently, information is lacking in the scientific literature that would allow are more detailed discrimination of the biochemical composition of intervillous and intravillous structures in the placenta. Also, enzyme expression and drug metabolism in the placenta was not accounted for in the models. Kinetic data of acetaminophen metabolites measured in the *ex vivo* cotyledon perfusion assay could be used to assess enzyme abundance in the placenta, although this is complicated by the apparent back-conversion of metabolites to the parent compound (20). Additionally, results of the parameter optimization suggested some identification difficulties when fitting the parameters. In fact, f_{in} and f_{out} showed a relative strong correlation with the partition coefficients indicating that either the permeability or the partitioning should be ideally fixed to avoid non-identification issues. Further studies are needed to better inform these parameter separately.

In conclusion, this study presents a novel *in silico* cotyledon perfusion model consisting of seven compartments that can be used to mechanistically investigate placental drug transfer. The structure of this model is congruent with that of the placental compartments in the maternal-fetal PBPK model which allows a direct transfer of parameters from the former in the latter model. While the time of delivery will determine the time of collection of paired samples, at least the maternal part of a study protocol can be informed by predictions based on PK models, including PBPK models. The simulated accumulation of acetaminophen in the trophoblasts of the presented model might be of concern as this could potentially affect prostaglandin synthesis and subsequently fetal exposure to prostaglandins. Yet, it should also be stressed again that the measured drug concentrations in the maternal and fetal reservoirs were only to a limited extent informative of accumulation in the trophoblasts, as indicated by the sensitivity analysis result. Further studies should investigate potential accumulation as well as placental metabolism of acetaminophen.

The developed *in silico* cotyledon perfusion model is freely shared on OSP GitHub (https://github.com/Open-Systems-Pharmacology) for further applications and/or refinements that were beyond the scope of this study. Importantly, due to the mechanistic nature of the developed models, predictions can, in principle, be scaled to earlier stages of pregnancy (at least to the early second trimester when the formation of the placental barrier is completed). As clinical data are difficult to obtain at earlier stages of pregnancy, PBPK modeling approaches may constitute a potentially powerful tool to evaluate and investigate placental drug transfer and ultimately improve pharmacotherapy in pregnant women.

DATA AVAILABILITY STATEMENT

The datasets analyzed for this study are referenced in the article. Clinical data reported by Mehraban et al. (18) can be obtained from Nisha Lakhi (NLakhi@rumcsi.or) upon reasonable request.

AUTHOR CONTRIBUTIONS

PM, KA, and AD designed the research and wrote the manuscript. PM and AD performed the research. PM, BN, JA, KC, KA, NL, and AD analyzed the data. All authors contributed to the article and approved the submitted version.

ACKNOWLEDGMENTS

The authors would like to thank Dr. Sigrid Conings for conducting and analyzing the *ex vivo* cotyledon perfusion experiments.

REFERENCES

1. Mitchell AA, Gilboa SM, Werler MM, Kelley KE, Louik C, Hernandez-Diaz S, et al. Medication use during pregnancy, with particular focus on prescription drugs: 1976–2008. *Am J Obstet Gynecol.* (2011) 205:51.e1–8. doi: 10.1016/j.ajog.2011.02.029
2. Engeland A, Bjørge T, Klungsøyr K, Hjellvik V, Skurtveit S, Furu K. Trends in prescription drug use during pregnancy and postpartum in Norway, 2005 to 2015. *Pharmacoepidemiol Drug Saf.* (2018) 27:995–1004. doi: 10.1002/pds.4577
3. Chaphekar N, Caritis S, Venkataramanan R. Model-informed dose optimization in pregnancy. *J Clin Pharmacol.* (2020) 60:S63–76. doi: 10.1002/jcph.1777
4. Codaccioni M, Bois F, Brochot C. Placental transfer of xenobiotics in pregnancy physiologically-based pharmacokinetic models: structure and data. *Computational Toxicol.* (2019) 12:100111. doi: 10.1016/j.comtox.2019.100111
5. Zhang Z, Unadkat JD. Development of a novel maternal-fetal physiologically based pharmacokinetic model II: verification of the model for passive placental permeability drugs. *Drug Metab Dispos.* (2017) 45:939–46. doi: 10.1124/dmd.116.073957
6. Atoyebi SA, Rajoli RK, Adejuyigbe E, Owen A, Bolaji O, Siccardi M, et al. Using mechanistic physiologically-based pharmacokinetic models to assess prenatal drug exposure: thalidomide versus efavirenz as case studies. *Eur J Pharm Sci.* (2019) 140:105068. doi: 10.1016/j.ejps.2019.105068
7. Codaccioni M, Brochot C. Assessing the impacts on fetal dosimetry of the modelling of the placental transfers of xenobiotics in a pregnancy

physiologically based pharmacokinetic model. *Toxicol Appl Pharmacol.* (2020) 409:115318. doi: 10.1016/j.taap.2020.115318
8. Liu XI, Momper JD, Rakhmanina NY, Green DJ, Burckart GJ, Cressey TR, et al. Prediction of maternal and fetal pharmacokinetics of dolutegravir and raltegravir using physiologically based pharmacokinetic modeling. *Clin Pharmacokinet.* (2020) 59:1433–50. doi: 10.1007/s40262-020-00897-9
9. Mendes MDS, Hirt D, Vinot C, Valade E, Lui G, Pressiat C, et al. Prediction of human fetal pharmacokinetics using *ex vivo* human placenta perfusion studies and physiologically based models. *Br J Clin Pharmacol.* (2016) 81:646–57. doi: 10.1111/bcp.12815
10. Mendes MDS, Lui G, Zheng Y, Pressiat C, Hirt D, Valade E, et al. A physiologically-based pharmacokinetic model to predict human fetal exposure for a drug metabolized by several CYP450 pathways. *Clin Pharmacokinet.* (2017) 56:537–50. doi: 10.1007/s40262-016-0457-5
11. Schalkwijk S, Buaben AO, Freriksen JJ, Colbers AP, Burger DM, Greupink R, et al. Prediction of fetal darunavir exposure by integrating human *ex-vivo* placental transfer and physiologically based pharmacokinetic modeling. *Clin Pharmacokinet.* (2018) 57:705–16. doi: 10.1007/s40262-017-0583-8
12. Freriksen JJ, Schalkwijk S, Colbers AP, Abduljalil K, Russel FG, Burger DM, et al. Assessment of maternal and fetal dolutegravir exposure by integrating *ex vivo* placental perfusion data and physiologically-based pharmacokinetic modeling. *Clin Pharmacol Ther.* (2020) 107:1352–61. doi: 10.1002/cpt.1748
13. Mian P, Allegaert K, Conings S, Annaert P, Tibboel D, Pfister M, et al. Integration of placental transfer in a fetal-maternal physiologically based pharmacokinetic model to characterize acetaminophen exposure and metabolic clearance in the fetus. *Clin Pharmacokinet.* (2020) 59:911–25. doi: 10.1007/s40262-020-00861-7
14. Liu XI, Momper JD, Rakhmanina N, van den Anker JN, Green DJ, Burckart GJ, et al. Physiologically based pharmacokinetic models to predict maternal pharmacokinetics and fetal exposure to emtricitabine and acyclovir. *J Clin Pharmacol.* (2020) 60:240–55. doi: 10.1002/jcph.1515
15. Szeto KX, Le Merdy M, Dupont B, Bolger MB, Lukacova V. PBPK modeling approach to predict the behavior of drugs cleared by kidney in pregnant subjects and fetus. *AAPS J.* (2021) 23:89. doi: 10.1208/s12248-021-00603-y
16. Tetro N, Moushaev S, Rubinchik-Stern M, Eyal S. The placental barrier: the gate and the fate in drug distribution. *Pharm Res.* (2018) 35:1–16. doi: 10.1007/s11095-017-2286-0
17. Nitsche JF, Patil AS, Langman LJ, Penn HJ, Derleth D, Watson WJ, et al. Transplacental passage of acetaminophen in term pregnancy. *Am J Perinatol.* (2017) 34:541–3. doi: 10.1055/s-0036-1593845
18. Mehraban S, Nematian S, Mehraban SS, Petrucci S, Tricorico G, Parnas Z, et al. Randomized control trial of intravenous acetaminophen for reduction of intrapartum maternal fever. *Am J Obstet Gynecol MFM.* (2021) 3:1–9. doi: 10.1016/j.ajogmf.2020.100287
19. Mian P, Van Den Anker JN, van Calsteren K, Annaert P, Tibboel D, Pfister M, et al. Physiologically based pharmacokinetic modeling to characterize acetaminophen pharmacokinetics and N-acetyl-p-benzoquinone imine (NAPQI) formation in non-pregnant and pregnant women. *Clin Pharmacokinet.* (2020) 59:97–110. doi: 10.1007/s40262-019-00799-5
20. Conings S, Tseke F, Van den Broeck A, Qi B, Paulus J, Amant F, et al. Transplacental transport of paracetamol and its phase II metabolites using the *ex vivo* placenta perfusion model. *Toxicol Appl Pharmacol.* (2019) 370:14–23. doi: 10.1016/j.taap.2019.03.004
21. Lippert J, Burghaus R, Edginton A, Frechen S, Karlsson M, Kovar A, et al. Open systems pharmacology community—an open access, open source, open science approach to modeling and simulation in pharmaceutical sciences. *CPT Pharmacometrics Syst Pharmacol.* (2019) 8:878–82. doi: 10.1002/psp4.12473
22. Beaulac-Baillargeon L, Rocheleau S. Paracetamol pharmacokinetics during the first trimester of human pregnancy. *Eur J Clin Pharmacol.* (1994) 46:451–4. doi: 10.1007/BF00191910
23. Allegaert K, Peeters MY, Beleyn B, Smits A, Kulo A, Van Calsteren K, et al. Paracetamol pharmacokinetics and metabolism in young women. *BMC Anesthesiol.* (2015) 15:1–11. doi: 10.1186/s12871-015-0144-3
24. Dallmann A, Ince I, Solodenko J, Meyer M, Willmann S, Eissing T, et al. Physiologically based pharmacokinetic modeling of renally cleared drugs in pregnant women. *Clin Pharmacokinet.* (2017) 56:1525–41. doi: 10.1007/s40262-017-0538-0
25. Shintaku K, Arima Y, Dan Y, Takeda T, Kogushi K, Tsujimoto M, et al. Kinetic analysis of the transport of salicylic acid, a nonsteroidal anti-inflammatory drug, across human placenta. *Drug Metab Dispos.* (2007) 35:772–8. doi: 10.1124/dmd.106.013029
26. Schmitt W. General approach for the calculation of tissue to plasma partition coefficients. *Toxicol In Vitro.* (2008) 22:457–67. doi: 10.1016/j.tiv.2007.09.010
27. Dallmann A, Ince I, Meyer M, Willmann S, Eissing T, Hempel G. Gestation-specific changes in the anatomy and physiology of healthy pregnant women: an extended repository of model parameters for physiologically based pharmacokinetic modeling in pregnancy. *Clin Pharmacokinet.* (2017) 56:1303–30. doi: 10.1007/s40262-017-0539-z
28. Valentin J. Basic anatomical and physiological data for use in radiological protection: reference values: ICRP publication 89: approved by the commission in September 2001. *Ann ICRP.* (2002) 32:1–277. doi: 10.1016/S0146-6453(03)00002-2
29. Open Systems Pharmacology. *Manual: Compounds: Definition and Work Flows.* Available online at: https://docs.open-systems-pharmacology.org/working-with-pk-sim/pk-sim-documentation/pk-sim-compounds-definition-and-work-flow#distribution (accessed on March 4, 2021).
30. Rodgers T, Leahy D, Rowland M. Physiologically based pharmacokinetic modeling 1: predicting the tissue distribution of moderate-to-strong bases. *J Pharm Sci.* (2005) 94:1259–76. doi: 10.1002/jps.20322
31. Rodgers T, Rowland M. Physiologically based pharmacokinetic modelling 2: predicting the tissue distribution of acids, very weak bases, neutrals and zwitterions. *J Pharm Sci.* (2006) 95:1238–57. doi: 10.1002/jps.20502
32. Poulin P, Theil FP. A priori prediction of tissue: plasma partition coefficients of drugs to facilitate the use of physiologically-based pharmacokinetic models in drug discovery. *J Pharm Sci.* (2000) 89:16–35. doi: 10.1002/(SICI)1520-6017(200001)89:1<16::AID-JPS3>3.0.CO;2-E
33. Poulin P, Schoenlein K, Theil FP. Prediction of adipose tissue: plasma partition coefficients for structurally unrelated drugs. *J Pharm Sci.* (2001) 90:436–47. doi: 10.1002/1520-6017(200104)90:4<436::aid-jps1002>3.0.co;2-p
34. Polin RA, Fox WW, Abman SH. *Fetal and Neonatal Physiology*. Amsterdam: Elsevier health sciences (2011).
35. Moniz C, Nicolaides K, Bamforth F, Rodeck C. Normal reference ranges for biochemical substances relating to renal, hepatic, and bone function in fetal and maternal plasma throughout pregnancy. *J Clin Pathol.* (1985) 38:468–72. doi: 10.1136/jcp.38.4.468
36. Bouazza N, Foissac F, Hirt D, Urien S, Benaboud S, Lui G, et al. Methodological approaches to evaluate fetal drug exposure. *Curr Pharm Des.* (2019) 25:496–504. doi: 10.2174/1381612825666190319102812
37. Noergaard M, Jensen PB, Gotfredsen DR, Bergholt T, Andersen JT, Mathiesen L. Therapeutic concentration of ciprofloxacin and transfer across the human term placenta. *Am J Obstet Gynecol.* (2021). doi: 10.1016/j.ajog.2021.05.032. [Epub ahead of print].
38. Russo FM, Conings S, Allegaert K, Van Mieghem T, Toelen J, Van Calsteren K, et al. Sildenafil crosses the placenta at therapeutic levels in a dually perfused human cotyledon model. *Am J Obstet Gynecol.* (2018) 219:619.e1–10. doi: 10.1016/j.ajog.2018.08.041
39. Freriksen JJ, Feyaerts D, van den Broek PH, van der Heijden O, van Drongelen J, van Hamersvelt H, et al. Placental disposition of the immunosuppressive drug tacrolimus in renal transplant recipients and in *ex vivo* perfused placental tissue. *Eur J Pharm Sci.* (2018) 119:244–8. doi: 10.1016/j.ejps.2018.04.017
40. Syme MR, Paxton JW, Keelan JA. Drug transfer and metabolism by the human placenta. *Clin Pharmacokinet.* (2004) 43:487–514. doi: 10.2165/00003088-200443080-00001
41. Myllynen P, Immonen E, Kummu M, Vähäkangas K. Developmental expression of drug metabolizing enzymes and transporter proteins in human placenta and fetal tissues. *Expert Opin Drug Metab Toxicol.* (2009) 5:1483–99. doi: 10.1517/17425250903304049
42. Stanley EL, Hume R, Visser TJ, Coughtrie MW. Differential expression of sulfotransferase enzymes involved in thyroid hormone metabolism during human placental development. *J Clin Endocrinol Metab.* (2001) 86:5944–55. doi: 10.1210/jcem.86.12.8081
43. Allegaert K, Mian P, Lapillonne A, van den Anker JN. Maternal paracetamol intake and fetal ductus arteriosus constriction or closure: a case

series analysis. *Br J Clin Pharmacol.* (2019) 85:245–51. doi: 10.1111/bcp.13778
44. Allegaert K, van den Anker JN, editors. *Perinatal and Neonatal Use of Paracetamol for Pain Relief. Seminars in Fetal and Neonatal Medicine.* Amsterdam: Elsevier (2017).
45. van den Anker J, Allegaert K. Acetaminophen use in pregnant women and their neonates: safe or unsafe till proven otherwise? *Neonatol Fetal Neonatal Res.* (2020) 117:249–51. doi: 10.1159/000506837
46. Saugstad OD. Acetaminophen and the developing brain: reason for concern? *Neonatology.* (2020) 117:245–8. doi: 10.1159/000505954
47. Granger JP, Alexander BT, Bennett WA, Khalil RA. Pathophysiology of pregnancy-induced hypertension. *Am J Hypertens.* (2001) 14:178S–85. doi: 10.1016/S0895-7061(01)02086-6
48. Nylund L, Lunell N-O, Lewander R, Persson B, Sarby B. Uteroplacental blood flow in diabetic pregnancy: measurements with indium 113m and a computer-linked gamma camera. *Am J Obstet Gynecol.* (1982) 144:298–302. doi: 10.1016/0002-9378(82)90582-8
49. Mazzanti L, Staffolani R, Rabini R, Romanini C, Cugini A, Benedetti G, et al. Modifications induced by gestational diabetes mellitus on cellular membrane properties. *Scand J Clin Lab Invest.* (1991) 51:405–10. doi: 10.3109/00365519109091633
50. Al-Okail MS, Al-Attas OS. Histological changes in placental syncytiotrophoblasts of poorly controlled gestational diabetic patients. *Endocr J.* (1994) 41:355–60. doi: 10.1507/endocrj.41.355
51. Meng Q, Shao L, Luo X, Mu Y, Xu W, Gao C, et al. Ultrastructure of placenta of gravidas with gestational diabetes mellitus. *Obstet Gynecol Int.* (2015) 2015:283124. doi: 10.1155/2015/283124

Conflict of Interest: AD is an employee of Bayer AG and uses Open Systems Pharmacology software, tools, and models in his professional role.

The remaining authors declare that the research was conducted in the absence of any commercial or financial relationships that could be construed as a potential conflict of interest.

Publisher's Note: All claims expressed in this article are solely those of the authors and do not necessarily represent those of their affiliated organizations, or those of the publisher, the editors and the reviewers. Any product that may be evaluated in this article, or claim that may be made by its manufacturer, is not guaranteed or endorsed by the publisher.

frontiers in Pediatrics

ORIGINAL RESEARCH
published: 13 October 2021
doi: 10.3389/fped.2021.721059

Characterization of Plasma Protein Alterations in Pregnant and Postpartum Individuals Living With HIV to Support Physiologically-Based Pharmacokinetic Model Development

*Sherry Zhao[1], Mary Gockenbach[1], Manuela Grimstein[2], Hari Cheryl Sachs[1], Mark Mirochnick[3], Kimberly Struble[4], Yodit Belew[4], Jian Wang[5], Edmund V. Capparelli[6,7], Brookie M. Best[6,7], Tamara Johnson[1], Jeremiah D. Momper[6] and Anil R. Maharaj[8]**

[1] Division of Pediatrics and Maternal Health, Office of Rare Diseases, Pediatrics, Urologic and Reproductive Medicine, Office of New Drugs, Center for Drug Evaluation and Research, U.S. Food and Drug Administration, Silver Spring, MD, United States, [2] Office of Clinical Pharmacology, Office of Translational Sciences, Center for Drug Evaluation and Research, U.S. Food and Drug Administration, Silver Spring, MD, United States, [3] Boston University School of Medicine, Boston, MA, United States, [4] Division of Antivirals, Office of Antimicrobials, Office of New Drugs, Center for Drug Evaluation and Research, U.S. Food and Drug Administration, Silver Spring, MD, United States, [5] Office of New Drugs, Center for Drug Evaluation and Research, U.S. Food and Drug Administration, Silver Spring, MD, United States, [6] Skaggs School of Pharmacy and Pharmaceutical Sciences, University of California, San Diego, San Diego, CA, United States, [7] Pediatrics Department, School of Medicine, San Diego-Rady Children's Hospital San Diego, University of California, San Diego, San Diego, CA, United States, [8] Faculty of Pharmaceutical Sciences, The University of British Columbia, Vancouver, BC, Canada*

Background: Alterations in plasma protein concentrations in pregnant and postpartum individuals can influence antiretroviral (ARV) pharmacokinetics. Physiologically-based pharmacokinetic (PBPK) models can serve to inform drug dosing decisions in understudied populations. However, development of such models requires quantitative physiological information (e.g., changes in plasma protein concentration) from the population of interest.

Objective: To quantitatively describe the time-course of albumin and α1-acid glycoprotein (AAG) concentrations in pregnant and postpartum women living with HIV.

Methods: Serum and plasma protein concentrations procured from the International Maternal Pediatric Adolescent AIDS Clinical Trial Protocol 1026s (P1026s) were analyzed using a generalized additive modeling approach. Separate non-parametric smoothing splines were fit to albumin and AAG concentrations as functions of gestational age or postpartum duration.

Results: The analysis included 871 and 757 serum albumin concentrations collected from 380 pregnant (~20 to 42 wks gestation) and 354 postpartum (0 to 46 wks postpartum) women, respectively. Thirty-six and 32 plasma AAG concentrations from 31 pregnant (~24 to 38 wks gestation) and 30 postpartum women (~2–13 wks postpartum), respectively, were available for analysis. Estimated mean albumin concentrations remained stable from 20 wks gestation to term (33.4 to 34.3 g/L);

OPEN ACCESS

Edited by:
Angela Birnbaum, University of Minnesota Twin Cities, United States

Reviewed by:
Robin Michelet, Freie Universität Berlin, Germany
Erik Sjögren, Uppsala University, Sweden
Ashwin Karanam, Pfizer, United States

***Correspondence:**
Anil R. Maharaj
anil.maharaj@ubc.ca

Specialty section:
This article was submitted to Obstetric and Pediatric Pharmacology, a section of the journal Frontiers in Pediatrics

Received: *05 June 2021*
Accepted: *09 September 2021*
Published: *13 October 2021*

Citation:
Zhao S, Gockenbach M, Grimstein M, Sachs HC, Mirochnick M, Struble K, Belew Y, Wang J, Capparelli EV, Best BM, Johnson T, Momper JD and Maharaj AR (2021) Characterization of Plasma Protein Alterations in Pregnant and Postpartum Individuals Living With HIV to Support Physiologically-Based Pharmacokinetic Model Development. Front. Pediatr. 9:721059. doi: 10.3389/fped.2021.721059

whereas, concentrations rapidly increased postpartum until stabilizing at ∼42.3 g/L 15 wk after delivery. Estimated AAG concentrations slightly decreased from 24 wks gestation to term (53.6 and 44.9 mg/dL) while postpartum levels were elevated at two wks after delivery (126.1 mg/dL) and subsequently declined thereafter. Computational functions were developed to quantitatively communicate study results in a form that can be readily utilized for PBPK model development.

Conclusion: By characterizing the trajectory of plasma protein concentrations in pregnant and postpartum women living with HIV, our analysis can increase confidence in PBPK model predictions for HIV antiretrovirals and better inform drug dosing decisions in this understudied population.

Keywords: albumin, α1-acid glycoprotein, pregnancy, postpartum, HIV, PBPK

INTRODUCTION

The Panel on Treatment of Pregnant Women with HIV Infection and Prevention of Perinatal Transmission recommends that all pregnant individuals[1] living with HIV initiate or maintain antiretroviral (ARV) therapy throughout pregnancy regardless of plasma HIV RNA or CD4 count (1). During the course of pregnancy, a myriad of anatomical and physiological changes occur that can lead to substantial alterations in ARV drug disposition (2, 3). Correspondingly, use of standard adult dosages in pregnant individuals may result in inappropriate drug exposures. Ensuring optimal ARV therapy in pregnant individuals living with HIV confers several benefits including preventing toxicity to both the mother and fetus, decreasing the risk of the development of drug resistance, maintaining viral suppression during pregnancy, and preventing mother-to-child HIV transmission (4). Nonetheless, many drugs have yet to be adequately studied in this population.

Physiologically based pharmacokinetic (PBPK) modeling is an approach that has the potential to provide *a priori* predictions of drug disposition in understudied populations, such as pregnant individuals. By incorporating biologically relevant physiological parameters, models may inform the design of clinical trials in pregnancy and provide estimates on when and to what extent dose adjustments might be needed (5, 6). Owing to the distinct anatomical and physiological differences between pregnant and non-pregnant individuals, several research groups have developed population PBPK models for pregnant individuals (7, 8). Notably, physiological information used to inform such models are predominately derived from Caucasian individuals with low-risk pregnancies. In comparison, pregnant individuals living with HIV represent a demographically diverse population (9). Such individuals typically receive multiple concomitant medications (10). Yet, quantitative physiological information on parameters influencing drug disposition in pregnant individuals living with HIV is limited. Consequently, currently published population PBPK models may not fully reflect the underlying physiology of pregnant individuals living with HIV.

Differences in plasma protein concentrations between individuals can lead to pronounced changes in fractions of unbound drug in plasma and subsequent alterations in systemic drug disposition, particularly for drugs that exhibit high degrees of plasma protein binding (>90% protein binding) (11, 12). Albumin and α1-acid glycoprotein (AAG) represent the two major plasma proteins responsible for binding of a majority of exogenously administered compounds (13). Literature reports evaluating gestational changes in plasma protein concentrations in pregnant individuals have been well-documented in the literature (14–16). However, due to a lack of information specific to pregnant individuals living with HIV, it remains unclear if historical data derived from individuals without HIV infection can be used to inform the development of PBPK models for this population.

After delivery, many of the physiologic changes associated with pregnancy take weeks to months to revert to their pre-pregnancy baseline (17). Studies on antibiotic pharmacology have demonstrated marked alterations in drug pharmacokinetics (PK) between early (2–3 days post-delivery) and late (>4 months post-delivery) postpartum periods (18, 19). Yet, few PBPK models have specifically been developed to estimate drug PK during this unique physiologic period (17). To inform the development of PBPK models capable of informing ARV dosing decisions in postpartum individuals living with HIV, data are needed to describe the physiological transition following delivery back to a non-pregnant state. Considering the important influence that plasma protein binding exerts on systemic drug disposition, this study sought to (1) quantitatively describe the time-course of serum/plasma protein concentrations (i.e., albumin and AAG) in pregnant and postpartum women living with HIV, (2) compare concentrations to values reported in pregnant and postpartum women without HIV infection, and (3) generate computational functions that describe the trajectory of serum/plasma protein concentrations in pregnant and postpartum women living with HIV to inform the prospective development of PBPK models.

[1]This article uses the term "pregnant individuals" to refer to all persons who can become pregnant regardless of gender identity. The terms "pregnant women living with HIV (PWLH)" and "postpartum women" are used in the Methods and Results section of the article because IMPAACT 1026s protocol specified that women were to be enrolled.

MATERIALS AND METHODS

Data Source

Our analysis evaluated serum and plasma protein concentrations procured from the International Maternal Pediatric Adolescent AIDS Clinical Trial (IMPAACT) Protocol 1026s (P1026s), a multicenter, multi-arm, open-label prospective opportunistic study of ARV and tuberculosis medications in pregnant and postpartum women (20). Pregnant women living with HIV (PWLH) as well as postpartum women receiving ARV medications as specified by the study protocol were eligible for enrollment. Each participant's ARV regimen was prescribed and managed by their treating physician. Key inclusion criteria during pregnancy included confirmed HIV diagnosis, receiving stable ARV treatment, and ≥20 wks gestation. Exclusion criteria included concomitant use of medications known to interfere with the PK of the medications being evaluated, multiple pregnancy (i.e., carrying multiple fetuses), and clinical or laboratory evidence of drug toxicity that would likely require changes in the medication regimen during the study. The protocol specified that women enrolled during pregnancy would remain in the study up to 24 wks after delivery. Intensive PK sampling and/or laboratory measurements were taken on multiple occasions including in the second trimester (20 to 26 gestational wks), third trimester (30 to 38 gestational wks), at delivery, and during the postpartum period (2 to 24 wks postpartum). Our analysis leveraged serum albumin and plasma AAG concentrations collected as part of these clinical evaluations. Demographic and anthropometric data including maternal age, weight, height, ethnicity, and country were collected. Additionally, pre-pregnancy weight was collected, if available.

Albumin in Pregnant and Postpartum Women Living With HIV

The time-course of serum albumin concentrations in pregnant and postpartum women living with HIV were described using a generalized additive modeling approach. Separate models were developed for the pregnant and postpartum periods. The start of the postpartum period coincided with the date of delivery. Models were developed using the Generalized Additive Models for Location, Scale, and Shape (gamlss) package in R (version 4.0.3; R Foundation for Statistical Computing, Vienna, Austria) (21). Non-parametric penalized beta-splines were used to model serum albumin concentrations (response variable) as a function of gestational age (weeks) or postpartum duration (weeks) (22). Models incorporating different error-distribution assumptions were generated and compared. In addition, models that permitted for changes in response variable variance as a function of gestational age or postpartum duration were evaluated. Model selection was guided by a combination of visual and quantitative appraisals including goodness-of-fit plots (i.e., quantile-quantile plots) and generalized Akaike information criterion (AIC) values (23). For the selected pregnancy and postpartum models, theoretical (model-based) time-dependent albumin quantiles associated with the 2.5th, 10th, 25th, 50th, 75th, 90th, and 97.5th percentiles were estimated. To evaluate the fit of model-derived quantiles, the percentage of observed data falling below each respective quantile was summarized for each dataset (pregnancy and postpartum). For models exhibiting an appropriate fit to the data, the percentage of observed data corresponding to each theoretical quantile should be congruent (e.g., 2.5% of observed data should fall below the model-derived quantile for the 2.5th percentile).

AAG in Pregnant and Postpartum Women Living With HIV

An initial assessment of the analysis dataset indicated that plasma AAG concentrations were not consistently reported. For each respective cohort (i.e., pregnancy and postpartum), <40 observations were available. Owing to the disparate nature of available AAG concentrations, the ability to examine different error distributions as well as alterations response variable variance, as conducted above, was limited. As such, our analysis exclusively focused on describing the time-course of the central tendency of plasma AAG concentrations in pregnant and postpartum women. Using the *smooth.spline()* function in R, separate cubic smoothing splines were fit to AAG concentrations (response variable) as functions of gestational age (weeks) or postpartum duration (weeks) in cohorts of pregnant and postpartum women, respectively.

Comparison to Serum/Plasma Concentrations From Women Without HIV Infection

Estimated serum/plasma protein concentrations (albumin and AAG) derived from our analysis were graphically compared to estimates for pregnant and postpartum women without HIV infection published by researchers affiliated with leading PBPK modeling platforms (i.e., Certara Simcyp™ and Open Systems Pharmacology PK-Sim®). Equations published by Abduljalil et al. and Dallmann et al. (7, 8) were used to facilitate these comparisons for pregnant women. Protein concentration estimates reflective of postpartum women were derived from Dallmann et al.'s published equation (17). The above-described equations were formulated following quantitative assessments of data collected over multiple publications from women without HIV.

Development of Computational Functions Describing Serum/Plasma Protein Concentrations in Pregnant and Postpartum Women Living With HIV

Several computational functions were developed to communicate the results of our analysis in a form that can be readily integrated into PBPK modeling platforms. Functions were generated using the open-source software R. For serum albumin, where the analysis included specific considerations for the central tendency, variance, and error distribution, four separate computational functions were developed. Developed functions provided estimates of (1) the arithmetic mean of serum albumin concentrations in pregnancy with increasing gestation, (2) quantiles of serum albumin concentrations in pregnancy, (3) the arithmetic mean of serum albumin concentrations in postpartum

women with increasing postpartum duration, and (4) quantiles of serum albumin concentrations in postpartum women.

Due to their lower computational complexity, parametric approximations of developed non-parametric models were incorporated into generated functions. Parametric polynomials were used to approximate the relationship between the central tendency (arithmetic mean) of serum albumin concentrations and time (i.e., gestational age or postpartum duration), as previously defined by corresponding non-parametric models. The degree of the polynomial was sequentially increased until the coefficient of determination (R^2) describing the polynomial's fit to estimates from the non-parametric model was >0.995. Quantile functions computing time-dependent estimates of serum albumin concentrations at specific percentiles were created by integrating the developed polynomials, describing the mean of albumin concentrations, and statistical considerations for the variance and error distribution of albumin values, as previously defined by corresponding non-parametric models. For AAG, where our analysis solely focused on describing the time-course of the central tendency of plasma AAG values, two computational functions were developed to describe arithmetic mean of AAG concentrations in (1) pregnant and (2) postpartum women. These functions were created using parametric polynomial approximations, as described above.

RESULTS

Demographics

Our analysis evaluated 871 serum albumin concentrations from 380 PWLH between ∼20 to 42 wks gestation (**Table 1**). For postpartum women living with HIV, 757 samples were evaluated from 354 women between 0 to 46 wks after delivery. In several instances, final study visits (i.e., 24 wks post-delivery) were delayed, resulting in clinical evaluations occurring up to several weeks after the protocol-defined end date. Two serum albumin concentrations present in the original dataset (1 pregnancy and 1 postpartum) that exhibited relatively high values compared to others (>60 g/L) were excluded from the analysis. Both the pregnant and postpartum albumin datasets were comprised of racially diverse cohorts. Black (i.e., Black African and Black or African American) women represented 47.4 and 46.9% of participants in the pregnancy and postpartum datasets, respectively. The majority of women were enrolled from the United States including 84.5 and 85.3% of women in the pregnancy and postpartum albumin datasets, respectively. The rest were enrolled from international sites. Concomitant ARV medications taken by women included in the albumin analysis are denoted in **Supplementary Table 1**.

Thirty-six plasma AAG concentrations collected from 31 PWLH between ∼24 to 38 wks gestation were included in the analysis (**Table 1**). The analysis additionally included 32 postpartum AAG concentrations collected from 30 women between ∼2 to 13 wks post-delivery. Evaluated plasma AAG concentrations were exclusively collected from participants enrolled in the United States. Black (i.e., Black or African American) women comprised 35.5 and 36.7% of the participants included in the pregnancy and postpartum AAG datasets, respectively. All women who contributed AAG concentrations for analysis were taking lopinavir/ritonavir (i.e., Kaletra; **Supplementary Table 1**).

Serum Albumin in PWLH

A generalized additive model incorporating a non-parametric smoother, a mixture-normal error distribution, and a constant error variance appropriately characterized the relationship between weeks gestation and serum albumin concentrations in PWLH (**Supplementary Figure 1**; **Supplementary Table 2**). The selected model utilized a combination of two normal (i.e., gaussian) distributions to describe the spread of serum albumin concentrations. Although an alternative model that additionally permitted for alterations in the variance of albumin concentrations with increasing gestation exhibited a lower AIC value compared to the selected model ($\Delta AIC = -2.034$; **Supplementary Table 2**), this difference was considered minute and, thus, a constant error variance model was adopted. Model-based quantiles adequately described the time-course of observed albumin concentrations in PWLH beyond 20 wks gestation (**Figure 1A**). This was additionally demonstrated by the high level of agreement between observed albumin concentrations and model-estimated quantiles (**Table 2**).

The estimated time-course for the central tendency (i.e., arithmetic mean) of serum albumin concentrations is displayed in **Figure 2A**. Model estimates were corroborated by average values computed from the observed data (**Supplementary Table 3**). In PWLH, average serum albumin concentrations remained relatively constant from 20 weeks gestations. Estimated values at 20 and 37 wks gestation were similar (34.3 and 33.4 g/L, respectively). In contrast, previously published equations describing the time-course of serum albumin concentrations in pregnant women without HIV infection denoted a decreasing trend (7, 8). For example, estimated serum albumin concentrations based on Dallmann et al.'s publication were 38.2 and 34.7 g/L at 20 and 37 wks gestation, respectively (8). Likewise, estimates from Abduljalil et al.'s published equation were 40.9 and 34.7 g/L, respectively (7). Notably, at term (i.e., 37 wks gestation), estimated values were similar between our analysis and those generated by competing equations.

As an additional evaluation, we compared the distribution of model predicted albumin concentrations at 20 wks, 28 wks, and term (i.e., 37 wks gestation) from our analysis to Dallmann et al.'s published equation (**Figures 3A–C**) (8). For the latter, albumin concentrations were approximated using a normal distribution with a standard deviation of 5.33 g/L. The difference in median values between the two analyses decreased with increasing gestation and were nearly congruent at term, where albumin concentrations of 34.1 and 34.8 g/L were estimated by our analysis and Dallmann et al.'s (8) equation, respectively. However, the distribution of albumin concentrations for PWLH exhibited a slight negative (left) skew whereas estimates from Dallmann et al.'s model were symmetrically distributed. The probability density associated with the upper tails of each respective distribution distinctly differed. At term, Dallmann et al.'s (8) equation exhibited a higher proportion of estimates exceeding

TABLE 1 | Demographic characteristics of the pregnant and postpartum women providing serum albumin and plasma AAG samples.

Demographic Parameters	Albumin dataset		AAG dataset	
	Pregnant (380 Women)	Postpartum (354 Women)	Pregnant (31 Women)	Postpartum (30 Women)
Country, *n* (%)				
Argentina	3 (0.8)	1 (0.3)	–	–
Botswana	12 (3.2)	12 (3.4)	–	–
Brazil	14 (3.7)	12 (3.4)	–	–
South Africa	2 (0.5)	2 (0.6)	–	–
Thailand	20 (5.3)	17 (4.8)	–	–
Uganda	8 (2.1)	8 (2.3)	–	–
United States	321 (84.5)	302 (85.3)	31 (100%)	30 (100%)
Race, *n* (%)				
Asian or Pacific Islander	24 (6.3)	22 (6.2)	–	–
Black African	22 (5.8)	22 (6.2)	–	–
Black or African American	158 (41.6)	144 (40.7)	11 (35.5)	11 (36.7)
Indigenous American	3 (0.8)	3 (0.8)	1 (3.2)	1 (3.3)
Other	5 (1.3)	5 (1.4)	–	–
Unknown/Unavailable	23 (6.1)	20 (5.9)	8 (25.9)	8 (26.7)
White (Caucasian)	145 (38.2)	138 (39)	11 (35.5)	10 (33.3)
Age (at delivery), years, Median (Q1, Q3)	29 (24, 34)	29 (24, 34)	29 (26.6, 33.5)	30 (27, 33.8)
Weight (pre-pregnancy), kg, Median (Q1, Q3)[1]	67.1 (57.9, 85.4)	67.8 (58.5, 84.8)	69.7 (60.5, 86.2)	69.7 (60.5, 86.2)
Body-Mass Index (pre-pregnancy), kg/m^2, Median (Q1, Q3)[1]	26.2 (22.7, 32.5)	26.4 (22.9, 32.7)	26.7 (22.8, 31.6)	26.7 (22.8, 31.6)
Weight (at delivery), kg, Median (Q1, Q3)[2]	79.5 (68.3, 94.5)	80.1 (68.5, 94.5)	86.5 (73.4, 97.7)	81.75 (73, 98.2)

AAG, α1-acid glycoprotein; Q1, First quartile; and Q3, Third quartile. [1]*Pre-pregnancy weights and body mass index values were missing for 116, 107, 8, and 7 individuals from the pregnancy albumin, postpartum albumin, pregnancy AAG, and postpartum AAG datasets, respectively.* [2]*Delivery weights were missing for 37, 34, 2, and 2 individuals from the pregnancy albumin, postpartum albumin, pregnancy AAG, and postpartum AAG datasets, respectively.*

40 g/L compared to our model (**Figure 3C**). For example, 16.7% of albumin concentrations at term were expected to be >40 g/L based on Dallmann et al.'s (8) model. In comparison, only 1.5% of estimates exceeded this threshold based on our model. An evaluation of the percent of observed data from PWLH that corresponded to quantiles generated from Dallmann et al.'s (8) model further highlighted this distributional mismatch (**Table 2**). Notably, observed data were discordant with upper model quantiles (75th, 90th, and 97.5th percentiles).

Serum Albumin in Postpartum Women Living With HIV

A generalized additive model incorporating a non-parametric smoother, a skew normal (type 2) error distribution, and time-dependent changes in error variance provided an appropriate fit to the data (**Supplementary Figure 2**; **Supplementary Table 4**). The selected distribution (i.e., skew normal type 2) exhibited a slight negative (left) skew (24). This is visually depicted in **Figure 1B**, where differences in albumin concentrations between subsequent lower percentiles are relatively larger compared to upper percentiles. The selected model employed different error variances for albumin concentrations ≤0.5 and >0.5 wks postpartum. For ≤0.5 wks postpartum, the estimated standard deviation of albumin concentrations was 4.86 g/L; whereas, beyond this period, a standard deviation of 3.64 g/L was estimated. Model quantiles exhibited a suitable fit to the data as demonstrated by the high degree of concordance with observed concentration values (**Table 2**).

The predicted time-course for the arithmetic mean of serum albumin concentrations during the postpartum period is displayed in **Figure 2B**. These estimates agreed with average values computed from the observed data (**Supplementary Table 5**). Average serum albumin concentrations slightly decreased immediately after birth. Estimated albumin concentrations at term (i.e., 37 wks gestation) based on the developed pregnancy model was 33.4 g/L; whereas, a value of 31.6 g/L was estimated at delivery based on the developed postpartum model. Serum albumin concentrations rapidly increased after delivery and stabilized to an average value of ∼42.3 g/L after 15 wks postpartum. Estimated albumin values were ∼75% (31.6 g/L) of this plateau value at delivery and increased to ∼90% (38.3 g/L) by 3 wks postpartum. A similar pattern was depicted by Dallmann et al.'s published equation, which described the trajectory of serum albumin concentrations in postpartum women without HIV infection (17). However, the denoted plateau value, achieved at ∼7 wks postpartum, was relatively higher (∼46.4 g/L). Nonetheless, the time-course

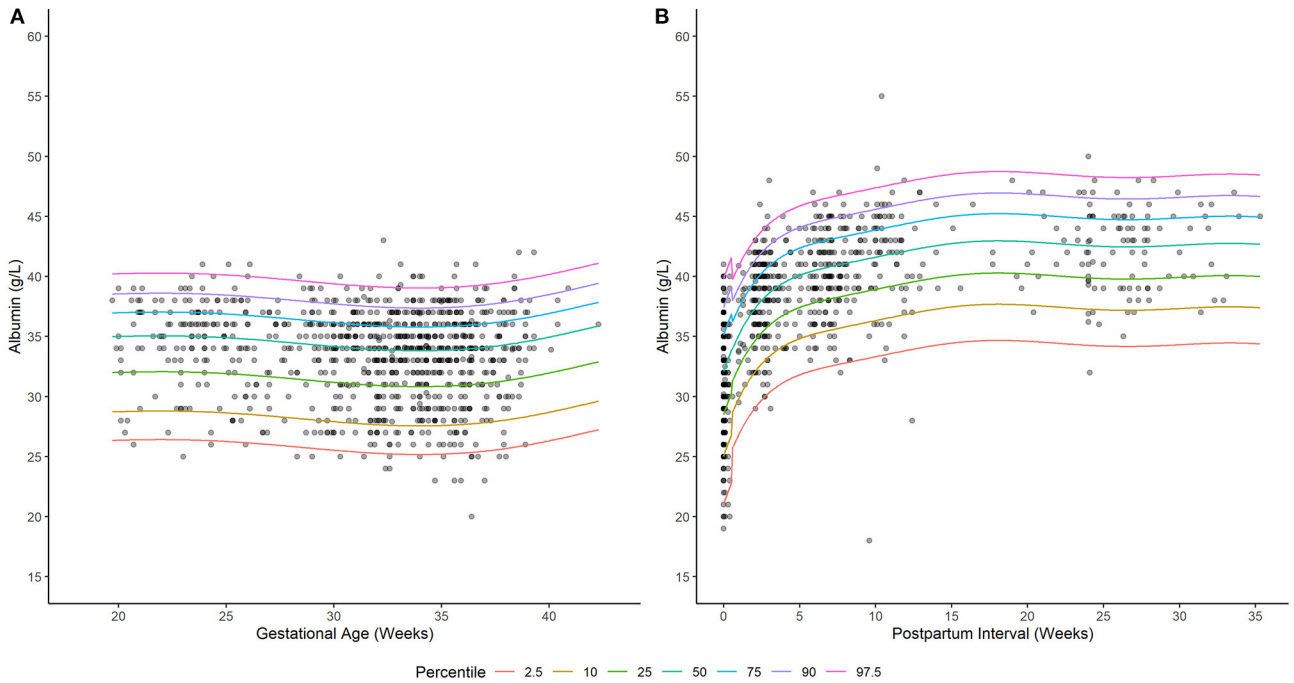

FIGURE 1 | Serum albumin concentrations in **(A)** pregnant and **(B)** postpartum women living with HIV. Solid lines depict model-based quantile estimates at denoted percentiles. Filled-circles depict observed serum albumin concentrations.

TABLE 2 | Percent of observed albumin concentrations in pregnant and postpartum women living with HIV that fall below model-predicted quantiles (associated with specified percentiles).

Dataset	Albumin pregnancy dataset		Albumin postpartum dataset
Model	P1026s (current study)	Dallmann et al. (8)	P1026s (current study)
Predicted Percentile			
2.5%	2.64%	1.95%	1.85%
10%	9.30%	13.55%	10.2%
25%	24.68%	29.97%	25.8%
50%	49.71%	69.23%	51.3%
75%	73.36%	96.56%	74.4%
90%	90.01%	99.66%	89.7%
97.5%	97.82%	100.00%	98.28%

of serum albumin concentrations was relatively similar to our analysis. For example, albumin concentrations estimated by Dallmann et al.'s (17) model were ∼66% (30.8 g/L) of their respective plateau value at delivery and increased to ∼90% (41.9 g/L) at 4 wks. A distributional comparison between our model and Dallmann et al.'s (17) was not instituted as the latter did not specify the variance and/or distribution of postpartum albumin values.

AAG in PWLH

Average plasma AAG concentrations, as estimated by a fitted smoothing spline, decreased linearly between 24- and 37-wks gestation (**Figure 4A**). Estimated AAG concentrations at these time points were 53.6 and 44.9 mg/dL, respectively. Previously published equations depicting the trajectory of plasma AAG concentrations in women without HIV infection depicted slightly higher values over similar time periods (7, 8). Nonetheless, these equations exhibited similar decreasing trends, albeit with slower rates of decrease. For example, estimated AAG concentrations at 24 and 37 weeks gestation based on Dallmann et al.'s published equation were 61.2 and 59.5 mg/dL, respectively (8); whereas, Abduljalil et al.'s equation depicted concentrations of 58.6 and 55.3 mg/dL, respectively (7).

AAG in Postpartum Women Living With HIV

Elevated plasma AAG concentrations were observed for samples collected closer to the date of delivery and decreased thereafter (**Figure 4B**). A smoothing spline fit to the data depicted a linear decreasing trend in average plasma AAG concentrations with increasing time after delivery. The estimated AAG concentration at 2 wks postpartum was 120.4 mg/dL, which was notably higher than the estimated value at term (44.9 mg/dL; 37 wks gestation) determined for PWLH. The fitted trajectory of AAG concentrations did not appear to reach a nadir value and was predicted to be 74.7 mg/dL at 12 wks postpartum. A previously published equation describing AAG concentrations in postpartum women without HIV infection displayed some similarities (17). The AAG concentration at 2 wks postpartum was estimated to be 126.1 mg/dL based on Dallmann et al.'s (17) published equation. Similar to our analysis, AAG concentrations decreased with increasing time after delivery. However, the rate of decline described by Dallmann et al. (17) was notably faster.

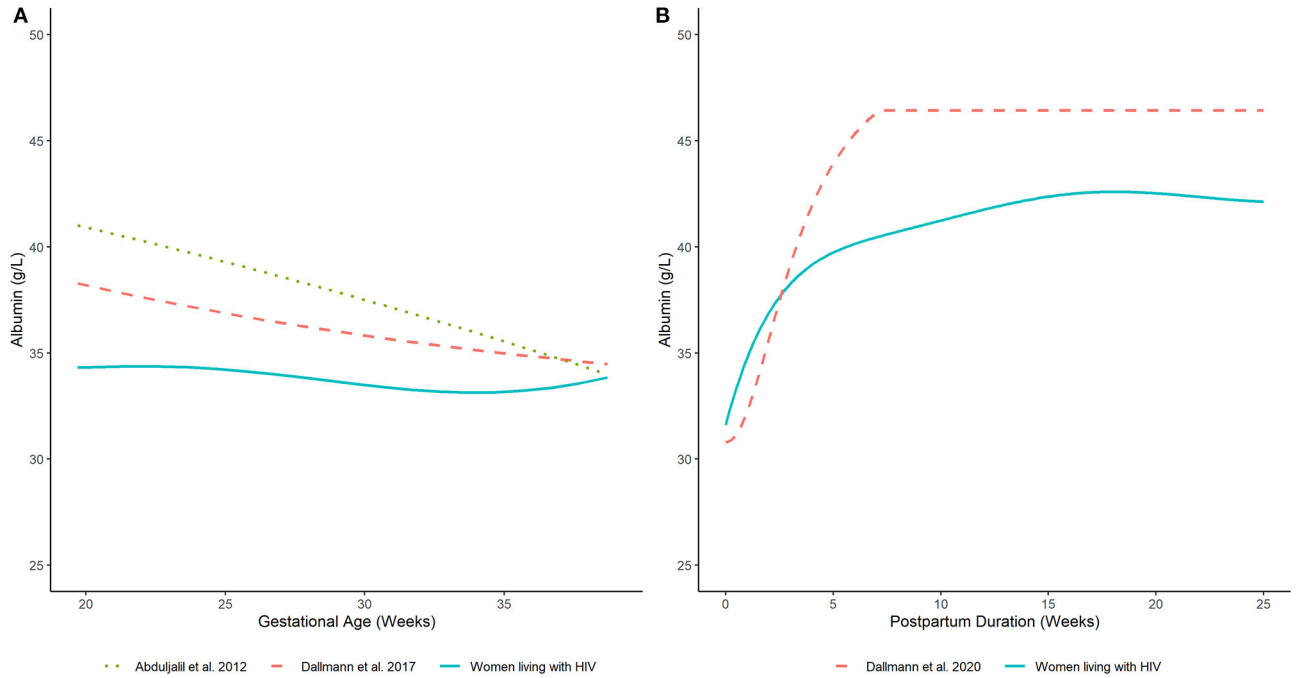

FIGURE 2 | Serum albumin concentrations in **(A)** pregnant and **(B)** postpartum women estimated by our analysis (women living with HIV) and other published equations (women without HIV infection) (7, 8, 17). Lines depict (arithmetic) mean albumin concentration estimates generated by competing models.

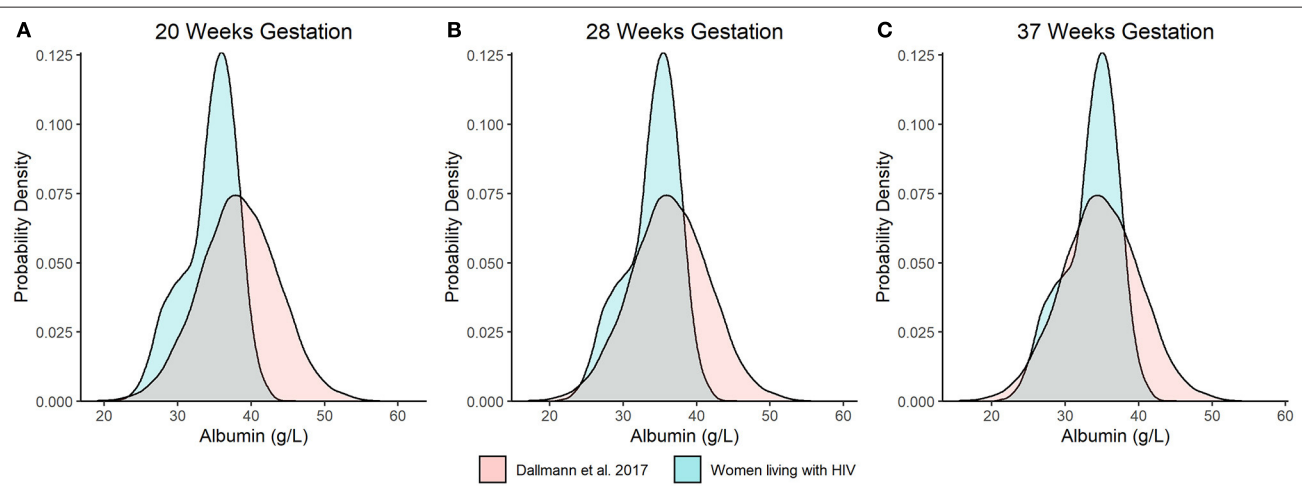

FIGURE 3 | Distributional comparison of predicted serum albumin concentration values at **(A)** 20, **(B)** 28, and **(C)** 37 wks gestation between our model and Dallmann et al.'s published equation (8). Distributions of serum albumin concentrations were generated over 10,000 stochastic simulations from each respective model/equation.

AAG concentrations rapidly declined until reaching a nadir of 70.1 mg/dL at ∼7 wks postpartum.

Computational Functions

Computational functions that output time-dependent estimates of albumin and AAG concentrations for pregnant and postpartum women living with HIV are provided in the **Supplementary Materials**. Two types of functions were developed: arithmetic mean and quantile functions. Arithmetic mean functions require one input, either gestational age or postpartum duration (weeks), and output corresponding estimates of serum/plasma protein concentration values. Quantile functions require two inputs: (1) gestational age or postpartum duration (weeks) and (2) a percentile value. These functions output time-dependent estimates of serum albumin concentrations corresponding to specified percentiles. An example script demonstrating the usage of the above-described functions, including how to generate stochastic albumin

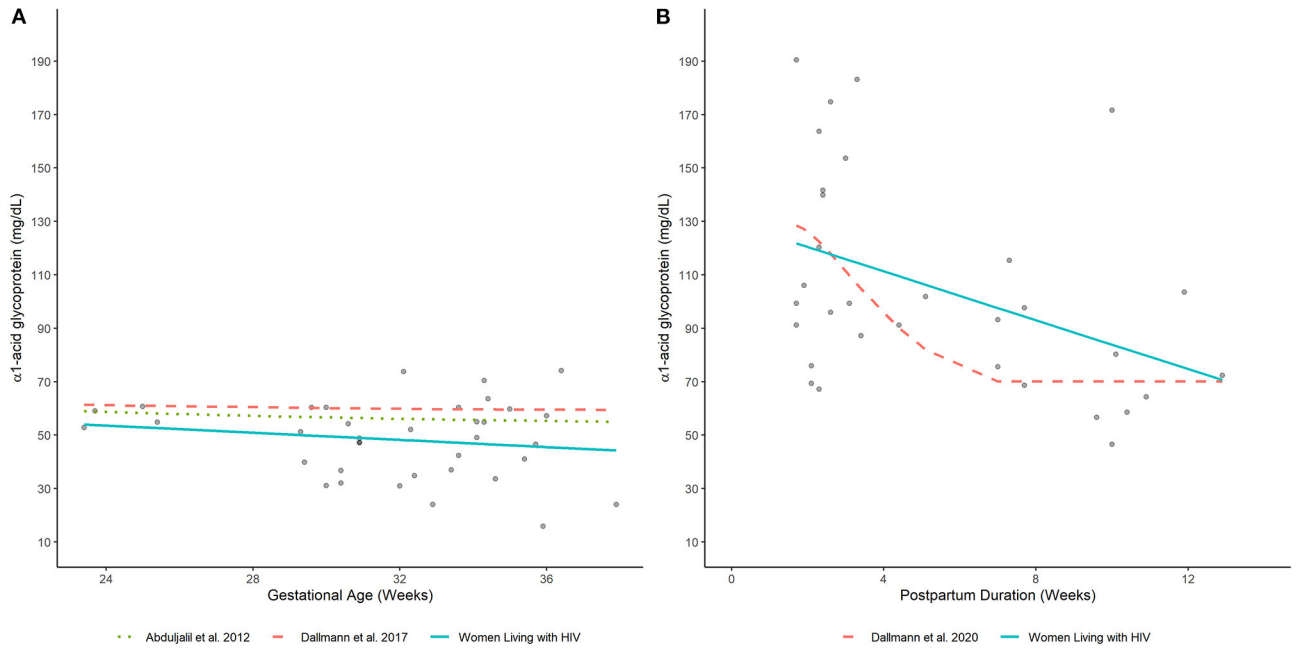

FIGURE 4 | Plasma AAG concentrations in **(A)** pregnant and **(B)** postpartum women estimated by our analysis (women living with HIV) and other published equations (women without HIV infection) (7, 8, 17). Lines depict (arithmetic) mean AAG concentration estimates generated by competing models. Filled-circles depict observed plasma AAG concentrations.

concentrations for the creation of virtual populations for prospective population PBPK model analyses, has also been provided in the **Supplementary Materials**.

DISCUSSION

To our knowledge, this quantitative analysis represents the first to specifically evaluate time-dependent changes in serum/plasma protein concentrations in pregnant and postpartum individuals living with HIV. Our analysis leveraged data collected from the IMPAACT Network's protocol 1026s, representing a large multicenter, multinational protocol designed to evaluate the pharmacokinetics of antiretroviral drugs during and after pregnancy. As such, the current analysis represents the largest assessments of serum/plasma protein concentrations in pregnant and postpartum individuals living with HIV to date. Pregnant individuals are generally excluded from drug development programs and clinical research trials, leading to the current paucity of drug safety and PK information in this population making it challenging to use many licensed drugs safely and effectively (25, 26). Although PBPK model analyses have the potential to generate *a priori* predictions of drug disposition in understudied populations, model development requires anatomical and physiological information specific to target populations of interest. By providing a quantitative description of protein concentrations in pregnant and postpartum individuals living with HIV, our study will serve to improve the development of PBPK models for this population. Furthermore, we have provided computational functions, developed using the open-source software R, to communicate our results in an interactive and transparent manner. Such functions can be directly integrated into PBPK modeling platforms.

Many ARV drugs exhibit high degrees of plasma protein binding (>90%), including several members of the integrase inhibitor and protease inhibitor classes (12, 27, 28). For such drugs, an understanding of the extent of plasma protein binding is considered critical for optimizing ARV therapy. Gestational changes in plasma protein concentrations can impact the extent of ARV plasma protein binding and subsequently contribute to pregnancy-associated alterations in drug PK. For example, the protease inhibitor lopinavir, which displays affinity for both albumin and AAG, exhibits pregnancy-associated changes in protein binding and PK (29). The fraction unbound of lopinavir in plasma increases by ∼12–20% in the second and third trimesters of pregnancy compared to postpartum values (30, 31). In addition, apparent clearance of lopinavir (co-administered with ritonavir) is increased by 31–58% between these periods (31–33). The observed increase in fraction unbound aligns with depicted physiological differences in serum/plasma protein concentrations between pregnant and postpartum individuals, as demonstrated by our analysis and along with others (30, 31). However, the observed increase in apparent clearance for lopinavir, which when co-administered with ritonavir exhibits characteristics similar to that of a low extraction ratio drug, exceeds the proportional increase that would be expected if PK alterations were due to changes plasma protein binding alone (34). This indicates that other physiological changes need to be considered in tandem with changes in protein binding to rationally inform ARV dosing in pregnancy. As such, our analysis

serves to describe only one facet of the complex physiological changes that occur during pregnancy.

Therapeutic goals of ARV therapy in pregnancy are focused toward maintaining maternal health while preventing vertical viral transmission (4). Correspondingly, both maternal and fetal ARV drug exposures are of interest. Several physiological parameters can influence the extent of fetal drug exposure including the magnitude of maternal drug exposure and the relative distribution of drugs between fetal and maternal plasma (F_p/M_p) (35, 36). Differences between maternal and fetal plasma protein concentrations is a key factor impacting drug-specific F_p/M_p values (36). By integrating maternal plasma protein concentration estimates from our analysis with data on fetal plasma protein concentrations, this work can contribute toward improving predictions of fetal drug exposure in pregnant individuals living with HIV.

Although many physiological changes transpire post-delivery, our current understanding of the time-course of such changes is limited. In studies evaluating ARV pharmacology in pregnant and postpartum individuals, postpartum individuals are typically evaluated at a single time point several weeks after delivery (i.e., $\geq$6 weeks) and merely serve as a control group to permit for assessments of pregnancy-associated changes in ARV PK (37–39). Use of PBPK modeling may offer an alternative approach for predicting the time-course of PK changes that occur immediately post-delivery and beyond. A recent publication by Dallmann et al. highlighted the potential utility of such models (17). The researchers developed a PBPK model for amoxicillin in pregnancy (3rd trimester) and the early postpartum period (1.5–3.8 h post-delivery). The model was able to recapitulate observed PK data in postpartum individuals, albeit with a slight underprediction of clearance. Our findings will contribute to the development of such models for individuals living with HIV by improving our understanding of how plasma protein concentrations change during the postpartum period.

Our analysis distinctly differs from other previously published research describing the time-course of plasma protein concentrations in pregnant and postpartum individuals (7, 8, 17). Previously published equations were generated using aggregated data from literature sources that focused on Caucasian individuals with low-risk pregnancies and no other medical conditions (7, 8, 17). In contrast, our analysis utilized data from individuals living with HIV and included a racially diverse cohort. In terms of methodology, our analysis utilized a generalized additive modeling approach to fit non-parametric smoothers to the data. An advantage of this approach is that the form of the relationship between variables is driven by the dataset itself (40); whereas, for parametric models, which were used to develop the previously published equations, the form of the relationship between variables is pre-defined by the user (7, 8, 17). As previous studies describing the time-course of plasma protein concentrations in pregnant and postpartum individuals living with HIV are lacking, use of generalized additive modeling was considered to be additionally beneficial, permitting for trajectories to be derived based on the current dataset rather than relying on patterns depicted from other populations. Use of a generalized additive modeling approach also permitted us to evaluate the distributional form of albumin concentrations, which was possible due to the availability of individualized data from IMPAACT's P1026s study. In contrast, previously published equations were developed using aggregated data from the literature, making such distributional evaluations challenging (7, 8, 17). For development population PBPK models, there is an interest in generating virtual populations whose anatomy and physiology vary according to biologically relevant distributions. Mismatches in the distribution between virtually generated populations and the target population will serve to reduce confidence in model predictions. Our analysis demonstrated a high-level of incongruence between albumin quantiles generated from a previously published equation and observed data from pregnant individuals living with HIV, particularly at higher percentile values (**Table 2**) (8). Accordingly, use of the above-described equation to generate a virtual population reflective of pregnant individuals living with HIV would likely result in biased estimates of PK variability for drugs that are highly protein-bound. By characterizing the distributional form of serum albumin concentrations, our work can serve to improve confidence in population PBPK model predictions for pregnant and postpartum individuals living with HIV.

There are several limitations associated with our analysis that should be highlighted. First, a relatively low number of AAG samples were available for analysis. Estimated smoothing splines depicted linear relationships between AAG concentrations and gestational age/postpartum duration. As smoothing splines are fit using penalized regression, it is likely that the amount of observed data was insufficient to permit the model from deviating from a linear approximation owing to a relatively high (smoothness) penalty factor (41). Correspondingly, the presented work should be viewed as a preliminary analysis of the time-course of AAG concentrations in pregnant and postpartum individuals living with HIV. Second, for several individuals within each dataset, protein concentrations were measured longitudinally (i.e., contributing multiple samples). As our analysis approach (i.e., generalized linear modeling) implicitly assumed datapoints were independent, the presence of multiple observations per individuals may have inserted some bias into our model estimates. Nonetheless, as the majority of individuals contributed $\leq$2 samples (e.g., 270/380 and 230/354 participants contributed $\leq$2 albumin concentrations to the pregnancy and postpartum datasets, respectively) toward each respective dataset, development of a mixed-effect model to account for such features (i.e., multiple samples per patient) was not pursued. Lastly, although our analysis depicted unique trends in the time-course of protein concentrations for individuals living with HIV (**Figures 2**, **4**), it lacked the capacity to identify the causative factor perpetuating such discrepancies. Other investigations have also observed lower albumin concentrations among cohorts of subjects with HIV-infection relative to non-HIV infected subjects (42, 43). However, due to demographic and socioeconomic differences that exist between individuals living with HIV and individuals without HIV infection, there may be several etiological factors responsible for such differences (e.g., racial, ethnic, nutritional, pathophysiological, etc.). As a preliminary analysis for this work, assessment of

the trajectory of albumin concentrations by race was conducted (**Supplementary Figure 3**). This comparison did not provide striking evidence for racial differences in the time-course of albumin concentrations in pregnant and postpartum individuals living with HIV. Correspondingly, a generalized approach that described the time-course of protein concentrations across the entire cohort was adopted.

In summary, our analysis characterized the trajectory of serum albumin and plasma AAG concentrations in pregnant and postpartum individuals living with HIV. This work is particularly informative for the development of population PBPK models for this population, as their physiology may not be adequately described within current models. The results of our analysis have been compiled into computational functions developed using open-source software, permitting for easy integration into prospectively developed PBPK models. By doing so, our results can serve to inform the development of future clinical trials evaluating ARV pharmacology in pregnant and postpartum individuals living with HIV.

DATA AVAILABILITY STATEMENT

The data analyzed in this study is subject to the following licenses/restrictions: Due the ethical restrictions in the study's informed consent documents and in the International Maternal Pediatric Adolescent AIDS Clinical Trials (IMPAACT) Network's approved human subjects protection plan, data cannot be made publicly available. However, data can be made available to interested researchers upon request to the IMPAACT Statistical and Data Management Center's data access committee with the agreement of the IMPAACT Network. Requests to access these datasets should be directed to dac.data@fstrf.org.

ETHICS STATEMENT

The studies involving human participants were reviewed and approved by all relevant Ethics or Human Subjects Protection Committees at all participating sites. IMPAACT P1026s is registered at ClinicalTrials.gov (https://clinicaltrials.gov/ct2/show/NCT00042289). All participants contributing data to the current analysis gave written informed consent, permission or assent in accordance with the Declaration of Helsinki. The patients/participants provided their written informed consent to participate in this study.

AUTHOR CONTRIBUTIONS

All co-authors reviewed, revised for content, and approved this article. SZ, MGo, JM, BB, MM, and AM made substantial contributions to the conception and design. BB and MM acquisition of data. SZ, MGo, MGr, HS, MM, KS, YB, JW, EC, BB, TJ, JM, and AM analysis or interpretation of data. All authors contributed to the article and approved the submitted version.

FUNDING

Overall support for the International Maternal Pediatric Adolescent AIDS Clinical Trials Network (IMPAACT) was provided by the National Institute of Allergy and Infectious Diseases (NIAID) with co-funding from the Eunice Kennedy Shriver National Institute of Child Health and Human Development (NICHD) and the National Institute of Mental Health (NIMH), all components of the National Institutes of Health (NIH), under Award Numbers UM1AI068632 (IMPAACT LOC), UM1AI068616 (IMPAACT SDMC) and UM1AI106716 (IMPAACT LC), and by NICHD contract number HHSN275201800001I. This project was supported by an appointment to the Research Fellowship Program at the Office of New Drugs, Center for Drug Evaluation and Research, U.S. Food and Drug Administration, administered by the Oak Ridge Institute for Science and Education through an interagency agreement between the U.S. Department of Energy and FDA (SZ and MGo). AM receives research support from the non-profit organization, Thrasher Research Fund (www.thrasherresearch.org).

SUPPLEMENTARY MATERIAL

The Supplementary Material for this article can be found online at: https://www.frontiersin.org/articles/10.3389/fped.2021.721059/full#supplementary-material

REFERENCES

1. Recommendations for the Use of Antiretroviral Drugs in Pregnant Women with HIV Infection and Interventions to Reduce Perinatal HIV Transmission in the United States. (accessed April 1, 2020).
2. Mirochnick M, Capparelli E. Pharmacokinetics of antiretrovirals in pregnant women. *Clin Pharmacokinet.* (2004) 43:1071–87. doi: 10.2165/00003088-200443150-00002
3. Feghali M, Venkataramanan R, Caritis S. Pharmacokinetics of drugs in pregnancy. *Semin Perinatol.* (2015) 39:512–9. doi: 10.1053/j.semperi.2015.08.003
4. Buckoreelall K, Cressey TR, King JR. Pharmacokinetic optimization of antiretroviral therapy in pregnancy. *Clin Pharmacokinet.* (2012) 51:639–59. doi: 10.1007/s40262-012-0002-0
5. Ke AB, Nallani SC, Zhao P, Rostami-Hodjegan A, Isoherranen N, Unadkat JD, et al. Physiologically based pharmacokinetic model to predict disposition of CYP2D6 and CYP1A2 metabolized drugs in pregnant women. *Drug Metab Dispos.* (2013) 41:801–13. doi: 10.1124/dmd.112.050161
6. Zheng L, Tang S, Tang R, Xu M, Jiang X, Wang L. Dose adjustment of quetiapine and aripiprazole for pregnant women using physiologically based pharmacokinetic modeling and simulation. *Clin Pharmacokinet.* (2020). doi: 10.1007/s40262-020-00962-3
7. Abduljalil K, Furness P, Johnson TN, Rostami-Hodjegan A, Soltani H. Anatomical, physiological and metabolic changes with gestational age during normal pregnancy: a database for parameters required in physiologically based pharmacokinetic modelling. *Clin Pharmacokinet.* (2012) 51:365–96. doi: 10.2165/11597440-000000000-00000
8. Dallmann A, Ince I, Meyer M, Willmann S, Eissing T, Hempel G. Gestation-specific changes in the anatomy and physiology of healthy pregnant women: an extended repository of model parameters for physiologically based pharmacokinetic modeling in pregnancy. *Clin Pharmacokinet.* (2017) 56:1303–30. doi: 10.1007/s40262-017-0539-z

9. AIDSinfo - UNAIDS. Elimination of mother-to-child transmission. Available online at: https://aidsinfo.unaids.org/. (accessed April 1, 2020).
10. Powis KM, Huo Y, Williams PL, Kacanek D, Jao J, Patel K, et al. Antiretroviral prescribing practices among pregnant women living with HIV in the United States, 2008-2017. *JAMA Netw Open.* (2019) 2:e1917669. doi: 10.1001/jamanetworkopen.2019.17669
11. Bohnert T, Gan LS. Plasma protein binding: from discovery to development. *J Pharm Sci.* (2013) 102:2953–94. doi: 10.1002/jps.23614
12. Boffito M, Back DJ, Blaschke TF, Rowland M, Bertz RJ, Gerber JG, et al. Protein binding in antiretroviral therapies. *AIDS Res Hum Retroviruses.* (2003) 19:825–35. doi: 10.1089/088922203769232629
13. Bteich M. An overview of albumin and alpha-1-acid glycoprotein main characteristics: highlighting the roles of amino acids in binding kinetics and molecular interactions. *Heliyon.* (2019) 5:e02879. doi: 10.1016/j.heliyon.2019.e02879
14. Pabby P. Changes in serum proteins during pregnancy. *J Obstet Gynaecol Br Emp.* (1960) 67:43–55. doi: 10.1111/j.1471-0528.1960.tb06949.x
15. Murphy MM, Scott JM, McPartlin JM, Fernandez-Ballart JD. The pregnancy-related decrease in fasting plasma homocysteine is not explained by folic acid supplementation, hemodilution, or a decrease in albumin in a longitudinal study. *Am J Clin Nutr.* (2002) 76:614–9. doi: 10.1093/ajcn/76.3.614
16. Macdonald HN, Good W. Changes in plasma total protein, albumin, urea and alpha-amino nitrogen concentrations in pregnancy and the puerperium. *J Obstet Gynaecol Br Commonw.* (1971) 78:912–7. doi: 10.1111/j.1471-0528.1971.tb00203.x
17. Dallmann A, Himstedt A, Solodenko J, Ince I, Hempel G, Eissing T. Integration of physiological changes during the postpartum period into a PBPK framework and prediction of amoxicillin disposition before and shortly after delivery. *J Pharmacokinet Pharmacodyn.* (2020) 47:341–59. doi: 10.1007/s10928-020-09706-z
18. Charles D, Larsen B. Pharmacokinetics of cefotaxime, moxalactam, and cefoperazone in the early puerperium. *Antimicrob Agents Chemother.* (1986) 29:873–6. doi: 10.1128/AAC.29.5.873
19. Charles D, Larsen B. Pharmacokinetics of piperacillin in the postpartum patient. *Gynecol Obstet Invest.* (1985) 20:194–8. doi: 10.1159/000298993
20. Pharmacokinetic Properties of Antiretroviral and Related Drugs During Pregnancy and Postpartum (NCT00042289). (2020) (accessed Apr 1, 2021).
21. Rigby RA, Stasinopoulos DM. Generalized additive models for location, scale and shape. *J R Stat Soc.* (2005) 54:507–54. doi: 10.1111/j.1467-9876.2005.00510.x
22. Eilers PHC, Marx BD. Flexible smoothing with B-splines and penalties. *Stat Sci.* (1996) 11:89–121. doi: 10.1214/ss/1038425655
23. Voncken L, Albers CJ, Timmerman ME. Model selection in continuous test norming with GAMLSS. *Assessment.* (2019) 26:1329–46. doi: 10.1177/1073191117715113
24. Rigby RA, Heller GZ, Stasinopoulos MD, De Bastiani F. *Distributions for Modelling Location, Scale, and Shape: Using GAMLSS in R. CRC Press.* (2017).
25. Sheffield JS, Siegel D, Mirochnick M, Heine RP, Nguyen C, Bergman KL, et al. Designing drug trials: considerations for pregnant women. *Clin Infect Dis.* (2014) 59:437. doi: 10.1093/cid/ciu709
26. Eke AC, Olagunju A, Momper J, Penazzato M, Abrams EJ, Best BM, et al. Optimizing pharmacology studies in pregnant and lactating women using lessons from HIV: a consensus statement. *Clin Pharmacol Ther.* (2020) 110:36–48. doi: 10.1007/s40262-020-00915-w
27. Flexner C. HIV-protease inhibitors. *N Engl J Med.* (1998) 338:1281–92. doi: 10.1056/NEJM199804303381808
28. van der Galien R, Ter Heine R, Greupink R, Schalkwijk SJ, van Herwaarden AE, Colbers A, et al. Pharmacokinetics of HIV-integrase inhibitors during pregnancy: mechanisms, clinical implications and knowledge gaps. *Clin Pharmacokinet.* (2019) 58:309–23. doi: 10.1007/s40262-018-0684-z
29. Gulati A, Boudinot FD, Gerk PM. Binding of lopinavir to human alpha1-acid glycoprotein and serum albumin. *Drug Metab Dispos.* (2009) 37:1572–5. doi: 10.1124/dmd.109.026708
30. Aweeka FT, Stek A, Best BM, Hu C, Holland D, Hermes A, et al. Lopinavir protein binding in HIV-1-infected pregnant women. *HIV Med.* (2010) 11:232–8. doi: 10.1111/j.1468-1293.2009.00767.x
31. Fayet-Mello A, Buclin T, Guignard N, Cruchon S, Cavassini M, Grawe C, et al. Free and total plasma levels of lopinavir during pregnancy, at delivery and postpartum: implications for dosage adjustments in pregnant women. *Antivir Ther.* (2013) 18:171–82. doi: 10.3851/IMP2328
32. Salem AH, Jones AK, Santini-Oliveira M, Taylor GP, Patterson KB, Nilius AM, et al. No need for lopinavir dose adjustment during pregnancy: a population pharmacokinetic and exposure-response analysis in pregnant and nonpregnant HIV-infected subjects. *Antimicrob Agents Chemother.* (2015) 60:400–8. doi: 10.1128/AAC.01197-15
33. Stek AM, Mirochnick M, Capparelli E, Best BM, Hu C, Burchett SK, et al. Reduced lopinavir exposure during pregnancy. *AIDS.* (2006) 20:1931–9. doi: 10.1097/01.aids.0000247114.43714.90
34. Dumond JB, Rigdon J, Mollan K, Tierney C, Kashuba AD, Aweeka F, et al. Brief report: significant decreases in both total and unbound lopinavir and amprenavir exposures during coadministration: ACTG protocol A5143/A5147s results. *J Acquir Immune Defic Syndr.* (2015) 70:510–4. doi: 10.1097/QAI.0000000000000777
35. Liu XI, Momper JD, Rakhmanina NY, Green DJ, Burckart GJ, Cressey TR, et al. Prediction of maternal and fetal pharmacokinetics of dolutegravir and raltegravir using physiologically based pharmacokinetic modeling. *Clin Pharmacokinet.* (2020) 59:1433–50. doi: 10.1007/s40262-020-00897-9
36. Hill MD, Abramson FP. The significance of plasma protein binding on the fetal/maternal distribution of drugs at steady-state. *Clin Pharmacokinet.* (1988) 14:156–70. doi: 10.2165/00003088-198814030-00004
37. Eke AC, Wang J, Amin K, Shapiro DE, Stek A, Smith E, et al. Fosamprenavir with ritonavir pharmacokinetics during pregnancy. *Antimicrob Agents Chemother.* (2020) 64:e02260. doi: 10.1128/AAC.02260-19
38. Mulligan N, Best BM, Wang J, Capparelli EV, Stek A, Barr E, et al. Dolutegravir pharmacokinetics in pregnant and postpartum women living with HIV. *AIDS.* (2018) 32:729–37. doi: 10.1097/QAD.0000000000001755
39. Osiyemi O, Yasin S, Zorrilla C, Bicer C, Hillewaert V, Brown K, et al. Pharmacokinetics, antiviral activity, and safety of rilpivirine in pregnant women with HIV-1 infection: results of a phase 3b, multicenter, open-label study. *Infect Dis Ther.* (2018) 7:147–59. doi: 10.1007/s40121-017-0184-8
40. Mahmoud HFF. Parametric versus semi and nonparametric regression models. *arXiv preprint arXiv:1906.10221* (2019).
41. Perperoglou A, Sauerbrei W, Abrahamowicz M, Schmid M. A review of spline function procedures in R. *BMC Med Res Methodol.* (2019) 19:46–3. doi: 10.1186/s12874-019-0666-3
42. Papathakis PC, Rollins NC, Chantry CJ, Bennish ML, Brown KH. Micronutrient status during lactation in HIV-infected and HIV-uninfected South African women during the first 6 mo after delivery. *Am J Clin Nutr.* (2007) 85:182–92. doi: 10.1093/ajcn/85.1.182
43. Hattingh Z, Walsh C, Veldman F, Bester C. The metabolic profiles of HIV-infected and non-infected women in Mangaung, South Africa. *null.* (2009) 22:23–8. doi: 10.1080/16070658.2009.11734213

Author Disclaimer: The content is solely the responsibility of the authors and does not necessarily represent the official views of the NIH. The opinions expressed in this article are those of the authors and should not be interpreted as the position of the U.S. FDA and the cases being presented do not imply FDA's endorsement of the products.

Conflict of Interest: The authors declare that the research was conducted in the absence of any commercial or financial relationships that could be construed as a potential conflict of interest.

Publisher's Note: All claims expressed in this article are solely those of the authors and do not necessarily represent those of their affiliated organizations, or those of the publisher, the editors and the reviewers. Any product that may be evaluated in this article, or claim that may be made by its manufacturer, is not guaranteed or endorsed by the publisher.

frontiers in Pediatrics

ORIGINAL RESEARCH
published: 18 October 2021
doi: 10.3389/fped.2021.723006

Mechanistic Modeling of Placental Drug Transfer in Humans: How Do Differences in Maternal/Fetal Fraction of Unbound Drug and Placental Influx/Efflux Transfer Rates Affect Fetal Pharmacokinetics?

*Xiaomei I. Liu[1], Dionna J. Green[2], John N. van den Anker[1], Natella Y. Rakhmanina[3,4], Homa K. Ahmadzia[5], Jeremiah D. Momper[6], Kyunghun Park[7], Gilbert J. Burckart[7] and André Dallmann[8]**

[1] Division of Clinical Pharmacology, Children's National Hospital, Washington, DC, United States, [2] Office of Pediatric Therapeutics, Office of the Commissioner, US Food and Drug Administration, Silver Spring, MD, United States, [3] Division of Infectious Diseases, Children's National Hospital, Washington, DC, United States, [4] Technical Strategies and Innovation, Elizabeth Glaser Pediatric AIDS Foundation, Washington, DC, United States, [5] Division of Maternal-Fetal Medicine, Department of Obstetrics and Gynecology, School of Medicine and Health Sciences, The George Washington University, Washington, DC, United States, [6] Skaggs School of Pharmacy and Pharmaceutical Sciences, University of California, San Diego, La Jolla, CA, United States, [7] Office of Clinical Pharmacology, US Food and Drug Administration, Silver Spring, MD, United States, [8] Pharmacometrics/Modeling and Simulation, Research and Development, Pharmaceuticals, Bayer AG, Leverkusen, Germany

OPEN ACCESS

Edited by:
Alfredo Vannacci, University of Florence, Italy

Reviewed by:
Ashwin Karanam, Pfizer, United States
Jiao Zheng, Shanghai Jiaotong University, China

***Correspondence:**
André Dallmann
andre.dallmann@bayer.com

Specialty section:
This article was submitted to Obstetric and Pediatric Pharmacology, a section of the journal Frontiers in Pediatrics

Received: *09 June 2021*
Accepted: *13 September 2021*
Published: *18 October 2021*

Citation:
Liu XI, Green DJ, van den Anker JN, Rakhmanina NY, Ahmadzia HK, Momper JD, Park K, Burckart GJ and Dallmann A (2021) Mechanistic Modeling of Placental Drug Transfer in Humans: How Do Differences in Maternal/Fetal Fraction of Unbound Drug and Placental Influx/Efflux Transfer Rates Affect Fetal Pharmacokinetics? Front. Pediatr. 9:723006. doi: 10.3389/fped.2021.723006

Background: While physiologically based pharmacokinetic (PBPK) models generally predict pharmacokinetics in pregnant women successfully, the confidence in predicting fetal pharmacokinetics is limited because many parameters affecting placental drug transfer have not been mechanistically accounted for.

Objectives: The objectives of this study were to implement different maternal and fetal unbound drug fractions in a PBPK framework; to predict fetal pharmacokinetics of eight drugs in the third trimester; and to quantitatively investigate how alterations in various model parameters affect predicted fetal pharmacokinetics.

Methods: The ordinary differential equations of previously developed pregnancy PBPK models for eight drugs (acyclovir, cefuroxime, diazepam, dolutegravir, emtricitabine, metronidazole, ondansetron, and raltegravir) were amended to account for different unbound drug fractions in mother and fetus. Local sensitivity analyses were conducted for various parameters relevant to placental drug transfer, including influx/efflux transfer clearances across the apical and basolateral membrane of the trophoblasts.

Results: For the highly-protein bound drugs diazepam, dolutegravir and ondansetron, the lower fraction unbound in the fetus vs. mother affected predicted pharmacokinetics in the umbilical vein by ≥10%. Metronidazole displayed blood flow-limited distribution across the placenta. For all drugs, umbilical vein concentrations were highly sensitive to changes in the apical influx/efflux transfer clearance ratio. Additionally, transfer

clearance across the basolateral membrane was a critical parameter for cefuroxime and ondansetron.

Conclusion: In healthy pregnancies, differential protein binding characteristics in mother and fetus give rise to minor differences in maternal-fetal drug exposure. Further studies are needed to differentiate passive and active transfer processes across the apical and basolateral trophoblast membrane.

Keywords: physiologically based pharmacokinetics (PBPK), placental drug transfer, maternal-fetal, pregnancy, mechanistic modeling

INTRODUCTION

Although drug use in pregnant women is frequent and increasing (1, 2), little is known about the different factors modulating placental transfer and fetal drug exposure. This knowledge is particularly important in an era where multiple approaches to therapy for the fetus are being considered (3, 4). As clinical studies involving pregnant women are difficult to conduct due to various considerations (5), other approaches are needed as alternative or complementary tools to elucidate maternal-fetal pharmacology. Among these tools, physiologically based pharmacokinetic (PBPK) modeling holds potential to improve the conceptual and quantitative understanding of maternal-fetal pharmacokinetics (6, 7). PBPK models integrate compound-specific properties (e.g., lipophilicity, molecular weight) and physiological and biological characteristics (e.g., organ volumes and blood flow rates) in a mechanistic framework (8). Whole-body PBPK models include multiple compartments which represent different organs and tissues that are arranged in a parallel circuit mimicking the blood flow in the circulatory system (9).

In recent years, numerous PBPK models for pregnant women have been developed and successfully evaluated with clinical data (10). Many of these models also described transfer of xenobiotics across the placenta and fetal pharmacokinetics (11). While much progress has been made in developing maternal-fetal PBPK models, many of these models lack a fully mechanistic description of the xenobiotic's placental transfer and partitioning between the maternal and fetal compartments. For example, differences in protein binding in maternal and fetal blood plasma have rarely been considered mechanistically. Yet, an altered fraction unbound of the drug in the fetal circulation might give rise to differences in drug exposure at steady-state, especially if the drug crosses the placenta exclusively *via* passive diffusion (12). Additionally, different influx and efflux transfer rates across the apical membrane of the trophoblast could be indicative of the presence of uptake or influx transporters (11, 13).

Hence, using a generic PBPK framework that can be extended to other drugs, the aims of this study were to (i) implement the unbound fraction of a drug in fetal model compartments; (ii) implement scaling factors for transplacental diffusion clearance that allow different influx and efflux transfer rates across the apical membrane of the trophoblasts; (iii) predict and evaluate maternal and fetal pharmacokinetics of a variety of drugs in the late third trimester with differential protein binding characteristics in the maternal and fetal organism when equal or different influx/efflux rates across the placenta are assumed; and (iv) quantify the effect of variations in maternal/fetal plasma protein binding, maternal blood flow rate to the placenta and placental influx/efflux rates on the predicted fetal pharmacokinetics through sensitivity analysis.

METHODS

Software

PBPK models were built with PK-Sim® and MoBi® which are available as open source tools through the Open Systems Pharmacology (OSP) software, version 9.1, *via* GitHub (https://github.com/Open-Systems-Pharmacology) (14). The updated model files described herein will be also uploaded there. The software R, version 3.6.3 (R Foundation for Statistical Computing, http://www.r-project.org) was used for graphics creation. Clinical data were digitized from published figures using WebPlotDigitizer, version 4.4 (https://automeris.io/WebPlotDigitizer/).

General Workflow

In previous studies, pregnancy PBPK models were built with the OSP software for the compounds acyclovir (15), cefuroxime (16), diazepam (17), dolutegravir (18), emtricitabine (15), metronidazole (17), ondansetron (17), and raltegravir (18). These models were successfully evaluated in non-pregnant adults, translated to pregnancy and the predicted maternal pharmacokinetics (16, 17) or predicted maternal and fetal pharmacokinetics at delivery (15, 18) were evaluated with clinical data. All models are freely available on OSP GitHub (https://github.com/Open-Systems-Pharmacology/Pregnancy-Models).

In this study, these models were used for further analyzing placental drug transfer. The development of additional non-pregnant PBPK models for other drugs and their extrapolation to and validation for pregnancy was beyond the scope of this study that focused exclusively on models that were already validated for pregnant women. Here, these models were updated by implementing the drug's fraction unbound in all fetal compartments as described in detail below. In contrast to previous studies (15, 18) the placental partition coefficients between maternal blood plasma and fetal intracellular space were predicted from the drug's physicochemical properties and the placental tissue composition. Additionally, the transfer clearance across the apical trophoblast membrane was estimated from *in*

vitro permeability measures as described below. Apart from these changes, no other model adjustments were made. Pregnancy-induced changes in relevant anatomical and physiological model parameter values, including clearance values, can be found in previous publications (15–18). After these structural model updates, maternal and fetal pharmacokinetics were predicted using different values for the maternal and fetal unbound drug fraction. Transfer rates across the placenta were initially kept equal in both directions (symmetrical transfer). Thereafter, local sensitivity analyses were conducted by varying the maternal blood flow to the placenta and the influx and efflux rates across the placental membrane.

Estimation of Fetal Fraction Unbound

Each drug's fraction unbound in fetal blood plasma (f_{u_fetus}) was estimated using the following equation that has been evaluated for various populations, including infants (19) and pregnant women (16):

$$f_{u\_fetus} = 1/\left(1 + \frac{1 - f_{u\_nonpreg}}{C_{prot\_nonpreg} \times f_{u\_nonpreg}} \times C_{prot\_fetus}\right) \quad (1)$$

Here, $f_{u\_nonpreg}$ is the fraction unbound of non-pregnant adults in plasma; $C_{prot\_nonpreg}$ is the concentration of binding proteins in the blood plasma in non-pregnant adults; C_{prot_fetus} is the concentration of binding proteins in fetal blood plasma. Values for C_{prot_fetus} were taken from a previously published meta-analysis (20). Implicit assumptions of this equation are that the number of adult and fetal protein binding sites and the drug's affinity to adult and fetal plasma proteins are the same and that the drug exclusively binds to one plasma protein only. **Table 1** lists for each drug the observed fraction unbound in non-pregnant subjects ($f_{u\_nonpreg}$) and the estimated maternal and fetal fraction unbound implemented in the PBPK model.

Structural Implementation of the Fetal Fraction Unbound in the Model

The structure of the pregnancy PBPK model is schematically shown in **Figure 1** and has been described in detail previously (16). Briefly, the fetal sub-structure of the pregnancy PBPK model consists of five compartments representing the fetal part of the placenta, the fetus, the amniotic fluid volume (which is not connected to other compartments) and the arterial and venous blood pools of the umbilical cord. Organ compartments are further sub-divided in the blood cells (*bc*), plasma (*pls*), interstitial (*int*), and intracellular compartment (*cell*).

Here, the ordinary differential equations (ODE) system of the fetal sub-structure was refined in MoBi® to account for fetal-specific protein binding. In MoBi® the ODEs are first defined for intercompartmental exchange processes in the passive transports building block; during set-up of a simulation, the ODEs are then generated for each compartment. In the following, the ODEs are first introduced for each intercompartmental exchange transport and then defined for the compartments.

TABLE 1 | Overview of the observed fraction unbound in non-pregnant subjects and the estimated fraction unbound in mother and fetus.

Drug	Fraction unbound in non-pregnant subjects	Maternal fraction unbound	Fetal fraction unbound
Acyclovir	0.85 (15)	0.88	0.86
Cefuroxime	0.67 (16)	0.73	0.68
Diazepam	0.020 (17)	0.027	0.021
Dolutegravir	0.0070 (18)	0.0088	0.0080
Emtricitabine	0.96 (15)	0.97	0.96
Metronidazole	0.89 (17)	0.92	0.89
Ondansetron	0.27 (17)	0.33	0.28
Raltegravir	0.17 (18)	0.24	0.23

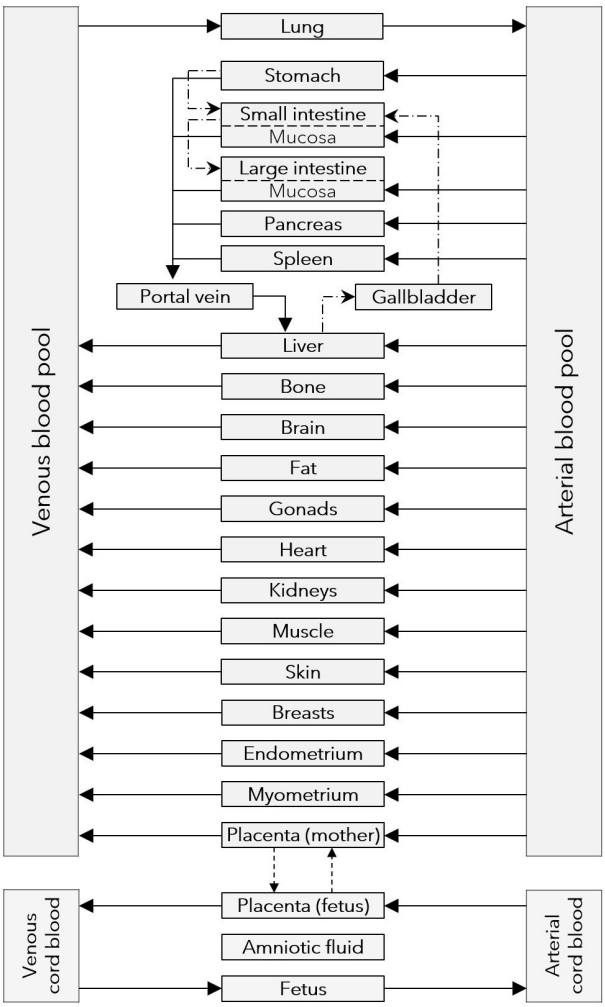

FIGURE 1 | Structure of the pregnancy PBPK models. Gray boxes represent compartments of the PBPK model; solid arrows denote drug transport *via* the organ blood flow; dashed arrows denote drug transport *via* passive diffusion; dash dotted lines denote drug transport *via* gastrointestinal motility or the biliary excretion route. PBPK, physiologically based pharmacokinetic.

Specifically, the ODEs in the fetal compartments describing drug exchange between plasma and blood cells (Equation 2), plasma and interstitial space (Equaton 3), and interstitial and intracellular space (Equation 4) were adjusted in the spatial structure building block section of MoBi® as described below. Note that Equations (2–4) only refer to the passive, gradient-driven drug exchange between the two sub-compartments.

$$\frac{dN_{bc}}{dt} = SA_{bc} \times P_{pls,bc} \times f_u \times \left(C_{pls} - \frac{C_{bc}}{K_{bc}}\right) \quad (2)$$

$$\frac{dN_{int}^{int\leftrightarrow pls}}{dt} = P_{end} \times SA_{end} \times f_u \times \left(C_{pls} - \frac{C_{int}}{K_{int,pls}}\right) \quad (3)$$

$$\frac{dN_{cell}}{dt} = P_{int,cell} \times SA_{int,cell} \times \left(K_{water,int} \times C_{int} - K_{water,cell} \times C_{cell}\right) \quad (4)$$

Here, N_{bc} denotes molar drug amount in blood cells (μmol), $N_{int}^{int\leftrightarrow pls}$ denotes molar drug amount in the interstitial compartment when only drug exchange between plasma and interstitial is considered (μmol); N_{cell} denotes molar drug amount in the intracellular compartment (μmol); C_{bc}, C_{cell}, C_{int} and C_{pls} denote the molar drug concentration in blood cells, intracellular space, interstitial space, and plasma, respectively (μmol/L); f_u the drug's fraction unbound in maternal blood plasma (which was originally assumed to be equal with the fraction unbound in fetal blood plasma); K_{bc}, $K_{int,pls}$, $K_{water,cell}$ and $K_{water,int}$ the partition coefficient between blood cells and plasma, interstitial and plasma, water and intracellular space and between water and interstitial space, respectively; N the molar drug amount (μmol); P_{end}, $P_{int,cell}$ and $P_{pls,bc}$ the drug's permeability through the endothelial, cellular, and blood cell membrane, respectively (assuming symmetrical transfer, i.e., equal permeability for both directions) (cm/min); and SA_{bc}, SA_{end}, and $SA_{int,cell}$ the total surface area of the endothelial, cellular and blood cell membrane, respectively (cm^2). The parameterization can be found elsewhere (16).

To account for the fetus-specific fraction of unbound drug in the model, Equations (2–4) were amended as described in the following. In all equations, f_u (the maternal fraction unbound) was substituted with f_{u_fetus} (the fetal fraction unbound) calculated from Equation (1).

Assuming that K_{bc} in Equation (2) is the same for the maternal and fetal organism and substituting f_u with f_{u_fetus} yields Equation (5).

$$\frac{dN_{bc}}{dt} = SA_{bc} \times P_{pls,bc} \times f_{u\_fetus} \times \left(C_{pls} - \frac{C_{bc}}{K_{bc}}\right) \quad (5)$$

In Equation (3), $K_{int,pls}$ was calculated according to the equation reported by Schmitt (21):

$$K_{int,pls} = \left(f_{water\_int} + \frac{f_{prot\_int}}{f_{prot\_pls}} \times \left(\frac{1}{f_{u\_fetus}} - f_{water\_pls}\right)\right) \times f_{u\_fetus} \quad (6)$$

where f_{water_pls} and f_{water_int} denote the fractional volume content of water in plasma and interstitial space, respectively; and f_{prot_pls} and f_{prot_int} denote the fractional volume content of proteins in plasma and interstitial space, respectively. Of note, f_{water_pls}, f_{water_int} and the ratio $\frac{f_{prot\_int}}{f_{prot\_pls}}$ were assumed to be the same as in the adult organism, namely 0.926 (22), 0.935 (22), and 0.37 (23), respectively. Inserting Equation (6) into Equation (3) yields Equation (7) which was used in the updated maternal-fetal PBPK model.

$$\frac{dN_{int}^{int\leftrightarrow pls}}{dt} = P_{end} \times SA_{end} \times f_{u\_fetus} \times \left(C_{pls} - \frac{C_{int}}{\left(f_{water\_int} + \frac{f_{prot\_int}}{f_{prot\_pls}} \times \left(\frac{1}{f_{u\_fetus}} - f_{water\_pls}\right)\right) \times f_{u\_fetus}}\right) \quad (7)$$

To refine Equation (4), $K_{water,int}$ and $K_{water,cell}$ were expressed as:

$$K_{water,int} = \frac{f_{u\_fetus}}{K_{int,pls}} \quad (8)$$

$$K_{water,cell} = \frac{f_{u\_fetus}}{K_{cell,pls}} \quad (9)$$

$K_{int,pls}$ is calculated according to Equation (6), while several equations were reported for predicting $K_{cell,pls}$, namely the PK-Sim Standard equation (24) and the equations proposed by Schmitt et al. (21), Rodgers et al. (25, 26), and Poulin et al. (27, 28). These equations—subsequently referred to as PK-Sim Standard, Schmitt, Rodgers and Rowland, and Poulin and Theil model—are implemented per default in the OSP software and use the global (i.e., maternal) fraction unbound which appears as a discrete multiplier in these equations. Hence, instead of manually changing the underlying equations, the default equations using the maternal fraction unbound were kept and Equation (9) were multiplied with the ratio of maternal to fetal fraction unbound as a correction factor ($\frac{f_u}{f_{u\_fetus}}$) so that the maternal fraction unbound cancels out and the fetal fraction unbound is included in the denominator:

$$K_{water,cell} = \frac{f_{u\_fetus}}{K_{cell,pls}} \times \frac{f_u}{f_{u\_fetus}} \quad (10)$$

Finally, inserting Equations (6, 8, and 10) in Equation (4) yields Equation (11):

$$\frac{dN_{cell}}{dt} = P_{int,cell} \times SA_{int,cell} \times \left(C_{int} \times \frac{1}{f_{water\_int} + \frac{f_{prot\_int}}{f_{prot\_pls}} \times \left(\frac{1}{f_{u\_fetus}} - f_{water\_pls}\right)} - C_{cell} \times \frac{f_u}{K_{cell,pls}}\right) \quad (11)$$

Fetal-specific changes of parameters appearing in Equation 11 and input variables thereof, such as the volume fraction of

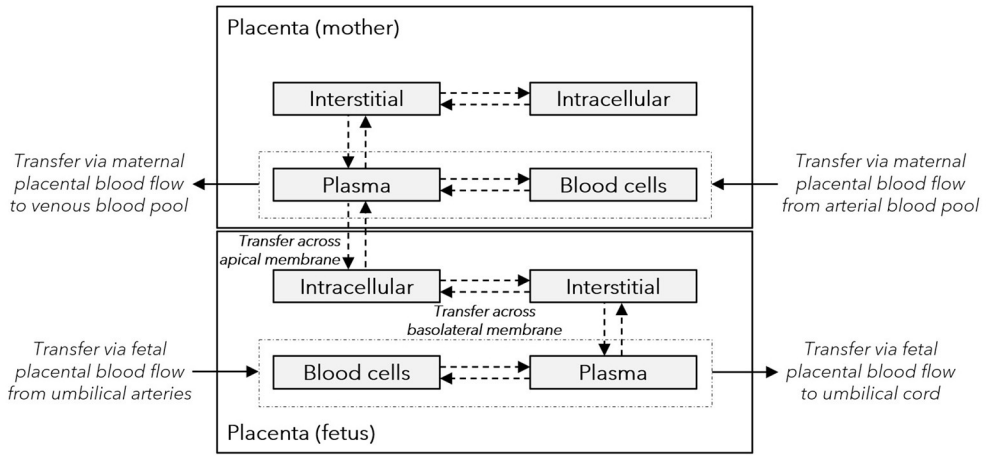

FIGURE 2 | Sub-structure of the placenta barrier in the pregnancy PBPK models. Gray boxes represent sub-compartments of the placenta structure implemented in the pregnancy PBPK model; dash-dotted boxes represent the vascular space; solid arrows denote drug transport *via* the organ blood flow; and dashed arrows denote drug transport *via* passive diffusion. The intracellular compartment in the fetal placenta represents the (syncytio)trophoblasts with the apical membrane facing toward the maternal plasma compartment and the basolateral membrane toward the fetal interstitial compartment. PBPK, physiologically based pharmacokinetic.

water and lipids in each tissue compartment which are needed to calculate $K_{cell,pls}$, were also accounted for. Quantitative data on these input variables was previously gathered from the literature (29). Equations (5, 7, and 11) were then used for all fetal compartments in the PBPK model.

Hence, the full equations for the rate of change of drug amount in the four compartments implemented in the updated maternal-fetal PBPK model were as follows:

$$d_t\begin{bmatrix} N_{bc} \\ N_{pls} \\ N_{int} \\ N_{cell} \end{bmatrix} = Q\begin{bmatrix} HCT \times \left(C_{bc}^{bp\_inflow} - C_{bc}\right) \\ (1-HCT) \times \left(C_{pls}^{bp\_inflow} - C_{pls}\right) \\ 0 \\ 0 \end{bmatrix} + E\begin{bmatrix} C_{bc} \\ C_{pls} \\ C_{int} \\ C_{cell} \end{bmatrix} \tag{12}$$

Here, Q denotes the blood flow of the compartment (L/min); HCT the hematocrit; $C_{bc}^{bp\_inflow}$ and $C_{bc}^{bp\_inflow}$ the molar drug concentration in the blood cells and plasma, respectively, of the blood pools that supplies the current compartment with blood (e.g., venous blood pool of the umbilical cord) (μmol/L) and E the passive drug exchange between the compartments driven by concentration gradients. Specifically, E was defined as the following 4 × 4 matrix:

Structural Implementation of Maternal-Fetal Drug Transfer in the Model

The sub-structure of the placenta barrier embedded in the pregnancy PBPK model is schematically illustrated in **Figure 2**. In this structure, maternal-fetal drug transfer occurs *via* the apical membrane of the trophoblast (represented in the model structure by the fetal intracellular compartment of the placenta). The ODE to describe maternal-fetal drug transfer was extended by adding scaling factors (f_{in} and f_{out}):

$$\frac{dN_{cell\_F}^{cell\_F \leftrightarrow pls\_M}}{dt} = f_{in} \times P_{pls,cell\_T} \times SA_{villi} \times f_u \times C_{pls\_M} - f_{out} \times P_{pls,cell\_T} \times SA_{villi} \times f_u \times \frac{C_{cell\_F}}{K_{cell,pls}} \tag{14}$$

In this equation, $N_{cell\_F}^{cell\_F \leftrightarrow pls\_M}$ is the molar drug amount in the fetal intracellular space of the placenta (trophoblasts) when only the maternal-fetal drug exchange process is considered (μmol); f_{in} and f_{out} are influx and efflux scaling factors, respectively; $P_{pls,cell\_T}$ is the permeability across the apical membrane of the trophoblasts (cm/min); SA_{villi} is the surface area of the fetal villi (cm²); C_{pls_M} and C_{cell_F} is the molar drug concentration in the maternal blood plasma of the placenta and fetal intracellular sub-space of the placenta, respectively (μmol/L); and $K_{cell,pls}$ is the placental partition coefficient between the fetal intracellular and the maternal blood plasma sub-space.

$$E = f_{u\_fetus}\begin{bmatrix} -P_{pls,bc} \times \frac{SA_{bc}}{K_{bc}} & P_{pls,bc} \times SA_{bc} & 0 & 0 \\ P_{pls,bc} \times \frac{SA_{bc}}{K_{bc}} & -P_{pls,bc} \times SA_{bc} - P_{end} \times SA_{end} & P_{end} \times \frac{SA_{end}}{K_{int,pls}} & 0 \\ 0 & P_{end} \times SA_{end} & -P_{end} \times \frac{SA_{end}}{K_{int,pls}} - P_{int,cell} \times \frac{SA_{int,cell}}{K_{int,pls}} & P_{int,cell} \times \frac{SA_{int,cell} \times f_u}{f_{u\_fetus} \times K_{cell,pls}} \\ 0 & 0 & P_{int,cell} \times \frac{SA_{int,cell}}{K_{int,pls}} & -P_{int,cell} \times \frac{SA_{int,cell} \times f_u}{f_{u\_fetus} \times K_{cell,pls}} \end{bmatrix} \tag{13}$$

For $K_{cell,pls}$, the same calculation method is used as for the other compartments in the PBPK model, i.e., the PK-Sim Standard, Schmitt, Rodgers and Rowland, or Poulin and Theil method. Information on the placenta tissue composition has been reported previously (29). The product of $P_{pls,cell} \times SA_{villi}$, also termed apical transfer clearance, was calculated according to a previously published *in vitro-to-in vivo* extrapolation approach (30). This approach uses midazolam as an *in vivo* calibrator and scales the passive diffusion clearance of another drug from its apparent permeability across epithelial cell lines (e.g., Caco-2 cells). An exception was emtricitabine; since no apparent *in vitro* permeability value could be found in the literature, the product of $P_{pls,cell} \times SA_{villi}$ was set to a previously reported value (15) estimated based on the *ex vivo* cotyledon perfusion assay (31). **Table 2** lists for each drug the method for predicting the tissue-to-plasma partition coefficients in the PBPK model together with the predicted value for $K_{cell,pls}$ between the fetal intracellular and the maternal blood plasma compartment as well as the values for the apparent permeability in Caco-2 cells and the resulting apical transfer clearance. It should be stressed that this clearance refers to the drug transfer across the apical membrane of the fetal trophoblasts. Of note, the selection of a method for predicting the partition coefficients of a given drug (as listed in **Table 2**) was done during development of the non-pregnant, adult PBPK model. During this process, several partition coefficient methods were tested. The method with the best simulation result (i.e., lowest squared error) was chosen and subsequently used in the maternal-fetal PBPK model [further information on the development of the non-pregnant, adult PBPK models can be found elsewhere (15–18)].

Note that in the original model, f_{in} and f_{out} in Equation (14) have a value of 1 and that for values <1 the apical transfer clearance is reduced, whereas for values >1 the apical transfer clearance is increased. In addition, similar scaling factors were introduced in the equation describing transfer across the basolateral membrane of the trophoblast (Equation 4), i.e., from the fetal intracellular compartment to the interstitial compartment in the placenta (see **Figure 2**).

Clinical Data

Clinical data for the investigated drugs herein were taken from the literature (18, 39–47) and are listed for each drug in **Table 3**. Blood samples were obtained from maternal peripheral venous blood and umbilical vein blood plasma at delivery. The timing of blood sampling relative to dose administration was highly heterogeneous due to the random nature in the time of delivery. Hence, for some drugs, e.g., acyclovir, cefuroxime and diazepam, few or no clinical data were available for the early absorption/distribution phase, whereas for others, e.g., ondansetron and metronidazole, few or no observed data were available in the elimination phase at delivery. Of note, clinical studies for diazepam investigated pharmacokinetics after doses of 5 mg (46) and 10 mg (45, 47) and studies for cefuroxime doses of 1,500 mg (42) and 750 mg (41). Here, the reported concentrations of diazepam and cefuroxime were normalized to the 10 and 750 mg dose, respectively, assuming linear pharmacokinetics.

Evaluation of Predictive Model Performance

Pharmacokinetics was predicted at delivery in a virtual population of 500 pregnant women. The predictive model performance was assessed by visual comparison of predicted drug concentrations in the maternal blood plasma and the umbilical vein blood plasma at delivery with the clinical data described above and listed in **Table 3**. In addition to visual assessment of the predictive model performance, the mean prediction error (MPE) (%) and mean squared error (MSE) were calculated as follows:

$$MPE = \frac{100}{n} \sum \frac{C_{sim,i} - C_{obs,i}}{C_{obs,i}} \tag{15}$$

$$MSE = \frac{1}{n} \sum \left(C_{obs,i} - C_{sim,i}\right)^2 \tag{16}$$

where $C_{sim,i}$ and $C_{obs,i}$ is the simulated and observed concentration at timepoint i, respectively; and n the total number of observed concentrations.

TABLE 2 | Overview of the methods for predicting the tissue-to-plasma partition coefficients of each drug in the PBPK model and placental transfer model parameters.

Drug	Method for predicting tissue-to-plasma partition coefficients in the PBPK model	Placental partition coefficient	Caco-2 cell permeability (cm/s)	Apical transfer clearance (L/min)
Acyclovir	PK-Sim Standard (24)	0.74	0.3×10^{-6} (32)	0.059
Cefuroxime	Schmitt (21)	0.61	1.2×10^{-6} (33)	0.20
Diazepam	PK-Sim Standard (24)	0.079	8.9×10^{-5} (34)	15.1
Dolutegravir	Rodgers and Rowland (25, 26)	0.16	2.5×10^{-6} (35)	0.43
Emtricitabine	Rodgers and Rowland (25, 26)	0.83	NA	0.019 (31)
Metronidazole	Rodgers and Rowland (25, 26)	0.80	5.7×10^{-5} (36)	9.76
Ondansetron	Poulin and Theil (27, 28)	0.41	1.8×10^{-5} (37)	3.11
Raltegravir	Rodgers and Rowland (25, 26)	0.28	7.3×10^{-6} (38)	1.24

NA, not available; PBPK, physiologically based pharmacokinetic.

TABLE 3 | Characteristics of the clinical studies used for model evaluation.

Drug	Posology	Gestational age (weeks)	Maternal concentration values (*n*)	Fetal concentration values (*n*)	References
Acyclovir	400 mg TID, oral	39.9 [37–41][a]	9	19	(39)
Cefuroxime	750 mg single dose, IV	41 [37–42][b]	14	8	(41)
Cefuroxime	1,500 mg single dose, IV	32 [28–35][b]	22	7	(42)
Diazepam	10 mg single dose, IV	38 [37–40][b]	16	16	(45)
Diazepam	5 mg single dose, IV	38–40[c]	5	5	(46)
Diazepam	10 mg single dose, IV	NA[d]	6	6	(47)
Dolutegravir	50 mg QD, oral	38 [35–42][b]	20	20	(18)
Emtricitabine	400 mg single dose, oral	39 [33–42][b]	166	37	(40)
Metronidazole	500 mg single dose, IV	NA[d]	21	12	(44)
Ondansetron	4 mg single dose, IV	39.1 [36.4–40.4][a]	46	9	(43)
Raltegravir	400 mg BID, oral	38 [36–40][b]	20	20	(18)

[a] *Expressed as arithmetic mean (range).*
[b] *Expressed as median (range).*
[c] *Expressed as range; median not reported.*
[d] *Gestational age at delivery not reported; in the model a gestational age of 40 weeks was assumed.*
BID, twice daily; IV, intravenous; NA, not available; PBPK, physiologically based pharmacokinetic; QD, once daily; TID, three times daily.

Sensitivity Analysis

Local sensitivity analyses were conducted using the updated maternal-fetal PBPK models to assess quantitatively how changes in various model parameters propagate to the model output. For each drug, the blood flow rate to the maternal intervillous space in the placenta was varied by factors of 0.5 and 2. Additionally, the apical and basolateral transfer clearance was varied as follows. For the apical transfer clearance, the scaling factors f_{in} and f_{out} in Equation (14) were varied both together by factors ranging from 2 to 10 and separately from each other (i.e., affecting either influx or efflux transfer clearance) by factors ranging from 0.5 to 2. The basolateral transfer clearance was varied by multiplying the product of $P_{int,cell} \times SA_{int,cell}$ (i.e., the transfer clearance) in Equation (4) by factors ranging from 1.5 to 10. Either the apical or the basolateral transfer clearance was modified during sensitivity analysis but not both at the same time.

The effect of variations in these parameters were only tested using the predicted umbilical vein concentrations as model output; maternal concentration predictions were not included as model output as it was previously shown that large changes in various placental transfer parameters (namely in the permeability across the apical trophoblast membrane and partition coefficient) did not significantly impact maternal plasma concentrations (18, 48).

Additionally, the area under the concentration-time curve from time zero (or, in case of multiple dose studies, time of last dose administration) to the time of the last observed concentration (AUC_{tlast}) was calculated from the observed data in maternal plasma and umbilical vein and compared with the predicted values.

RESULTS

The observed and predicted maternal plasma concentration-time profiles are shown in **Figure 3**. While the predicted median concentration-time profiles generally captured the clinical data, the observed interindividual variability was underestimated by the models. **Table 4** lists the MPEs for these predictions.

Figure 4 presents the observed and predicted plasma concentration-time profiles in the umbilical cord and **Table 4** lists the MPEs and MSEs for these predictions. For some drugs, such as ondansetron and metronidazole, visual assessment of the fetal prediction results was only possible within a relatively narrow time interval after dose administration because of lacking clinical data at later time points. Therefore, the predicted elimination phase could not be evaluated. For other drugs, e.g., acyclovir, few clinical data were available in the early distribution phase (i.e., before reaching the peak concentration in the fetus). No consistent trend for under- or overestimation was evident across the different predicted pharmacokinetic profiles. While for some drugs, such as diazepam and ondansetron, the pharmacokinetic profiles were overall adequately captured, the clinical data were underestimated for other drugs, e.g., acyclovir and dolutegravir, or, in the case of emtricitabine, overestimated. Of note, the relatively high MPE for emtricitabine (102.5%, see **Table 4**) could predominantly be attributed to two observed plasma concentrations in the absorption phase that were substantially overestimated (specially these concentrations were 0.0095 and 0.024 μg/mL at 0.8 and 3 h, respectively). For cefuroxime the clinical data showed high variability and contained very limited information, so that an adequate assessment of the predicted umbilical cord concentration was difficult. Similar to the pharmacokinetics predicted in maternal plasma, the observed interindividual variability was generally underestimated by the models.

Note that **Figure 4** also includes the prediction results that are obtained when setting the fetal fraction unbound value to that in the mother (i.e., equal fraction unbound values) to allow a visual assessment of the effect of plasma protein binding differences between the fetal and maternal circulatory

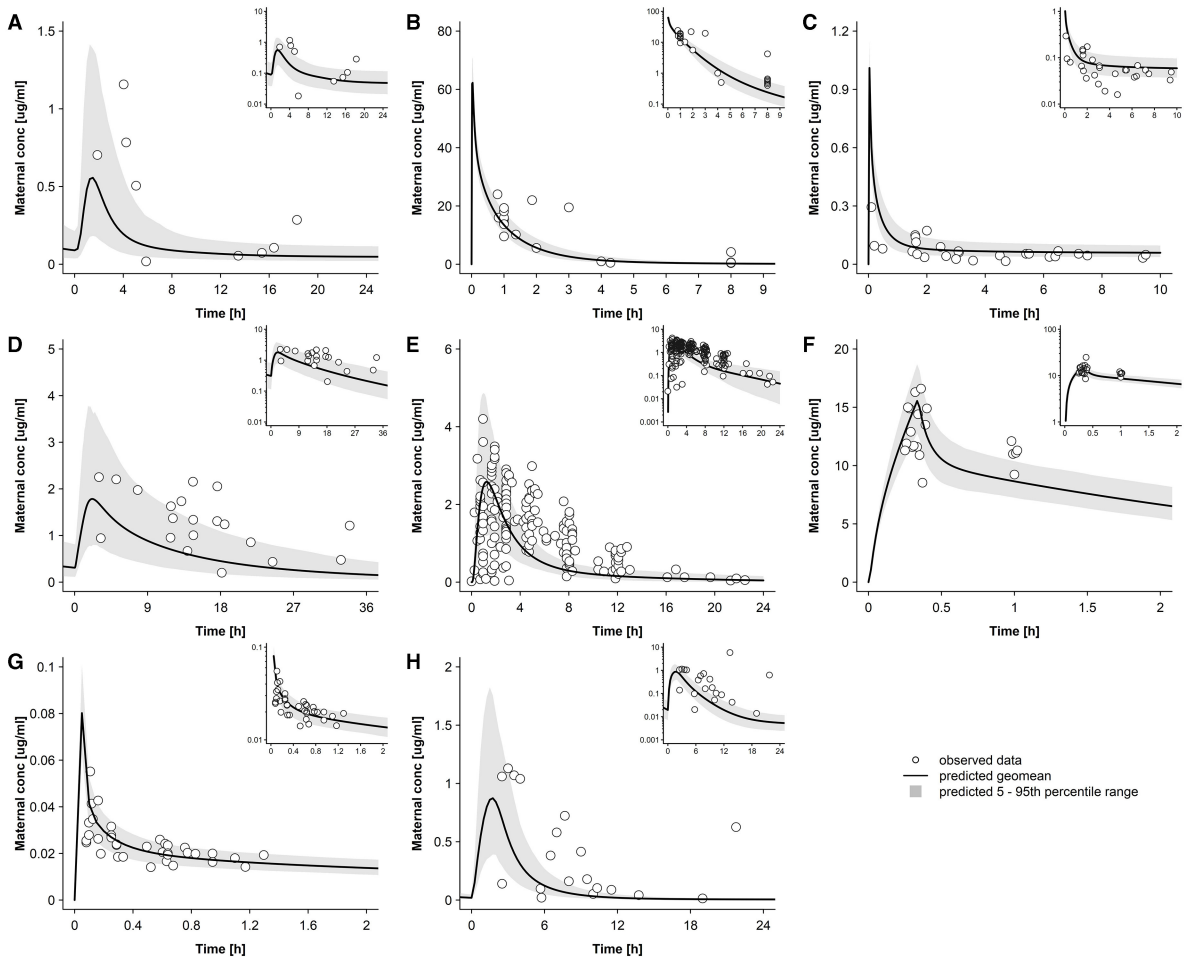

FIGURE 3 | Maternal plasma concentration–time profiles observed and predicted at delivery. Concentration-time profiles in the maternal peripheral blood plasma for acyclovir **(A)**, cefuroxime **(B)**, diazepam **(C)**, dolutegravir **(D)**, emtricitabine **(E)**, metronidazole **(F)**, ondansetron **(G)**, and raltegravir **(H)** at delivery in the third trimester. Semi-log scaled figures are shown as inset plot in the top-right corner of each panel. The time refers to the time after drug administration. Circles represent individual observed data; the solid line represents the predicted geomean and the shaded area the predicted 5th−95th percentile range. Observed data for acyclovir, cefuroxime, diazepam, dolutegravir, emtricitabine, metronidazole, ondansetron, and raltegravir were taken from Liu et al. (18), Leung et al. (39), Hirt et al. (40), Philipson and Stiernstedt (41), De Leeuw et al. (42), Elkomy et al. (43), Visser and Hund (44), Moore and McBride (45), Ridd et al. (46), and Mandelli et al. (47), respectively. conc, concentration.

TABLE 4 | Mean prediction errors and mean squared errors.

Drug	Maternal plasma concentrations		Umbilical vein concentrations	
	Mean prediction error (%)	Mean squared error	Mean prediction error (%)	Mean squared error
Acyclovir	16.9	0.17	15.7	0.12
Cefuroxime	−22.2	30.5	45.4	4.97
Diazepam	37.9	0.01	24.6	0.01
Dolutegravir	−37.2	0.68	−43.4	1.17
Emtricitabine	102.5	0.97	3.1	0.25
Metronidazole	0.9	13.5	−3.2	8.61
Ondansetron	4.4	7.0×10^{-5}	−41.2	2.0×10^{-5}
Raltegravir	−22.8	0.16	−23.3	0.51

system. For most drugs, differences in plasma protein binding between the mother and fetus translated into rather small differences in predicted umbilical cord concentrations. **Table 5** lists the predicted AUC_{tlast} for the umbilical cord plasma concentrations obtained when assuming equal maternal/fetal unbound drug fractions and when considering differential maternal/fetal protein binding. As can be seen in this table, the effect of assuming a different fetal fraction unbound on AUC_{tlast} was below 5% for some drugs but exceeded 10% in the case of highly-protein bound drugs (diazepam, dolutegravir and ondansetron); raltegravir was an exception, though. **Table 6** lists the observed and predicted AUC_{tlast} in maternal and umbilical vein plasma (when assuming differential maternal-fetal protein binding). In all but four cases, the observed AUC_{tlast} fell within the predicted 5th−95th percentile range.

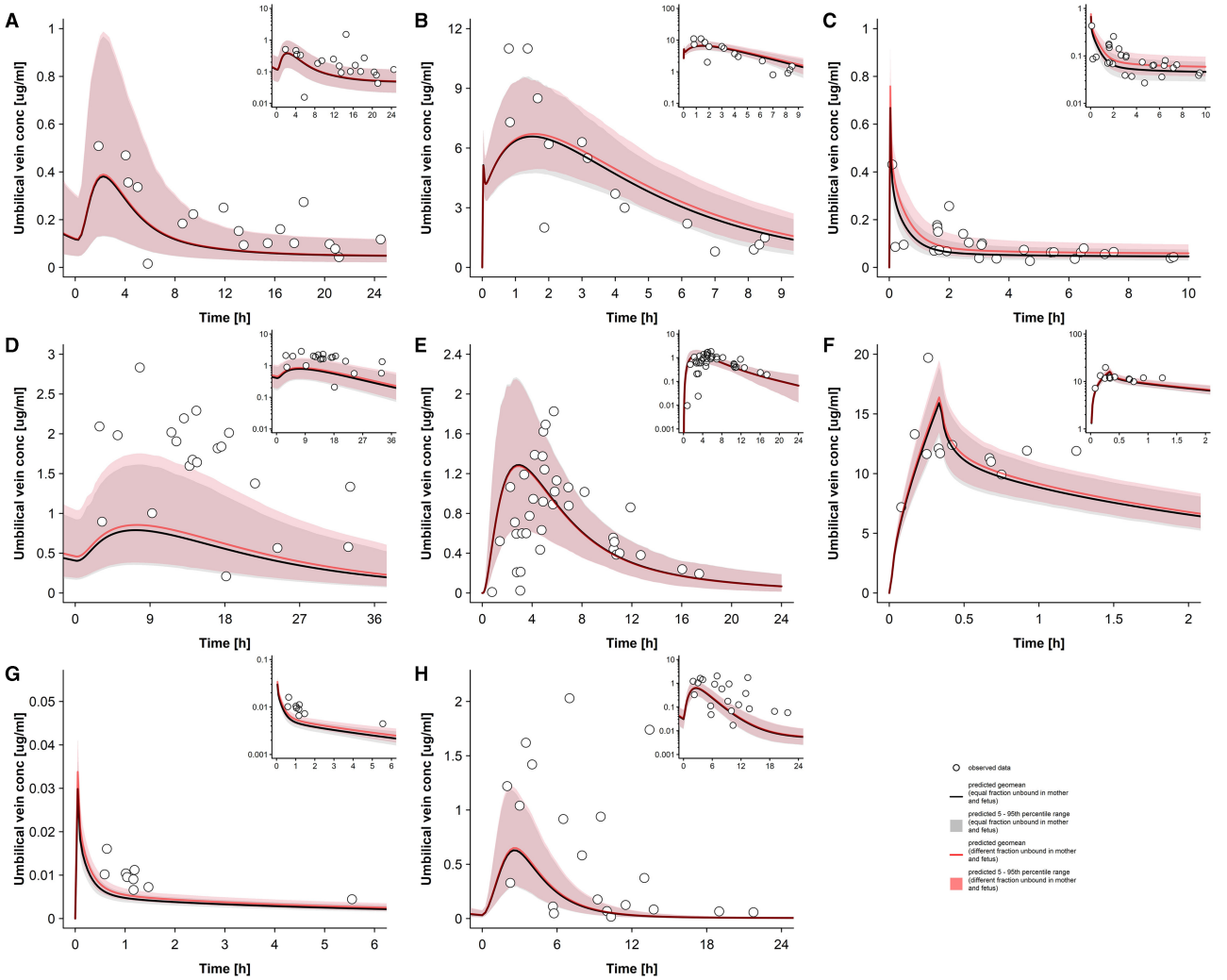

FIGURE 4 | Umbilical vein plasma concentration–time profiles observed and predicted at delivery. Concentration-time profiles in the umbilical vein plasma for acyclovir **(A)**, cefuroxime **(B)**, diazepam **(C)**, dolutegravir **(D)**, emtricitabine **(E)**, metronidazole **(F)**, ondansetron **(G)**, and raltegravir **(H)** at delivery in the third trimester. Semi-log scaled figures are shown as inset plot in the top-right corner of each panel. The time refers to the time after drug administration. Circles represent individual observed data; the solid line represents the predicted geomean and the shaded area the predicted 5th–95th percentile range. Red shades denote to predictions with different maternal/fetal unbound drug fractions and black/gray colors predictions with equal maternal and fetal unbound drug fractions. Observed data for acyclovir, cefuroxime, diazepam, dolutegravir, emtricitabine, metronidazole, ondansetron, and raltegravir were taken from Liu et al. (18), Leung et al. (39), Hirt et al. (40), Philipson and Stiernstedt (41), De Leeuw et al. (42), Elkomy et al. (43), Visser and Hund (44), Moore and McBride (45), Ridd et al. (46), and Mandelli et al. (47), respectively. conc, concentration.

Results of the sensitivity analysis are presented in **Figures 5**–**8**. **Figure 5** shows the predicted concentration-time profiles in the umbilical vein when maternal placental blood flow rate was varied two-fold. Within this range, the maternal placental blood flow rate did not significantly affect the predicted umbilical vein concentrations except for metronidazole. For all drugs, the maximum difference in AUC_{tlast} between the original model and the model with altered blood flow rate did not exceed 1%, except for cefuroxime and metronidazole where the maximum difference was 2.9 and 5.7% when the blood flow rate was increased two-fold and reduced two-fold, respectively.

Figures 6, **7** present the concentration-time profiles in the umbilical vein that were predicted with different apical influx and efflux transfer clearance scaling factors (f_{in} and f_{out}). As noted above, f_{in} and f_{out} modify the transfer clearance across the apical trophoblast membrane in the maternal-fetal and fetal-maternal direction, respectively. Changes in these parameters had only a negligible impact on maternal concentrations (data not shown). **Figure 6** presents pharmacokinetic predictions when f_{in} and f_{out} are both varied equally, i.e., when the transfer clearance ($P_{pls,cell} \times SA_{villi}$) is similarly changed in both the influx and efflux direction. As was expected for orally administered drugs, except for raltegravir, higher values for f_{in} and f_{out} gave rise to

TABLE 5 | Predicted drug exposure in umbilical vein plasma with equal and different maternal-fetal protein binding.

Drug	AUC_{tlast} predicted in umbilical vein plasma with equal maternal and fetal fraction unbound (μg h/mL)	AUC_{tlast} predicted in umbilical vein plasma with different maternal and fetal fraction unbound (μg h/mL)	Difference (%)
Acyclovir	1.9	2.0	5.3
Cefuroxime	36.5	38.2	4.7
Diazepam	0.67	0.85	26.9
Dolutegravir	15.0	16.5	10.0
Emtricitabine	10.2	10.1	−0.98
Metronidazole	12.3	12.7	3.3
Ondansetron	0.024	0.028	16.7
Raltegravir	3.0	3.2	6.7

AUC_{tlast}, area under the concentration-time curve from time zero (or, in case of multiple dose studies, time of last dose administration) to the time of the last observed concentration.

TABLE 6 | Observed and predicted drug exposure in mother and fetus.

Drug	AUC_{tlast} in maternal plasma (μg h/mL)		AUC_{tlast} in umbilical vein plasma (μg h/mL)	
	Observed	Predicted (geomean [*p5*; *p95*])	Observed	Predicted (geomean [*p5*; *p95*])
Acyclovir	3.7	1.9 [0.66; 5.1]	5.3	2.0 [0.70; 5.1]
Cefuroxime	39.0	43.9 [32.8; 61.9]	33.3	38.2 [27.5; 54.4]
Diazepam	0.50	0.86 [0.55; 1.4]	0.67	0.85 [0.55; 1.4]
Dolutegravir	37.5	19.4 [8.2; 42.9]	37.8	16.5 [7.2; 35.1]
Emtricitabine	15.9	10.6 [5.0; 19.7]	10.7	10.1 [5.3; 16.9]
Metronidazole	7.0	5.1 [4.2; 6.2]	13.8	12.7 [10.4; 15.2]
Ondansetron	0.11	0.10 [0.074; 0.12]	0.030	0.028 [0.022; 0.036]
Raltegravir	5.9	2.9 [1.3; 6.3]	7.7	3.2 [2.4; 6.3]

AUC_{tlast}, area under the concentration-time curve from time zero (or, in case of multiple dose studies, time of last dose administration) to the time of the last observed concentration; p5, 5th percentile; p95, 95th percentile.

greater peak concentrations (C_{max}) and a lower time at which C_{max} is reached (t_{max}). For intravenously administered drugs, variations in f_{in} and f_{out} only had a negligible effect on the predicted pharmacokinetic profiles.

Figure 7 shows predicted pharmacokinetic profiles when either f_{in} or f_{out} was changed, while the other one was kept unchanged at the original value of 1. It is important to note that these results are relative and will be different when the absolute transfer clearance ($P_{pls,cell} \times SA_{villi}$) is altered. As expected, these variations had a strong impact on the umbilical vein-to-maternal plasma concentration ratio. No consistent trend for under- or overestimation was found for the different drugs when apical influx or efflux transfer was altered. For some drugs (e.g., ondansetron and raltegravir), albeit not for all, a two-fold increase of the efflux transfer clearance showed results that were equivalent to a two-fold decrease in the influx transfer clearance.

The results for sensitivity analysis when varying the transfer clearance across the basolateral membrane are shown in **Figure 8**. These results were informative in that they revealed that the basolateral transfer clearance was also a sensitive parameter for some drugs, e.g., for cefuroxime and raltegravir.

DISCUSSION

Fetal therapeutics is rapidly becoming a reality both for drugs given to the mother and for gene and stem cell therapy delivered to the fetus. For drugs that are administered to the mother with the intent of treating the fetus, a further understanding of maternal to fetal drug transfer will be required. This study refined the ODE system of a previously published pregnancy PBPK model by implementing the fetal-specific unbound drug fraction in the model. Additionally, scaling factors were integrated in the model to account for asymmetrical drug transfer across the apical and basolateral membranes of the trophoblast. Using the refined model, maternal and fetal pharmacokinetics were predicted for eight different drugs. It was further investigated how different unbound drug fractions in the maternal and fetal circulatory system and different apical and basolateral influx/efflux transfer clearances impact the predicted drug concentrations in the umbilical vein.

In this study, apical transfer clearance was estimated using a previously proposed *in vitro-to-in vivo* extrapolation of a drug's passive diffusion clearance (30). This extrapolation approach appears attractive because *in vitro* permeability values required as input are often readily available in the literature. Although it was initially only proposed for drugs crossing the placenta exclusively *via* passive diffusion (30), this approach also yielded adequate results for ondansetron which is a substrate of P-glycoprotein [P-gp, also referred to as multidrug resistance protein 1 (MDR1)] (49), an efflux transporter expressed in the apical membrane of trophoblasts (50). On the other hand, for dolutegravir and raltegravir which are also P-gp substrates (51, 52), this approach substantially underestimated the clinical observations (**Figure 4**). Furthermore, for acyclovir, a substrate of various efflux transporters expressed in the placenta, such as the multidrug and toxin extrusion proteins (MATE) 1/2-K (53), it was expected that this approach would result in an overestimation of umbilical vein concentrations as efflux is not considered in the estimated apical transfer clearance value; yet, the presented results showed that an even higher placental transfer clearance would be required to adequately describe the data. Hence, the overall suitability of this approach for parameterizing placental transfer in PBPK models remains inconclusive. Importantly, a refined version of this approach has been proposed very recently (54) and merits further evaluation with additional drugs.

The predicted variability in maternal and, to a lesser extent, umbilical vein concentrations was generally underestimated (**Figures 3**, **4**). To some extent, this was expected because

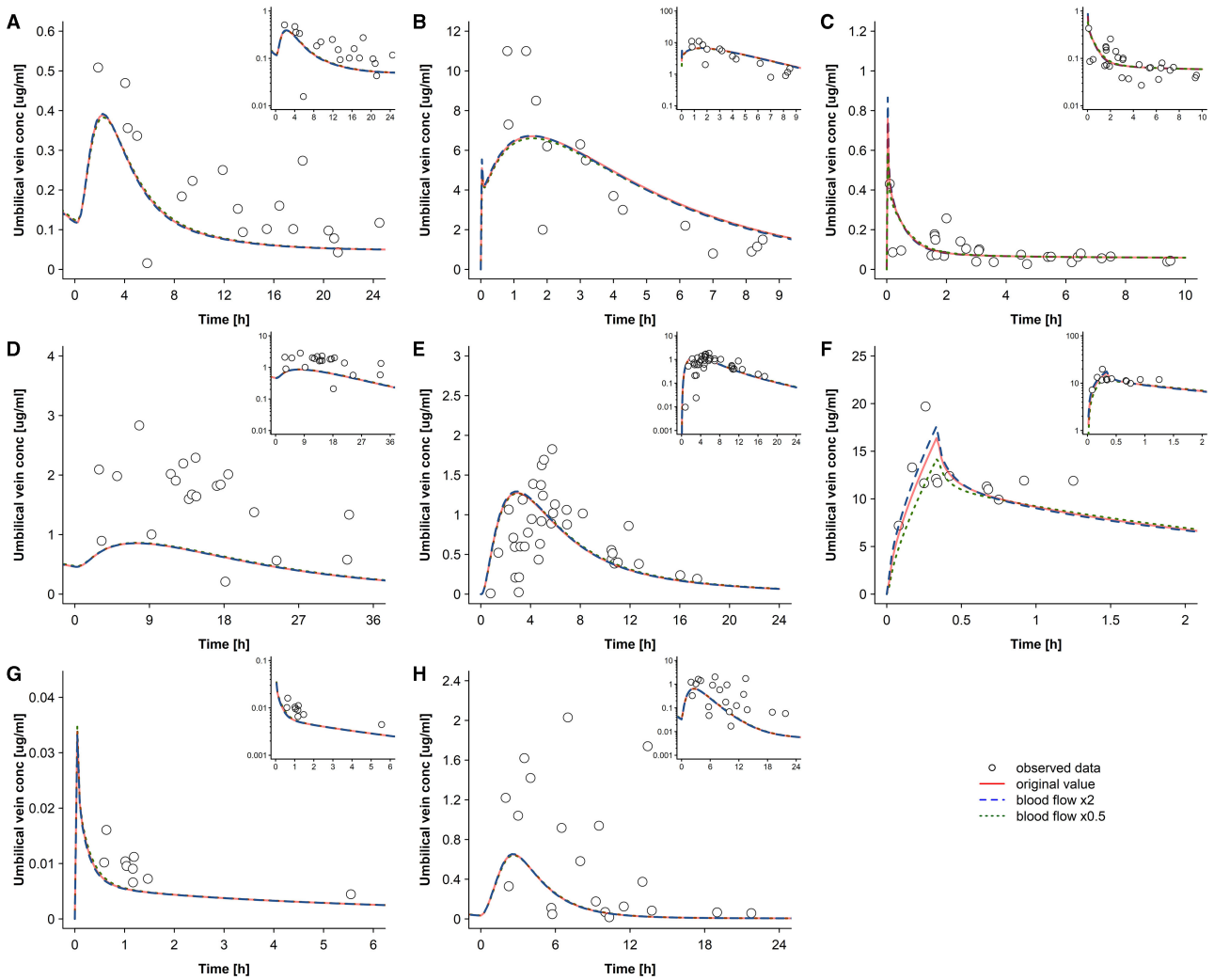

FIGURE 5 | Sensitivity analysis for the maternal placental blood flow rate. Concentration-time profiles in the umbilical vein plasma for acyclovir **(A)**, cefuroxime **(B)**, diazepam **(C)**, dolutegravir **(D)**, emtricitabine **(E)**, metronidazole **(F)**, ondansetron **(G)**, and raltegravir **(H)** at delivery in the third trimester. Semi-log scaled figures are shown as inset plot in the top-right corner of each panel. The time refers to the time after drug administration. Circles represent individual observed data and the lines represents the predicted geomean concentrations with different blood flow rates to the maternal placenta. Observed data for acyclovir, cefuroxime, diazepam, dolutegravir, emtricitabine, metronidazole, ondansetron, and raltegravir were taken from Liu et al. (18), Leung et al. (39), Hirt et al. (40), Philipson and Stiernstedt (41), De Leeuw et al. (42), Elkomy et al. (43), Visser and Hund (44), Moore and McBride (45), Ridd et al. (46), and Mandelli et al. (47), respectively. conc, concentration.

the variability in anatomical and physiological parameters integrated in the PBPK models stems from observations in non-laboring women (29). While relatively little is known about changes in fetal physiological parameters during delivery, maternal physiological parameters, particularly those related to hemodynamics, show substantial variation during the peripartum period. For example, cardiac output is 13–31% higher in the first stage of labor compared to the pre-parturient level (55, 56) and can temporarily increase by ∼20–60% during cesarean delivery, especially if uterotonics, e.g., oxytocin or carbetocin, are co-administered (57). This might give rise to temporary changes in various organ blood flows which could in turn contribute to increased variability in drug distribution and elimination. For drugs with a blood-flow limited distribution behavior across the placenta, such as metronidazole, a potential increase in maternal placental blood flow during labor can be expected to increase the distribution across the placenta leading to higher drug exposure in the fetus (further discussed below). Furthermore, elimination is relatively insensitive toward potential changes in liver blood flow for drugs that have a low to intermediate hepatic extraction ratio (all drugs investigated herein). For example, for diazepam, metronidazole, and ondansetron, a 30% increase in both hepatic arterial and portal vein blood flow increased clearance by only 0.3, 0.9, and 4.1%, respectively (data not shown). The clearance of high extraction drugs depends more on liver blood flow and might therefore be substantially increased during labor.

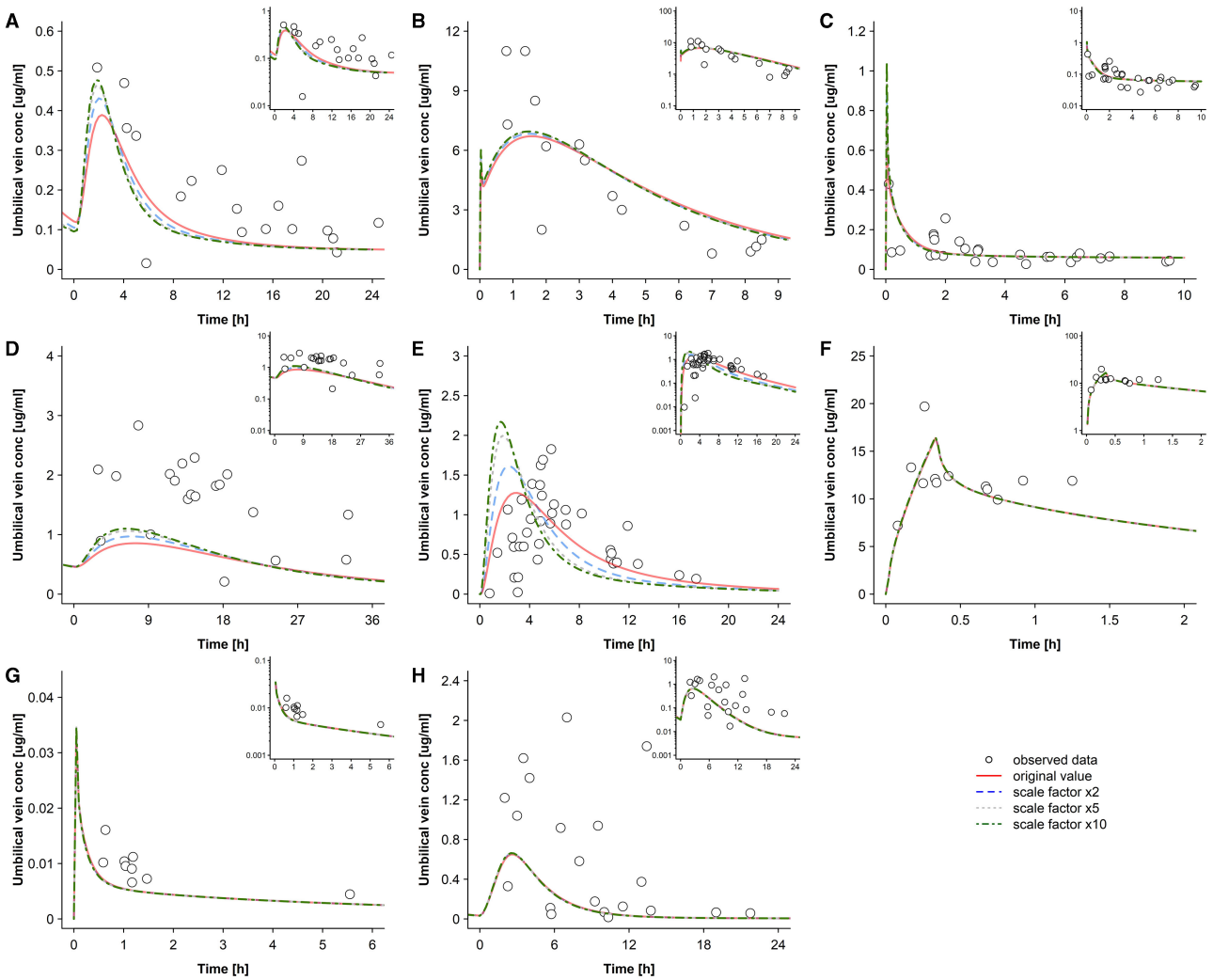

FIGURE 6 | Sensitivity analysis for the transfer clearance across the apical trophoblast membrane where both influx and efflux clearance are equally varied. Concentration-time profiles in the umbilical vein plasma for acyclovir **(A)**, cefuroxime **(B)**, diazepam **(C)**, dolutegravir **(D)**, emtricitabine **(E)**, metronidazole **(F)**, ondansetron **(G)**, and raltegravir **(H)** at delivery in the third trimester. Semi-log scaled figures are shown as inset plot in the top-right corner of each panel. Circles represent individual observed data and the lines represents the predicted geomean concentrations with different transfer clearances across the apical trophoblast membrane (both influx and efflux transfer clearance are equally altered). Observed data for acyclovir, cefuroxime, diazepam, dolutegravir, emtricitabine, metronidazole, ondansetron, and raltegravir were taken from Liu et al. (18), Leung et al. (39), Hirt et al. (40), Philipson and Stiernstedt (41), De Leeuw et al. (42), Elkomy et al. (43), Visser and Hund (44), Moore and McBride (45), Ridd et al. (46), and Mandelli et al. (47), respectively. conc, concentration.

While the effect of labor on cardiac output is relatively well-characterized, the effect on organ blood flows (e.g., for the placenta and liver) is unknown which complicates integrating these factors in a PBPK model.

Along a similar line, an overestimation of the maternal clearance of raltegravir and dolutegravir may have led to an underestimation of both maternal and fetal drug exposure. In these cases, increasing maternal plasma concentrations (e.g., by reducing UGT-mediated clearance or the unbound drug fraction) also improved predictions in the umbilical cord. This stresses again that maternal physiological changes need to be adequately captured in PBPK models since maternal and fetal pharmacokinetics are intimately connected.

The unbound drug fraction was estimated in this study from reported maternal and fetal albumin serum levels. Albumin does not cross the placenta (58, 59) and hence fetal albumin is exclusively of fetal origin. Fetal albumin is synthesized at a higher rate in the early third trimester vs. late third trimester (60) where the difference between fetal and maternal albumin concentrations diminishes. The findings of this study demonstrate that slight differences in maternal-fetal protein binding at term delivery generally have a rather small effect on the predicted umbilical cord concentrations (see **Table 5**). At quasi-equilibrium, it can be expected that the predicted concentration ratio between maternal and umbilical vein concentrations will approach the ratio of maternal to fetal fraction unbound.

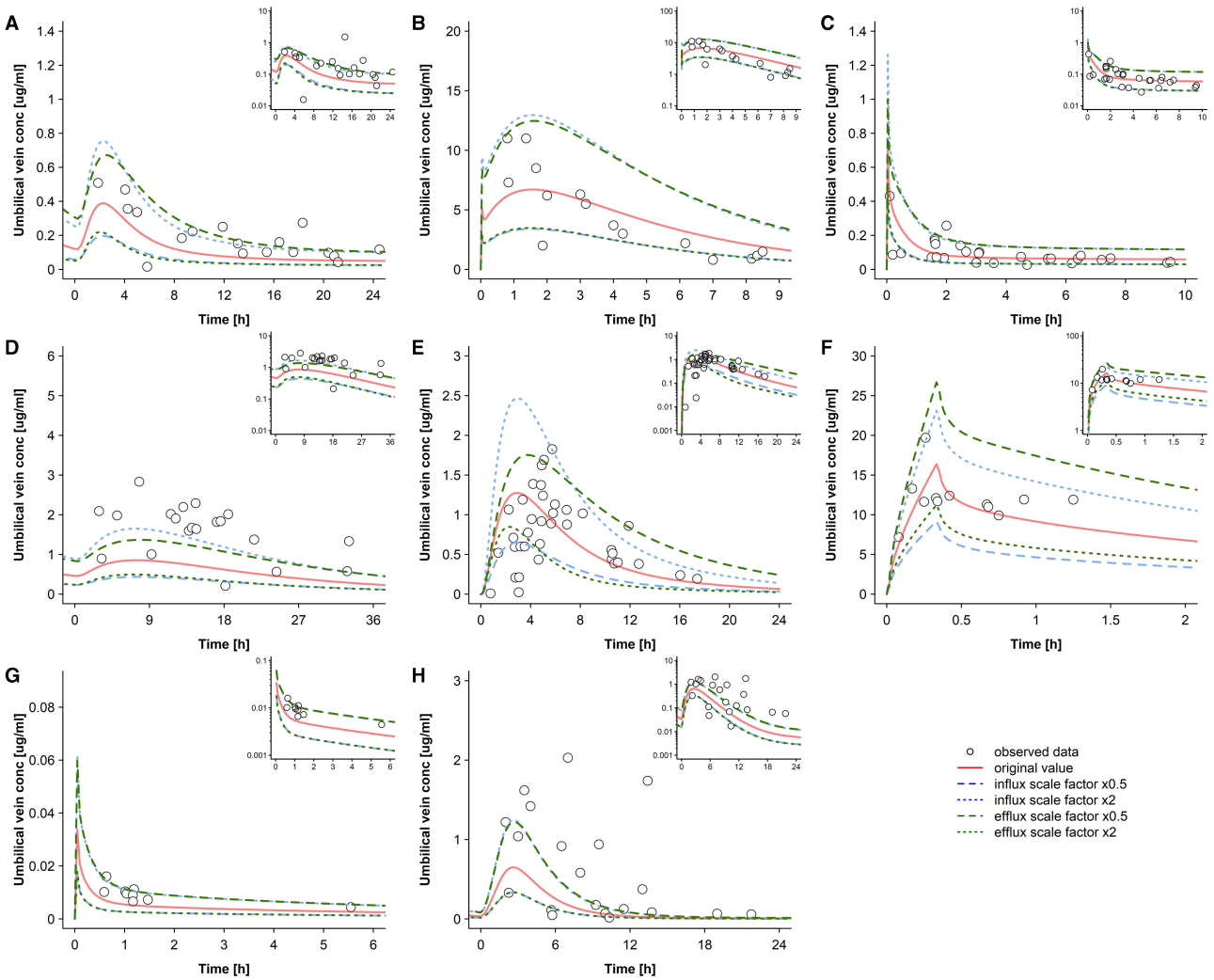

FIGURE 7 | Sensitivity analysis for the transfer clearance across the apical trophoblast membrane where either influx or efflux clearance is varied. Concentration-time profiles in the umbilical vein plasma for acyclovir **(A)**, cefuroxime **(B)**, diazepam **(C)**, dolutegravir **(D)**, emtricitabine **(E)**, metronidazole **(F)**, ondansetron **(G)**, and raltegravir **(H)** at delivery in the third trimester. Semi-log scaled figures are shown as inset plot in the top-right corner of each panel. The time refers to the time after drug administration. Circles represent individual observed data and the lines represents the predicted geomean concentrations with different transfer clearances across the apical trophoblast membrane (either influx or efflux transfer clearance is altered). Observed data for acyclovir, cefuroxime, diazepam, dolutegravir, emtricitabine, metronidazole, ondansetron, and raltegravir were taken from Liu et al. (18), Leung et al. (39), Hirt et al. (40), Philipson and Stiernstedt (41), De Leeuw et al. (42), Elkomy et al. (43), Visser and Hund (44), Moore and McBride (45), Ridd et al. (46), and Mandelli et al. (47), respectively. conc, concentration.

When calculating the fetal unbound drug fraction according to Equation (1), it was assumed that the drug binds to one protein only (namely albumin) and that the number of adult and fetal protein binding sites as well as the drug's affinity to adult and fetal plasma proteins are the same. The assumption that albumin is the exclusive protein binding partner may contribute to an underestimation of the fetal unbound fraction of a drug with mixed binding to albumin or α1-acidic glycoprotein because the relative concentration difference between fetal and adult α1-acidic glycoprotein is considerably larger than that for albumin [α1-acidic glycoprotein: 0.21 g/L in the fetus at 38 weeks of gestation vs. 0.70 g/L in non-pregnant adults; albumin: 38.6 g/L in the fetus at 38 weeks of gestation vs. 46.4 g/L in non-pregnant adults (20, 29)]. Relatively little information could be found in the scientific literature to falsify (or verify) the assumption of equal number of protein binding sites and binding affinity of adult and fetal albumin. Investigating diazepam binding to albumin, Viani et al. (61) reported 0.83 and 1.02 number of albumin binding sites (expressed as moles of drug per mole of albumin) for fetal and adult serum, respectively, and an association constant of 1.36×10^{-5} and 1.00×10^{-5} M^{-1} to fetal and adult albumin, respectively. Calculation of the fetal unbound fraction from these values according to a previously described method (16, 19) yields a value of 0.024 for diazepam instead of 0.021 (**Table 1**) which is closer to the maternal value of 0.027 and would hence lead to a lower difference between predicted maternal and fetal plasma

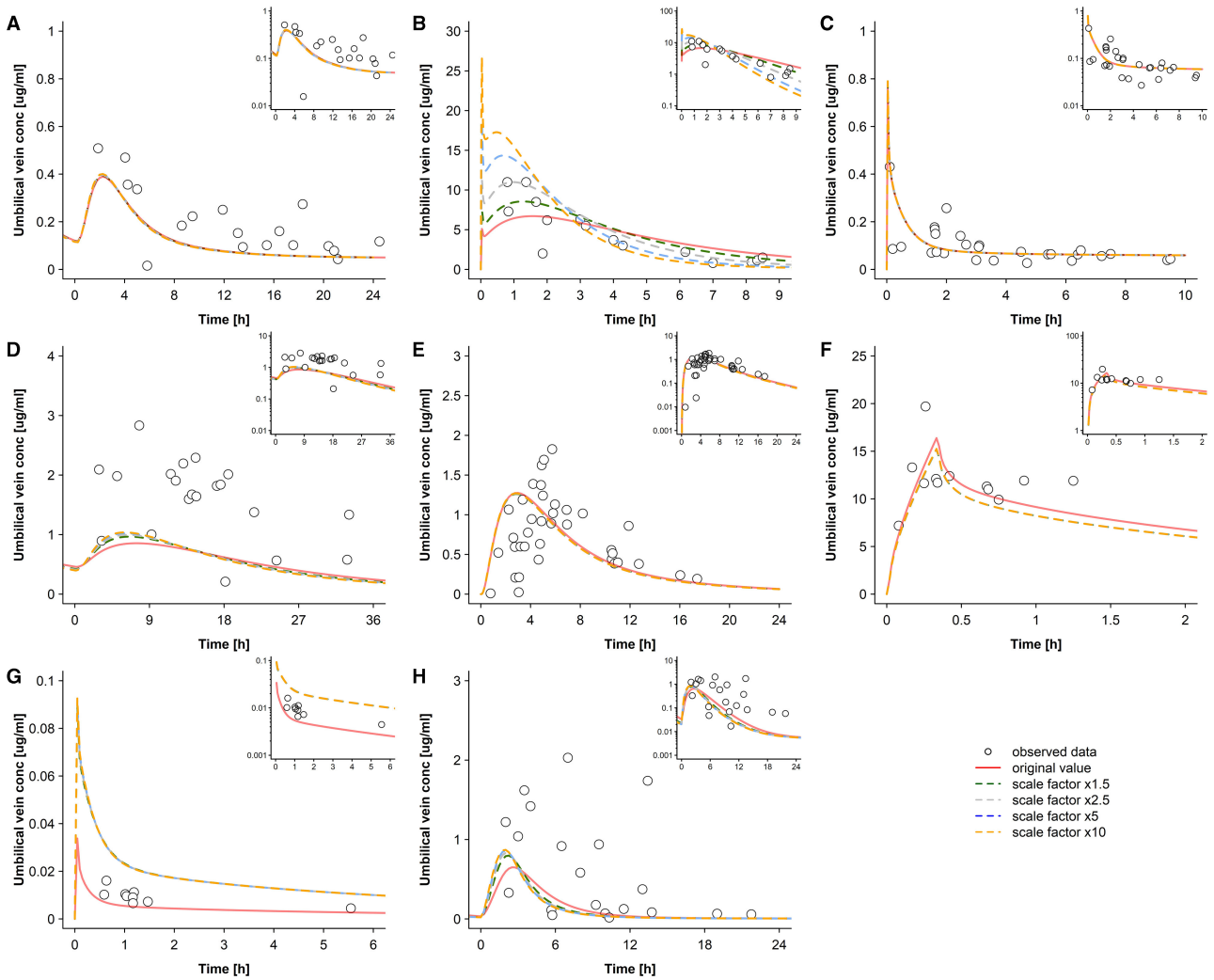

FIGURE 8 | Sensitivity analysis for the transfer clearance across the basolateral trophoblast membrane. Concentration-time profiles in the umbilical vein plasma for acyclovir **(A)**, cefuroxime **(B)**, diazepam **(C)**, dolutegravir **(D)**, emtricitabine **(E)**, metronidazole **(F)**, ondansetron **(G)**, and raltegravir **(H)** at delivery in the third trimester. Semi-log scaled figures are shown as inset plot in the top-right corner of each panel. The time refers to the time after drug administration. Circles represent individual observed data and the lines represents the predicted geomean concentrations with different transfer clearances across the basolateral trophoblast membrane (both influx and efflux transfer clearance are equally altered). Observed data for acyclovir, cefuroxime, diazepam, dolutegravir, emtricitabine, metronidazole, ondansetron, and raltegravir were taken from Liu et al. (18), Leung et al. (39), Hirt et al. (40), Philipson and Stiernstedt (41), De Leeuw et al. (42), Elkomy et al. (43), Visser and Hund (44), Moore and McBride (45), Ridd et al. (46), and Mandelli et al. (47), respectively. conc, concentration.

concentrations. Without further experimental data, though, it is difficult to evaluate the calculated fetal unbound fraction of the other investigated drugs. This highlights the need to further measure the fetal unbound fraction of diverse drugs in clinical samples and use these data to develop, train or validate methods for calculating the unbound fraction of a drug.

For drugs weakly or moderately bound to albumin (fraction unbound $>$ ~30%), the differences in fetal/maternal protein binding can, under normal conditions, be expected to be rather low at term delivery because the difference between fetal and maternal albumin concentration diminishes toward term (20, 29). However, they may become more relevant at earlier stages of pregnancy. For example, in a paired analysis, Krauer et al. (62) observed that the fetal/maternal albumin concentration ratio was around 0.66 $\pm$ 0.30 (mean $\pm$ standard deviation) between 16 and 25 weeks of gestation and increased thereafter, reaching 1.20 $\pm$ 0.18 at $>$35 weeks of gestation. Additionally, differences in fetal/maternal fraction of unbound drug may be exaggerated in diseased states that have been observed to be associated with maternal or fetal hypoalbuminemia, such as preeclampsia and eclampsia (63) or severe hydrops fetalis (64). Finally, for drugs predominantly binding to α1-acidic glycoprotein, larger differences between maternal and fetal fraction of unbound drug may be expected as the observed fetal/maternal concentration ratio of α1-acidic glycoprotein rises only to 0.37 $\pm$ 0.23 (mean $\pm$ standard deviation) at term (62). This highlights that differential

protein binding characteristics, although found to be generally only of minor importance in this study, might be relevant in various scenarios and should hence be structurally considered in PBPK models.

Interestingly, the observed pharmacokinetic profiles in the umbilical vein could not be captured for all drugs when placental transfer clearance, estimated from reported Caco-2 permeability (**Table 2**), was assumed to be equal in both maternal-fetal and fetal-maternal direction (**Figure 4**). For example, the umbilical vein concentrations of acyclovir, dolutegravir, and raltegravir were systematically underestimated and could not be improved when increasing the total blood flow to the placenta (**Figure 5**) or the total flux across the apical membrane (**Figure 6**). In fact, with the exception of metronidazole, the concentrations predicted in the umbilical vein were not sensitive to changes in the maternal placental blood flow, at least not within the tested range (**Figure 5**). These findings suggest that the distribution of these drugs across the placenta barrier is not limited by blood flow, but rather by the permeability through the trophoblasts' apical membrane at the fetal-maternal interface. This is an expected finding because for all drugs the product of the fraction of unbound drug (**Table 1**) and the apical transfer clearance rate (**Table 2**) is considerably lower than the mean placental blood flow of the mother (∼0.75 L/min), except for metronidazole where the latter product amounts to 9.0 L/min which makes the transplacental distribution of metronidazole blood flow-limited. Hence, alterations in placental hemodynamics induced by labor and delivery might be of concern for this drug.

Although transfer clearance across the apical membrane was a sensitive parameter for orally administered drugs (except raltegravir), higher parameter values did not substantially improve the model performance (**Figure 6**). With equal apical transfer clearance in both influx and efflux direction, the ratio of predicted maternal to umbilical vein plasma concentrations at quasi-equilibrium was solely influenced by differential protein binding characteristics (**Figure 4**).

While the placental partition coefficients (**Table 2**) did influence intracellular concentrations in the trophoblasts, concentrations in the maternal and umbilical vein blood were not affected by this parameter (data not shown). For example, higher values for the maternal blood plasma-to-fetal intracellular partition coefficients led to higher intracellular drug concentrations in the trophoblast without significantly influencing maternal and umbilical vein plasma concentrations. This was expected because the values of the partition coefficient between maternal blood plasma and fetal intracellular space are similar to the values of the partition coefficient between fetal blood plasma and fetal intracellular space. Changes in umbilical vein concentrations will only be observed if the maternal blood plasma-to-fetal intracellular partition coefficient is changed while keeping the fetal blood plasma-to-fetal intracellular partition coefficient unchanged as has been shown previously (18, 48). The effect of such asymmetrical changes in placental partition coefficients is similar to alterations in the efflux transfer clearance; for example, as can be seen from Equation (14), a two-fold increase in $K_{cell,pls}$ will yield the same results as reducing f_{out} by a factor of 0.5.

For several drugs (e.g., dolutegravir, ondansetron, and raltegravir), the clinical data could be better described when a higher influx-to-efflux transfer clearance ratio was applied in the models (**Figure 7**). Yet, it is difficult to draw general conclusions from these findings because they all relate to specific apical transfer clearance values (**Table 2**) which may be inaccurate as discussed above. For example, to improve the model predictions for dolutegravir, ondansetron and raltegravir, a higher influx-to-efflux ratio seemed to be necessary (**Figure 7**); however, since these drugs are P-gp substrates (49, 51, 52), a lower influx-to-efflux ratio would be biologically plausible. This might suggest that the applied *in vitro-to-in vivo* extrapolation approach underestimates the absolute apical transfer clearance for these drugs; in turn, a higher absolute apical transfer clearance could then accommodate a lower influx-to-efflux ratio. This hypothesis seems to be in line with findings from *in vitro* studies. When comparing various studies that quantified P-gp expression relative to that of the housekeeping gene GAPDH (glyceraldehyde-3-phosphate dehydrogenase), higher P-gp expression was found in Caco-2 cells (65–67) than in (syncytio)trophoblasts (68, 69). These expression data corroborate the hypothesis that, compared to Caco-2 cells, a weaker effect of P-gp mediated efflux can be expected for the placenta barrier. As can be seen from Equation (14), it is unfortunately not possible to use these PBPK models for estimation of both the apical transfer clearance and the factor modulating efflux clearance (f_{out}) because of non-identifiability issues.

Even if the transfer clearance across the apical membrane is accurately parameterized, the transfer clearance across the basolateral membrane of the trophoblast may also play an important role as was found, e.g., for cefuroxime and ondansetron (**Figure 8**). In the presented PBPK models, the basolateral transfer clearance was estimated as product of the drug's organ permeability (2.73×10^{-6} and 1.69×10^{-2} cm/min for cefuroxime and ondansetron, respectively) and the surface area between the trophoblasts' intracellular and interstitial space (on average ∼56,700 dm^2). For cefuroxime, but not for ondansetron, the resulting basolateral transfer clearance was lower than the apical transfer clearance (0.015 vs. 0.20 L/min for cefuroxime and 96 vs. 3.11 L/min for ondansetron). These findings illustrate that an adequate parameterization of placental drug transfer should consider both apical and basolateral transfer clearance rates.

In addition to the model parameters investigated herein (placental blood flow, apical and basolateral influx and efflux clearance rates and differential protein binding in mother and fetus), the degree of a drug's ionization could also affect placental transfer as only the non-ionized drug fraction can cross the trophoblast membrane. The pH of the fetal blood is ∼0.1 log unit lower than that of the maternal blood. Although this is generally of less concern under normal conditions, the pH difference may be exaggerated in the case of fetal asphyxia, or in situations of severe maternal hemorrhage and coagulopathy requiring blood transfusions (70). In the case of weakly basic drugs, a lower pH value of the fetal blood is associated with a higher fraction of the ionized

form of the drug leading to ion trapping and higher drug concentrations in the fetal blood as has been observed e.g., for bupivacaine (71) and lidocaine (72). Among the drugs investigated herein, only ondansetron is weakly basic with a pKa of 7.80 (73) which might have partly contributed to the underestimation of ondansetron concentrations in the umbilical vein.

As stated above, it is difficult to accurately identify mechanisms of the misfit between predicted and observed pharmacokinetics because multiple factors can affect the predictions in a similar fashion. For example, ondansetron pharmacokinetics could be better described by either a higher fetal fraction unbound; a higher ratio of influx-to-efflux transfer clearance across the apical membrane; a higher transfer clearance across the basolateral membrane; by potentially accounting for the different pH value in fetal blood; or by a combination of all these factors. This indicates that further clinical data of well-characterized drugs are required to systematically inform placental blood flow rates, passive and active transfer processes as well the effect of differential protein binding and pH values between maternal and fetal blood.

Another limitation of the presented maternal-fetal PBPK models is the lack of a mechanistic integration of drug transporters in the placenta. On a physiological level, the differences in influx/efflux diffusion clearances might be attributed to the presence of drug transporters in the placenta. The presented findings highlight the fact that an adequate parametrization of transporter activities in the apical and basolateral membrane of the trophoblasts is crucial for predicting fetal drug exposure. Currently, the integration of placental transporters in PBPK models is hampered by the scarce information on transporter abundance in the (syncytio)trophoblasts.

Additionally, placental metabolism has not been accounted for in this study. Yet, the expression or activity of numerous drug-metabolizing enzymes has been found to be absent in the human term placenta (74, 75). In fact, the enzymes involved in the metabolism of the drugs investigated herein—except for acyclovir and emtricitabine—are either not expressed or not functionally active in the term placenta. To the best of our knowledge, the expression of aldehyde oxidase, which is responsible for metabolism of acyclovir [∼10% of the dose in non-pregnant adults (15)], has not yet been studied in the human term placenta, while the enzyme involved in metabolism of emtricitabine [∼29% of the dose in non-pregnant adults (15)] is not identified. Therefore, it appears unlikely that placental transfer of the investigated drugs could have been influenced by placental metabolism. Still, for other drugs, especially those with a high extraction ratio, placental metabolism, if present *in vivo*, should be accounted for in the model as this would potentially decrease the net flux of drug across the placenta.

Finally, this study was limited to eight drugs. It is evident that further models and additional clinical data from both mother and fetus are needed to further advance our understanding of placental drug transfer. While pregnant women have historically been excluded from clinical trials, the lack of drug studies in pregnant women has been recognized as a major health issue (76). There seems to be a slow paradigm shift arguing in favor of the inclusion of pregnant women in clinical research (77–79) which is also, at least to some extent, reflected by recent guidance documents from the US Food and Drug Administration (FDA) (7). Hence, it can be expected that more clinical data in pregnant women will be generated within the next years. Analyzing these data with modeling and simulation techniques will help to interpret these data by mathematical abstraction and thus generate further insights in maternal-fetal pharmacology.

In conclusion, our current understanding of drug transfer kinetics across the placenta is only rudimentary. The findings indicate that, in the late third trimester, differential protein binding characteristics in the maternal and fetal system give rise to only minor differences in maternal-fetal exposure to albumin-bound drugs, especially if protein binding is low or moderate. Differences in placental influx and efflux clearance, however, were found to be highly relevant stressing the importance of drug transporters in the placenta. Hence, further clinical studies are required to better disentangle and quantify both passive and active transfer processes across the apical and basolateral membrane of the trophoblast. This updated PBPK model structure is freely shared on OSP GitHub (https://github.com/Open-Systems-Pharmacology) for further applications and/or refinements that were beyond the scope of this study. Ultimately, once the confidence in maternal-fetal PBPK models has been established, these models might be, among other approaches, a powerful tool to support informed decision making for a safe and efficient pharmacotherapy targeting the mother and/or fetus.

DATA AVAILABILITY STATEMENT

The original contributions presented in the study are publicly available. This data can be found here: GitHub (https://github.com/Open-Systems-Pharmacology).

AUTHOR CONTRIBUTIONS

AD designed the research. XL, GB, and AD wrote the manuscript. XL and AD performed the research. XL, DG, JA, NR, HA, JM, KP, GB, and AD analyzed the data. All authors contributed to the article and approved the submitted version.

ACKNOWLEDGMENTS

The authors would like to thank Mark Mirochnick for critically reviewing the manuscript.

REFERENCES

1. Mitchell AA, Gilboa SM, Werler MM, Kelley KE, Louik C, Hernandez-Diaz S, et al. Medication use during pregnancy, with particular focus on prescription drugs: 1976-2008. *Am J Obstet Gynecol.* (2011) 205:51.e1–e8. doi: 10.1016/j.ajog.2011.02.029
2. Lupattelli A, Spigset O, Twigg MJ, Zagorodnikova K, Mardby AC, Moretti ME, et al. Medication use in pregnancy: a cross-sectional, multinational web-based study. *BMJ Open.* (2014) 4:e004365. doi: 10.1136/bmjopen-2013-004365
3. Moon-Grady AJ, Baschat A, Cass D, Choolani M, Copel JA, Crombleholme TM, et al. Fetal treatment 2017: the evolution of fetal therapy centers-a joint opinion from the international fetal medicine and surgical society (ifmss) and the north american fetal therapy network (naftnet). *Fetal Diagn Ther.* (2017) 42:241–8. doi: 10.1159/000475929
4. Sharma D, Tsibizova VI. Current perspective and scope of fetal therapy: part 2. *J Matern Fetal Neonatal Med*. (2020). doi: 10.1080/14767058.2020.1839881. [Epub ahead of print].
5. Endicott S, Haas DM. The current state of therapeutic drug trials in pregnancy. *Clin Pharmacol Ther.* (2012) 92:149–50. doi: 10.1038/clpt.2012.81
6. Cole S, Coppola P, Kerwash E, Nooney J, Lam SP. Pharmacokinetic characterization to enable medicine use in pregnancy, the potential role of physiologically-based pharmacokinetic modeling: a regulatory perspective. *CPT Pharmacometr Syst Pharmacol.* (2020) 9:547–9. doi: 10.1002/psp4.12551
7. Green DJ, Park K, Bhatt-Mehta V, Snyder D, Burckart GJ. Regulatory considerations for the mother, fetus and neonate in fetal pharmacology modeling. *Front Pediatr.* (2021) 9:698611. doi: 10.3389/fped.2021.698611
8. Krishnan K, Loizou GD, Spendiff M, Lipscomb JC, Andersen ME. PBPK modeling: a primer. In: Krishnan K, Andersen ME, editors. *Quantitative Modeling in Toxicology.* Chippenham: John Wiley & Sons Ltd. (2010). p. 21–58.
9. Nestorov I. Whole body pharmacokinetic models. *Clin Pharmacokinet.* (2003) 42:883–908. doi: 10.2165/00003088-200342100-00002
10. Chaphekar N, Caritis S, Venkataramanan R. Model-informed dose optimization in pregnancy. *J Clin Pharmacol.* (2020) 60:S63–S76. doi: 10.1002/jcph.1777
11. Codaccioni M, Bois F, Brochot C. Placental transfer of xenobiotics in pregnancy physiologically-based pharmacokinetic models: structure and data. *Comput Toxicol.* (2019) 12:100111. doi: 10.1016/j.comtox.2019.100111
12. Hill MD, Abramson FP. The significance of plasma protein binding on the fetal/maternal distribution of drugs at steady-state. *Clin Pharmacokinet.* (1988) 14:156–70. doi: 10.2165/00003088-198814030-00004
13. Codaccioni M, Brochot C. Assessing the impacts on fetal dosimetry of the modelling of the placental transfers of xenobiotics in a pregnancy physiologically based pharmacokinetic model. *Toxicol Appl Pharmacol.* (2020) 409:115318. doi: 10.1016/j.taap.2020.115318
14. Lippert J, Burghaus R, Edginton A, Frechen S, Karlsson M, Kovar A, et al. Open systems pharmacology community-an open access, open source, open science approach to modeling and simulation in pharmaceutical sciences. *CPT Pharmacometr Syst Pharmacol.* (2019) 8:878–82. doi: 10.1002/psp4.12473
15. Liu XI, Momper JD, Rakhmanina N, van den Anker JN, Green DJ, Burckart GJ, et al. Physiologically based pharmacokinetic models to predict maternal pharmacokinetics and fetal exposure to emtricitabine and acyclovir. *J Clin Pharmacol.* (2020) 60:240–55. doi: 10.1002/jcph.1515
16. Dallmann A, Ince I, Solodenko J, Meyer M, Willmann S, Eissing T, et al. Physiologically based pharmacokinetic modeling of renally cleared drugs in pregnant women. *Clin Pharmacokinet.* (2017) 56:1525–41. doi: 10.1007/s40262-017-0538-0
17. Dallmann A, Ince I, Coboeken K, Eissing T, Hempel G. A physiologically based pharmacokinetic model for pregnant women to predict the pharmacokinetics of drugs metabolized via several enzymatic pathways. *Clin Pharmacokinet.* (2018) 57:749–68. doi: 10.1007/s40262-017-0594-5
18. Liu XI, Momper JD, Rakhmanina NY, Green DJ, Burckart GJ, Cressey TR, et al. Prediction of maternal and fetal pharmacokinetics of dolutegravir and raltegravir using physiologically based pharmacokinetic modeling. *Clin Pharmacokinet.* (2020) 59:1433–50. doi: 10.1007/s40262-020-00897-9
19. McNamara PJ, Alcorn J. Protein binding predictions in infants. *AAPS PharmSci.* (2002) 4:E4. doi: 10.1208/ps040104
20. Abduljalil K, Jamei M, Johnson TN. Fetal physiologically based pharmacokinetic models: systems information on fetal blood components and binding proteins. *Clin Pharmacokinet.* (2020) 59:629–42. doi: 10.1007/s40262-019-00836-3
21. Schmitt W. General approach for the calculation of tissue to plasma partition coefficients. *Toxicol In Vitro.* (2008) 22:457–67. doi: 10.1016/j.tiv.2007.09.010
22. Valentin J. Basic anatomical and physiological data for use in radiological protection: reference values: ICRP Publication 89: approved by the Commission in September (2001). *Ann ICRP.* (2002) 32:1–277. doi: 10.1016/S0146-6453(03)00002-2
23. Sloop CH, Dory L, Roheim PS. Interstitial fluid lipoproteins. *J Lipid Res.* (1987) 28:225–37. doi: 10.1016/S0022-2275(20)38701-0
24. *Open Systems Pharmacology Manual: Compounds: Definition and Work Flows.* (2021). Available online at: https://docs.open-systems-pharmacology.org/working-with-pk-sim/pk-sim-documentation/pk-sim-compounds-definition-and-work-flow#distribution (accessed September 20, 2021).
25. Rodgers T, Leahy D, Rowland M. Physiologically based pharmacokinetic modeling 1: predicting the tissue distribution of moderate-to-strong bases. *J Pharm Sci.* (2005) 94:1259–76. doi: 10.1002/jps.20322
26. Rodgers T, Rowland M. Physiologically based pharmacokinetic modelling 2: predicting the tissue distribution of acids, very weak bases, neutrals and zwitterions. *J Pharm Sci.* (2006) 95:1238–57. doi: 10.1002/jps.20502
27. Poulin P, Theil FP. A priori prediction of tissue: plasma partition coefficients of drugs to facilitate the use of physiologically-based pharmacokinetic models in drug discovery. *J Pharm Sci.* (2000) 89:16–35. doi: 10.1002/(SICI)1520-6017(200001)89:1<16::AID-JPS3>3.0.CO;2-E
28. Poulin P, Schoenlein K, Theil FP. Prediction of adipose tissue: plasma partition coefficients for structurally unrelated drugs. *J Pharm Sci.* (2001) 90:436–47. doi: 10.1002/1520-6017(200104)90:4<436::AID-JPS1002>3.0.CO;2-P
29. Dallmann A, Ince I, Meyer M, Willmann S, Eissing T, Hempel G. Gestation-specific changes in the anatomy and physiology of healthy pregnant women: an extended repository of model parameters for physiologically based pharmacokinetic modeling in pregnancy. *Clin Pharmacokinet.* (2017) 56:1303–30. doi: 10.1007/s40262-017-0539-z
30. Zhang Z, Unadkat JD. Development of a novel maternal-fetal physiologically based pharmacokinetic model II: verification of the model for passive placental permeability drugs. *Drug Metab Dispos.* (2017) 45:939–46. doi: 10.1124/dmd.116.073957
31. Mendes MDS, Hirt D, Vinot C, Valade E, Lui G, Pressiat C, et al. Prediction of human fetal pharmacokinetics using *ex vivo* human placenta perfusion studies and physiologically based models. *Br J Clin Pharmacol.* (2016) 81:646–57. doi: 10.1111/bcp.12815
32. Shah P, Jogani V, Mishra P, Mishra AK, Bagchi T, Misra A. *In vitro* assessment of acyclovir permeation across cell monolayers in the presence of absorption enhancers. *Drug Dev Ind Pharm.* (2008) 34:279–88. doi: 10.1080/03639040701655952
33. Barrett M, Lawrence M, Hutt A, Lansley A. Stereoselective absorption and hydrolysis of cefuroxime axetil diastereomers using the Caco-2 cell monolayer model. *Eur J Drug Metab Pharmacokinet.* (1997) 22:409–13. doi: 10.1007/BF03190978
34. Haslam IS, O'Reilly DA, Sherlock DJ, Kauser A, Womack C, Coleman T. Pancreatoduodenectomy as a source of human small intestine for Ussing chamber investigations and comparative studies with rat tissue. *Biopharm Drug Dispos.* (2011) 32:210–21. doi: 10.1002/bdd.751
35. Grießinger JA, Hauptstein S, Laffleur F, Netsomboon K, Bernkop-Schnürch A. Evaluation of the impact of multivalent metal ions on the permeation behavior of dolutegravir sodium. *Drug Dev Ind Pharm.* (2016) 42:1118–26. doi: 10.3109/03639045.2015.1115869
36. Hurdle JG, Heathcott AE, Yang L, Yan B, Lee RE. Reutericyclin and related analogues kill stationary phase *Clostridium difficile* at achievable colonic concentrations. *J Antimicrob Chemother.* (2011) 66:1773–6. doi: 10.1093/jac/dkr201
37. Gan L-S, Hsyu P-H, Pritchard JF, Thakker D. Mechanism of intestinal absorption of ranitidine and ondansetron: transport across Caco-2 cell monolayers. *Pharm Res.* (1993) 10:1722–5. doi: 10.1023/A:1018965929419
38. Moss DM, San Kwan W, Liptrott NJ, Smith DL, Siccardi M, Khoo SH, et al. Raltegravir is a substrate for SLC22A6: a putative mechanism for the

interaction between raltegravir and tenofovir. *Antimicrob Agents Chemother.* (2011) 55:879–87. doi: 10.1128/AAC.00623-10
39. Leung DT, Henning PA, Wagner EC, Blasig A, Wald A, Sacks SL, et al. Inadequacy of plasma acyclovir levels at delivery in patients with genital herpes receiving oral acyclovir suppressive therapy in late pregnancy. *J Obstetr Gynaecol Canada.* (2009) 31:1137–43. doi: 10.1016/S1701-2163(16)34374-2
40. Hirt D, Urien S, Rey E, Arrive E, Ekouevi DK, Coffie P, et al. Population pharmacokinetics of emtricitabine in human immunodeficiency virus type 1-infected pregnant women and their neonates. *Antimicrob Agents Chemother.* (2009) 53:1067–73. doi: 10.1128/AAC.00860-08
41. Philipson A, Stiernstedt G. Pharmacokinetics of cefuroxime in pregnancy. *Am J Obstet Gynecol.* (1982) 142:823–8. doi: 10.1016/S0002-9378(16)32526-1
42. De Leeuw JW, Roumen FJ, Bouckaert PX, Cremers HM, Vree TB. Achievement of therapeutic concentrations of cefuroxime in early preterm gestations with premature rupture of the membranes. *Obstet Gynecol.* (1993) 81:255–60.
43. Elkomy MH, Sultan P, Carvalho B, Peltz G, Wu M, Clavijo C, et al. Ondansetron pharmacokinetics in pregnant women and neonates: towards a new treatment for neonatal abstinence syndrome. *Clin Pharmacol Ther.* (2015) 97:167–76. doi: 10.1002/cpt.5
44. Visser A, Hundt H. The pharmacokinetics of a single intravenous dose of metronidazole in pregnant patients. *J Antimicrob Chemother.* (1984) 13:279–83. doi: 10.1093/jac/13.3.279
45. Moore RG, McBride WG. The disposition kinetics of diazepam in pregnant women at parturition. *Eur J Clin Pharmacol.* (1978) 13:275–84. doi: 10.1007/BF00716363
46. Ridd MJ, Brown KF, Nation RL, Collier CB. The disposition and placental transfer of diazepam in cesarean section. *Clin Pharmacol Ther.* (1989) 45:506–12. doi: 10.1038/clpt.1989.65
47. Mandelli M, Morselli P, Nordio S, Pardi G, Principi N, Sereni F, et al. Placental transfer of diazepam and its disposition in the newborn. *Clin Pharmacol Ther.* (1975) 17:564–72. doi: 10.1002/cpt1975175564
48. Mian P, Allegaert K, Conings S, Annaert P, Tibboel D, Pfister M, et al. Integration of placental transfer in a fetal-maternal physiologically based pharmacokinetic model to characterize acetaminophen exposure and metabolic clearance in the fetus. *Clin Pharmacokinet.* (2020) 59:911–25. doi: 10.1007/s40262-020-00861-7
49. Schinkel AH, Wagenaar E, Mol C, van Deemter L. P-glycoprotein in the blood-brain barrier of mice influences the brain penetration and pharmacological activity of many drugs. *J Clin Invest.* (1996) 97:2517–24. doi: 10.1172/JCI118699
50. Dallmann A, Liu XI, Burckart GJ, van den Anker J. Drug transporters expressed in the human placenta and models for studying maternal-fetal drug transfer. *J Clin Pharmacol.* (2019) 59:S70–S81. doi: 10.1002/jcph.1491
51. Reese MJ, Savina PM, Generaux GT, Tracey H, Humphreys JE, Kanaoka E, et al. *In vitro* investigations into the roles of drug transporters and metabolizing enzymes in the disposition and drug interactions of dolutegravir, a HIV integrase inhibitor. *Drug Metab Dispos.* (2013) 41:353–61. doi: 10.1124/dmd.112.048918
52. Hoque MT, Kis O, De Rosa MF, Bendayan R. Raltegravir permeability across blood-tissue barriers and the potential role of drug efflux transporters. *Antimicrob Agents Chemother.* (2015) 59:2572–82. doi: 10.1128/AAC.04594-14
53. Nies AT, Damme K, Schaeffeler E, Schwab M. Multidrug and toxin extrusion proteins as transporters of antimicrobial drugs. *Expert Opin Drug Metab Toxicol.* (2012) 8:1565–77. doi: 10.1517/17425255.2012.722996
54. Anoshchenko O, Storelli F, Unadkat JD. Successful prediction of human fetal exposure to P-gp substrate drugs using the proteomics-informed relative expression factor approach and PBPK modeling and simulation. *Drug Metab Dispos.* (2021). doi: 10.1124/dmd.121.000538. [Epub ahead of print].
55. Hendricks CH, Quilligan EJ. Cardiac output during labor. *Am J Obstet Gynecol.* (1956) 71:953–72. doi: 10.1016/0002-9378(56)90720-7
56. Robson S, Dunlop W, Boys R, Hunter S. Cardiac output during labour. *Br Med J (Clin Res Ed).* (1987) 295:1169–72. doi: 10.1136/bmj.295.6607.1169
57. Rosseland LA, Hauge TH, Grindheim G, Stubhaug A, Langesæter E. Changes in blood pressure and cardiac output during cesarean delivery: the effects of oxytocin and carbetocin compared with placebo. *Anesthesiology.* (2013) 119:541–51. doi: 10.1097/ALN.0b013e31829416dd
58. Dancis J, Lind J, Oratz M, Smolens J, Vara P. Placental transfer of proteins in human gestation. *Am J Obstet Gynecol.* (1961) 82:167–71. doi: 10.1016/S0002-9378(16)36111-7
59. Gitlin D, Kumate J, Urrusti J, Morales C. The selectivity of the human placenta in the transfer of plasma proteins from mother to fetus. *J Clin Invest.* (1964) 43:1938–51. doi: 10.1172/JCI105068
60. van den Akker CH, Schierbeek H, Rietveld T, Vermes A, Duvekot JJ, Steegers EA, et al. Human fetal albumin synthesis rates during different periods of gestation. *Am J Clin Nutr.* (2008) 88:997–1003. doi: 10.1093/ajcn/88.4.997
61. Viani A, Cappiello M, Pacifici GM. Binding of diazepam, salicylic acid and digitoxin to albumin isolated from fetal and adult serum. *Dev Pharmacol Ther.* (1991) 17:100–8. doi: 10.1159/000457505
62. Krauer B, Dayer P, Anner R. Changes in serum albumin and α1-acid glycoprotein concentrations during pregnancy: an analysis of fetal-maternal pairs. *BJOG Int J Obstet Gynaecol.* (1984) 91:875–81. doi: 10.1111/j.1471-0528.1984.tb03700.x
63. Dai D-M, Cao J, Yang H-M, Sun H-M, Su Y, Chen Y-Y, et al. Hematocrit and plasma albumin levels difference may be a potential biomarker to discriminate preeclampsia and eclampsia in patients with hypertensive disorders of pregnancy. *Clin Chim Acta.* (2017) 464:218–22. doi: 10.1016/j.cca.2016.12.001
64. Pasman SA, Meerman RH, Vandenbussche FP, Oepkes D. Hypoalbuminemia: a cause of fetal hydrops? *Am J Obstet Gynecol.* (2006) 194:972–5. doi: 10.1016/j.ajog.2006.02.028
65. Pfrunder A, Gutmann H, Beglinger C, Drewe J. Gene expression of CYP3A4, ABC-transporters (MDR1 and MRP1-MRP5) and hPXR in three different human colon carcinoma cell lines. *J Pharm Pharmacol.* (2003) 55:59–66. doi: 10.1111/j.2042-7158.2003.tb02434.x
66. Nakamura T, Sakaeda T, Ohmoto N, Moriya Y, Komoto C, Shirakawa T, et al. Gene expression profiles of ABC transporters and cytochrome P450 3A in Caco-2 and human colorectal cancer cell lines. *Pharm Res.* (2003) 20:324–7. doi: 10.1023/A:1022251910820
67. Zrieki A, Farinotti R, Buyse M. Cyclooxygenase inhibitors down regulate P-glycoprotein in human colorectal Caco-2 cell line. *Pharm Res.* (2008) 25:1991–2001. doi: 10.1007/s11095-008-9596-1
68. Sun M, Kingdom J, Baczyk D, Lye S, Matthews S, Gibb W. Expression of the multidrug resistance P-glycoprotein, (ABCB1 glycoprotein) in the human placenta decreases with advancing gestation. *Placenta.* (2006) 27:602–9. doi: 10.1016/j.placenta.2005.05.007
69. Wang C, Li H, Luo C, Li Y, Zhang Y, Yun D, et al. The effect of maternal obesity on the expression and functionality of placental P-glycoprotein: implications in the individualized transplacental digoxin treatment for fetal heart failure. *Placenta.* (2015) 36:1138–47. doi: 10.1016/j.placenta.2015.08.007
70. Elmer J, Wilcox SR, Raja AS. Massive transfusion in traumatic shock. *J Emerg Med.* (2013) 44:829–38. doi: 10.1016/j.jemermed.2012.11.025
71. Datta S, Alper MH, Ostheimer GW, Brown WU, Weiss JB. Effects of maternal position on epidural anesthesia for cesarean section, acid-base status, and bupivacaine concentrations at delivery. *J Am Soc Anesthesiol.* (1979) 50:205–9. doi: 10.1097/00000542-197903000-00007
72. Bozynski MEA, Rubarth LB, Patel JA. Lidocaine toxicity after maternal pudendal anesthesia in a term infant with fetal distress. *Am J Perinatol.* (1987) 4:164–6. doi: 10.1055/s-2007-999764
73. Somers G, Harris A, Bayliss M, Houston J. The metabolism of the 5HT3 antagonists ondansetron, alosetron and GR87442 I: a comparison of *in vitro* and *in vivo* metabolism and *in vitro* enzyme kinetics in rat, dog and human hepatocytes, microsomes and recombinant human enzymes. *Xenobiotica.* (2007) 37:832–54. doi: 10.1080/00498250701485575
74. Myllynen P, Immonen E, Kummu M, Vähäkangas K. Developmental expression of drug metabolizing enzymes and transporter proteins in human placenta and fetal tissues. *Expert Opin Drug Metab Toxicol.* (2009) 5:1483–99. doi: 10.1517/17425250903304049
75. Kazma JM, van den Anker JN, Allegaert K, Dallmann A, Ahmadzia HK. Role of placenta in drug metabolism and drug transfer. In: Aranda JV, van den Anker JN, editors. *Yaffe and Aranda's Neonatal and Pediatric Pharmacology:*

Therapeutic Principles in Practice, 5th Edn. Philadelphia, PA: Lippincott Williams & Wilkins (2021). p. 119–34.
76. Zajicek A, Giacoia G. Obstetric clinical pharmacology: coming of age. *Clin Pharmacol Ther.* (2007) 81:481–2. doi: 10.1038/sj.clpt.6100136
77. Lyerly AD, Little MO, Faden R. The second wave: toward responsible inclusion of pregnant women in research. *Int J Fem Approaches Bioeth.* (2008) 1:5–22. doi: 10.3138/ijfab.1.2.5
78. Lyerly AD, Little MO, Faden RR. Reframing the framework: toward fair inclusion of pregnant women as participants in research. *Am J Bioeth.* (2011) 11:50–2. doi: 10.1080/15265161.2011.560353
79. Chervenak FA, McCullough LB. An ethically justified framework for clinical investigation to benefit pregnant and fetal patients. *Am J Bioeth.* (2011) 11:39–49. doi: 10.1080/15265161.2011.562595

Conflict of Interest: AD is an employee of Bayer AG and uses Open Systems Pharmacology software, tools, and models in his professional role.

The remaining authors declare that the research was conducted in the absence of any commercial or financial relationships that could be construed as a potential conflict of interest.

Publisher's Note: All claims expressed in this article are solely those of the authors and do not necessarily represent those of their affiliated organizations, or those of the publisher, the editors and the reviewers. Any product that may be evaluated in this article, or claim that may be made by its manufacturer, is not guaranteed or endorsed by the publisher.

frontiers in Pediatrics

REVIEW
published: 03 November 2021
doi: 10.3389/fped.2021.733823

Maternal-Fetal Pharmacology of Drugs: A Review of Current Status of the Application of Physiologically Based Pharmacokinetic Models

Nupur Chaphekar[1], *Prerna Dodeja*[1], *Imam H. Shaik*[1], *Steve Caritis*[2] *and Raman Venkataramanan*[1,2,3]*

[1] Department of Pharmaceutical Sciences, School of Pharmacy, University of Pittsburgh, Pittsburgh, PA, United States, [2] Department of Obstetrics, Gynecology and Reproductive Sciences, Magee Women's Hospital of UPMC, School of Medicine, University of Pittsburgh, Pittsburgh, PA, United States, [3] Department of Pathology, School of Medicine, University of Pittsburgh, Pittsburgh, PA, United States

Pregnancy and the postpartum period are associated with several physiological changes that can alter the pharmacokinetics (PK) and pharmacodynamics (PD) of drugs. For certain drugs, dosing changes may be required during pregnancy and postpartum to achieve drug exposures comparable to what is observed in non-pregnant subjects. There is very limited data on fetal exposure of drugs during pregnancy, and neonatal exposure through transfer of drugs via human milk during breastfeeding. Very few systematic clinical pharmacology studies have been conducted in pregnant and postpartum women due to ethical issues, concern for the fetus safety as well as potential legal ramifications. Over the past several years, there has been an increase in the application of modeling and simulation approaches such as population PK (PopPK) and physiologically based PK (PBPK) modeling to provide guidance on drug dosing in those special patient populations. Population PK models rely on measured PK data, whereas physiologically based PK models incorporate physiological, preclinical, and clinical data into the model to predict drug exposure during pregnancy. These modeling strategies offer a promising approach to identify the drugs with PK changes during pregnancy to guide dose optimization in pregnancy, when there is lack of clinical data. PBPK modeling is also utilized to predict the fetal exposure of drugs and drug transfer via human milk following maternal exposure. This review focuses on the current status of the application of PBPK modeling to predict maternal and fetal exposure of drugs and thereby guide drug therapy during pregnancy.

Keywords: maternal, fetal, pharmacology, pregnancy, PBPK

OPEN ACCESS

Edited by:
André Dallmann, Bayer, Germany

Reviewed by:
Marc Codaccioni, Agence Nationale de Sécurité du Médicament et des Produits de Santé (ANSM), France
Blessy George, United States Food and Drug Administration, United States

***Correspondence:**
Raman Venkataramanan
rv@pitt.edu

Specialty section:
This article was submitted to Obstetric and Pediatric Pharmacology, a section of the journal Frontiers in Pediatrics

Received: *30 June 2021*
Accepted: *16 September 2021*
Published: *03 November 2021*

Citation:
Chaphekar N, Dodeja P, Shaik IH, Caritis S and Venkataramanan R (2021) Maternal-Fetal Pharmacology of Drugs: A Review of Current Status of the Application of Physiologically Based Pharmacokinetic Models. Front. Pediatr. 9:733823. doi: 10.3389/fped.2021.733823

Pregnant women take one to three medications on an average in addition to the routine iron and vitamin supplements recommended during pregnancy (1). Pregnant women take medications for acute illnesses such as nausea and vomiting, upper respiratory tract and urinary tract infections or for chronic conditions such as psychiatric disorders, HIV infection, epilepsy, organ transplantation, rheumatological conditions, or substance abuse disorder. Pharmacotherapy is also needed for pregnancy-induced conditions like hypertensive disorder, preterm labor and gestational diabetes (2). Pregnant women and their fetuses are orphan populations with regards to information on the

safety and efficacy of drugs. Ninety eight percent of the drugs approved in the United States between 2000 and 2010 have insufficient data on drug dosing during pregnancy, while seventy percent of them have no data on drug use in pregnancy (3). Pregnant women are excluded from clinical studies due to ethical, fetal safety and medico-legal concerns. Therefore, there is limited data available on PK and PD of drugs used in pregnancy. **Table 1** lists the issues and potential confounding factors contributing to the lack of PK and PD data in pregnancy. Current dosing recommendations in pregnancy are based on data obtained from non-pregnant population. In this context, modeling and simulation techniques like PopPK or PBPK can provide additional information regarding appropriate drug dosing in this special population. A summary of ideal studies that could be conducted during pregnancy and the next best alternative or alternate approaches that can be used when a clinical study is not practical to obtain necessary data, is presented in **Table 2**.

PHYSIOLOGICAL CHANGES DURING PREGNANCY

Several physiological changes occur during pregnancy that help support the growth and development of the fetus. The absorption, distribution, metabolism and excretion processes of drugs can be altered during pregnancy and may contribute to altered PK of drugs. **Table 3** summarizes pregnancy mediated physiological changes that can impact PK processes. Reduced gastrointestinal motility and delayed gastric emptying time during pregnancy can reduce drug absorption. There is an increase in gastric pH during pregnancy which can lead to changes in absorption of acidic drugs due to increased ionization (10, 11). A systematic study evaluating the impact of changes in drug absorption on pharmacokinetics after intravenous vs. oral administration during pregnancy and postpartum is lacking. Several physiological changes may alter drug distribution such as increased plasma volume, maternal plasma protein dilution or organ volume variation (fat) (12–14). The expression and activity of certain CYP enzymes change during pregnancy which may lead to change in metabolism of selected substrates. The metabolism of drugs catalyzed by cytochrome P450 (CYP) isoenzymes CYP3A4, CYP2D6, CYP2C9 and certain uridine glucuronosyltransferases (UGT) isoenzymes UGT1A4 and UGT1A9 is increased during pregnancy (15) and the metabolism of CYP1A2 and CYP2C19 substrates is decreased during pregnancy (15, 16).

Accumulating *in-vivo* and *in-vitro* data suggests that the increased levels of steroid hormones during pregnancy might be responsible for altered metabolism of certain substrates (17). For example, UGT1A1 up-regulation was seen in progesterone treated HEPG2 cells co-transfected with PXR as compared to control cells. An increase in the glucuronidation (UGT1A4) was observed in 17-beta estradiol treated HEPG2 cells co-transfected with ERα receptor (18). Progesterone treatment caused up-regulation of UGT1A in pregnant humanized UGT1A/ PXR mice as opposed to pregnant humanized UGT1A mice with PXR knockout suggesting the role of PXR activation leading to the up-regulation of UGT1A enzymes (19). The renal excretion of drugs is increased during pregnancy due to a 60–80% increase in renal blood flow and a 50% increase in glomerular filtration rate (20). To date there is limited data available elucidating the effect of pregnancy on intestinal, hepatic and renal transporters involved in the absorption, distribution, efflux, secretion and reabsorption of drugs.

TABLE 1 | Need for designed pharmacological studies performed during pregnancy, lactation and postpartum.

Scope of the problem	Contributors to the problem
• Inadequate pharmacological studies performed during pregnancy, lactation and postpartum • Limited data on pregnancy mediated changes in drug exposure and response • Optimal dosing for pregnant, lactating, postpartum women unclear for most medications • Impact of drug exposure on fetal growth and development is unclear for almost all medications used during pregnancy • Limited data on drug transfer through breast feeding • Limited incentive for industries (safety—liability issues)	• Pregnancy is an exclusion in most clinical trials • Inadequate funding for clinical pharmacology research in pregnant, lactating and postpartum women • Inadequate number of investigators qualified to perform or engaged in such studies • Inconvenient study designs for participants • Need for innovative sampling techniques and modeling approaches

PBPK MODELING TO PREDICT DRUG EXPOSURE DURING PREGNANCY

Model-based approaches can provide some information regarding drug exposure and drug dosing in various patient populations when direct clinical data is not available. PBPK is a tool that can be used to predict drug exposure in such patient populations. This model-predicted data can be used to optimize drug dosing in special patient populations and can be further fine-tuned as more clinical data becomes available.

PBPK is a mechanistic approach that has been used in the drug development processes to determine safe and optimal doses to be used in clinical trials, estimate drug exposure in special populations and also to predict drug-drug interactions (21). It can be used as a viable alternative to generate clinical data in special patient populations. Regulatory agencies such as the US FDA and the European Medicines Agency have accepted the use of PBPK modeling to facilitate the decision-making process for conducting a clinical study in submissions for Investigational New Drug and New Drug Applications (22–24). PBPK models are multicompartmental models in which each compartment corresponds to one or more organ and is interconnected by the circulatory system. It integrates important physiological parameters (e.g., blood flow, enzyme

TABLE 2 | Ideal studies in pregnancy and alternative approaches.

Ideal studies	Next best alternatives	Alternate approaches
• Drug exposure studies (Pharmacokinetics over a dosing interval) in first, second, third trimester and post-partum • Drug response studies over a dosing interval (first, second, third trimester and post-partum) • Maternal drug safety assessments (first, second, third trimester and post-partum) • Fetal / Neonatal drug safety assessments (monitoring of neonates and newborn) • Drug excretion in breast milk (total amount excreted in breast milk over a dosing interval)	• Surrogate drug exposure studies (limited sampling strategy or trough level) in first, second, third trimesters and post-partum • Limited drug response studies (first, second, third trimester and post-partum) • Placental (*in vitro*) perfusion studies • Cord blood sampling for fetal exposure assessments • Milk to plasma ratio for drugs in lactating women • Placental perfusion studies • Placenta on a chip study	• Predictions based on probe drug studies for DME and transporters • Population PK modeling • PBPK modeling and simulations

TABLE 3 | Physiological changes and potential impact on PK of drugs.

Pharmacokinetic parameter	Effect of pregnancy	Potential impact on pharmacokinetics	Clinical example
Absorption	Decrease in gastrointestinal motility and gastric emptying time Increase in gastric pH Increase in gastrointestinal blood flow Alterations in enzymes and transporters involved in absorption of drugs	Increase or decrease in the rate of absorption Increase or decrease in bioavailability	Aspirin C_{max} decreased by 29% during pregnancy (4) Lower C_{max} of metoprolol during pregnancy (5)
Distribution	Increase in cardiac output Increase in total body water and fat Decrease in plasma protein binding	Increase in volume of distribution	Increase in volume of distribution of metoprolol during pregnancy (5)
Metabolism	Alterations of CYP and UGT enzyme activity Increase in hepatic blood flow	Increase or decrease in metabolism of substrates	Decrease in clearance of caffeine (CYP1A2 substrate) during pregnancy (6) Increase in Clearance of lamotrigine (UGT1A4 substrate) during pregnancy as compared to postpartum (7)
Excretion	Increase in renal blood flow Increase in glomerular filtration rate Alterations of enzymes and transporters involved in tubular reabsorption and secretion	Increase in renal excretion Increase or decrease in tubular reabsorption and secretion	Unbound renal secretion of digoxin increased during pregnancy due to increased P-gP activity (8) Increased renal secretion and renal clearance of amoxicillin during pregnancy as compared to postpartum (9)

and transporter abundance, cardiac output, glomerular filtration rate) and drug related parameters (blood-to-plasma ratio, plasma protein binding, permeability, solubility, *in vitro* metabolism or transport) which are known to influence drug PK and PD (25). **Figure 1A** represents an example of a minimal PBPK model (26) and **Figure 1B** represents an example of a PBPK model with each tissue/organ in the body being considered as a separate compartment (27). Pregnancy creates the need for additional compartments in the PBPK model. **Figure 2** depicts the structure of pregnancy-PBPK (p-PBPK) model used in three different PBPK modeling software. The most important compartment in a p-PBPK model is the fetal unit. This is combined into a single "lumped" compartment known as the fetoplacental unit in the Simcyp and GastroPlus software. The fetoplacental unit incorporates the fetus, placenta, amniotic fluid, membranes and umbilical cord as depicted in **Figures 2A,B**. However, in the Open Systems Pharmacology software package, each of these units are considered discrete and accounted for separately, along with the inclusion of myometrium and endometrium, as seen in **Figure 2C**. **Table 4** summarizes the physiological parameters that are considered in the Simcyp p-PBPK model.

CURRENT STATUS OF PREGNANCY PBPK MODELS

Physiological changes during pregnancy are gestational age dependent. For example, the activity of UGT1A4 increased by 200% during the first and second trimesters and by 300% during the third trimester leading to increased clearance of lamotrigine (7). Similarly, the changes in organ blood flow, activity of certain metabolic enzymes and transporters are dependent on gestational age. The p-PBPK models incorporate these gestational age-related physiological changes into a normal PBPK model to simulate pregnant population. These p-PBPK models can then be used to predict the gestational age dependent pharmacokinetics of different drugs.

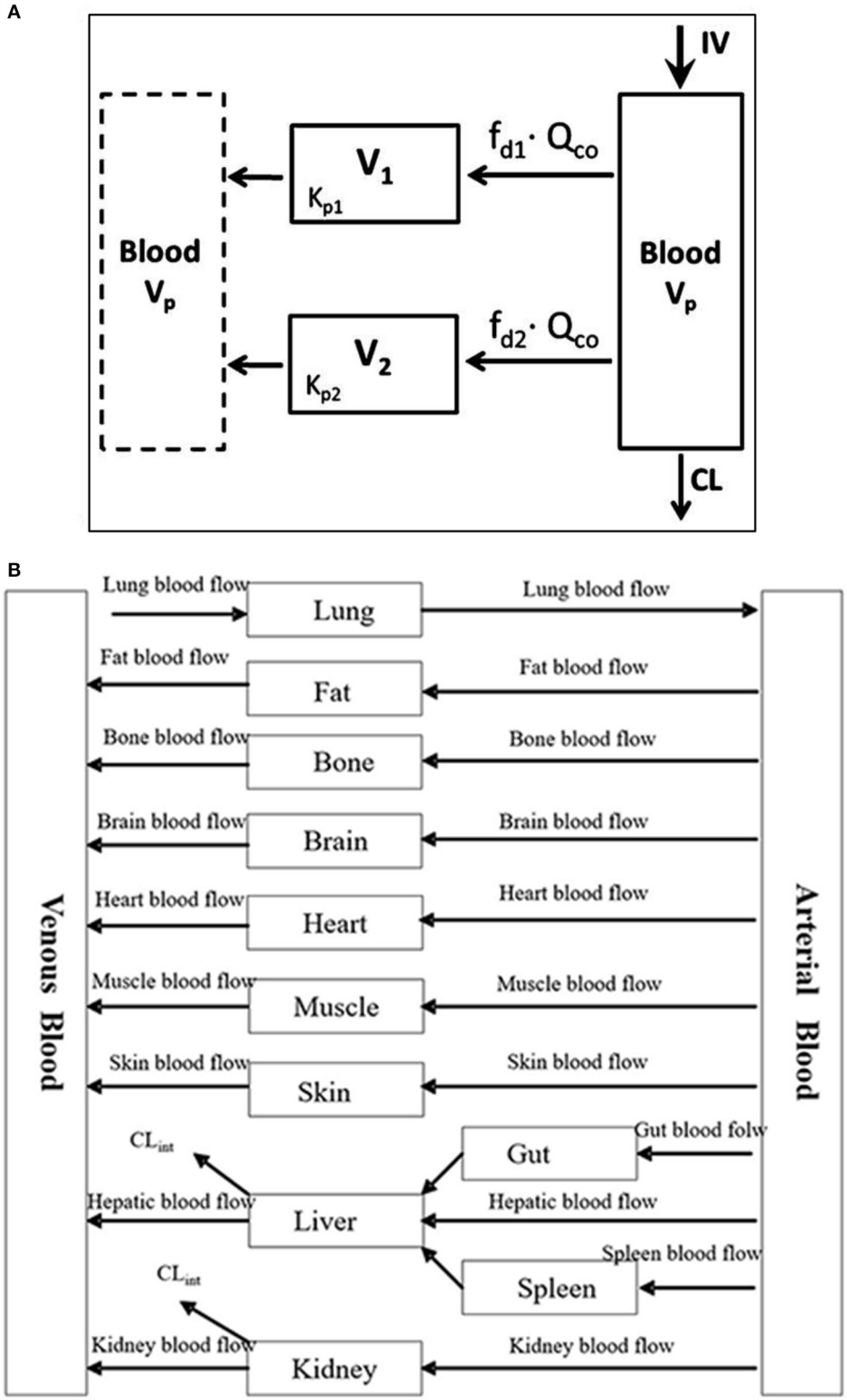

FIGURE 1 | (A) Minimal PBPK model with two tissue compartments (26). **(B)** Example of a PBPK model (27).

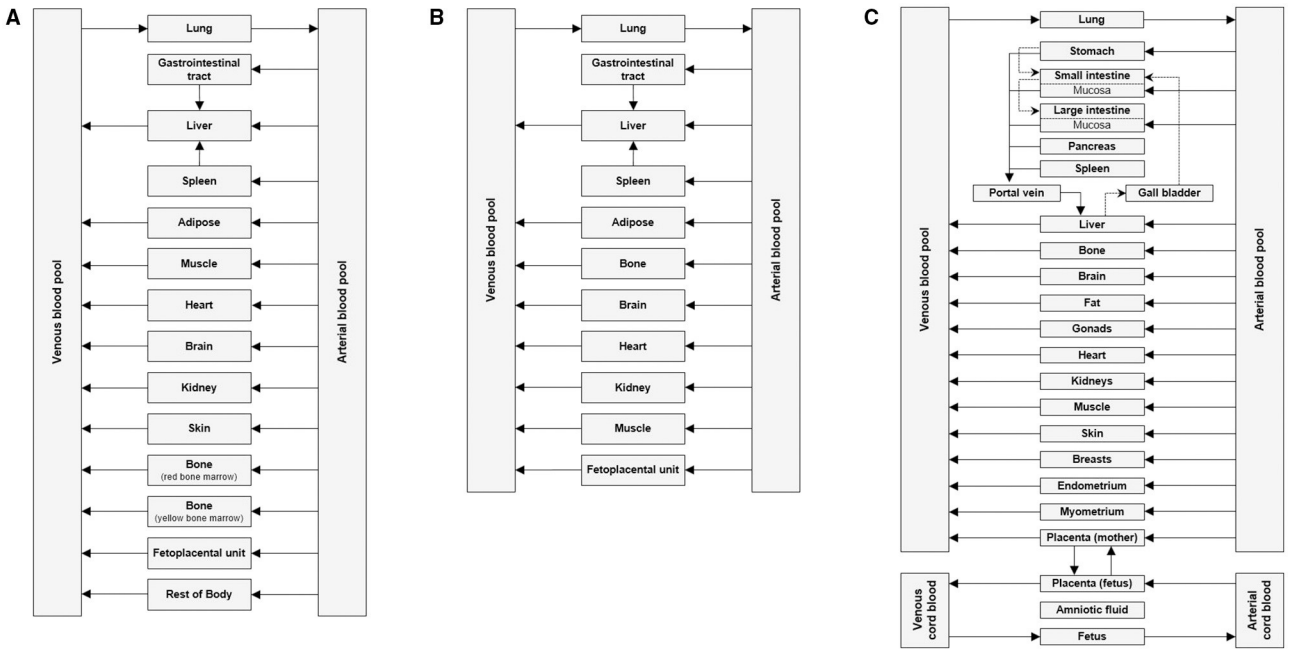

FIGURE 2 | Basic structure of p-PBPK model in **(A)** Gatsroplus **(B)** SimCyp and **(C)** Open Systems Pharmacology (28).

TABLE 4 | Physiological parameters that are modified for pregnancy prediction in Simcyp p-PBPK model.

List of parameters
Cardiac output
Total body weight
Total fat
Plasma volume
Red blood cell volume
Hematocrit
Serum albumin
Skin blood flow rate
Adipose blood flow rate
Renal blood flow rate
Fetoplacental unit blood flow rate
Enzyme and transporter activity

Several p-PBPK models have been developed and evaluated for antiretroviral, anti-malarial, psychoactive drugs, drugs used for the treatment of substance use disorder and environmental chemicals. Although these models have been able to predict the pharmacokinetics of certain drugs during pregnancy reasonably well, there are still several challenges that remain unresolved. There is no/limited information available to fully evaluate all the assumptions that are used in such models. There is paucity of data on combined effect of pregnancy and disease state (e.g., diabetes, malaria, hypertensive disorder) on gestational age-related changes in various physiological parameters and hence the predictions must be interpreted with caution. Data for drug elimination kinetics are typically scaled from *in-vitro* cell culture experiments and these experiments do not account for all the physiological changes which necessitates additional extrapolation factors to be incorporated. There is lack of information regarding changes in all drug metabolizing enzyme and transporter activity across gestational ages. Enzyme or transporter activity determined using probe drug data is specific to the trimester in which the study was conducted and cannot be extrapolated to other trimesters.

An exhaustive literature search was conducted using PubMed with the keywords *PBPK and pregnancy*. The results from the search with clinical observations are listed in **Table 5** with specific examples discussed below.

REVIEW OF PREGNANCY PBPK MODELS REPORTED IN THE LITERATURE

PBPK modeling has been used as a tool to guide and optimize drug dosing in pregnancy for several drugs and scenarios discussed below.

Drug Based Studies

Ziprasidone is an antipsychotic drug used to treat schizophrenia and other psychiatric disorders. It is administered orally and is metabolized by CYP3A4 primarily in the liver. Biesdorf et al. established a PBPK model to predict drug exposure during pregnancy using the Simcyp inbuilt pregnancy population which includes gestational age-related changes in blood flow, glomerular filtration rate, plasma protein binding etc. Since the model used the pregnancy population in Simcyp, some physiological changes that were not very specific to the route of elimination of Ziprasidone were also incorporated. The model

TABLE 5 | Review of published p-PBPK models.

Compound	Route of administration	Clinical observations	Recommended dose adjustment based on PBPK modeling	Software	Reference
Acetaminophen	IV and oral dosing	Lower acetaminophen concentrations during pregnancy as compared to non-pregnant women	No dose adjustments since there is lack of data on toxicity of the metabolite NAPQI	Open Systems Pharmacology®	(29)
Amoxicillin	IV bolus and infusion	Increased renal clearance during pregnancy and postpartum	May need increased dosing No clinical recommendations	Open Systems Pharmacology®	(30)
Betamethasone	IV, IM and oral dosing	Increased clearance during pregnancy	No clinical recommendations	Simcyp®	(31)
Buprenorphine	Sublingual	Decreased buprenorphine exposure during pregnancy as compared to postpartum	Increased dose/ more frequent dosing	Simcyp	(32)
Caffeine	Oral dosing	Increased maternal and fetal exposure during pregnancy due to reduced CYP1A2 activity	Limit caffeine intake	GastroPlus®	(33)
Caffeine, Midazolam, Nifedipine, Metoprolol Ondansetron, Granisetron, Diazepam and Metronidazole	IV and oral dosing	Increase in clearance of CYP2A6, CYP2E1, CYP2D6 and CYP3A4 substrates and decreased clearance of CYP1A2 and CYP2C19 substrates	Likely changes in dosing No clinical recommendations	Open Systems Pharmacology®	(34)
Caffeine, Metoprolol, Midazolam	IV Bolus, Oral dosing	100% increase, 30% decrease and a 35% decrease in the exposure of caffeine, metoprolol, and midazolam respectively during pregnancy	Decreased dose for caffeine and increased dose for metoprolol and midazolam	Simcyp®	(35)
Cefazolin, Cefuroxime, Cefradine	IV and oral dosing	Increased clearance of the three drugs during pregnancy	Increased dose during pregnancy	Open Systems Pharmacology®	(36)
Ceftazidime, Cefuroxime, Fluconazole, Aztreonam, Imipenem, Ceftriaxone	IV and Oral dosing	Decrease of *in vivo* drug exposure (for all 6 drugs) in pregnant women due to increased renal clearance	No dose changes	Simcyp®	(37)
Cefuroxime, Cefazoline	IV infusion, IV bolus or infusion	Model accurately predicts changes in renal clearance for both drugs, however inclusion of postpartum data is necessary for fine tuning	No clinical recommendations	GastroPlus®	(38)
Darunavir boosted with ritonavir	Oral dosing	Decreased Darunavir exposure during second and third trimester of pregnancy	Increased dose or dosing frequency during pregnancy	Simcyp®	(39)
Dolutegravir	Oral dosing	Dose of 50 mg q.d Dolutegravir provides sufficient fetal exposure, resulting in 90% viral inhibition	No dose changes	Berkeley Madonna	(40)
Dolutegravir, Raltegravir	Oral dosing	Decreased exposure during pregnancy	No dose changes	Open Systems Pharmacology®	(41)
Emtricitabine and Acyclovir	Oral dosing	Lower emtricitabine and acyclovir concentrations during pregnancy with the lowest concentrations during the third trimester	No dose changes	Open Systems Pharmacology®	(42)
Emtricitabine, Dolutegravir, Raltegravir	Oral dosing	Neonatal washout kinetics observed for all three drugs	No clinical recommendations	Open Systems Pharmacology®	(43)
Indomethacin	Oral dosing	Higher indomethacin clearance during second trimester as compared to non-pregnant women.	Higher dosing requirement during pregnancy	Gastroplus®	(44)

(Continued)

TABLE 5 | Continued

Compound	Route of administration	Clinical observations	Recommended dose adjustment based on PBPK modeling	Software	Reference
Indomethacin	Oral dosing	Decrease in indomethacin exposure by 14, 24, and 32% in the first, second and third trimester respectively, compared to non-pregnant women.	Additional clinical studies warranted to provide optimal dosing recommendations	Simcyp®	(45)
Metformin, digoxin, emtricitabine, midazolam	Oral dosing	Decreased exposure during pregnancy due to increased clearance	No clinical recommendations	GastroPlus®	(46)
Metformin, Tacrolimus, Oseltamivir	Oral dosing	Increased renal clearance of metformin during pregnancy as compared to postpartum. 20 % decrease in AUC of tacrolimus between 1st and 3rd trimester. AUC of parent drug (oseltamivir) similar but AUC of metabolite (oseltamivir carboxylate) 30% lower during pregnancy.	No clinical recommendations	Simcyp®	(47)
Methadone, Glyburide, Phenytoin	Oral dosing	Increased clearance of methadone and glyburide during pregnancy as compared to postpartum	No clinical recommendations	Simcyp®	(48)
Midazolam, Nifedipine, Indinavir	Oral dosing	Increased clearance during pregnancy	No clinical recommendations	MATLAB	(49)
Midazolam, Theophylline, Zidovudine, Nevirapine, Emtricitabine, Lamivudine, Ondansetron, Diazepam, Metronidazole, Cefuroxime	IV and oral dosing	Increase in fetal exposure with pregnancy age for all drugs	No clinical recommendations	GNU MCSim	(50)
Piperaquine	Oral dosing	Pharmacokinetics unchanged as compared to non-pregnant women	No need for dosage adjustment	Simcyp®	(51)
Quetiapine	Oral dosing	Decreased concentrations during pregnancy	Dose increase during pregnancy	Simcyp®	(52)
Quetiapine, Aripiprazole	Oral and IV dosing	Progressively decreased plasma concentrations throughout pregnancy	Dose for both drugs needs to be increased in the second and third trimesters.	Open Systems Pharmacology®	(53)
Tenofovir, emtricitabine, lamivudine	IV and Oral dosing	Increase in renal clearance of drugs during pregnancy	No need for dosage adjustment	Simcyp®	(54)
Theophylline, Paroxetine, Clonidine, Dextromethorphan	Oral dosing	Increased concentration of theophylline during third trimester. 100–200% induction of CYP2D6 during third trimester adequately describes the pharmacokinetics of paroxetine, clonidine and dextromethorphan during pregnancy.	No clinical recommendations	Simcyp®	(55)
Ziprasidone	Oral dosing	No significant difference in exposure as compared to non-pregnant women	No dose adjustment necessary	Simcyp®	(56)

predicted exposures correlated well with the clinical data and exposure of ziprasidone during pregnancy at 6, 20, and 34 weeks of gestation. Since the exposure of ziprasidone during pregnancy was comparable to non-pregnant women, no dose adjustment is recommended during pregnancy for this drug (56). Ke et al. developed a PBPK model to evaluate maternal exposure of

the antenatal corticosteroids dexamethasone and betamethasone which are primarily metabolized by CYP3A4. In this model, the fraction of dexamethasone metabolized by CYP3A4 was obtained from a clinical DDI study with itraconazole. However, for betamethasone, an *in-vitro* study was conducted to investigate the role of CYP3A4 in its metabolism. Ideally a clinical DDI study should be conducted to verify the fraction of betamethasone metabolized by CYP3A4 (31).

Quetiapine, an antipsychotic drug metabolized mainly by CYP3A4 and CYP2D6, shows decreased exposure during pregnancy possibly due to known increase in the activity of these two enzymes. A PBPK modeling approach was used to optimize the dosing regimen to target a predetermined therapeutic range (52). Though the model recommended a dose increase during pregnancy, information about the pregnancy mediated changes on PD is also needed to implement the recommended change in the dose during pregnancy.

Probe Drug-Based Studies

PBPK models developed previously have been also modified/refined to determine the exposure of substrates during pregnancy. Ke et al. refined a previously published PBPK model to include CYP3A4 activity changes during the third trimester based on data from the probe drug midazolam and used it to predict the exposures of nifedipine and indinavir in pregnancy. The site of CYP3A4 induction during the third trimester was proposed to be mainly the liver (49). However, subsequent models were not able to reproduce these findings. The model by De Sousa Mendes *et al* showed that a 90–100% CYP3A4 induction is required to capture the PK changes in third trimester for drugs metabolized by CYP3A4 (57). Whereas the model by Dallmann et al. using Open Systems Pharmacology suggested that a 60% induction in liver and intestine CYP3A4 is enough to describe the observed PK changes (58). There is still ongoing discussion regarding the magnitude and site of CYP3A4 induction in pregnancy and there are several shortcomings with using probe drug data for CYP3A4 assessments of CYP3A activity for other drugs. The models developed cannot be applied to predict the pharmacokinetics of other drugs and also for evaluating the pharmacokinetics across different trimesters.

Renally Cleared Drugs

Liu et al. developed a p-PBPK model for emtricitabine and acyclovir which are antiviral drugs primarily excreted unchanged in the urine by glomerular filtration and tubular secretion (42). The model had several limitations such as not accounting for potential changes in gastrointestinal absorption due to pregnancy. Additionally, since intravenous data for acyclovir in women was not available, observed drug concentrations were extrapolated based on PK data from men. A previously developed PopPK model for ganciclovir, a drug in the same class as acyclovir, has shown higher ganciclovir clearance in women than men after correcting for individual body surface area and glomerular filtration (59). Therefore, it is likely that there may be a significant underestimation of acyclovir as well in the model developed by Liu et al.

Pregnancy and Genotype Impact

A limited number of PBPK models in the literature have evaluated the impact of genotype on pharmacokinetics of drugs during pregnancy. Efavirenz which is used for the treatment of human immunodeficiency virus (HIV) is metabolized by the highly polymorphic enzyme CYP2B6. Though both 400 mg and 600 mg doses show similar efficacy, a 400 mg dose is suggested to avoid dose related toxicities. However, there is limited data on the PK of 400 mg dose in pregnancy. p-PBPK model developed by Chetty et al. using Simcyp evaluated the pharmacokinetics after a reduced dose of 400 mg in CYP2B6 extensive metabolizers. The model predicted that approximately 57% of extensive metabolizers would show trough concentrations below the therapeutic target during third trimester, suggesting dose reduction during pregnancy may lead to therapeutic failure in extensive metabolizers (60). The utility of this model to predict drug exposure in rapid and ultra-rapid metabolizers during pregnancy remains unknown. Additionally, evidence suggests that race and ethnicity have an impact on CYP2B6 activity. The model by Chetty et al. has been developed and evaluated only for the Caucasian population and therefore the generalizability of the model to other populations is questionable. Models incorporating other inbuilt populations such as in Simcyp (e.g., Japanese, Chinese etc.) can be used to optimize drug dosing in the non-Caucasian populations (61).

Pregnancy and Drug Response

p-PBPK models have also been extended to determine the PD effect of drugs used in pregnancy. Darakjian et al. developed a PBPK-PD model for caffeine in pregnancy. The PD model evaluated the effect of caffeine on phosphodiesterase enzyme (PE), cyclic adenosine monophosphate (cAMP) and epinephrine levels, which are factors associated with increased miscarriage risk. Increased caffeine plasma levels due to reduction in CYP1A2 activity during pregnancy led to greater inhibition of the PE enzyme, higher cAMP and greater increase of epinephrine levels which could increase the risk of pregnancy loss. Despite not being validated, the model was able to predict the increased concentration of caffeine in the fetoplacental compartment indicating its potential utility (33). Alqahtani et al. developed a PBPK-PD model to estimate concentrations of indomethacin in the second trimester of pregnancy and to support dose adjustment based on PD rationale in the pregnant population. Although the PBPK-PD model suggested a higher indomethacin dosing requirement during pregnancy, it cannot be directly used in clinical practice without further *in-vivo* validation (44).

Pregnancy and Drug Interactions

PBPK models can be potentially used to predict drug-drug interactions in pregnancy when it is difficult to conduct clinical studies in vulnerable populations. Piperaquine is an antimalarial drug used during pregnancy. Approximately 1 million pregnancies in sub-Saharan Africa are complicated with co-infection of human immunodeficiency virus (HIV) and malaria, however there is paucity of data on anti-HIV medication mediated exposure changes of piperaquine during pregnancy

(62). Olafuyi et al. developed a PBPK model to predict the drug-drug interaction potential between piperaquine and anti-HIV drugs (ritonavir and efavirenz) for Thai, Papua New Guinean, and Sudanese populations. The model showed no change in piperaquine PK due to co-administration of anti-HIV drugs and indicated no need for a change in the dose (51).

CURRENT STATUS OF p-PBPK MODELS USED TO DETERMINE FETAL EXPOSURE

The p-PBPK model becomes more complex upon addition of the fetoplacental unit since the model requires inclusion of placental transfer parameters, fetus and placental enzyme and transporter kinetics and blood flow to various additional anatomical units to predict exposure in fetus.

The *in-vitro* placental perfusion model is one of the tools used to study transplacental transfer of drugs (63). It can also be used to investigate the effect of exogenous and endogenous chemicals on maternal and fetal perfusion and transfer. It offers several advantages as the placental barrier is maintained and separate perfusion of the maternal and fetal side can be achieved. However, information about transplacental drug transfer and expression of enzymes and transporters during different stages of pregnancy cannot be obtained as the tissue for perfusion studies is normally available only at the time of delivery. The placenta is in a metabolically static state during these experiments as compared to the metabolically changing state during different stages of pregnancy (63, 64). Transplacental transfer parameters like diffusion, clearance index, elimination constant and placenta partition coefficient can be obtained from these experiments and incorporated in a PBPK model to predict fetal exposure later in pregnancy. The placental perfusion has been instrumental in developing PBPK models and has been used for predicting fetal exposure of dolutegravir, tenofovir, emtricitabine, and nevirapine (40, 57, 65).

Another approach is to incorporate data from *in-vitro* experiments using placental tissue, microsomes or human placental cell lines. Mian et al. developed a PBPK model to predict fetal exposure of acetaminophen. Different methods to estimate the placental transfer (ex *vivo* cotyledon perfusion experiments or scaling based on Caco-2 cell permeability experiments, physicochemical properties in MoBi) were incorporated in the model and the predictions show a comparable fetal exposure. Maturation of enzymes in the fetal liver was accounted for to determine the molar dose fraction of acetaminophen converted to N-acetyl-p-benzoquinone imine. The model incorporating the ex-*vivo* perfusion model data showed the best correlation with observed cord blood data for acetaminophen but may not hold true for all compounds (29). There is limited information available on placental enzymes and transporters in particular at various stages of pregnancy and further studies in this area would be helpful in developing IVIVE for placental clearance across various trimesters. Data obtained from primary placental cells, human choriocarcinoma cells or placenta-on-a-chip model may be more physiologically relevant to obtain transplacental parameters (66, 67). Protein abundance information for placental transporters which is available from recent reports can be incorporated into maternal-fetal PBPK models to further improve the model predictions (68).

Animal models offer another promising approach but differences in hemodynamics and placental structure can pose challenges in extrapolation of animal data to humans. The gestational age and the associated changes in physiology differ substantially between animals and humans requiring correction factors while extrapolating these data to humans. A PBPK model to predict fetal exposure of a brominated flame retardant, BDE-47 was developed by parameterizing the model with concentrations of BDE-47 from the literature and previous pharmacokinetic and toxicokinetic studies. This model was able to predict the fetal concentrations of BDE-47 in rats after maternal exposure within one standard deviation of the experimental data indicating its potential to be extrapolated to other species including humans after careful consideration of anatomical and physiological differences in placental structure and function (69).

Abduljalil et al. reviewed the literature for studies evaluating changes in fetal parameters (e. g., body weight, body surface area, body water, abdominal circumference, body fat) during fetal growth. This data was used to create mathematical algorithms to describe changes in these fetal parameters with gestational age which can potentially be added to the fetal PBPK model (70).

Transplacental transfer parameters from *in silico* models, *in vitro* and *ex vivo* studies have been incorporated into p-PBPK models. Codaccioni et al. developed p-PBPK model for ten compounds using four different models of placental exchange based on *in vitro*, *ex vivo*, and *in silico* information. The non-pregnant and pregnant as well as fetal PK simulations were compared with observed profiles at delivery for each of the ten compounds. A comparison of the model predictions across different trimesters of pregnancy yielded inconclusive results. These models can be optimized and potentially be used based on the purpose of the study and type of data and resources available (50). In the absence of clinical data to evaluate the fetal PBPK models, umbilical cord concentrations observed at delivery were used. Zhang et al. developed a maternal-fetal PBPK model which incorporated gestational age-related changes in fetal physiologic parameters such as fetal serum albumin, liver volume, uterus blood flow etc. Sensitivity analysis identified that a single time-point umbilical venous/ maternal plasma ratio is not reflective of the fetal exposure (71). The various gaps in knowledge for modeling maternal-fetal pharmacology are summarized in **Table 6**.

An exhaustive literature search was conducted using PubMed with the keywords *PBPK and fetal exposure*. The publications from the search describing the development and validation of p-PBPK models to determine fetal exposure are presented in **Table 7**.

EXAMPLES OF p-PBPK MODELS TO PREDICT FETAL EXPOSURE OF DRUGS

Fetal drug exposure is normally important from a fetal safety perspective. From efficacy point of view while normally one is

interested in maternal drug exposure, there are conditions where fetal exposure is also important to maximize efficacy. Darunavir, an anti-HIV drug, primarily metabolized by CYP3A4 is routinely administered with CYP3A4 inhibitor ritonavir to maintain higher plasma concentrations during pregnancy. p-PBPK model was developed by incorporating information from *ex vivo* human placental perfusion studies to simulate fetal exposure after different dosing regimens (72). The model was validated by comparing maternal, fetal and amniotic fluid concentrations. The fetal concentration was compared with the single time-point umbilical cord concentration obtained at delivery. The model was able to capture the observed clinical data thus indicating that the placental perfusion data can be successfully integrated into p-PBPK models to predict fetal blood concentration at term. This approach is especially beneficial in the case of anti-HIV drugs to ensure that the half-maximal effective concentration is achieved in the fetus and the mother.

Zhang et al. developed a model to predict the placental transfer of passively diffusing drugs. The transplacental transfer parameters for zidovudine and theophylline were obtained using midazolam as the calibrator. The model was validated using single time-point maternal plasma and umbilical cord concentrations and the model was able to successfully predict the concentrations observed in patients. However, this model can only be used for drugs that undergo passive diffusion across the placenta. The use of a more sensitive calibrator that can predict placental transfer of a wide range of drugs with different physiochemical properties can enhance the utility of this model to predict fetal exposure of other drugs (82).

PBPK modeling has also been used to predict the fetal exposure to environmental chemicals (83). Bisphenol A (BPA) is an environmental chemical ingested through dietary and non-dietary sources. It is rapidly converted to nontoxic conjugates BPA-glucuronide (BPAG) and BPA-sulfate (BPAS) *via* glucuronidation and sulfation pathways. Sharma et al. developed a PBPK model for predicting the fetal exposure of bisphenol A which was evaluated against the observed BPA concentrations in cord blood, fetus liver and amniotic fluid following exposure from maternal blood (76). Parametrization of glucuronidation in fetus was done by scaling of *in-vitro* adult hepatocyte data in the absence of data from fetal hepatocytes which could have been a valuable addition to the model. Additionally, incorporating information on conjugation and deconjugation of BPA in placenta and fetus could lead to better prediction of the fetal exposure using this model.

Physiologically based toxicokinetic (PBTK) models are mathematical models that integrate absorption, distribution, metabolism and excretion processes for chemicals in biological

TABLE 6 | Current gaps in modeling maternal-fetal pharmacology.

Maternal pharmacology	Fetal pharmacology
1. Lack of data on time course of changes in expression and activities of various phase 1 and 2 enzymes during pregnancy and postpartum 2. Lack of data on Time course of changes in various transporters during pregnancy and postpartum 3. Lack of data from same person during and post-delivery 4. Lack of PD measures—Relationship between exposure and response 5. Lack of information on potential impact of other comorbid conditions on PK/PD 6. Lack of PBPK models of biologics	1. Actual fetal exposure / blood and tissue concentration prediction not available—need for validation with meaningful clinical data 2. Lack of data on exposure response relationship in fetus 3. Placental enzymes and transporter expression data to incorporate transplacental transfer in PBPK model 4. Maternal-placental-fetal drug partitioning—factors impacting this such as plasma protein binding in mother, fetus, and role of placental transporters

TABLE 7 | List of published p-PBPK models to predict fetal exposure.

Compound	Species in which model was developed and validated	Software	References
Darunavir	Humans	Simcyp®	(72)
Dolutegravir	Humans	Berkeley Madonna	(40)
Dolutegravir	Humans-neonates	SimBiology®	(73)
Zidovudine, Theophylline	Humans	Simcyp®/ Matlab	(74)
Acetaminophen	Humans	Open Systems Pharmacology®	(75)
Nevirapine	Humans	R	(57)
Tenofovir, emtricitabine	Humans	Simcyp®, R	(65)
BDE-47 (polybrominated diphenyl ether)	Male, female (pregnant and non-pregnant rats)	ACSL® (Advanced Continuous Simulation Language)	(69)
Bisphenol A	Humans	R	(76)
Perfluorooctanoic acid (PFOA) and Perfluorooctane sulfate (PFOS)	Humans	ACSL® (Advanced Continuous Simulation Language)	(77)
Manganese	Humans	ACSL® (Advanced Continuous Simulation Language)	(78)
Thalidomide, Efavirenz	Humans	Simbiology®	(79)
Napthalene	Humans	CFD-PBPK	(80)
2,3,7,8-Tetrachlorodibenzo-p-dioxin (TCDD)	Pregnant female rats	ACSL® (Advanced Continuous Simulation Language)	(81)

systems. These models can serve as a tool to inform health risk assessments. They are traditionally based on extrapolating simulations in animal model to predict human exposure. For instance, Gingrich et al. developed a pregnancy specific p-PBTK model to predict bisphenol A and bisphenol S exposures in fetus (84). The model was calibrated using pregnant sheep data and results were extrapolated to assess the risk in humans However, this latter step remains uncertain due to major differences in placental physiology and structure between the species. More recently, high throughput toxicokinetic (HTTK) modeling has been used as an alternative in which models are parametrized with *in vitro* data, structure-derived physicochemical properties (e.g., QSAR) or species specific physiological data for several chemicals (85).

PBPK Modeling to Predict Drug Exposure in Neonates

Bunglawala et al. built a neonatal PBPK model for dolutegravir using pediatric clinical data with assumptions that solubility, body composition and transporter expression were similar to adults (73). However, development and age-related changes are known but were not accounted in the model. Further, the possibility of drug exposure through maternal breast milk or placenta was not considered, though it is known that dolutegravir readily crosses the placenta.

In contrast to the approach described above, Liu et al. developed a PBPK model to link prenatal and postnatal pharmacokinetics using previously published p-PBPK models for emtricitabine, dolutegravir and raltegravir (43). The total drug amounts in fetal compartments at term delivery were predicted and incorporated as initial conditions in the neonatal PBPK model to predict drug concentrations in neonatal elimination phase after birth. Emtricitabine is eliminated unchanged in the urine by glomerular filtration and active tubular secretion mediated by Organic Cation Transporter 2 (OCT2). The OCT2 ontogeny applied in this model is based on data obtained from one term newborn only (86). Hence, additional *in-vitro* and clinical data are needed to further incorporate the ontogeny of OCT2 in the neonatal PBPK models. Additionally, the model should be tested and verified with information from other compounds as well as coupled maternal-fetal-neonatal PBPK models to understand early neonatal pharmacokinetics.

PBPK Modeling to Predict Transfer of Drugs Through Human Milk and Infant Exposure

Maternal milk is a rich source of nourishment and breast-feeding is encouraged by the U.S. Department of Health and Human Services due to the beneficial effects for the mother as well as the infant. Maternal factors such as age, parity, breastfeeding patterns, milk composition and volume and physicochemical properties of the drug such as protein binding, molecular weight and lipophilicity affect the amount of drug transferred into human milk. Clinical studies focusing on quantifying the human milk exposure of drugs are needed. In the absence of clinical data, PBPK models have attempted to quantify infant exposure through human milk by integrating a breast tissue compartment. Loccisano et al. successfully developed a PBPK model to determine exposure of PFOA and PFOS in fetus and in infant through milk by extrapolating a previously developed and evaluated model in rats (77). As additional information on drug elimination kinetics in fetus and infant becomes available, it could be incorporated in to the model for better prediction of drug exposure in neonates (87).

Two differing approaches implemented in the prediction of infant exposure using PBPK are based on the method of drug uptake into human milk from plasma. One approach considers diffusion from drug in plasma via the breast tissue as done in PBPK modeling for lactational transfer of methylmercury (88). The other approach considers the direct passage of drug into the breast milk without considering the breast tissue as in the PBPK model to determine the infant exposure of organic pollutants (89).

Merrill et al. developed a PBPK model to predict perchlorate and iodide kinetics and subsequent perchlorate induced inhibition of iodide uptake in lactating mothers. The model was parameterized using data from previous models in male rat, lactating rat and non-pregnant women. However, this model has not been evaluated for perchlorate kinetics in humans due to lack of available clinical data (90). Isoniazid exposure to infant through breast milk was predicted using a validated PBPK model which accounted for the polymorphic expression of isoniazid metabolizing enzyme, N-acetyltransferase 2 (fast and slow metabolizers). Drug exposure was highest in slow metabolizing infants of slow metabolizing mothers, but the observed levels were still less than the infant exposure limit which is 10% of the maternal dose. The model was developed using information from ICRP reports which are generated based on data mainly from Caucasian population and should be cautiously extrapolated to other populations (82).

CONCLUSIONS

There has been tremendous progress over the past few years in the use of PBPK modeling to predict maternal and fetal exposure of drugs. By integrating physiological data, preclinical data, and clinical data, PBPK can be used to predict maternal and fetal exposure and guide optimization of maternal dosing during pregnancy when pharmacokinetic studies cannot be readily performed. Even though validation of these models is challenging due to limited clinical data, *in-vitro* and *ex-vivo* experimental data can be utilized to help predict fetal exposure of drugs. PBPK modeling can also serve as a tool to guide drug dosing during breastfeeding based on drug transfer through human milk. In summary, PBPK modeling offers promise as a potential tool to predict maternal and fetal exposure of drugs and thereby guide therapy in this special population.

AUTHOR CONTRIBUTIONS

NC: conception or design of the work, acquisition, analysis or interpretation of data for the work, drafting the work, provide approval for publication of the content, and agree to be accountable for all aspects of the work. PD and IS: revising it critically for important intellectual content, provide approval for publication of the content, and agree to be accountable for all aspects of the work. SC and RV: conception or design of the work, revising it critically for important intellectual content, provide approval for publication of the content, and agree to be accountable for all aspects of the work. All authors contributed to the article and approved the submitted version.

FUNDING

This work is partially funded by grants from the Eunice Kennedy Shriver National Institute of Child Health and Human Development (NICHD, HD047905) through the Obstetric Pharmacology Research Center (OPRC).

REFERENCES

1. Mitchell AA, Gilboa SM, Werler MM, Kelley KE, Louik C, Hernandez-Diaz SS. National Birth Defects Prevention, Medication use during pregnancy, with particular focus on prescription drugs: 1976-2008. *Am J Obstet Gynecol.* (2011) 205:51 e1–8. doi: 10.1016/j.ajog.2011.02.029
2. Judith CF, Rubin D, Loffredo C. The Baltimore-Washington Infant Study Group, Use of prescription and non-prescription drugs in pregnancy. *J Clin Epidemiol.* (1993) 46:581–9. doi: 10.1016/0895-4356(93)90132-K
3. Adam MP, Polifka JE, Friedman JM. Evolving knowledge of the teratogenicity of medications in human pregnancy. *Am J Med Genet C Semin Med Genet.* (2011) 157C:175–82. doi: 10.1002/ajmg.c.30313
4. Shanmugalingam R, Wang X, Munch G, Fulcher I, Lee G, Chau K, et al. A pharmacokinetic assessment of optimal dosing, preparation, and chronotherapy of aspirin in pregnancy. *Am J Obstet Gynecol.* (2019) 221:255 e1–255 e9. doi: 10.1016/j.ajog.2019.04.027
5. Hogstedt S, Bo Lindberg MD, Peng DR, Regardh CG, Rane A. Pregnancy induced increase in metoprolol metabolism. *Clin Pharmacol Ther.* (1985) 37:688–92. doi: 10.1038/clpt.1985.114
6. H.R.a.Knutti CSR, Effect of the pregnancy on pharmacokinetics of caffeine, European Journal of Clinical Pharmacology (1981) 121-126. doi: 10.1007/BF00637512
7. N.D. Pennell PB, Stowe ZN, Helmers SL, Montgomery JQ, Henry TR. Impact of pregnancy and childbirth on metabolism of lamotrigine. *Neurology.* (2004) 62:292. doi: 10.1212/01.WNL.0000103286.47129.F8
8. Hebert MF, Easterling TR, Kirby B, Carr DB, Buchanan ML, Rutherford T, Thummel KE, Fishbein DP, Unadkat JD, Effects of pregnancy on CYP3A and P-glycoprotein activities as measured by disposition of midazolam and digoxin: a University of Washington specialized center of research study. *Clin Pharmacol Ther.* (2008) 84:248–53. doi: 10.1038/clpt.2008.1
9. Andrew MA, Easterling TR, Carr DB, Shen D, Buchanan ML, Rutherford T, Bennett R, Vicini P, Hebert MF, Amoxicillin pharmacokinetics in pregnant women: modeling and simulations of dosage strategies. *Clin Pharmacol Ther.* (2007) 81:547–56. doi: 10.1038/sj.clpt.6100126
10. Waldum HL, Serum group 1 pepsinogens during pregnancy. *Scand J Gastroent.* (1980) 15:61–3. doi: 10.3109/00365528009181433
11. Vasicka LT, Bright ARH. Peptic ulcer and pregnancy, review of hormonal relationships and a report of one case of massive gastrointestinal hemorrhage. *Obstet Gynecol Surv.* (1957) 12:1–13. doi: 10.1097/00006254-195702000-00001
12. Dawes M, Chowienczyk PJ. Drugs in pregnancy. Pharmacokinetics in pregnancy. *Best Pract Res Clin Obstet Gynaecol.* (2001) 15:819–26. doi: 10.1053/beog.2001.0231
13. Cheung LT, CK, Swaminathan R, Urinary excretion of some enzymes and proteins during pregnancy. *Clin Chem.* (1989) 35:1978–80. doi: 10.1093/clinchem/35.9.1978
14. Erman A, Neri A, Sharoni R, Rabinov M, Kaplan B, Rosenfeld JB, et al. Enhanced urinary albumin excretion after 35 weeks of gestation and during labour in normal pregnancy. *Scand J Clin Lab Invest.* (1992) 52:409–13. doi: 10.3109/00365519209088376
15. Isoherranen N, Thummel KE. Drug metabolism and transport during pregnancy: how does drug disposition change during pregnancy and what are the mechanisms that cause such changes? *Drug Metab Dispos.* (2013) 41:256–62. doi: 10.1124/dmd.112.050245
16. Tracy TS, Venkataramanan R, Glover DD, Caritis SNH. National Institute for Child, U Human Development Network of Maternal-Fetal-Medicine, Temporal changes in drug metabolism (CYP1A2, CYP2D6 and CYP3A Activity) during pregnancy. *Am J Obstet Gynecol.* (2005) 192:633–9. doi: 10.1016/j.ajog.2004.08.030
17. Jeong H. Altered drug metabolism during pregnancy: hormonal regulation of drug-metabolizing enzymes. *Expert Opin Drug Metab Toxicol.* (2010) 6:689–99. doi: 10.1517/17425251003677755
18. Chen H, Yang K, Choi S, Fischer JH, Jeong H. Up-regulation of UDP-glucuronosyltransferase (UGT) 1A4 by 17beta-estradiol: a potential mechanism of increased lamotrigine elimination in pregnancy. *Drug Metab Dispos.* (2009) 37:1841–7. doi: 10.1124/dmd.109.026609
19. Chen S, Yueh MF, Evans RM, Tukey RH. Pregnane-x-receptor controls hepatic glucuronidation during pregnancy and neonatal development in humanized UGT1 mice. *Hepatology.* (2012) 56:658–67. doi: 10.1002/hep.25671
20. Davison JM, Dunlop W. Renal hemodynamics and tubular function normal human pregnancy. *Kidney Int.* (1980) 18:152–61. doi: 10.1038/ki.1980.124
21. Khalil F, Laer S. Physiologically based pharmacokinetic modeling: methodology, applications, and limitations with a focus on its role in pediatric drug development. *J Biomed Biotechnol.* (2011) 2011:907461. doi: 10.1155/2011/907461
22. Luzon E, Blake K, Cole S, Nordmark A, Versantvoort C, Berglund EG. Physiologically based pharmacokinetic modeling in regulatory decision-making at the European Medicines Agency. *Clin Pharmacol Ther.* (2017) 102:98–105. doi: 10.1002/cpt.539
23. Wagner C, Pan Y, Hsu V, Sinha V, Zhao P. Predicting the effect of CYP3A inducers on the pharmacokinetics of substrate drugs using physiologically based pharmacokinetic (PBPK) modeling: an analysis of PBPK submissions to the US FDA. *Clin Pharmacokinet.* (2016) 55:475–83. doi: 10.1007/s40262-015-0330-y
24. Wagner C, Pan Y, Hsu V, Grillo JA, Zhang L, Reynolds KS, Sinha V, Zhao P. Predicting the effect of cytochrome P450 inhibitors on substrate drugs: analysis of physiologically based pharmacokinetic modeling submissions to the US Food and Drug Administration. *Clin Pharmacokinet.* (2015) 54:117–27. doi: 10.1007/s40262-014-0188-4
25. Jones H, Rowland-Yeo K, Basic concepts in physiologically based pharmacokinetic modeling in drug discovery and development. *CPT Pharmacometrics Syst Pharmacol.* (2013) 2:e63. doi: 10.1038/psp.2013.41
26. Cao Y, Jusko WJ. Applications of minimal physiologically-based pharmacokinetic models. *J Pharmacokinet Pharmacodyn.* (2012) 39:711–23. doi: 10.1007/s10928-012-9280-2
27. Zhuang X, Lu C. PBPK modeling and simulation in drug research and development. *Acta Pharm Sin B.* (2016) 6:430–40. doi: 10.1016/j.apsb.2016.04.004
28. Dallmann A, Pfister M, van den Anker J, Eissing T. *Physiologically based pharmacokinetic modeling in pregnancy: a systematic review of published models. Clin Pharmacol Ther.* (2018) 104:1110–24. doi: 10.1002/cpt.1084
29. Mian P, van den Anker JN, van Calsteren K, Annaert P, Tibboel D, Pfister M, et al. Physiologically based pharmacokinetic modeling to characterize acetaminophen pharmacokinetics and N-Acetyl-p-Benzoquinone Imine (NAPQI) formation in non-pregnant and pregnant women. *Clin Pharmacokinet.* (2020) 59:97–110. doi: 10.1007/s40262-019-00799-5

30. Dallmann A, Himstedt A, Solodenko J, Ince I, Hempel G, Eissing T. Integration of physiological changes during the postpartum period into a PBPK framework and prediction of amoxicillin disposition before and shortly after delivery. *J Pharmacokinet Pharmacodyn.* (2020) 47:341–59. doi: 10.1007/s10928-020-09706-z
31. Ke AB, Milad MA, Evaluation of maternal drug exposure following the administration of antenatal corticosteroids during late pregnancy using physiologically-based pharmacokinetic modeling. *Clin Pharmacol Ther.* (2019) 106:164–73. doi: 10.1002/cpt.1438
32. Zhang H, Kalluri HV, Bastian JR, Chen H, Alshabi A, Caritis SN, et al. Gestational changes in buprenorphine exposure: A physiologically-based pharmacokinetic analysis, *Br J Clin Pharmacol.* (2018) 84:2075–87. doi: 10.1111/bcp.13642
33. Darakjian LI, Kaddoumi A. Physiologically based pharmacokinetic/pharmacodynamic model for caffeine disposition in pregnancy. *Mol Pharm.* (2019) 16:1340–9. doi: 10.1021/acs.molpharmaceut.8b01276
34. Dallmann A, Ince I, Coboeken K, Eissing T, Hempel G. A physiologically based pharmacokinetic model for pregnant women to predict the pharmacokinetics of drugs metabolized via several enzymatic pathways. *Clin Pharmacokinet.* (2018) 57:749–68. doi: 10.1007/s40262-017-0594-5
35. Gaohua L, Abduljalil K, Jamei M, Johnson TN, Rostami-Hodjegan A. A pregnancy physiologically based pharmacokinetic (p-PBPK) model for disposition of drugs metabolized by CYP1A2, CYP2D6 and CYP3A4. *Br J Clin Pharmacol.* (2012) 74:873–85. doi: 10.1111/j.1365-2125.2012.04363.x
36. Dallmann A, Ince I, Solodenko J, Meyer M, Willmann S, Eissing T, et al. Physiologically based pharmacokinetic modeling of renally cleared drugs in pregnant women. *Clin Pharmacokinet.* (2017) 56:1525–41. doi: 10.1007/s40262-017-0538-0
37. Song L, Yu Z, Xu Y, Li X, Liu X, Liu D, et al. Preliminary physiologically based pharmacokinetic modeling of renally cleared drugs in Chinese pregnant women. *Biopharm Drug Dispos.* (2020) 41:248–67. doi: 10.1002/bdd.2243
38. Szeto KX, Le Merdy M, Dupont B, Bolger MB, Lukacova V, PBPK Modeling approach to predict the behavior of drugs cleared by kidney in pregnant subjects and fetus. *The AAPS J.* (2021) 23:89. doi: 10.1208/s12248-021-00603-y
39. Colbers A, Greupink R, Litjens C, Burger D, Russel FG. Physiologically based modelling of darunavir/ritonavir pharmacokinetics during pregnancy. *Clin Pharmacokinet.* (2016) 55:381–96. doi: 10.1007/s40262-015-0325-8
40. Freriksen JJM, Schalkwijk S, Colbers AP, Abduljalil K, Russel FGM, Burger DM, et al. Assessment of maternal and fetal dolutegravir exposure by integrating ex *vivo* placental perfusion data and physiologically-based pharmacokinetic modeling. *Clin Pharmacol Ther.* (2020) 107:1352–61. doi: 10.1002/cpt.1748
41. Liu XI, Momper JD, Rakhmanina NY, Green DJ, Burckart GJ, Cressey TR, et al. *Prediction of maternal and fetal pharmacokinetics of dolutegravir and raltegravir using physiologically based pharmacokinetic modeling, Clin Pharmacokinet.* (2020) 59:1433–50. doi: 10.1007/s40262-020-00897-9
42. Liu XI, Momper JD, Rakhmanina N, van den Anker JN, Green DJ, Burckart GJ. Physiologically based pharmacokinetic models to predict maternal pharmacokinetics and fetal exposure to emtricitabine and acyclovir. *J Clin Pharmacol.* (2020) 60:240–55. doi: 10.1002/jcph.1515
43. Liu XI, Momper JD, Rakhmanina NY, Green DJ, Burckart GJ, Cressey TR, et al. *Physiologically based pharmacokinetic modeling framework to predict neonatal pharmacokinetics of transplacentally acquired emtricitabine, dolutegravir, and raltegravir. Clin Pharmacokinet.* (2021) 60:795–809. doi: 10.1007/s40262-020-00977-w
44. Subbian S, Alqahtani S, Kaddoumi A. Development of physiologically based pharmacokinetic/pharmacodynamic model for indomethacin disposition in pregnancy. *Plos ONE.* (2015) 10:e0139762. doi: 10.1371/journal.pone.0139762
45. Pillai VC, Shah M, Rytting E, Nanovskaya TN, Wang X, Clark SM, et al. Prediction of maternal and fetal pharmacokinetics of indomethacin in pregnancy. *Br J Clin Pharmacol.* (2021). doi: 10.1111/bcp.14960
46. Xia B, Heimbach T, Gollen R, Nanavati C, He H, A simplified PBPK modeling approach for prediction of pharmacokinetics of four primarily renally excreted and CYP3A metabolized compounds during pregnancy. *AAPS J.* (2013) 15:1012–24. doi: 10.1208/s12248-013-9505-3
47. Jogiraju VK, Avvari S, Gollen R, Taft DR. Application of physiologically based pharmacokinetic modeling to predict drug disposition in pregnant populations. *Biopharm Drug Dispos.* (2017) 38:426–38. doi: 10.1002/bdd.2081
48. Ke AB. Expansion of a PBPK model to predict disposition in pregnant women of drugs cleared via multiple enzymes including CYP2B6, CYP2C9 and CYP2C19. *British Journal of Clinical Pharmacology.* (2013) 77:554–70. doi: 10.1111/bcp.12207
49. Ke AB, Nallani SC, Zhao P, Rostami-Hodjegan A, Unadkat JD. A PBPK model to predict disposition of CYP3A-metabolized drugs in pregnant women: verification and discerning the site of CYP3A induction. *CPT Pharmacometrics Syst Pharmacol.* (2012) 1:e3. doi: 10.1038/psp.2012.2
50. Codaccioni M, Brochot C. Assessing the impacts on fetal dosimetry of the modelling of the placental transfers of xenobiotics in a pregnancy physiologically based pharmacokinetic model. *Toxicol Appl Pharmacol.* (2020) 409:115318. doi: 10.1016/j.taap.2020.115318
51. Olafuyi O, Coleman M, Badhan RKS, The application of physiologically based pharmacokinetic modelling to assess the impact of antiretroviral-mediated drug-drug interactions on piperaquine antimalarial therapy during pregnancy. *Biopharm Drug Dispos.* (2017) 38:464–78. doi: 10.1002/bdd.2087
52. Badhan RKS, Macfarlane H. Quetiapine dose optimisation during gestation: a pharmacokinetic modelling study. *J Pharm Pharmacol.* (2020) 72:670–81. doi: 10.1111/jphp.13236
53. Zheng L, Tang S, Tang R, Xu M, Jiang X, Wang L. Dose adjustment of quetiapine and aripiprazole for pregnant women using physiologically based pharmacokinetic modeling and simulation. *Clin Pharmacokinet.* (2021) 60:623–35. doi: 10.1007/s40262-020-00962-3
54. De Sousa Mendes M, Hirt D, Urien S, Valade E, Bouazza N, Foissac F, et al. Physiologically-based pharmacokinetic modeling of renally excreted antiretroviral drugs in pregnant women. *Br J Clin Pharmacol.* (2015) 80:1031–41. doi: 10.1111/bcp.12685
55. Ke AB, Nallani SC, Zhao P, Rostami-Hodjegan A, Isoherranen N, Unadkat JD. A physiologically based pharmacokinetic model to predict disposition of CYP2D6 and CYP1A2 metabolized drugs in pregnant women. *Drug Metab Dispos.* (2013) 41:801–13. doi: 10.1124/dmd.112.050161
56. Biesdorf C, Martins FS, Sy SKB, Diniz A. Physiologically-based pharmacokinetics of ziprasidone in pregnant women. *Br J Clin Pharmacol.* (2019) 85:914–23. doi: 10.1111/bcp.13872
57. De Sousa Mendes M, Lui G, Zheng Y, Pressiat C, Hirt D, Valade E, et al. A physiologically-based pharmacokinetic model to predict human fetal exposure for a drug metabolized by several CYP450 pathways. *Clin Pharmacokinet.* (2017) 56:537–50. doi: 10.1007/s40262-016-0457-5
58. Dallmann A, Solodenko J, Ince I, Eissing T. Applied concepts in PBPK. Modeling: how to extend an open systems pharmacology model to the special population of pregnant women. *CPT Pharmacometrics Syst Pharmacol.* (2018) 7:419–31. doi: 10.1002/psp4.12300
59. Perrottet N, Csajka C, Pascual M, Manuel O, Lamoth F, Meylan P, et al. Population pharmacokinetics of ganciclovir in solid-organ transplant recipients receiving oral valganciclovir. *Antimicrob Agents Chemother.* (2009) 53:3017–23. doi: 10.1128/AAC.00836-08
60. Chetty M, Danckwerts MP, Julsing A, Prediction of the exposure to a 400-mg daily dose of efavirenz in pregnancy: is this dose adequate in extensive metabolisers of CYP2B6? *Eur J Clin Pharmacol.* (2020) 76:1143–1150. doi: 10.1007/s00228-020-02890-4
61. Ilic K, Hawke RL, Thirumaran RK, Schuetz EG, Hull JH, Kashuba AD, et al. The influence of sex, ethnicity, and CYP2B6 genotype on bupropion metabolism as an index of hepatic CYP2B6 activity in humans. *Drug Metab Dispos.* (2013) 41:575–81. doi: 10.1124/dmd.112.048108
62. Uneke CJ, Ogbonna A, Malaria and HIV co-infection in pregnancy in sub-Saharan Africa: impact of treatment using antimalarial and antiretroviral agents. *Trans R Soc Trop Med Hyg.* (2009) 103:761–7. doi: 10.1016/j.trstmh.2008.06.017
63. M.K.a.Golan A. *In-vitro* models using human placenta to study fetal exposure of drugs. *Clinical Medicine: Reproductive Health.* (2008) 15-24. doi: 10.4137/CMRH.S974
64. Conings S, Amant F, Annaert P, Van Calsteren K. Integration and validation of the ex *vivo* human placenta perfusion model. *J Pharmacol Toxicol Methods.* (2017) 88:25–31. doi: 10.1016/j.vascn.2017.05.002

65. De Sousa Mendes M, Hirt D, Vinot C, Valade E, Lui G, Pressiat C, et al. Prediction of human fetal pharmacokinetics using ex *vivo* human placenta perfusion studies and physiologically based models. *Br J Clin Pharmacol.* (2016) 81:646–57. doi: 10.1111/bcp.12815
66. Evseenko DA, Paxton JW, Keelan JA. ABC drug transporter expression and functional activity in trophoblast-like cell lines and differentiating primary trophoblast. *Am J Physiol Regul Integr Comp Physiol.* (2006) 290:R1357–65. doi: 10.1152/ajpregu.00630.2005
67. Pemathilaka RL, Reynolds DE, Hashemi NN. Drug transport across the human placenta: review of placenta-on-a-chip and previous approaches. *Interface Focus.* (2019) 9:20190031. doi: 10.1098/rsfs.2019.0031
68. Anoshchenko O, Prasad B, Neradugomma NK, Wang J, Mao Q, Unadkat JD. Gestational age-dependent abundance of human placental transporters as determined by quantitative targeted proteomics. *Drug Metab Dispos.* (2020) 48:735–41. doi: 10.1124/dmd.120.000067
69. Emond C, Raymer JH, Studabaker WB, Garner CE, Birnbaum LS. A physiologically based pharmacokinetic model for developmental exposure to BDE-47 in rats. *Toxicol Appl Pharmacol.* (2010) 242:290–8. doi: 10.1016/j.taap.2009.10.019
70. Abduljalil K, Johnson TN, Rostami-Hodjegan A, Fetal physiologically-based pharmacokinetic models: systems information on fetal biometry and gross composition. *Clin Pharmacokinet.* (2018) 57:1149–71. doi: 10.1007/s40262-017-0618-1
71. Zhang Z, Imperial MZ, Patilea-Vrana GI, Wedagedera J, Gaohua L, Unadkat JD, Development of a Novel Maternal-Fetal Physiologically Based Pharmacokinetic Model I: Insights into Factors that Determine Fetal Drug Exposure through Simulations and Sensitivity Analyses. *Drug Metab Dispos.* (2017) 45:920–38. doi: 10.1124/dmd.117.075192
72. Schalkwijk S, Buaben AO, Freriksen JJM, Colbers AP, Burger DM, Greupink R. Russel FGM, prediction of fetal darunavir exposure by integrating human ex-*vivo* placental transfer and physiologically based pharmacokinetic modeling. *Clin Pharmacokinet.* (2018) 57:705–16. doi: 10.1007/s40262-017-0583-8
73. Bunglawala F, Rajoli RKR, Mirochnick M, Owen A, Siccardi M. Prediction of dolutegravir pharmacokinetics and dose optimization in neonates via physiologically based pharmacokinetic (PBPK) modelling. *J Antimicrob Chemother.* (2020) 75:640–7. doi: 10.1093/jac/dkz506
74. Zhang Z, Unadkat JD. Development of a novel maternal-fetal physiologically based pharmacokinetic model II: Verification of the model for passive placental permeability drugs. *Drug Metab Dispos.* (2017) 45:939–46. doi: 10.1124/dmd.116.073957
75. Mian P, Allegaert K, Conings S, Annaert P, Tibboel D, Pfister M, van Calsteren K, et al. Integration of placental transfer in a fetal-maternal physiologically based pharmacokinetic model to characterize acetaminophen exposure and metabolic clearance in the fetus. *Clin Pharmacokinet.* (2020) 59:911–25. doi: 10.1007/s40262-020-00861-7
76. Sharma RP, Schuhmacher M, Kumar V. The development of a pregnancy PBPK Model for Bisphenol A and its evaluation with the available biomonitoring data. *Sci Total Environ.* (2018) 624:55–68. doi: 10.1016/j.scitotenv.2017.12.023
77. Loccisano AE, Longnecker MP, Campbell JL, Jr., Andersen ME, Clewell HJ, 3rd. Development of PBPK models for PFOA and PFOS for human pregnancy and lactation life stages. *J Toxicol Environ Health A.* (2013) 76:25–57. doi: 10.1080/15287394.2012.722523
78. Yoon M, Schroeter JD, Nong A, Taylor MD, Dorman DC, Andersen ME, et al. Physiologically based pharmacokinetic modeling of fetal and neonatal manganese exposure in humans: describing manganese homeostasis during development. *Toxicol Sci.* (2011) 122:297–316. doi: 10.1093/toxsci/kfr141
79. Atoyebi SA, Rajoli RKR, Adejuyigbe E, Owen A, Bolaji O, Siccardi M, et al. Using mechanistic physiologically-based pharmacokinetic models to assess prenatal drug exposure: Thalidomide versus efavirenz as case studies. *Eur J Pharm Sci.* (2019) 140:105068. doi: 10.1016/j.ejps.2019.105068
80. Dustin Kapraun F, Schlosser PM, Nylander-French LA, Kim D, Yost EE, Druwe IL. A PBPK model for napthalene with inhalation and skin routes of exposure. *Toxicological Sciences.* (2020) 177:377–91. doi: 10.1093/toxsci/kfaa117
81. Emond C, Birnbaum LS, DeVito MJ. Physiologically based pharmacokinetic model for developmental exposures to TCDD in the rat. Toxicol Sci. (2004) 80:115–33. doi: 10.1093/toxsci/kfh117
82. Garessus EDG, Mielke H, Gundert-Remy U. Exposure of infants to isoniazid via breast milk after maternal drug intake of recommended doses is clinically insignificant irrespective of metaboliser status. A physiologically-based pharmacokinetic (PBPK) modelling approach to estimate drug exposure of infants via breast-feeding. *Front Pharmacol.* (2019) 10:5. doi: 10.3389/fphar.2019.00005
83. Brochot C, Casas M, Manzano-Salgado C, Zeman FA, Schettgen T, Vrijheid M, Bois FY, Prediction of maternal and foetal exposures to perfluoroalkyl compounds in a Spanish birth cohort using toxicokinetic modelling. *Toxicol Appl Pharmacol.* (2019) 379:114640. doi: 10.1016/j.taap.2019.114640
84. Gingrich J, Filipovic D, Conolly R, Bhattacharya S, Veiga-Lopez A. Pregnancy-specific physiologically-based toxicokinetic models for bisphenol A and bisphenol S. *Environ Int.* (2021) 147:106301. doi: 10.1016/j.envint.2020.106301
85. Pearce RG, Setzer RW, Strope CL, Wambaugh JF, Sipes NS. httk: R package for high-throughput toxicokinetics. *J Stat Softw.* (2017) 79:1–26. doi: 10.18637/jss.v079.i04
86. Cheung KWK, van Groen BD, Spaans E, van Borselen MD, de Bruijn A, Simons-Oosterhuis Y, et al. A comprehensive analysis of ontogeny of renal drug transporters: mRNA analyses, quantitative proteomics, and localization. *Clin Pharmacol Ther.* (2019) 106:1083–92. doi: 10.1002/cpt.1516
87. Clewell RA, Gearhart JM. Pharmacokinetics of toxic chemicals in breast milk: Use of PBPK models to predict infant exposure. *Environmental Health Perspectives.* (2002) 110:A333–A337. doi: 10.1289/ehp.021100333
88. Ou L, Wang H, Chen C, Chen L, Zhang W, Wang X. Physiologically based pharmacokinetic (PBPK) modeling of human lactational transfer of methylmercury in China. *Environ Int.* (2018) 115:180–7. doi: 10.1016/j.envint.2018.03.018
89. Verner MA, Ayotte P, Muckle G, Charbonneau M, Haddad S. A physiologically based pharmacokinetic model for the assessment of infant exposure to persistent organic pollutants in epidemiologic studies. *Environ Health Perspect.* (2009) 117:481–7. doi: 10.1289/ehp.0800047
90. Merrill EA, Clewell RA, Robinson PJ, Jarabek AM, Gearhart JM, Sterner TR, et al. PBPK model for radioactive iodide and perchlorate kinetics and perchlorate-induced inhibition of iodide uptake in humans. *Toxicol Sci.* (2005) 83:25–43. doi: 10.1093/toxsci/kfi017

Conflict of Interest: The authors declare that the research was conducted in the absence of any commercial or financial relationships that could be construed as a potential conflict of interest.

Publisher's Note: All claims expressed in this article are solely those of the authors and do not necessarily represent those of their affiliated organizations, or those of the publisher, the editors and the reviewers. Any product that may be evaluated in this article, or claim that may be made by its manufacturer, is not guaranteed or endorsed by the publisher.

frontiers in Pharmacology

ORIGINAL RESEARCH
published: 19 January 2022
doi: 10.3389/fphar.2021.793346

Physiologically Based Pharmacokinetic Modeling in Pregnant Women Suggests Minor Decrease in Maternal Exposure to Olanzapine

Liang Zheng[1,2], *Hongyi Yang*[2], *André Dallmann*[3], *Xuehua Jiang*[2], *Ling Wang*[2]* *and Wei Hu*[1]*

[1]Department of Clinical Pharmacology, The Second Hospital of Anhui Medical University, Hefei, China, [2]Department of Clinical Pharmacy and Pharmacy Administration, West China School of Pharmacy, Sichuan University, Chengdu, China, [3]Pharmacometrics/Modeling and Simulation, Research and Development, Pharmaceuticals Bayer AG, Leverkusen, Germany

Pregnancy is accompanied by significant physiological changes that might affect the *in vivo* drug disposition. Olanzapine is prescribed to pregnant women with schizophrenia, while its pharmacokinetics during pregnancy remains unclear. This study aimed to develop a physiologically based pharmacokinetic (PBPK) model of olanzapine in the pregnant population. With the contributions of each clearance pathway determined beforehand, a full PBPK model was developed and validated in the non-pregnant population. This model was then extrapolated to predict steady-state pharmacokinetics in the three trimesters of pregnancy by introducing gestation-related alterations. The model adequately simulated the reported time-concentration curves. The geometric mean fold error of C_{max} and AUC was 1.14 and 1.09, respectively. The model predicted that under 10 mg daily dose, the systematic exposure of olanzapine had minor changes (less than 28%) throughout pregnancy. We proposed that the reduction in cytochrome P4501A2 activity is counteracted by the induction of other enzymes, especially glucuronyltransferase1A4. In conclusion, the PBPK model simulations suggest that, at least at the tested stages of pregnancy, dose adjustment of olanzapine can hardly be recommended for pregnant women if effective treatment was achieved before the onset of pregnancy and if fetal toxicity can be ruled out.

Keywords: olanzapine, PBPK, pregnancy, metabolic enzymes, pharmacokinetics

OPEN ACCESS

Edited by:
Venkata Kashyap Yellepeddi, The University of Utah, United States

Reviewed by:
Robin Michelet, Freie Universität Berlin, Germany
Shinya Ito, Hospital for Sick Children, Canada

***Correspondence:**
Ling Wang
wlin_scu@scu.edu.cn
Wei Hu
huwei@ahmu.edu.cn

Specialty section:
This article was submitted to Obstetric and Pediatric Pharmacology, a section of the journal Frontiers in Pharmacology

Received: *12 October 2021*
Accepted: *23 December 2021*
Published: *19 January 2022*

Citation:
Zheng L, Yang H, Dallmann A, Jiang X, Wang L and Hu W (2022) Physiologically Based Pharmacokinetic Modeling in Pregnant Women Suggests Minor Decrease in Maternal Exposure to Olanzapine. Front. Pharmacol. 12:793346. doi: 10.3389/fphar.2021.793346

INTRODUCTION

The peak incidence of many psychiatric illnesses such as schizophrenia in women occurs during their reproductive years (Kulkarni et al., 2015). The prescription of second-generation antipsychotics (SGAs) to pregnant women has been steadily increasing in the last 20 years. The latest statistics from ten countries show that up to 2% of pregnant women use SGAs (Reutfors et al., 2020). Though concerns about the safety of antipsychotics during pregnancy persist, some large-scale clinical studies in recent years suggested that exposure to SGAs does not confer an increased risk of congenital malformations (Huybrechts et al., 2016; Damkier and Videbech, 2018). Given the severe consequences without pharmacotherapy, off-label use of antipsychotics during pregnancy may

be inevitable. Except for concerns about fetal safety, clinicians often face another major challenge, i.e., optimizing dosage regimens to obtain effective maternal treatment.

The potential benefits of therapeutic drug monitoring (TDM) to optimize pharmacotherapy are particularly obvious in psychiatry and neurology. The TDM task force of the German Society of Neuropsychopharmacology and Pharmacopsychiatry (Arbeitsgemeinschaft für Neuropsychopharmakologie und Pharmakopsychiatrie [AGNP]) had given many antipsychotics a high recommendation strength for conducting TDM (Hiemke et al., 2018). For olanzapine, a reference concentration range of 20–80 ng/ml was recommended. On the other hand, pregnancy introduces conspicuous changes in various anatomical, physiological, and biological properties, for instance, organ blood flow and hormone levels. Those alterations will influence drug disposition and further their system exposure (Kazma et al., 2020). According to a comprehensive review, gestation-associated changes in pharmacokinetics widely exist (Pariente et al., 2016). Blood concentrations of commonly prescribed antipsychotics perphenazine, quetiapine, and aripiprazole decrease sharply in late pregnancy, suggesting effective treatment may not be achieved in this period with the pregestational dosing regimen (Westin et al., 2018). However, a paucity in complete pharmacokinetic reports makes it challenging to implement dose adjustment for pregnant women.

Physiologically based pharmacokinetic (PBPK) modeling serves as a critical pharmacometrics tool to make reliable pharmacokinetic predictions in special populations. The number of new drug application submissions to the US Food and Drug Administration (FDA) that included PBPK modeling for pediatric drug development has continued to grow over the past decade (Corriol-Rohou and Cheung, 2019) and the role of PBPK modeling for pregnant women in a regulatory context has been discussed recently (Coppola et al., 2021; Green et al., 2021). Since PBPK is a mechanism-based modeling method, the combined effects of multiple gestation-related physiological changes on drug disposition can be incorporated. The confidence in current pregnant modeling tools is restricted by a lack of robust data around the understanding of some metabolic enzymes and transporters and how gestation and genotypes affect drug exposure jointly (Abduljalil and Badhan, 2020). Despite these shortages, PBPK modeling seems promising to address an imperative query: whether dose adjustment is required during pregnancy. In a previous study, we proposed optimized dosage regimens of quetiapine and aripiprazole for the pregnant population using PBPK modeling and simulation (Zheng et al., 2021).

Olanzapine undergoes extensive metabolism in the liver. Several enzymes, namely cytochrome P450 (CYP) 1A2, 2C8, 3A4, flavin monooxygenase 3 (FMO3), and glucuronyltransferase (UGT) 1A4, are responsible for the metabolism. Six metabolic pathways of olanzapine have been identified, and some metabolic pathways such as N-demethylation are mediated by different enzymes (**Supplementary Figure S1**) (Kassahun et al., 1997; Korprasertthaworn et al., 2015). UGT1A4 catalyzes 10-N-glucuronidation and 4′-N-glucuronidation, whose metabolites account for 23% of an administered oral dose in non-pregnant adults (Kassahun et al., 1997). The precise proportions of other metabolites generated by oxidases have not been determined. The *in vivo* pharmacological effects are believed to be derived mainly from the parent drug (Hiemke et al., 2018). Though the principal metabolic enzyme CYP1A2 reveals a sharp reduction in its metabolic ability during pregnancy, plasma concentrations of olanzapine appear to be not markedly changed according to therapeutic drug monitoring data reported from Norwegian hospitals (Tracy et al., 2005; Westin et al., 2018). Thus, this study aims to develop a whole-body PBPK model for olanzapine to evaluate the change in systemic exposure of olanzapine throughout pregnancy. The results of this study will be beneficial for rational antipsychotic medication in this vulnerable population.

MATERIALS AND METHODS

Software and General Workflow

We used Open Systems Pharmacology Suite incorporating PK-Sim® and MoBi® (https://github.com/Open-Systems-Pharmacology) to implement the modeling work. The software is freely distributed under the GPLv2 license (Lippert et al., 2019). Parameter identification and sensitivity analysis were conducted within PK-Sim®. The reported plasma time-concentration data were digitized using WebPlotDigitizer version 4.2 (Ankit Rohatgi, Austin, United States). Plot creation and statistical analysis were conducted with OriginPro® (OriginLab, Northampton, United States).

An overview of the 27-compartment pregnancy model structure and general modeling workflow is depicted in **Figure 1**. As the first step, we constructed the adult PBPK model of olanzapine using the default 18-compartment model structure designed for small molecules (Willmann et al., 2003). The model was validated with pharmacokinetic data under multiple scenarios, including studies in pediatrics and smokers. The validated model was then scaled to the pregnant population after modifying gestation-related anatomy/physiology and changes in protein binding, metabolism, and renal excretion.

Clinical Data

We searched and extracted the published clinical pharmacokinetic data of olanzapine and classified them into the test set and validation set. To avert differences caused by pharmaceutical preparations, we excluded studies not using the reference-listed drug (Zyprexa®) or generic drugs proved to be bioequivalent. The detailed subject demographics and dosing information are provided in **Supplementary Table S1**. The test set used to assist modeling is a clinical drug-drug interaction (DDI) study conducted in adult males. This study reported single-dose (10 mg) oral pharmacokinetic profiles with or without co-administration with the strong CYP1A2 inhibitor fluvoxamine (Wang et al., 2004).

Model Development and Evaluation

The input compound-specific parameters for model development are listed in **Table 1**. Lipophilicity (measured as logP value) and

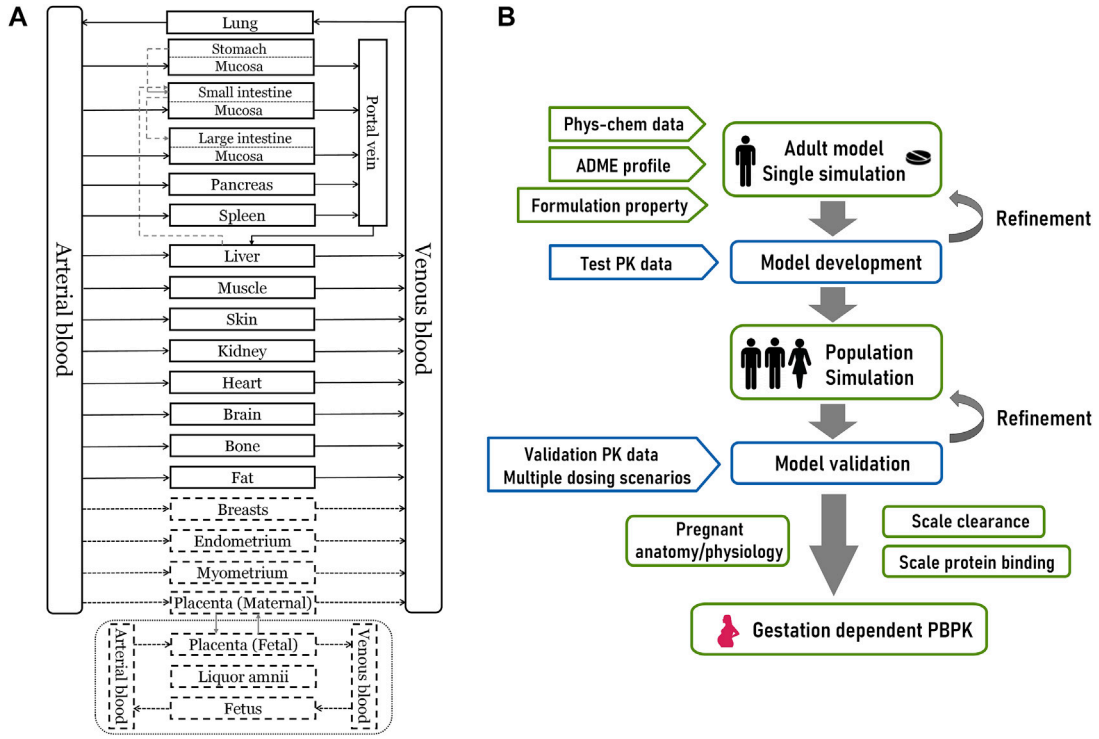

FIGURE 1 | The overall design of this modeling study **(A)** A 27-compartment physiological model of pregnant women in Mobi®. The dotted portion is nine gestation-specific compartments **(B)** The schematic diagram for PBPK modeling workflow. Phys-chem, physicochemical; ADME, absorption, distribution, metabolism, and excretion.

TABLE 1 | Summary of input compound parameters of olanzapine PBPK model.

Parameters	Values/Methods	Source
LogP	2.85	modified from reported values (2.77, 2.89) Ela et al. (2004), Urmila Sri Syamala (2013)
f_u (non-pregnant adults)	0.07	drug label[b]
MW (g/mol)	312.4	—
dissociation type	Monoprotic base	—
PKa	7.24	Callaghan et al. (1999)
solubility (μg/ml)	145.4	Urmila Sri Syamala (2013)
dissolution time (50% dissolved, min)	10	Ding (2012)
transcellular permeability (cm/min)	3.85E-6	parameter identification
partition coefficients	Schmitt	Schmitt (2008)
cellular permeabilities	Charge dependent Schmitt	Schmitt (2008)
$CL_{int,CYP1A2}$ (L/h)	26.67	fitted to $f_{m,CYP1A2}$
$CL_{int,CYP3A4}$ (L/h)	0.82	fitted to $f_{m,CYP3A4}$
$CL_{int,CYP2C8}$ (L/h)	2.14	fitted to $f_{m,CYP2C8}$
$CL_{int,FMO3}$ (L/h)	4.05	fitted to $f_{m,FMO3}$
$CL_{int,UGT1A4}$ (L/h)	20.06	fitted to $f_{m,UGT1A4}$
$f_{m,CYP1A2}$[a]	0.50	calculated
$f_{m,UGT1A4}$[a]	0.23	Kassahun et al. (1997)
$f_{m,CYP3A4}/f_{m,CYP2C8}/f_{m,FMO3}$[a]	0.067	assumed
GFR fraction	1.0	assumed
CL_{TSspec} (L/min)	0.31	fitted to f_R
f_R	0.07	Kassahun et al. (1997)

logP, lipophilicity; MW, molecular weight; pKa, acid dissociation constant; CL_{int}, intrinsic clearance; f_m, fraction metabolized by a specific enzyme; f_u, fraction unbound; GFR, glomerular filtration fraction; CL_{TSspec}, specific clearance by tubular secretion; f_R, fraction excreted via kidney.

[a]*please note that these parameters are not model input parameters, but model output values calculated from the simulated pharmacokinetics and that they differ in pregnant women.*

[b]*official drug label of Zyprexa® (https://www.accessdata.fda.gov/drugsatfda_docs/label/2009/022173lbl.pdf).*

intestinal transcellular permeability were optimized using the Monte-Carlo algorithm. Tissue-to-plasma partition coefficients and cellular permeabilities were calculated by the Schmitt and Charge-dependent Schmitt method, respectively. For *in vivo* clearance, we first determined the contributions of each pathway to the total clearance. Olanzapine was eliminated primarily by hepatic metabolism, while direct renal excretion (f_R), composed of glomerular filtration and tubular secretion, accounted for only 7% of an administered oral dose (Kassahun et al., 1997). The dose fraction metabolized by UGT1A4 was set to 0.23, corresponding to the proportion of recovery as glucuronide conjugates from urine and feces (Kassahun et al., 1997). The contribution of CYP1A2 was reckoned to be 0.50 based on data from the abovementioned DDI study according to the Rowland-Matin equation (**Eq. 1**) (Elsby et al., 2012). A validated PBPK model of fluvoxamine developed by Britz et al. was used for model development (Britz et al., 2019).

$$\frac{AUC_i}{AUC} = \frac{F_{g,\ i}}{F_g} \times \frac{1}{\frac{\sum f_m \times f_{m,\ CYP1A2}}{1+\frac{I_u}{K_i}} + \left(1 - \sum f_m \times f_{m,\ CYP1A2}\right)} \quad (1)$$

Further details of using **Eq. 1** to calculate the dose fraction metabolized by CYP1A2, including a description of the variables in this equation, is provided in the supplementary material. Contributions of secondary enzymes involved in olanzapine metabolism including CYP2C8, CYP3A4, and FMO3 were roughly estimated to be equal. Olanzapine exhibited dose-dependent pharmacokinetics, and metabolic saturation was not observed; therefore, we used first-order processes to define metabolism according to .

$$v = CL_{int,E} \times S \quad (2)$$

$CL_{int,E}$ is the normalized intrinsic clearance (L/min) obtained by fitting to the test set data and to the fraction metabolized through each enzyme (f_m) determined before. S is substrate amount (μmol) and v the reaction rate (μM/min).

Sensitivity of the final model to single parameters (local sensitivity analysis) was measured as relative change of area under the concentration-time curve (AUC, ng·h/mL) after a single oral dose or AUC from time of the last dose administration to infinity after multiple administrations. Parameters were included in the analysis if they were optimized or associated with optimized parameters or if they might have a substantial impact due to calculation methods. Sensitivity to a parameter was calculated according to .

$$Sensitivity = \frac{\Delta AUC}{AUC} \times \frac{p}{\Delta p} \quad (3)$$

where ΔAUC = change of the simulated AUC, AUC = simulated AUC with the original parameter value, Δp = change of the examined model parameter value, and p = original model parameter value. A sensitivity value of +1.0 denotes that a 10% increase of the examined parameter causes a 10% increase of the simulated AUC (Hanke et al., 2018).

For model evaluation, population simulations to the validation set were performed. The simulated time-concentration curves were compared with the observed ones. The geometric mean fold error (GMFE) for observed C_{max} (ng/ml), t_{max} (h), and AUC as an index of quantitative assessment was calculated according to .

$$GMFE = 10^{\left(\sum \left|\lg\left(\frac{predicted\ PK\ parameter}{observed\ PK\ parameter}\right)\right|\right)/n} \quad (4)$$

where n is the number of simulated studies. The predicted and observed PK parameters used geometric or arithmetic means depending on reports of clinical studies. If not available, the parameters were calculated by non-compartment analysis using the concentration data. A GMFE value less than two suggests satisfactory predictive performance (Britz et al., 2019). A more detailed description of model development and evaluation is provided in the Supplemental Material.

Extrapolation to the Pregnant Population

The pregnancy model with anatomic physiological alterations was developed by Dallmann et al. and described in detail in several publications (Dallmann et al., 2017a; Dallmann et al., 2017b). The model was built in MoBi® and exported to PK-Sim® for population simulation. The following compound-related parameters were considered for adjustments in the pregnancy model. The unbound fraction in plasma during pregnancy was deduced from the base value measured in non-pregnant adults according to **Eqs 5**, **6** (Dallmann et al., 2017b).

$$f_u = \frac{1}{1 + K_A \times P/MW_{albumin}} \quad (5)$$

$$P\left(\frac{g}{L}\right) = 14.7 \exp(-0.0454FW) + 31.7 \quad (6)$$

where f_u is the plasma unbound fraction of olanzapine, K_A is the equilibrium association constant (μmol^{-1}), P represents the albumin concentration in plasma in a specific fertilization week of pregnancy (μmol/L), $MW_{albumin}$ is the molecular weight of albumin (g/mol), and FW denotes fertilization weeks, which is calculated by subtracting 2 weeks from the gestational week. To calculate the fraction unbound in pregnancy, K_A was first calculated for non-pregnant adults by re-arranging **Eq. 1** using a value of 0.07 for the fraction unbound in non-pregnant adults (see **Table 1**) and 31.7 g/L for the albumin concentration (Dallmann et al., 2017a). Thereafter, the fraction unbound in pregnancy was calculated from **Eqs 5**, **6** using the same K_A value for pregnant women as for non-pregnant adults.

Renal clearances (glomerular filtration, tubular secretion, and renal plasma clearance) are technically interpreted as passive transport processes in the model. Their values as listed in **Table 1** are normalized to the volume of kidney and can be left unchanged in pregnancy (Dallmann et al., 2017b). Drug metabolism was modified by activity change of metabolic enzymes taking fertilization week as the independent variable.

CYP1A2

CYP1A2 activity changes during pregnancy can be reflected by changes in the apparent clearance of caffeine which is described by **Eq. 7** (Dallmann et al., 2018a).

$$CYP1A2\ activity\ change\ (\%) = 0.0291FW^2 - 2.77FW \quad (7)$$

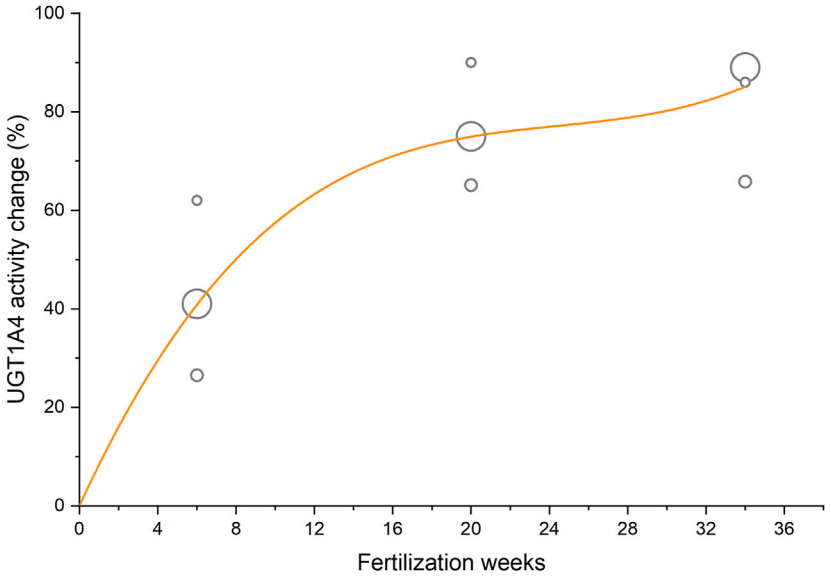

FIGURE 2 | Activity change of UGT1A4 during pregnancy taking lamotrigine apparent clearance as an indicator. The circle area reflects the sample size of clinical studies, and the curve represents the fitted regression equation.

UGT1A4

The antiepileptic drug lamotrigine was mainly eliminated through N-glucuronidation which is predominantly catalyzed by UGT1A4 *in vivo* (Wang et al., 2015). Previous studies reported the apparent clearances of lamotrigine in 7, 11, and 53 cases of women before and during pregnancy (Tran et al., 2002; Petrenaite et al., 2005; Pennell et al., 2008). By taking fertilization week as the independent variable and the sample size as weight, a cubic function describing the relative change of lamotrigine apparent clearance was fitted to these data by non-linear regression (**Figure 2** and **Eq. 8**).

$$\boldsymbol{UGT1A4\ activity\ change}(\%) = 8.669\boldsymbol{FW} - 0.339\boldsymbol{FW}^2 + 0.00462\boldsymbol{FW}^3 \quad (8)$$

CYP3A4

Eq. 9 describing CYP3A4 induction during pregnancy was derived based on the PBPK modeling of CYP3A4 probe substrate midazolam in pregnant women (Ke and Milad, 2019).

$$\boldsymbol{CYP3A4\ activity}\ (\%) = 1.00736 + 0.00564\boldsymbol{FW} + 0.00172\boldsymbol{FW}^2 - 0.00003\boldsymbol{FW}^3 \quad (9)$$

CYP2C8

Quantitative information on CYP2C8 activity during pregnancy was not reported; therefore, CYP2C8-mediated clearance was assumed to remain unchanged in the pregnancy model.

FMO3

The N′-oxidation of nicotine is catalyzed solely by FMO_3. Hukkanen et al. proposed that the ratio of urinary excretion of nicotine N′-oxide to the plasma area under the curve of nicotine could be an active indicator of FMO_3 (excluding the effect of slightly higher urine pH during pregnancy on urinary excretion of nicotine) (Hukkanen et al., 2005). According to this study, FMO_3 activity is increased by 58% in late pregnancy.

The setting of compound-related parameters in the pregnancy model is listed in **Table 2**.

TABLE 2 | The setting of compound-related parameters in the pregnancy model. Parameters were adjusted based on their baseline values presuming 6-, 20-, and 34-weeks fertilization as representative of first, second, and third trimesters, respectively.

Parameters	1st trimester	2nd trimester	3rd trimester
f_u	0.075	0.085	0.091
$CL_{int,CYP1A2}$ (L/h)	22.40	14.13	9.87
$CL_{int,CYP3A4}$ (L/h)	0.89	1.28	1.64
$CL_{int,CYP2C8}$ (L/h)	2.14	2.14	2.14
$CL_{int,FMO3}$ (L/h)	4.05	4.05	7.11
$CL_{int,UGT1A4}$ (L/h)	28.24	35.04	36.91

Pregnant Simulation

We created three virtual pregnant groups based on fertilization week ranges, including first trimester (1–11 weeks), second trimester (12–26 weeks), and third trimester (27–38 weeks), with a non-pregnant population (20–40 years old) as the reference population. Each virtual population contained 1,000 individuals. The model was applied to predict the steady-state pharmacokinetics of olanzapine in non-pregnant and pregnant women under 10 mg daily dose, which is a recommended starting and commonly used dose.

RESULTS

Olanzapine PBPK Model Development

As shown in **Figure 3** and **Table 3**, the olanzapine model adequately simulates mean pharmacokinetic profiles of a

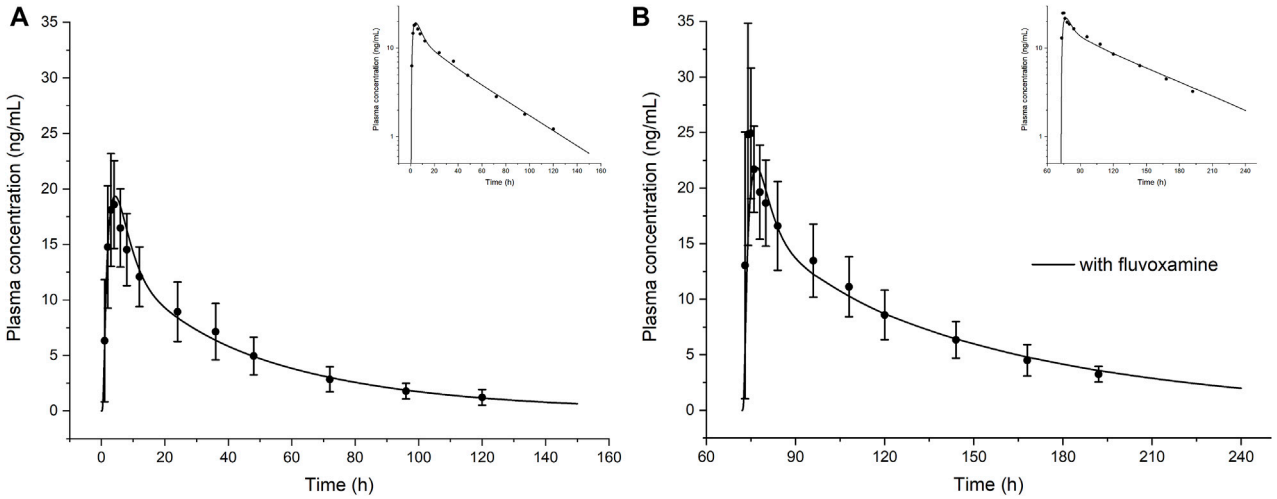

FIGURE 3 | The model-simulated concentration-time curve of olanzapine after a single oral dose of 10 mg in healthy volunteers in the absence **(A)** or presence **(B)** of co-administered CYP1A2 inhibitor fluvoxamine. Curves are from the model prediction and observed mean plasma concentrations with standard deviations are shown as circles with error bars. The top right corners show the log scale figures. Figure B calculated the actual sampling time starting from day 4 that was different from the original literature.

TABLE 3 | Simulated and observed pharmacokinetic parameters of olanzapine from model development.

–	Single dose			Co-administered with fluvoxamine	
	C_{max} (ng/ml)	$AUC_{0-\infty}$ (ng*h/mL)	CL/F (L/h)	$C_{max}R$	AUCR
Simulated	19.4	701.0	14.3	1.13	1.88
Reported	18.6	728.5	14.6	1.34	1.76

C_{max}, peak concentration; $AUC_{0-\infty}$, area under the concentration-time curve from time zero to infinity; CL/F, apparent clearance; $C_{max}R$, c_{max} ratio; AUCR, AUC, ratio.

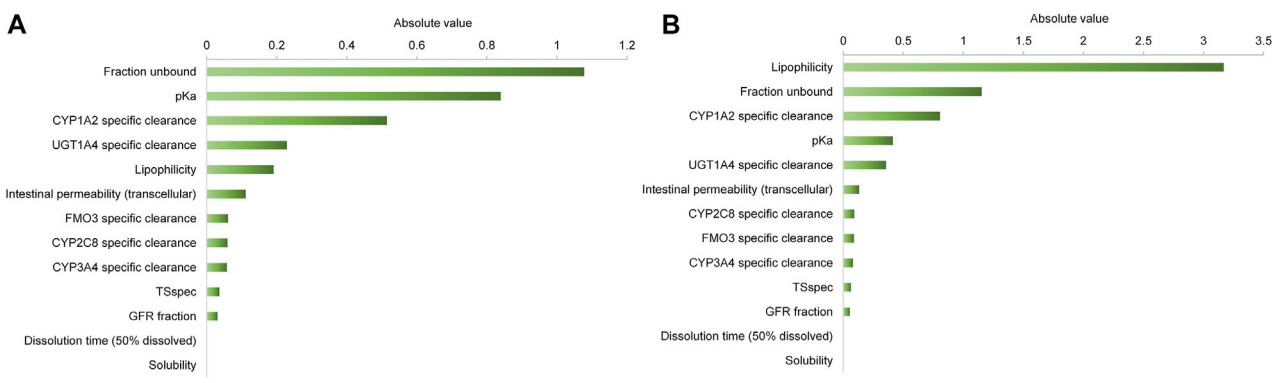

FIGURE 4 | Sensitivity analysis of the olanzapine model. Sensitivity of the final model to single parameters was measured as relative change of $AUC_{0\infty}$ after a single oral dose **(A)** or AUC from time of the last dose to infinity after multiple administrations **(B)**. A sensitivity value of +1.0 denotes that a 10% increase of the examined parameter causes a 10% increase of the simulated AUC.

10 mg single oral dose with and without co-administration with fluvoxamine. The prediction errors for C_{max} and AUC are less than 4.5%. When co-administered with fluvoxamine, the predicted C_{max} ratio ($C_{max}R$) and AUC ratio (AUCR) are 1.13 and 1.88, respectively, compared to the reported values of 1.34 and 1.76. The contributions of each clearance pathway have been consistent with reported values. Sensitivity analysis (**Figure 4**) indicates that the fraction unbound is the most sensitive parameter (−1.24) for systemic exposure to olanzapine after a single oral dose, followed by pKa (−1.02), specific clearances of

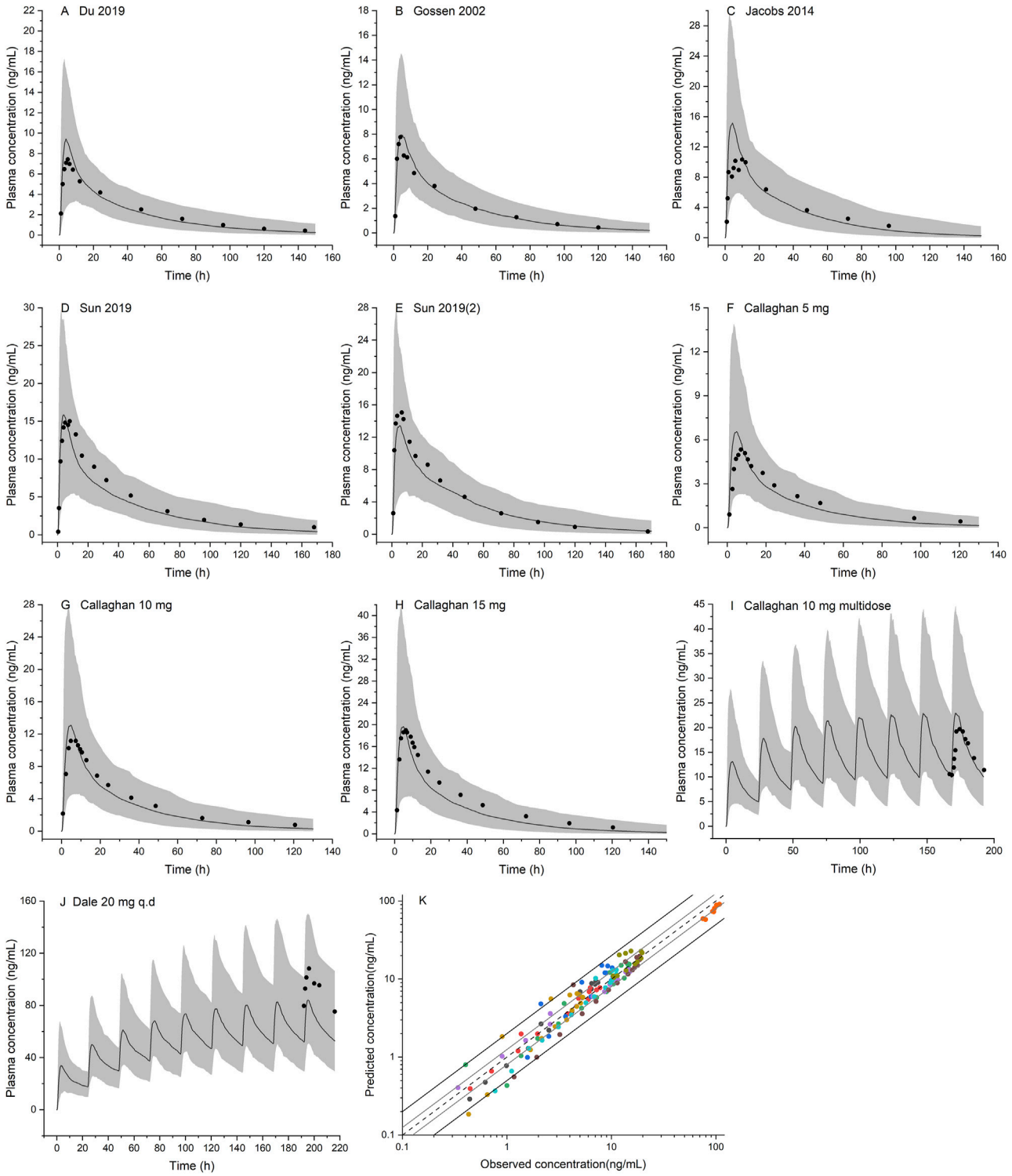

FIGURE 5 | Population PBPK simulations for olanzapine in the non-pregnant population **(A–J)** Predicted median plasma concentrations are shown as dark lines, and shaded areas indicate 5th to 95th prediction range. Black dots are observed mean plasma concentrations extracted from clinical studies **(K)** Goodness of fit plot for model prediction of olanzapine plasma concentrations. Different colors represent observed-to-predicted concentration data from different simulations in figure **A–J**. The observed data are from published studies with references provided in the **Supplementary Material**.

TABLE 4 | Predicted and observed pharmacokinetic parameters of olanzapine and geometric mean fold errors from model validation.

Study	Methods	$C_{max}/C_{max\text{-}ss}$ (ng/ml)	$AUC/AUC_{\tau\text{-}ss}$ (ng·h/mL)	t_{max} (h)
Du et al. (2020)	Predicted	8.1	298.3	4.4
	Observed	7.8	341.4	5.0
	FE	1.04	0.87	0.88
Gossen (2002)	Predicted	7.2	264.1	4.9
	Observed	7.6	272.0	3.0
	FE	0.95	0.97	1.63
Callaghan 1999	Predicted	7.0	217.8	4.0
	Observed	5.4	236.7	7.0
	FE	1.30	0.92	0.57
Jacobs (2014)	Predicted	13.4	426.2	4.3
	Observed	13.2	436.9	6.0
	FE	1.02	0.98	0.72
Sun (2019a)	Predicted	17.2	710.3	3.9
	Observed	17.5	711.5	7.0
	FE	0.98	1.00	0.56
Sun (2019b)	Predicted	14.5	651.7	4.2
	Observed	16.7	629.2	5.0
	FE	0.87	1.04	0.84
Callaghan 1999	Predicted	14.0	436.5	4.0
	Observed	11.2	460.3	4.8
	FE	1.25	0.95	0.83
Callaghan 1999	Predicted	21.0	653.1	4.0
	Observed	19.0	755.1	6.2
	FE	1.10	0.86	0.65
Callaghan 1999	Predicted	24.8	423.1	3.7
	Observed	19.7	388.6	6.2
	FE	1.26	1.09	0.60
Dale 2000	Predicted	92.2	1731	3.0
	Observed	115.6	2,220	4.0
	FE	0.80	0.78	0.75
	GMFE	1.14	1.09	1.44

FE, fold error; GMFE, geometric mean fold error; $C_{max\text{-}ss}$, steady-state peak concentration; $AUC_{\tau\text{-}ss}$, steady-state AUC, of a dosing interval; t_{max} time to reach peak concentration.

CYP1A2 (−0.51) and UGT1A4 (−0.23), and lipophilicity (−0.19) among all included model parameters. As to multiple dosing, logP is the most sensitive parameter (3.17), followed by fraction unbound, CYP1A2 specific clearance, and pKa.

Olanzapine Model Verification

Ten population PBPK simulations for the validation data set were conducted and are shown in **Figure 5**. More than 95% of the predicted drug concentrations are within a twofold error range of the measured values, and about 62% are within 1.25-fold error range according to the goodness-of-fit plot (**Figure 5K**). The mean absolute prediction errors of the plasma concentrations for all simulated studies are less than 42% (**Supplementary Table S2**). The fold errors for predicted/observed C_{max} and AUC are within the range of 0.75–1.30, and GMFE of C_{max} and AUC is 1.14 and 1.09, respectively (**Table 4**). In a pediatric simulation (Dale 2000), the model predicts a slightly lower plasma exposure in children aged 10–18.

Pharmacokinetic Prediction in the Pregnant Population

Simulations of steady-state pharmacokinetics were performed during the first (6 weeks), second (20 weeks), and third (34 weeks) trimesters of pregnancy, in comparison with that of baseline. Fraction unbound shows a moderate increase across the first (7.1%), second (21.4%), and third (30.0%) trimester. CYP1A2 activity decreases, while UGT1A4, CYP3A4, and FMO3 are upregulated; as a result, the intrinsic clearance alters less than 20% throughout pregnancy. Overall, PBPK modeling predicts a limited impact of gestation on plasma concentrations of olanzapine (**Figure 6**). The fluctuation of mean plasma concentration under 10 mg daily dose is basically stable but an effective treatment concentration (20 ng/ml) cannot be guaranteed to achieve at any time in a dosing interval of late pregnancy. The steady-state C_{max}, $AUC_{\tau\text{-}ss}$, and half-life of olanzapine show slight changes (not more than 28%) throughout pregnancy (**Table 5**). The apparent total clearance (CL/F) are increased by up to 37.1% until the late

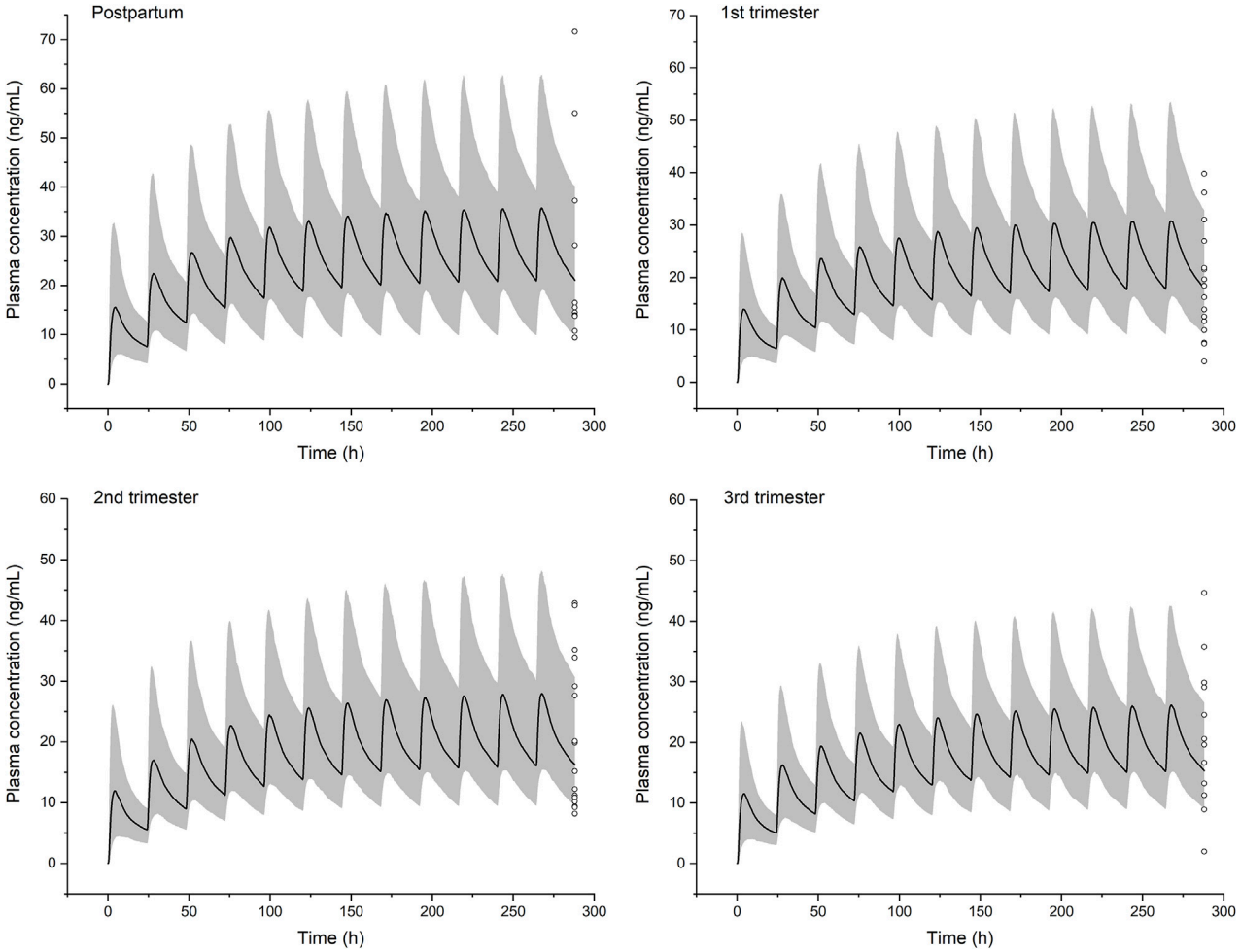

FIGURE 6 | Simulated pharmacokinetic profiles of olanzapine in non-pregnant women and women in the three stages of pregnancy receiving 10 mg daily dose. Median plasma concentrations are shown as dark lines, and shaded areas indicate 5th to 95th prediction range. Circles are individual olanzapine concentration data in pregnant women with schizophrenia collected from therapeutic drug monitoring (TDM) (Westin et al., 2018). It was recommended that TDM samples are collected as trough levels at steady state.

TABLE 5 | Model-predicted steady state pharmacokinetic parameters of olanzapine during pregnancy under 10 mg daily dose. Data shown as geometric means.

—	$C_{max\text{-}ss}$ (ng/ml)	$AUC_{\tau\text{-}ss}$ (ng·h/mL)	$t_{1/2}$ (h)	CL_{ss}/F
Postpartum	35.1	653.5	32.7	15.3
1st trimester	30.5 (–13.1%)	562.9 (–11.5%)	32.5 (+0.31%)	17.8 (+16.1%)
2nd trimester	27.5 (–21.6%)	511.2 (–21.8%)	33.1 (+1.22%)	19.6 (+27.8%)
3rd trimester	25.8 (–26.5%)	476.5 (–27.1%)	33.6 (+2.75%)	21.0 (+37.1%)

$C_{max\text{-}ss}$, steady-state peak concentration; $AUC_{\tau\text{-}ss}$, steady-state AUC of a dosing interval; $t_{1/2}$, half life; CL_{ss}/F, steady-state apparent clearance. Within brackets are relative changes during pregnancy compared to the baseline.

pregnancy. Based on the model prediction, the average steady-state trough concentrations of olanzapine in the first, second, and third trimester of pregnancy are decreased by 12.4, 22.6, and 28.3%, respectively. The magnitude of predicted decrease is slightly higher than the observed one calculated from TDM data. (**Table 6**).

DISCUSSION

This study developed a PBPK model of olanzapine using a 'middle-out' strategy and gave pharmacokinetic predictions for the pregnant population. To our knowledge, this is the first pregnant PBPK modeling study for olanzapine.

TABLE 6 | The mean steady state trough concentrations of olanzapine predicted by the PBPK model and reported TDM data-based regression curve (Westin et al., 2018).

Method	BaselineConc	6 weeks gestation		20 weeks gestation		34 weeks gestation	
		Conc	Change	Conc	Change	Conc	Change
PBPK model	22.6	19.8	−12.4%	17.5	−22.6%	16.2	−28.3%
Regression curve	21.3	20.9	−1.9%	20.1	−5.6%	19.3	−9.4%

Previous olanzapine PBPK modeling studies for non-pregnant adults described olanzapine clearance based on *in vitro* data (Polasek et al., 2018; Sun et al., 2020), while this study applied a different strategy. Because direct *in vitro* to *in vivo* extrapolation of the contribution of an enzyme to the total drug metabolism is often associated with great uncertainty (Zhang et al., 2020), we calculated this important parameter for major enzymes using *in vivo* data (mass balance and clinical DDI study). CYP1A2 has long been regarded as the primary enzyme for olanzapine metabolism, and its contribution was first determined to be 50%. Unlike typical highly polymorphic enzymes such as CYP2C9 and CYP2D6, genetic polymorphisms of CYP1A2 contribute little to the interindividual pharmacokinetic variability of olanzapine (Na Takuathung et al., 2019). Therefore, CYP1A2 polymorphisms were not considered in this study. The major circulating metabolite of olanzapine is the 10-N-glucuronide, whose formation can be attributed to UGT1A4 and UGT2B10 with the former having a much higher catalytic activity than UGT2B10 (Soderberg and Dahl, 2013). Besides, sensitivity analysis shows that fraction unbound, pKa, logP, and CYP1A2 and UGT1A4-mediated clearance are the most sensitive parameters, while logP is much more sensitive following multiple administrations. This impact leads to a visibly different time to reach the plateau under multiple doses, probably because of late back-distribution from compartments where olanzapine accumulates, that significantly affect AUC of the last dose (data not shown). As a result, a higher sensitivity to logP was observed after multiple administrations. Because the Charge-dependent Schmitt method for calculating cellular permeabilities considers the effect of electric charge, pKa becomes a relatively important parameter.

We speculated that the reduction in CYP1A2 activity during pregnancy is counteracted by the induction of other enzymes, especially UGT1A4. To this date, different studies have reported controversial results on hepatic blood flow during pregnancy. Therefore, the gestation-related physiology engine for creating virtual pregnant populations assumed unchanged absolute liver blood flow (Dallmann et al., 2017a). Alterations in CL/F should be mainly attributed to changes in (unbound fraction) x (intrinsic clearance) especially when olanzapine has a relatively low extraction ratio (<0.3). Fraction unbound, CYP1A2 and UGT1A4-mediated clearances are the most significant ones among all tested parameters modified during pregnancy (**Figure 4**). CYP1A2 activity decreases by up to 60% to late pregnancy. Meanwhile, UGT1A4 activity increases by 85% on average, whereas there is a slight alteration in fraction unbound, as calculated according to **Eq. 5**. As a result, the mean plasma concentrations of olanzapine are generally stable. On the other hand, the reliability of model predictions is potentially affected by several factors that cannot be accurately clarified at the current stage. First, the sensitivity analysis indicated that attention should be paid to the calculated fraction unbound. Although the calculation method (**Eq. 5**) has been evaluated for other drugs, the results stress the importance of a correct value for fraction unbound during pregnancy. For an extensively metabolized drug like olanzapine, increase in fraction unbound contributes to a higher hepatic clearance with a great possibility. Therefore, it should be beneficial to measure a precise fraction unbound of olanzapine in future clinical studies to confirm or refine the value used in the PBPK model. Second, it is currently undetermined whether gestation changes drug absorption from the gastrointestinal tract. In this model, settings for drug absorption were not specifically modified compared to non-pregnant women. Drug absorption is indeed a challenge requiring further investigation. There might be several gestation-related factors affecting drug absorption, for instance, prolongation in gastrointestinal transit time, and enlargement in intestinal villi surface area (Dallmann et al., 2018b; Koren and Pariente, 2018). However, we haven't developed mathematical explanations for these factors due to inadequate quantitative human data. Since clinical data for C_{max}/t_{max} are lacking, the simulated absorption cannot be evaluated. This stresses again the need for further clinical data during pregnancy, ideally full pharmacokinetic profiles instead of trough concentrations. Third, uncertainty in clearance contribution of some minor enzymes during model development, though we estimated it had a minimal impact. Besides, there are conflicting reports on the exact magnitude of CYP3A4 induction in pregnant women. Some studies suggest that a 2-fold induction in the third trimester is plausible, whereas others suggest a lower activity increase (such as 27%) (Nylen et al., 2011). A previous modeling study used a weighted mean of 60% induction (Dallmann et al., 2018a). Assuming a 60% activity increase in the third trimester, the model predicts a C_{max} of 26.3 ng/ml and $AUC_{\tau\text{-}ss}$ of 488.1 ngh/mL, which show negligible differences from the current data. Therefore, among all relevant enzymes, CYP1A2 and UGT1A4 activity during pregnancy are critical determinants of olanzapine clearance. More quantitative data reflecting activity changes of metabolic enzymes are needed to enhance the predictive performance of pregnant PBPK modeling.

According to the TDM data and PBPK predictions, dose adjustments appear to be not urgently needed for pregnant women. Neither has a report that pregnant women show a higher treatment failure rate under the same doses. But we should notice that TDM data have indicated a considerable interindividual variability in trough concentrations (Westin et al., 2018). Therefore, TDM has its unique strength in the

individualized dosing that could not be replaced. Effective treatment before gestation is essential to olanzapine usage during pregnancy with an unchanged dosage regimen.

A limitation of this study is that fetal exposure to olanzapine has not been addressed. In order to estimate the placental transfer of drugs, data from *in vitro* cell models and *ex vivo* placental perfusion are preferred. Additionally, umbilical cord blood concentration data during delivery would be needed to validate the model predictions (Dallmann et al., 2019). Unfortunately, these pieces of information on olanzapine are lacking. Recent studies have made beneficial attempts to explore the maternal-fetal drug transfer and exposure ratio with the abovementioned approaches using acetaminophen as a model drug (Mian et al., 2020; Mian et al., 2021). These studies provide helpful references in the analysis of fetal pharmacokinetics of olanzapine in the future. We urgently need more long-term studies with large samples to clarify the efficacy and adverse impacts on fetuses and determine management strategies for antipsychotics.

CONCLUSION

In summary, this study developed a PBPK model of olanzapine to evaluate the maternal exposure of this commonly prescribed antipsychotic in the pregnant population. The predictive performance was validated with various clinical pharmacokinetic studies. According to the presented PBPK simulations, the steady-state pharmacokinetics of olanzapine is slightly, and probably not clinically significantly altered during pregnancy. Combined with the TDM data, the model suggests that dose adjustment cannot be formulated for pregnant women, at least at the tested stages of pregnancy, if effective treatment was achieved before the onset of pregnancy, while fetal safety certainly needs continuous surveillance.

DATA AVAILABILITY STATEMENT

The raw data supporting the conclusions of this article will be made available by the authors, without undue reservation.

AUTHOR CONTRIBUTIONS

LZ, XJ, and LW contributed to the conception of the study. LZ and HY performed the study. LZ and WH wrote the first draft. AD revised the draft and contributed valuable suggestions. WH and LW provided final approval of the manuscript.

FUNDING

The National Natural Science Foundation of China (Grant No. 81573789) provided the funding for this research. The publication fee is covered by The Second Hospital of Anhui Medical University.

SUPPLEMENTARY MATERIAL

The Supplementary Material for this article can be found online at: https://www.frontiersin.org/articles/10.3389/fphar.2021.793346/full#supplementary-material.

REFERENCES

Abduljalil, K., and Badhan, R. K. S. (2020). Drug Dosing during Pregnancy-Opportunities for Physiologically Based Pharmacokinetic Models. *J. Pharmacokinet. Pharmacodyn* 47 (4), 319–340. doi:10.1007/s10928-020-09698-w

Britz, H., Hanke, N., Volz, A. K., Spigset, O., Schwab, M., Eissing, T., et al. (2019). Physiologically-Based Pharmacokinetic Models for CYP1A2 Drug-Drug Interaction Prediction: A Modeling Network of Fluvoxamine, Theophylline, Caffeine, Rifampicin, and Midazolam. *CPT Pharmacometrics Syst. Pharmacol.* 8 (5), 296–307. doi:10.1002/psp4.12397

Callaghan, J. T., Bergstrom, R. F., Ptak, L. R., and Beasley, C. M. (1999). Olanzapine. Pharmacokinetic and Pharmacodynamic Profile. *Clin. Pharmacokinet.* 37 (3), 177–193. doi:10.2165/00003088-199937030-00001

Coppola, P., Kerwash, E., and Cole, S. (2021). Physiologically Based Pharmacokinetics Model in Pregnancy: A Regulatory Perspective on Model Evaluation. *Front. Pediatr.* 9, 687978. doi:10.3389/fped.2021.687978

Corriol-Rohou, S., and Cheung, S. Y. A. (2019). Industry Perspective on Using MIDD for Pediatric Studies Requiring Integration of Ontogeny. *J. Clin. Pharmacol.* 59 (Suppl. 1), S112–S119. doi:10.1002/jcph.1495

Dallmann, A., Ince, I., Coboeken, K., Eissing, T., and Hempel, G. (2018a). A Physiologically Based Pharmacokinetic Model for Pregnant Women to Predict the Pharmacokinetics of Drugs Metabolized via Several Enzymatic Pathways. *Clin. Pharmacokinet.* 57 (6), 749–768. doi:10.1007/s40262-017-0594-5

Dallmann, A., Ince, I., Meyer, M., Willmann, S., Eissing, T., and Hempel, G. (2017a). Gestation-Specific Changes in the Anatomy and Physiology of Healthy Pregnant Women: An Extended Repository of Model Parameters for Physiologically Based Pharmacokinetic Modeling in Pregnancy. *Clin. Pharmacokinet.* 56 (11), 1303–1330. doi:10.1007/s40262-017-0539-z

Dallmann, A., Ince, I., Solodenko, J., Meyer, M., Willmann, S., Eissing, T., et al. (2017b). Physiologically Based Pharmacokinetic Modeling of Renally Cleared Drugs in Pregnant Women. *Clin. Pharmacokinet.* 56 (12), 1525–1541. doi:10.1007/s40262-017-0538-0

Dallmann, A., Mian, P., Van den Anker, J., and Allegaert, K. (2019). Clinical Pharmacokinetic Studies in Pregnant Women and the Relevance of Pharmacometric Tools. *Curr. Pharm. Des.* 25 (5), 483–495. doi:10.2174/1381612825666190320135137

Dallmann, A., Pfister, M., van den Anker, J., and Eissing, T. (2018b). Physiologically Based Pharmacokinetic Modeling in Pregnancy: A Systematic Review of Published Models. *Clin. Pharmacol. Ther.* 104 (6), 1110–1124. doi:10.1002/cpt.1084

Damkier, P., and Videbech, P. (2018). The Safety of Second-Generation Antipsychotics during Pregnancy: A Clinically Focused Review. *CNS Drugs* 32 (4), 351–366. doi:10.1007/s40263-018-0517-5

Ding, Y. (2012). Comparison of Dissolution of Olanzapine Tablets From Different Manufacturers. *Anti-Infection Pharmacy* 04, 290–292.

Du, P., Li, P., Liu, H., Zhao, R., Zhao, Z., and Yu, W. (2020). Open-Label, Randomized, Single-Dose, 2-Period, 2-Sequence Crossover, Comparative Pharmacokinetic Study to Evaluate Bioequivalence of 2 Oral Formulations of Olanzapine Under Fasting and Fed Conditions. *Clin. Pharmacol. Drug Dev.* 9 (5), 621–628. doi:10.1002/cpdd.743

Ela, A. A. E., Härtter, S., Schmitt, U., Hiemke, C., Spahn-Langguth, H., and Langguth, P. (2004). Identification of P-Glycoprotein Substrates and Inhibitors Among Psychoactive Compounds - Implications For Pharmacokinetics of

Selected Substrates. *J. Pharm. Pharmacol.* 56 (8), 967–975. doi:10.1211/0022357043969

Elsby, R., Hilgendorf, C., and Fenner, K. (2012). Understanding the Critical Disposition Pathways of Statins to Assess Drug-Drug Interaction Risk during Drug Development: It's Not Just about OATP1B1. *Clin. Pharmacol. Ther.* 92 (5), 584–598. doi:10.1038/clpt.2012.163

Gossen, D., de Suray, J. M., Vandenhende, F., Onkelinx, C., and Gangji, D. (2002). Influence of Fluoxetine on Olanzapine Pharmacokinetics. *AAPS PharmSci.* 4 (2), E11. doi:10.1208/ps040211

Green, D. J., Park, K., Bhatt-Mehta, V., Snyder, D., and Burckart, G. J. (2021). Regulatory Considerations for the Mother, Fetus and Neonate in Fetal Pharmacology Modeling. *Front. Pediatr.* 9, 698611. doi:10.3389/fped.2021.698611

Grothe, D. R., Calis, K. A., Jacobsen, L., Kumra, S., DeVane, C. L., Rapoport, J. L., et al. (2000). Olanzapine Pharmacokinetics in Pediatric and Aolescent Inpatients with Childhood-Onset Schizophrenia. *J. Clin. Psychopharmacol.* 20 (2), 220–225. doi:10.1097/00004714-200004000-00015

Hanke, N., Frechen, S., Moj, D., Britz, H., Eissing, T., Wendl, T., et al. (2018). PBPK Models for CYP3A4 and P-Gp DDI Prediction: A Modeling Network of Rifampicin, Itraconazole, Clarithromycin, Midazolam, Alfentanil, and Digoxin. *CPT Pharmacometrics Syst. Pharmacol.* 7 (10), 647–659. doi:10.1002/psp4.12343

Hiemke, C., Bergemann, N., Clement, H. W., Conca, A., Deckert, J., Domschke, K., et al. (2018). Consensus Guidelines for Therapeutic Drug Monitoring in Neuropsychopharmacology: Update 2017. *Pharmacopsychiatry* 51 (1-02), e1–62. doi:10.1055/s-0043-11649210.1055/s-0037-1600991

Hukkanen, J., Dempsey, D., Jacob, P., 3rd, and Benowitz, N. L. (2005). Effect of Pregnancy on a Measure of FMO3 Activity. *Br. J. Clin. Pharmacol.* 60 (2), 224–226. doi:10.1111/j.1365-2125.2005.02406.x

Huybrechts, K. F., Hernández-Díaz, S., Patorno, E., Desai, R. J., Mogun, H., Dejene, S. Z., et al. (2016). Antipsychotic Use in Pregnancy and the Risk for Congenital Malformations. *JAMA Psychiatry* 73 (9), 938–946. doi:10.1001/jamapsychiatry.2016.1520

Jacobs, B. S., Colbers, A. P., Velthoven-Graafland, K., Schouwenberg, B. J., and Burger, D. M. (2014). Effect of Fosamprenavir/Ritonavir on the Pharmacokinetics of Single-Dose Olanzapine in Healthy Volunteers. *Int. J. Antimicrob Agents* 44 (2), 173–177. doi:10.1016/j.ijantimicag.2014.03.014

Kassahun, K., Mattiuz, E., Nyhart, E., Jr., Obermeyer, B., Gillespie, T., Murphy, A., et al. (1997). Disposition and Biotransformation of the Antipsychotic Agent Olanzapine in Humans. *Drug Metab. Dispos* 25 (1), 81–93.

Kazma, J. M., van den Anker, J., Allegaert, K., Dallmann, A., and Ahmadzia, H. K. (2020). Anatomical and Physiological Alterations of Pregnancy. *J. Pharmacokinet. Pharmacodyn* 47 (4), 271–285. doi:10.1007/s10928-020-09677-1

Ke, A. B., and Milad, M. A. (2019). Evaluation of Maternal Drug Exposure Following the Administration of Antenatal Corticosteroids during Late Pregnancy Using Physiologically-Based Pharmacokinetic Modeling. *Clin. Pharmacol. Ther.* 106 (1), 164–173. doi:10.1002/cpt.1438

Koren, G., and Pariente, G. (2018). Pregnancy- Associated Changes in Pharmacokinetics and Their Clinical Implications. *Pharm. Res.* 35 (3), 61. doi:10.1007/s11095-018-2352-2

Korprasertthaworn, P., Polasek, T. M., Sorich, M. J., McLachlan, A. J., Miners, J. O., Tucker, G. T., et al. (2015). *In Vitro* Characterization of the Human Liver Microsomal Kinetics and Reaction Phenotyping of Olanzapine Metabolism. *Drug Metab. Dispos* 43 (11), 1806–1814. doi:10.1124/dmd.115.064790

Kulkarni, J., Storch, A., Baraniuk, A., Gilbert, H., Gavrilidis, E., and Worsley, R. (2015). Antipsychotic Use in Pregnancy. *Expert Opin. Pharmacother.* 16 (9), 1335–1345. doi:10.1517/14656566.2015.1041501

Lippert, J., Burghaus, R., Edginton, A., Frechen, S., Karlsson, M., Kovar, A., et al. (2019). Open Systems Pharmacology Community-An Open Access, Open Source, Open Science Approach to Modeling and Simulation in Pharmaceutical Sciences. *CPT Pharmacometrics Syst. Pharmacol.* 8 (12), 878–882. doi:10.1002/psp4.12473

Mian, P., Allegaert, K., Conings, S., Annaert, P., Tibboel, D., Pfister, M., et al. (2020). Integration of Placental Transfer in a Fetal-Maternal Physiologically Based Pharmacokinetic Model to Characterize Acetaminophen Exposure and Metabolic Clearance in the Fetus. *Clin. Pharmacokinet.* 59 (7), 911–925. doi:10.1007/s40262-020-00861-7

Mian, P., Nolan, B., van den Anker, J. N., van Calsteren, K., Allegaert, K., Lakhi, N., et al. (2021). Mechanistic Coupling of a Novel In Silico Cotyledon Perfusion Model and a Physiologically Based Pharmacokinetic Model to Predict Fetal Acetaminophen Pharmacokinetics at Delivery. *Front. Pediatr.* 9, 733520. doi:10.3389/fped.2021.733520

Na Takuathung, M., Hanprasertpong, N., Teekachunhatean, S., and Koonrungsesomboon, N. (2019). Impact of CYP1A2 Genetic Polymorphisms on Pharmacokinetics of Antipsychotic Drugs: a Systematic Review and Meta-Analysis. *Acta Psychiatr. Scand.* 139 (1), 15–25. doi:10.1111/acps.12947

Nylén, H., Sergel, S., Forsberg, L., Lindemalm, S., Bertilsson, L., Wide, K., et al. (2011). Cytochrome P450 3A Activity in Mothers and Their Neonates as Determined by Plasma 4β-Hydroxycholesterol. *Eur. J. Clin. Pharmacol.* 67 (7), 715–722. doi:10.1007/s00228-010-0984-1

Pariente, G., Leibson, T., Carls, A., Adams-Webber, T., Ito, S., and Koren, G. (2016). Pregnancy-Associated Changes in Pharmacokinetics: A Systematic Review. *PLoS MedARTN* 13 (11), e1002160. doi:10.1371/journal.pmed.1002160

Pennell, P. B., Peng, L., Newport, D. J., Ritchie, J. C., Koganti, A., Holley, D. K., et al. (2008). Lamotrigine in Pregnancy: Clearance, Therapeutic Drug Monitoring, and Seizure Frequency. *Neurology* 70 (22), 2130–2136. doi:10.1212/01.wnl.0000289511.20864.2a

Petrenaite, V., Sabers, A., and Hansen-Schwartz, J. (2005). Individual Changes in Lamotrigine Plasma Concentrations during Pregnancy. *Epilepsy Res.* 65 (3), 185–188. doi:10.1016/j.eplepsyres.2005.06.004

Polasek, T. M., Tucker, G. T., Sorich, M. J., Wiese, M. D., Mohan, T., Rostami-Hodjegan, A., et al. (2018). Prediction of Olanzapine Exposure in Individual Patients Using Physiologically Based Pharmacokinetic Modelling and Simulation. *Br. J. Clin. Pharmacol.* 84 (3), 462–476. doi:10.1111/bcp.13480

Reutfors, J., Cesta, C. E., Cohen, J. M., Bateman, B. T., Brauer, R., Einarsdóttir, K., et al. (2020). Antipsychotic Drug Use in Pregnancy: A Multinational Study from Ten Countries. *Schizophr Res.* 220, 106–115. doi:10.1016/j.schres.2020.03.048

Schmitt, W. (2008). General Approach for the Calculation of Tissue to Plasma Partition Coefficients. *Toxicol In Vitro* 22 (2), 457–467. doi:10.1016/j.tiv.2007.09.010

Soderberg, M. M., and Dahl, M. L. (2013). Pharmacogenetics of Olanzapine Metabolism. *Pharmacogenomics* 14 (11), 1319–1336. doi:10.2217/pgs.13.120

Sun, L., McDonnell, D., Liu, J., and von Moltke, L. (2019a). Bioequivalence of Olanzapine Given in Combination With Samidorphan as a Bilayer Tablet (ALKS 3831) Compared With Olanzapine-Alone Tablets: Results From a Randomized, Crossover Relative Bioavailability Study. *Clin. Pharmacol Drug Dev.* 8 (4), 459–466. doi:10.1002/cpdd.601

Sun, L., McDonnell, D., Yu, M., Kumar, V., and von Moltke, L. (2019b). A Phase I Open-Label Study to Evaluate the Effects of Rifampin on the Pharmacokinetics of Olanzapine and Samidorphan Administered in Combination in Healthy Human Subjects. *Clin. Drug Investig.* 39 (5), 477–484. doi:10.1007/s40261-019-00775-8

Sun, L., von Moltke, L., and Rowland Yeo, K. (2020). Physiologically-Based Pharmacokinetic Modeling for Predicting Drug Interactions of a Combination of Olanzapine and Samidorphan. *CPT Pharmacometrics Syst. Pharmacol.* 9 (2), 106–114. doi:10.1002/psp4.12488

Tracy, T. S., Venkataramanan, R., Glover, D. D., and Caritis, S. N. (2005). Temporal Changes in Drug Metabolism (CYP1A2, CYP2D6 and CYP3A Activity) during Pregnancy. *Am. J. Obstet. Gynecol.* 192 (2), 633–639. doi:10.1016/j.ajog.2004.08.030

Tran, T. A., Leppik, I. E., Blesi, K., Sathanandan, S. T., and Remmel, R. (2002). Lamotrigine Clearance during Pregnancy. *Neurology* 59 (2), 251–255. doi:10.1212/wnl.59.2.251

Urmila Sri Syamala, R. S. K. (2013). Self Nanoemulsifying Drug Delivery System of Olanzapine for Enhanced Oral Bioavailability: In vitro, In vivo Characterisation and In vitro -In vivo Correlation. *J. Bioequiv. Availab.* 05 (05). doi:10.4172/jbb.1000159

Wang, C. Y., Zhang, Z. J., Li, W. B., Zhai, Y. M., Cai, Z. J., Weng, Y. Z., et al. (2004). The Differential Effects of Steady-State Fluvoxamine on the Pharmacokinetics of Olanzapine and Clozapine in Healthy Volunteers. *J. Clin. Pharmacol.* 44 (7), 785–792. doi:10.1177/0091270004266621

Wang, Q., Liang, M., Dong, Y., Yun, W., Qiu, F., Zhao, L., et al. (2015). Effects of UGT1A4 Genetic Polymorphisms on Serum Lamotrigine Concentrations in Chinese Children with Epilepsy. *Drug Metab. Pharmacokinet.* 30 (3), 209–213. doi:10.1016/j.dmpk.2014.12.007

Westin, A. A., Brekke, M., Molden, E., Skogvoll, E., Castberg, I., and Spigset, O. (2018). Treatment with Antipsychotics in Pregnancy: Changes in Drug Disposition. *Clin. Pharmacol. Ther.* 103 (3), 477–484. doi:10.1002/cpt.770

Willmann, S., Lippert, J., Sevestre, M., Solodenko, J., Fois, F., and Schmitt, W. (2003). PK-sim: a Physiologically Based Pharmacokinetic 'whole-Body' Model. *Biosilico* 1 (4), 121–124. doi:10.1016/S1478-5382(03)02342-4

Zhang, X., Yang, Y., Grimstein, M., Fan, J., Grillo, J. A., Huang, S. M., et al. (2020). Application of PBPK Modeling and Simulation for Regulatory Decision Making and its Impact on US Prescribing Information: An Update on the 2018-2019 Submissions to the US FDA's Office of Clinical Pharmacology. *J. Clin. Pharmacol.* 60 (Suppl. 1), S160–S178. doi:10.1002/jcph.1767

Zheng, L., Tang, S., Tang, R., Xu, M., Jiang, X., and Wang, L. (2021). Dose Adjustment of Quetiapine and Aripiprazole for Pregnant Women Using Physiologically Based Pharmacokinetic Modeling and Simulation. *Clin. Pharmacokinet.* 60 (5), 623–635. doi:10.1007/s40262-020-00962-3

Conflict of Interest: AD is an employee of Bayer AG and uses Open Systems Pharmacology software, tools, and models in his professional role.

The remaining authors declare that the research was conducted in the absence of any commercial or financial relationships that could be construed as a potential conflict of interest.

Publisher's Note: All claims expressed in this article are solely those of the authors and do not necessarily represent those of their affiliated organizations, or those of the publisher, the editors and the reviewers. Any product that may be evaluated in this article, or claim that may be made by its manufacturer, is not guaranteed or endorsed by the publisher.

Advantages of publishing in Frontiers

OPEN ACCESS
Articles are free to read for greatest visibility and readership

FAST PUBLICATION
Around 90 days from submission to decision

HIGH QUALITY PEER-REVIEW
Rigorous, collaborative, and constructive peer-review

TRANSPARENT PEER-REVIEW
Editors and reviewers acknowledged by name on published articles

Frontiers
Avenue du Tribunal-Fédéral 34
1005 Lausanne | Switzerland

Visit us: www.frontiersin.org
Contact us: frontiersin.org/about/contact

REPRODUCIBILITY OF RESEARCH
Support open data and methods to enhance research reproducibility

DIGITAL PUBLISHING
Articles designed for optimal readership across devices

FOLLOW US
@frontiersin

IMPACT METRICS
Advanced article metrics track visibility across digital media

EXTENSIVE PROMOTION
Marketing and promotion of impactful research

LOOP RESEARCH NETWORK
Our network increases your article's readership